Profiling the kinome in oncogenic Ras mutant cells

Thesis submitted in accordance with the requirements of the University of Liverpool for the degree of Doctor in Philosophy (or other degree as appropriate) by:

Leah Jane Wilson

August 2020

Some of the data presented in this Thesis was previously presented in my review:

New Perspectives, Opportunities, and Challenges in Exploring the Human Protein Kinome (Wilson *et al.*, 2018).

Profiling the kinome in oncogenic Ras mutant cells

Leah Jane Wilson

RAS Proteins (KRAS4A, KRAS4B, NRAS and HRAS) are small GTPases involved in normal cellular proliferation, differentiation and apoptosis. Mutations in RAS, rendering it in the active GTP-bound state, are present in around 20% of human cancers, making it the subject of many years intensive research. Despite this, there has been limited success in targeting the RAS pathway due to the complex nature of RAS biology. Studies have shown that although highly homologous, the RAS isoforms are not functionally redundant. Furthermore, different activating RAS codon mutations illicit different signalling responses.

Our work aimed at understanding the differential signalling outputs within the RAS pathway and the wider signalling network.

Most understanding of RAS isoform biology has derived from ectopic expression experiments; however, there is a general consensus that studying endogenous RAS signalling is desirable. We have used a panel of isogenic SW48 colorectal cancer cells harbouring different RAS codon mutations to profile kinome-wide responses. The human protein kinome comprises 535 kinases and these key signalling components are frequently dysregulated in human cancers. We propose that each RAS mutant activates distinct kinase driven tumourigenic pathways.

Using NanoString technology, we characterised the transcript-level expressed kinome in each RAS mutant isogenic cell line. We identified a subset of 401 kinases expressed in SW48 cells that show differential expression. In order to build a more comprehensive kinome profile, we next measured protein kinase expression in the RAS mutant cells. Using beads conjugated to a broad specificity kinase inhibitor, we enriched the kinome fraction from cell lysates and quantified 177 protein kinases by mass spectrometry. Integrating this data with the NanoString and pre-existing proteomic datasets has enabled us to

infer likely protein expression and/or activation differences within the kinomes of Ras mutant SW48 cells.

The combination of methodologies that have been optimised allow large scale profiling of kinome expression and in some cases differential kinase activation. The data generated from these global kinase assays identify kinase nodes sensitive to isoform-specific Ras signalling.

Table of contents

List of Figures

List of Tables

Abbreviations

AML	Acute myeloid leukaemia
ATCC	American Type Culture Collection
ATP	Adenosine triphosphate
BCA	Bicinchoninic acid protein assay
COI	Cytochrome C oxidase I assay testing
CRC	Colorectal cancer
DE	Differential expression
EGF	Epidermal growth factor
eGFP	Enhanced green fluorescent protein
Ephs	Ephrin receptor tyrosine kinases
ePK	Eukaryotic protein kinase
ER	Endoplasmic reticulum
FBS	Foetal bovine serum
FDA	Food and Drug Administration
FDR	False discovery rate
FTI	Farnesyl transferase inhibitor
GAP	Guanine activating protein
GDP	Guanosine diphosphate
GEF	Guanine exchange factor
GTP	Guanosine triphosphate
HGF	Hepatocyte growth factor
HVR	Hypervariable region
iTRAQ	Isobaric tags for relative and absolute quantitation
KD	Knockdown
LC	Liquid chromatography
LFQ	Label free quantification
MAPK	Mitogen-Activated Protein Kinase
mCRC	Metastatic colorectal cancer
MIB	Multiplexed inhibitor bead
MIB/MS	Multiplexed inhibitor bead/Mass spectrometry
MS/MS	Tandem mass spectrometry
MUT	Mutant
NS	NanoString
NSCLC	Non-small cell lung cancer
PBS	Phosphate-buffered saline
PCR	Polymerase chain reaction
PDAC	Pancreatic ductal adenocarcinoma
PROTAC	Proteolysis targeting chimera
PTM	Post translational modification

RA	RAS association domain
rAAV	Recombinant adeno-associated virus
RBD	RAS binding domain
RNAi	RNA interference
ROS	Reactive oxygen species
RTK	Receptor tyrosine kinase
SDS-PAGE	SDS polyacrylamide electrophoresis
shRNA	Short hairpin RNA
SILAC	Stable Isotope Labelling with Amino acids in Cell culture
siRNA	Small interfering RNA
STR	Short Tandem Repeat profiling
TCGA	American Type Culture Collection
TK	Tyrosine kinase
TKI	Tyrosine kinase inhibitors
TNBC	Triple negative breast cancer
WT	Wild type

Acknowledgements

This PhD has been one of the most challenging yet rewarding opportunities that I have undertaken in my life. To achieve this requires support and guidance in many forms and I have been remarkably fortunate to have had both in abundance.

I wish to express my deepest appreciation to my supervisors, Prof Ian Prior and Prof Judy Coulson for their patient guidance, encouragement and personal support. I have been extremely lucky to have supervisors who have cared so much and been willing to give their time so generously. I would like to thank my supervisors at Astra Zeneca, Dr Paul Smith and Dr Sarah Ross whose insight and guidance has been invaluable throughout the course of this PhD. I would also like to acknowledge BBSRC for funding this work.

I am grateful for the inspiration, advice and friendship of my colleagues on the 5th floor past and present. Particularly, I would like to express my gratitude to Dr Adam Linley for being a patient teacher during the early stages of my PhD. I would like to pay special regards to Dr Fiona Hood and Dr Emma Rusilowicz-Jones for both their professional and personal support during the course of my PhD. You have become great friends and I will really miss our office. I also wish to thank everyone in the MCSUIP and JMC labs who make up a remarkable group of people who contribute to a fun, welcoming and stimulating working environment.

A special thanks goes to my parents for their unwavering love and encouragement, without whom I would never have enjoyed so many opportunities in life. Dad- you really are an inspiration.

And finally, to my wonderful husband, Mike. You have provided me with so much love, laughter and support. I know it may be cliché to say I couldn't have done this without you- but I really couldn't!

Chapter 1 : Introduction

The Ras superfamily of small guanosine triphosphatases (GTPases) comprise over 150 human members. The family is subdivided into five groups based on sequence homology: Ras, Rho, Ran, Rab and Arf (Wennerberg, Rossman and Der, 2005). The RAS family were the founding members of small GTPases and have been the subject of intense research due to their crucial role in oncogenesis. These small GTPases are involved in the acquisition of all the hallmarks of cancer as defined by Hanahan and Weinberg (Hanahan and Weinberg, 2011). Although similar to the α subunit of heterotrimeric G proteins in biochemistry and function, Ras GTPases function as monomeric G proteins (Hurley *et al.*, 1984). RAS proteins act as binary molecular switches that cycle between a GDP-bound inactive form and a GTP-bound active form (Gibbs *et al.*, 1984; McGrath *et al.*, 1984; Sweet *et al.*, 1984) (section 1.2.1). Once in the active GTP-bound form, RAS can illicit many downstream signalling responses that control multiple cellular processes that drive tumorigenesis. These processes include all of the hallmarks of cancer: sustaining proliferative signalling, evading growth suppressors, resisting cell death, enabling replicative immortality, inducing angiogenesis, and activating invasion and metastasis (Hanahan and Weinberg, 2011).

1.1. The discovery of RAS

1.1.1. RAS Retroviruses

The discovery of RAS genes originally stemmed from studies of potently transforming retroviruses that were conducted throughout the 1960s (Malumbres and Barbacid, 2003). The studies of retroviruses that induced the formation of sarcomas in animals and transformed cells in culture, provided the first evidence of RAS involvement in cancer. In 1964, Jennifer Harvey isolated the Harvey murine sarcoma virus (HA-MuSV) by passage of a murine leukaemia virus in rats (HARVEY, 1964). A few years later in 1967, Werner H. Kirsten isolated the Kirsten murine sarcoma virus (Ki-MSV) by passage of

murine leukaemia viruses in rats (Kirsten and Mayer, 1967). These initial discoveries provide the basis for their current gene names; the RAS gene family name is derived from the fact they were found to induce rat sarcomas, whilst their individual gene names hail from their discoverers' (Karnoub and Weinberg, 2008).

Scolnick and colleagues conducted an array of pioneering studies throughout the 1970s that underpins much of our understanding of the fundamental properties of cellular RAS proteins (see section 1.2) (Scolnick *et al.*, 1973; Scolnick and Parks, 1974; Scolnick, Papageorge and Shih, 1979; Shih *et al.*, 1979b; Willingham *et al.*, 1980). Although, initially identified as a viral component that induced transformation in rats, a study in 1974 revealed that the transforming properties of these viruses were in fact, a normal component of the rat genome (Scolnick and Parks, 1974). Despite this, it wasn't until sometime later that experiments linked RAS directly to human cancer.

1.1.2. RAS human oncogenes

In the early 1970s, scientists were able to transfer DNA into mammalian cells by transfection, following the precipitation of DNA using calcium phosphate (Hill and Hillova, 1971). The focus on these initial studies was to determine the effect of DNA transfection and as a result, deduce gene function. By 1978, Wigler et al. had adapted the method so that a single copy of eukaryotic DNA could be transferred into mammalian cells. Focus then shifted to determine whether the transfected DNA had the ability to transform cells (Wigler *et al.*, 1978). In 1979, Weinberg and colleagues first applied the method in NIH3T3 mouse fibroblast cells; DNA isolated from chemically transformed mouse cells caused morphological transformation (foci) when transfected into the NIH3T3 cells in culture (Shih *et al.*, 1979a). The ability of NIH3T3 cells to become morphologically transformed by a single gene enabled researchers to measure the oncogenic potential of a gene of interest, an assay that is still widely used today (Jainchill, Aaronson and Todaro, 1969). However, there was a lack of confidence in these first reports. Although NIH3T3 cells were immortalized, they had been shown to become spontaneously transformed when

continuously cultured at high confluency (Malumbres and Barbacid, 2003). Furthermore, no evidence was presented in the report that indicated that the DNA was efficiently transfected into the cells.

Any scepticism was resolved over the following years after the assay was used to identify the transforming activity of DNA isolated from human cancer cell lines. The focus formation assay was used firstly to clone a human transforming gene isolated from human bladder carcinoma cells (Krontiris and Cooper, 1981) and later studies that identified transforming activity in lung, colon and leukaemia cell lines also provided further evidence of the presence of transforming genes in human cancer (Perucho *et al.*, 1981; Murray *et al.*, 1981; Shih *et al.*, 1981).

Whilst efforts were made to identify and isolate the human oncogenes that were responsible for NIH3T3 cell transformation, a surprising discovery was made (Cox and Der, 2010). In 1982, three independent groups discovered that the transforming genes isolated from human bladder cancer cells were homologous to the Harvey and Kirsten sarcoma viruses identified in the 1960s (Santos *et al.*, 1982; Der, Krontiris and Cooper, 1982; Parada *et al.*, 1982). Furthermore, studies later that year revealed that HRAS was activated in human bladder carcinomas by a single amino acid substitution at codon 12 (Taparowsky *et al.*, 1982; Reddy *et al.*, 1982; Tabin *et al.*, 1982) and similar observations were made for activated KRAS in lung and colon tumour cells (Capon *et al.*, 1983). Moreover, the same single missense mutation at codon 12 was found in the viral RAS genes (Cox and Der, 2010).

However, the notion that a single point mutation could induce transformation in cells was scrutinised by the scientific community (Malumbres and Barbacid, 2003) and this presumption was later revised when it was discovered that activated HRAS alone could not transform primary fibroblast cells (Land, Parada and Weinberg, 1983). Instead, it was shown that concurrent activation of an oncogene or suppression of tumour suppressor gene is required to promote transformation, a concept that is critical to our current understanding

of the multistep pathway to carcinogenesis (Vogelstein *et al.*, 1988; Hruban *et al.*, 2000).

In 1983, a third RAS gene was discovered in a human neuroblastoma cell line (Hall *et al.*, 1983; Shimizu *et al.*, 1983). Considering, it had not been previously identified in retrovirus studies and it was first described as a neuroblastoma transforming gene, it was designated the name NRAS (Cox and Der, 2010).

Over the next few years, RAS mutations were detected in several human tumour cell lines (Pulciani *et al.*, 1982). Furthermore, mutant RAS genes were identified in patient tumours and not in normal tissue, thus providing evidence that this phenomenon was not an artefact of the NIH3T3 cell model (Feig *et al.*, 1984; Santos *et al.*, 1984). It is now widely accepted that RAS is one of the most prevalently mutated oncogenes in human cancers, mutated in approximately 20% of all cancer patients (section 1.3) (Prior, Hood and Hartley, 2020).

1.2. RAS regulation

1.2.1. The RAS GDP/GTP cycle

Early biochemical studies focusing on the RAS retroviral genes provided the first indication that RAS may function as a GTPase (Scolnick *et al.*, 1973; Scolnick and Parks, 1974). The discovery by Scolnick and colleagues that the viral RAS genes encode a 21kDa protein subsequently led to studies to characterise the function of RAS proteins (Shih *et al.*, 1979b). One of the many key discoveries, was that RAS proteins bind to guanine-containing nucleotides with high affinity (Scolnick, Papageorge and Shih, 1979). This finding, along with the fact that RAS has a similar amino acid homology to the alpha subunit of G proteins sparked speculation that like other G proteins, RAS functions as a GDP/GTP regulated binary switch (Hurley *et al.*, 1984).

In 1984, three groups confirmed that RAS proteins were in fact GTPases, cycling between an inactive GDP-bound state and an active GTP-bound state (Gibbs *et al.*, 1984; McGrath *et al.*, 1984; Sweet *et al.*, 1984). Moreover, authors revealed that intrinsic GTP hydrolysis was significantly reduced in mutant proteins vs. wild-type proteins. These studies provided the first indication that impaired GTPase activity leading to preferential binding of GTP may be responsible for the transformation of cancer cells.

The studies that followed provided an explanation as to why point mutations at codon 12 and 61 of RAS resulted in constitutively activated proteins; McCormick et al. reported that an antibody that specifically recognised the region of codon 12 on HRAS blocked the binding of GTP (Clark *et al.*, 1985), whilst another study revealed that several mutations in HRAS at position 61 impaired GTP hydrolysis (Der, Finkel and Cooper, 1986). Collectively, these studies showed that mutations in RAS impair GTP hydrolysis rendering proteins in the active GTP-bound state.

However, the impaired GTPase activity of mutant vs. wild-type proteins observed in vitro was not enough to justify RAS activity in vivo, and therefore

researchers endeavoured to understand how the RAS GDP/GTP cycle was being regulated (Malumbres and Barbacid, 2003; Cox and Der, 2010).

A breakthrough came in 1987 when the first GTPase activating protein (RasGAP) was identified (Trahey and McCormick, 1987). In a study using xenopus oocytes, Trahey and McCormick discovered a protein that stimulated the GTPase activity of wild-type proteins but not mutant proteins; The cytosolic protein stimulated the hydrolysis of GTP-bound wild-type proteins more than 200-fold, however there was little effect on the NRAS codon 12 mutants (Trahey and McCormick, 1987). The following year the group purified the protein and described it as p120RasGAP (Trahey *et al.*, 1988). Shortly after the discovery of the first RasGAP, a second RAS inactivating protein, Neurofibromin (NF1), was identified in a study of patients with neurofibromatosis (Wallace *et al.*, 1990). When the NF1 gene, which is mutated in Neurofibromatosis disease was cloned, scientists discovered that there was a region of significant sequence homology to p120RasGAP (Ballester *et al.*, 1990; Xu *et al.*, 1990). Moreover, this region was shown to interact with and inactivate RAS (Martin *et al.*, 1990).

In parallel to the discovery of RasGAPs, research efforts focused on identifying activating regulators of RAS that induce GTP binding. The first evidence of proteins that facilitated the exchange of GDP to GTP on RAS was provided in genetic studies of yeast and Drosophila. Firstly, the guanine nucleotide exchange factor (GEF), CDC25, was shown to regulate RAS activity in *Saccharomyces cerevisiae* (Robinson *et al.*, 1987; Broek *et al.*, 1987) whilst, the RasGEF, Son of Sevenless (SOS) was identified in a genetic study of Drosophila and was later found to be related to the yeast CDC25 gene (Rogge, Karlovich and Banerjee, 1991; Bonfini *et al.*, 1992). Soon thereafter, the first mammalian RasGEFs, were identified (Downward *et al.*, 1990; Wolfman and Macara, 1990). Structural and functional analyses of the Drosophila SOS gene and the yeast CDC25 gene revealed homologous mammalian proteins that included Son of Sevenless 1 (SOS1) and RAS nucleotide releasing factor 1 (RASGRF1) (Bowtell *et al.*, 1992; Wei *et al.*, 1992).

In the years following, several more RasGEFs and RasGAPs were identified, some of which are highlighted in Figure 1.1 (Bos, Rehmann and Wittinghofer, 2007). It is now widely accepted that RAS functions as a GDP/GTP regulated binary switch which is controlled by RasGAPs and RasGEFs (Figure 1.1). RasGAPs stimulate intrinsic GTPase hydrolysis to promote the formation of (inactive) RAS-GDP, whilst RasGEFs promote the dissociation of GDP to facilitate the formation of (active) RAS-GTP (Mitin, Rossman and Der, 2005). Mutations in RAS render it in its active GTP-bound state and is typically a result of GAP insensitivity, whereby GAP mediated GTP hydrolysis is disrupted causing an accumulation of active RAS (Moore *et al.*, 2020). However, mutations that increase the rate of GEF mediated GDP/GTP exchange have also been described (Hunter *et al.*, 2015). See section 1.3.2 for more details of the individual RAS mutants.

The determination of the crystal structures of RAS provided a better understanding of the structural dynamics of RAS proteins cycling between the inactive and active conformations (de Vos *et al.*, 1988). Comparison of the GDP-bound and GTP-bound structures of RAS revealed two key regions of conformational change referred to as switch 1 (residues 30-40) and switch 2 (residues 60-76) (Milburn *et al.*, 1990; Schlichting *et al.*, 1990). In the active conformation, hydrogen bonds form between the γ-phosphate of GTP and the threonine and glycine residues (T35, G60) of the switch 1 and switch 2 regions respectively. Upon GTP hydrolysis, the γ-phosphate is released and the switch regions return to the relaxed inactive conformation (Vetter and Wittinghofer, 2001). The conformational change in these regions is critical for the interaction between RAS and its upstream regulators or downstream effectors (Karnoub and Weinberg, 2008) (see section 1.2.4 for more information on RAS structure).

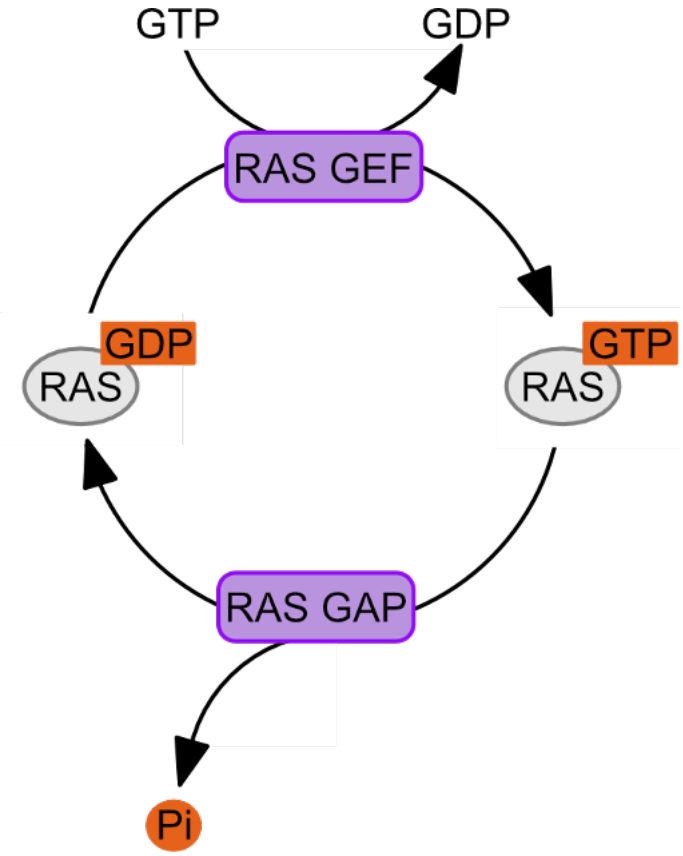

	Gene name	Protein name
GEFs	SOS1/2	SOS1/2
	RASGRP 1-4	RASGRP 1-4
	RASGRF 1/2	RASGRF 1/2
GAPs	RASA1	p120 RasGAP
	RASA2	GAP1 M/RASA2
	RASA3	GAP1 (IP4BP)
	RASA4	CAPRI
	RASAL1	RASL1
	SYNGAP	SynGAP
	NF1	Neurofibromin 1
	GAPVD1	GAPVD1
	DAB2IP	DAB2IP

Figure 1.1. Regulation of RAS activity.

RAS GEFs stimulate the exchange GDP to GTP thus, resulting in the formation of a pool of active GTP-bound RAS. In contrast, RAS GAPs accelerate the intrinsic GTPase activity of RAS thus promoting in the formation of inactive GDP-bound protein. Known regulators of the RAS GDP/GTP cycle are highlighted in table above.

1.2.2. Upstream regulation of RAS

Another important advance in our understanding of how RAS is regulated came from studies linking mitogenic signalling and RAS activation. Initial evidence indicating that mitogenic signalling may control RAS GTPase activity came from an early study conducted in NIH3T3 cells. Scientists revealed that Epidermal Growth Factor (EGF) treatment stimulated guanine nucleotide binding of cellular HRAS (Kamata and Feramisco, 1984). The following year, further evidence was provided in studies conducted by Stacey et al. that utilised a monoclonal antibody targeting RAS. The microinjection of the antibody into NIH3T3 cells prevented serum induced DNA synthesis thus indicating that RAS was essential for signalling downstream of extracellular mitogens (Mulcahy, Smith and Stacey, 1985).

The first direct link between upstream mitogenic signalling and RAS regulation came from a study linking the cell surface platelet derived growth factor receptor (PDGF) and RasGAP p120. The study revealed that stimulation of the PDGF receptor induced the tyrosine phosphorylation of RasGAP p120, resulting in its translocation to the cell membrane where it can regulate RAS (Molloy *et al.*, 1989).

Further evidence came from seminal studies linking the cell surface epidermal growth factor receptor (EGFR) and RAS activation. In *Caenorhabditis elegans*, a novel protein was identified named sem-5, that consisted of one SH2 domain and two SH3 domains (Clark, Stern and Horvitz, 1992). Authors reported that Sem-5, along with let-23 (EGFR like) and let-60 (RAS like) proteins were essential for vulval development in *Caenorhabditis elegans*. Concurrent with this discovery, a mammalian protein, GRB2, that exhibited notable structural and functional homology to sem-5 was identified in a study searching for proteins that bind to the intracellular tail of EGFR (Lowenstein *et al.*, 1992). Several studies later discovered that the SH2 and SH3 domain containing protein, GRB2 (sem-5) was the missing link between EGFR and the RASGEF, SOS1; Eight studies revealed that GRB2 was an adaptor protein, that could bind to EGFR via its SH2 domain at one end, and SOS via its two SH3 domains

at the other end (Olivier *et al.*, 1993; Rozakis-Adcock *et al.*, 1993; Simon, Dodson and Rubin, 1993; Egan *et al.*, 1993; Chardin *et al.*, 1993; Buday and Downward, 1993; Gale *et al.*, 1993; Li *et al.*, 1993). It was later shown that the formation of the EGFR: GRB2:SOS1 complex at the plasma membrane was crucial for RAS activation; When EGFR is activated, Grb2:SOS1 is recruited from the cytosol to the membrane where it can then activate RAS (Quilliam *et al.*, 1994; Aronheim *et al.*, 1994). Moreover, GRB2 can bind to other adaptor proteins (such as SHC and IRS-1) permitting the interaction of SOS1:RAS with several different receptor tyrosine kinases (RTKs) (Margolis and Skolnik, 1994).

These studies were crucial to our understanding of the signal transduction from extracellular stimuli to RAS. Moreover, these observations also emphasised the importance of subcellular localisation of RAS regulating proteins (see section 1.2.4). It is now widely accepted that several RTKs can activate downstream RAS. Upon activation, RTKs become auto phosphorylated on multiple tyrosine residues that in turn, recruit adaptor proteins containing SH2 domains to the cell membrane, where associated RASGEFs can activate RAS (Margolis and Skolnik, 1994).

1.2.3. RAS downstream effector signalling

In 1993, the first RAS effector, Raf, was discovered thus providing the final link in the RAS canonical signalling pathway. Several groups revealed that Raf preferentially binds to RAS in its active GTP-bound state rather than its inactive GDP-bound state (Wigler *et al.*, 1978; Zhang *et al.*, 1993; Warne, Viciana and Downward, 1993; Moodie *et al.*, 1993). Furthermore, it was reported that Raf is a potent competitive inhibitor of RasGAP proteins, such as p120 RasGAP and NF1 (Warne, Viciana and Downward, 1993). The role of Raf downstream of RAS was also verified in independent genetic studies of *Caenorhabditis elegans* and drosophila (Han *et al.*, 1993; Dickson *et al.*, 1992). Raf had been discovered as a retrovirus oncogene many years prior, thus the protein had already been well characterised (Rapp *et al.*, 1983). It was known that Raf activates downstream MEK and ERK thus, the RAS-RAF-MEK-ERK (MAPK)

signalling cascade was delineated (Gallego *et al.*, 1992) (Kyriakis *et al.*, 1992; Wood *et al.*, 1992; Howe *et al.*, 1992; Dent *et al.*, 1992).

RAS promotes cellular transformation through activating the downstream cascade and in turn, a number of different families of transcription factors. These include c-MYC, c-FOS, c-JUN and ETS1 that promote a wide variety of cellular processes including cell cycle entry, angiogenesis, and cell survival (Deng and Karin, 1994; Westwick *et al.*, 1994; Brunner *et al.*, 1994; Gimple and Wang, 2019). Furthermore, cytoplasmic ERK can also regulate a number of different downstream kinases, including ribosomal s6 kinases (RSKs) that regulate diverse cellular processes (Takács *et al.*, 2020). Recently, Nils Bluthgen and colleagues compiled a comprehensive ERK target phosphosite archive taken from various research studies; A list of 2507 phosphosites were compiled from various sources, including 659 direct and 1848 indirect ERK targets thus, highlighting the complexity of downstream signalling (Ünal, Uhlitz and Blüthgen, 2017). It is also important to note that activated ERK can also downregulate RAS activity by phosphorylating upstream components. For example, a negative feedback loop has been described whereby activated ERK phosphorylates SOS1 and as a result, the SOS1:GRB2 complex is uncoupled from the tyrosine residues of RTKs (Buday, Warne and Downward, 1995).

A short time after the discovery of Raf, a second RAS effector, Phosphatidylinositol 3-kinase (PI3K), was described. Although the association of PI3K and RAS had first been reported in 1991 (Sjölander *et al.*, 1991), it wasn't until 1994 that the kinase was accepted as a direct RAS effector when Julian Downward and colleagues revealed that RAS interacts with the catalytic p110 subunit of PI3K (Rodriguez-Viciana *et al.*, 1994). Like Raf, PI3K binds active RAS-GTP through its Ras Binding domain (RBD) (Rajalingam *et al.*, 2007). Upon activation by RAS, P13K phosphorylates Phosphatidylinositol 4,5-bisphosphate (PIP_2) leading to the production of Phosphatidylinositol (3,4,5)-trisphosphate (PIP_3) at the plasma membrane. Subsequently, AKT is recruited to the membrane and associates with PIP_3 through its PH domain. At the membrane, AKT can be activated through phosphorylation of tyrosine and

serine residues (T308 and S473) by PDK1 and mTORC2 respectively (Castellano and Downward, 2011). AKT has been shown to activate over 200 substrates including GSK3, mTOR, and FOXO family members that promote cell cycle progression, cell survival and metabolism (Manning and Toker, 2017).

In the meantime, a third RAS effector, Ral guanine nucleotide dissociation stimulator (RALGDS) was described (Cox and Der, 2010; Spaargaren and Bischoff, 1994). RALGDS associates with RAS through its RAS association (RA) domain and also acts as a GEF for RAL (RAS like protein) thus providing a bridge between RAS and RAL proteins (Rajalingam *et al.*, 2007; Hofer *et al.*, 1994) . Initial studies in mouse fibroblast NIH3T3 cells suggested a minimal role for RALGDS in RAS transformation (White *et al.*, 1996; Urano, Emkey and Feig, 1996). However later studies in human kidney cells revealed that the effector has a significant role in oncogenic RAS signalling (Hamad *et al.*, 2002). Furthermore, it was revealed that RalGDS is essential for transformation of HRAS mutant skin carcinoma cells (González-García *et al.*, 2005). Loss of function analyses provided further evidence of the importance of both RAL isoforms (RALA and RALB) as key modulators of oncogenic cell proliferation and survival (Chien and White, 2003). The study used RNAi to define the roles of each isoform in transformation. It was revealed that RALA is required for anchorage independent proliferation of cancer cells, whilst RALB prevents transformed cells from programmed cell death via sec5/TBK1 (Chien and White, 2003; Chien *et al.*, 2006).

The growing family of RAS effectors now comprise more than nine different classes of effectors (Raf, PI3K, RALGDS, Tiam, RASSF, Rin1, Af6, PLCε and PKCζ) (Rajalingam *et al.*, 2007). Some are highlighted in Figure 1.2. In broad terms Ras effectors can be described as GEFs/GAPs regulating other GTPases and kinases. Most attention has focussed on RAF-MEK-ERK and the PI3K due to their significant contributions to oncogenesis. Ral has also been relatively well studied although it is still unclear if it supports oncogenic Ras function in all contexts. Of the remaining effectors, two of the most characterised effectors are Tiam1 and RASSF5 (Nore1).

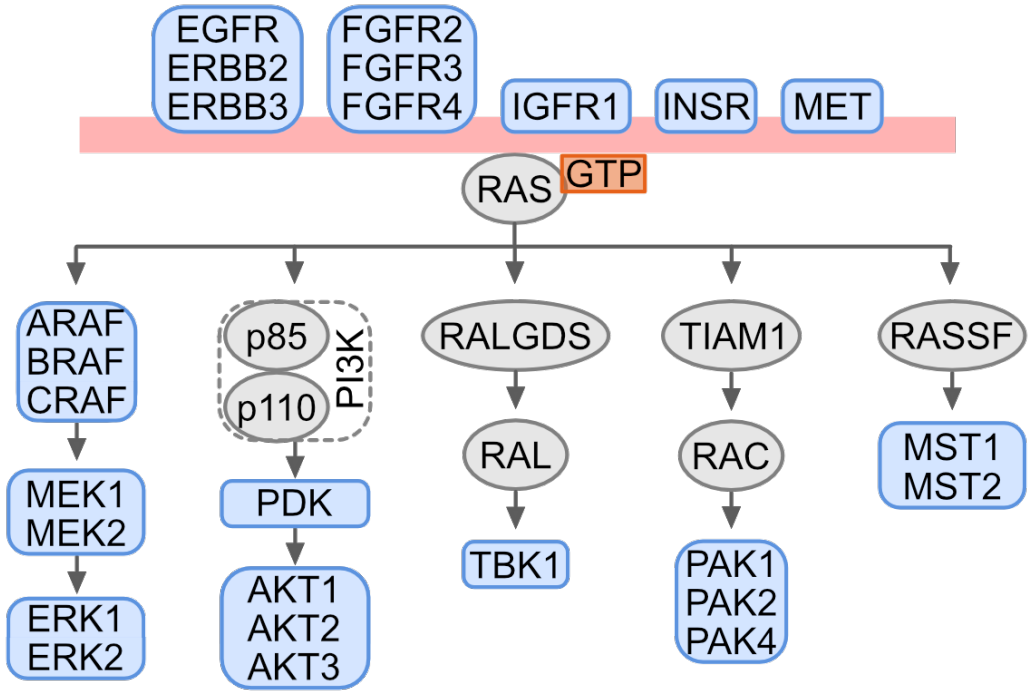

Figure 1.2. RAS signalling network

Several RTKs have been shown to activate RAS. Upon activation, RAS binds to its downstream effectors. RAS-GTP preferentially binds to Ras binding domain (RBD) or Ras association (RA) domain containing effectors. There are over nine different families, some of the best characterised effector- signalling cascades are highlighted above. Many upstream and downstream nodes within the Ras network are kinases (highlighted in blue).

T lymphoma invasion and metastasis protein (Tiam1) is a RAC specific GEF that mediates the activation of RAC through RAS (Rajalingam *et al.*, 2007). Channing Der and colleagues first described Tiam1 as a RAS effector that preferentially binds to RAS-GTP through a RAS binding domain (Lambert *et al.*, 2002). Concurrent with this discovery, it was reported that Tiam1 is essential for HRAS induced skin tumour formation in mice indicating the importance of RAS-Tiam1 interaction in human cancer (Malliri *et al.*, 2002). Upon activation by RAS, Tiam1 promotes the formation of RAC-GTP leading to the phosphorylation of the p21 activated kinases (PAK) (Manser *et al.*, 1994). TIAM1-PAK signalling predominantly controls proteins regulating cytoskeleton rearrangement and migration, but has also been implicated in cell growth and survival (Takács *et al.*, 2020).

RAS association domain family (RASSF) possess a RA domain, but no catalytic function (Rajalingam *et al.*, 2007). The most characterised RASSF, Nore1 (RASSF5), acts as a scaffold between active RAS and the proapoptotic proteins mammalian sterile-20-like protein kinases (MST1/2) (Khokhlatchev *et al.*, 2002). Thus, RASSF proteins act as a tumour suppressors through MST induced cell cycle arrest and apoptosis (Vos and Clark, 2006) and may act as a homeostatic mechanism to prolonged RAS signalling.

Many RAS effector signalling pathways have been established that control diverse cellular functions. However, it is important to note that RAS induced oncogenesis occurs through a complex network of signalling nodes, rather than just the simple linear pathways highlighted above. Feed forward signalling, cross talk between multiple downstream effector pathways and negative feedback loops all contribute to RAS induced oncogenesis. Another layer of complexity is added by the fact that the convergence of downstream pathways will also be dependent on signalling intensity and duration (Hornberg *et al.*, 2005). Understanding the context dependence of downstream effector signalling will be key for our understanding of RAS biology.

1.2.4. Post-translational mechanisms of RAS regulation

As previously mentioned, most of our understanding of how RAS is regulated was derived from early studies of RAS retroviruses. It was appreciated in the early stages of RAS research that RAS was not solely controlled by its GDP/GTP cycle, but that recruitment of cytosolic RAS to the membrane was essential for its activation. Evidence first emerged in 1980 when Ha-MuSV p21 protein was detected on the inner leaflet of the plasma membrane by electron microscopy (Willingham *et al.*, 1980). Scolnick and colleagues also reported that viral HRAS contained tightly bound lipids which facilitated its interaction with the membrane (Sefton *et al.*, 1982). Moreover, in 1984 Lowy et al. revealed that lipid binding and membrane association through a cysteine residue (C186) at the C-terminus of RAS is essential for the transforming activity of RAS (Willumsen *et al.*, 1984a). Based on the critical importance of the cysteine residue, authors correctly hypothesised that no more than 3 amino

acids are cleaved during lipid processing (Willumsen *et al.*, 1984b). Others also speculated that cysteine 186 was the site of palmitoylation due to the fact that viral HRAS could incorporate palmitate acid (Buss and Sefton, 1986).

These initial findings prompted a series of experiments that fully defined the molecular mechanisms of RAS lipid processing (Karnoub and Weinberg, 2008). It was revealed that actually, several steps of post-translational modifications (PTMs) are required for the stable association of RAS proteins in the membrane (Hancock *et al.*, 1991).

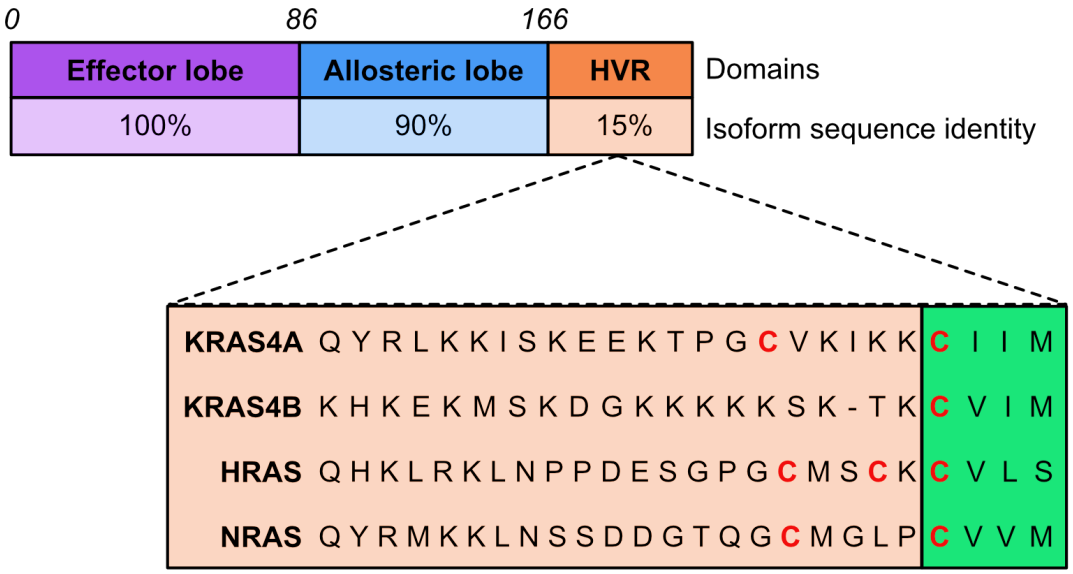

Figure 1.3. RAS structure

The three RAS genes encode four RAS isoforms. The isoforms share almost complete sequence homology in the G domain. The G domain consists of the effector lobe, which is essential for effector interactions, and the allosteric lobe which connects the effector lobe to membrane associated residues. The hypervariable region (HVR) is the only region of significant sequence divergence. A series of post-translational modifications of the HVR promote recruitment to the membrane where they can become activated. Once activated, conformational changes occur in the switch 1 (residues 30-40) and switch 2 (residues 60-76) regions that allow for effector engagement and downstream signalling.

Although highly homologous, each RAS isoform has a region of significant sequence divergence in the C-terminal hypervariable region (HVR) (Figure 1.3) (Mo, Coulson and Prior, 2018). The HVR encompasses 23/24 amino acids which undergo a series of PTMs that promote recruitment and binding to the membrane where they can function (Prior and Hancock, 2012). Each isoform shares a CAAX box motif at the extreme C-termini that is sequentially processed; Firstly, the cysteine residue is prenylated by farnesyl protein transferase (Casey *et al.*, 1989). This initial step promotes the affinity of cytosolic RAS to the endoplasmic reticulum (ER) where additional enzymes required for CAAX processing are localised (Prior and Hancock, 2012). At the ER, the AAX motif is cleaved off by Ras-converting enzyme (Rce1) and the cysteine residue is carboxymethylated by isoprenyl cysteine transferase (ICMT) (Hancock and Parton, 2005).

Although the latter step produces hydrophobic proteins that weakly associate with membranes, it was shown that a second signal, upstream of the CAAX motif, is required for stable association with the membrane (Hancock *et al.*, 1991). For KRAS4B, the second signal is a region of 6 polybasic lysine residues that provide an electrostatic interaction with the hydrophilic heads in the plasma membrane (Hancock, Paterson and Marshall, 1990). The second signal for the other three RAS isoforms is palmitoylation. HRAS is palmitoylated on cysteine residues 181 and 184 whilst NRAS and KRAS4A are mono palmitoylated on cysteine residues 181 and 180 respectively (Hancock *et al.*, 1989). It is important to note that the second signal determines how each RAS isoform is trafficked and where in the membrane they are localised (Mo, Coulson and Prior, 2018). Palmitoylated RAS proteins traffic through the Golgi to the membrane, whereas unpalmitoylated KRAS4B bypasses the Golgi and traffics through the cytosol to the membrane (Choy *et al.*, 1999; Apolloni *et al.*, 2000). Once at the plasma membrane, the HVR motifs regulate the interactions of each isoform with different microdomains that contain different RAS regulators and effectors (Prior *et al.*, 2003) (Casar *et al.*, 2009). Thus, differential compartmentalisation of the RAS isoforms is thought to contribute to the isoform-specific differences in signalling (Abankwa *et al.*, 2010; Omerovic, Laude and Prior, 2007).

1.3. RAS contribution to cancer

1.3.1. Isoform-specific RAS signalling

In vivo studies have shown that although highly homologous, the four RAS isoforms (HRAS, NRAS, KRAS4A and KRAS4B) are not functionally redundant (Mo, Coulson and Prior, 2018). It was originally shown that, only the KRAS4B isoform was essential for normal mouse embryogenesis. Whilst NRAS and HRAS double knockout mice were healthy, KRAS ablation was embryonic lethal (Koera *et al.*, 1997; Esteban *et al.*, 2001). However, a later study showed that there was no specific requirement for KRAS in mouse development. When HRAS was expressed in the KRAS locus, mice were viable, despite the mice later displaying cardiomyopathy (Potenza *et al.*, 2005). Furthermore, mice heterozygous for KRAS that lack NRAS function are embryonic lethal suggesting partial overlap between the RAS gene family (Johnson *et al.*, 1997). This suggests that isoform specific differences in development arise from RAS gene expression patterns, rather than the specific function of the RAS protein itself. However, it is important to note that KRAS may still have a role in healthy development (Mo, Coulson and Prior, 2018).

Other evidence of isoform specific differences comes from the fact that the isoforms have different mutation frequencies; KRAS is most frequently mutated in cancer, mutated in 69% of all cancers, compared with 22% for NRAS and 9% for HRAS (Mo, Coulson and Prior, 2018). Moreover, each isoform is differentially associated with specific cancers: KRAS is strongly associated with pancreatic, colorectal and lung tumours, NRAS is frequently mutated in melanomas and HRAS is predominantly mutated in Head and Neck Cancers (Figure 1.4) (Prior, Lewis and Mattos, 2012).

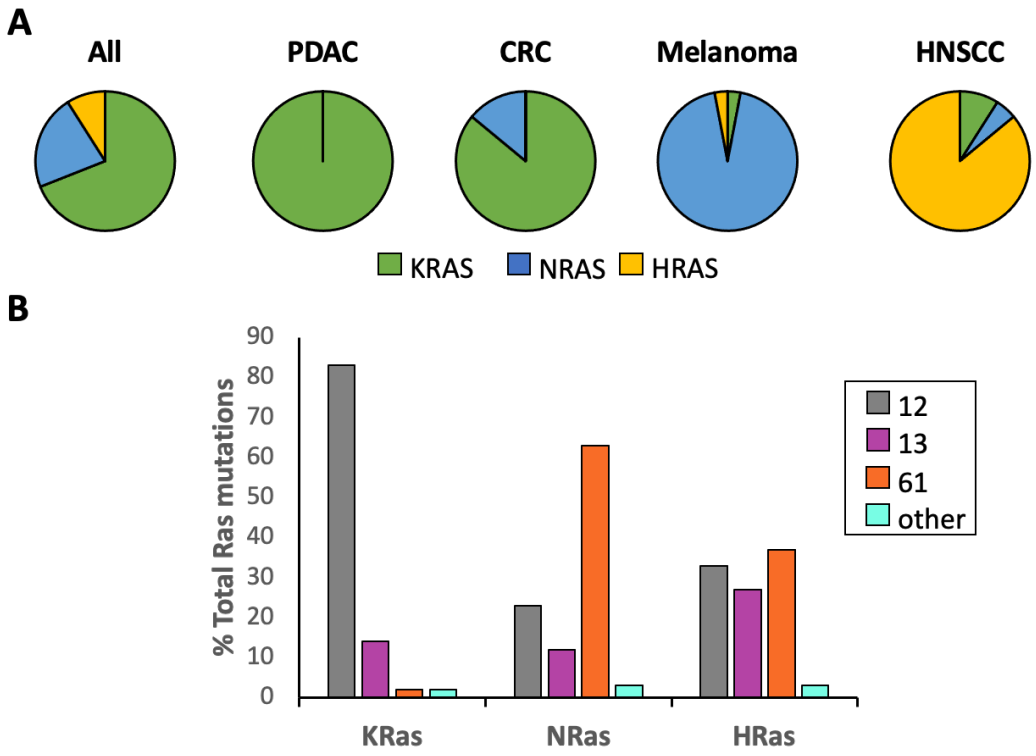

Figure 1.4. Ras mutations in cancer

A) Despite being highly homologous, each isoform is not functionally redundant. Each individual RAS isoform exhibits differential and preferential coupling to specific cancers. Pie charts display RAS mutational frequencies per cancer type. Pie chart colours: green, KRAS; blue, NRAS; yellow, HRAS. B) Ras-isoform–specific codon mutation bias. K-Ras is typically mutated at codon 12, whereas N-Ras favours codon 61. H-Ras displays intermediate behaviour. Bar chart colours: grey, codon 12; purple, codon 13; orange, codon 61. Data taken from previous studies using TCGA and COSMIC datasets (Prior, Lewis and Mattos, 2012; Mo, Coulson and Prior, 2018) .

The mechanistic basis for isoform specific frequencies remains poorly understood. Most understanding of RAS isoform biology has derived from ectopic expression experiments. The studies describe preferential coupling of each isoform with key Ras effector pathways. KRAS was shown to be a more potent activator of the MAPK pathway whereas HRAS and NRAS were shown to more potently activate the PI3K pathway (Yan *et al.*, 1998; Voice *et al.*, 1999). This is in contrast to findings from studies using cell lines or mouse models with endogenously expressed mutant RAS; Very little evidence of preferential coupling to Ras effectors was presented. Instead, significant heterogeneity for effector requirements was displayed for each isoform

suggesting that RAS signalling is more context dependent (Tuveson *et al.*, 2004; Omerovic *et al.*, 2008).

Despite this, functional differences between the RAS isoforms have been described. A study using genetically engineered mice with inducible expression of different oncogenic RAS isoforms in the endogenous loci, revealed unique functions of KRAS and NRAS in human colon cancer. Only mutationally activated KRAS, not NRAS, can promote colonic epithelium proliferation thus, providing an insight into KRAS mutation bias in colorectal cancer (Haigis *et al.*, 2008). Moreover, the study revealed activated KRAS mediates oncogenesis through a non-canonical pathway that includes RAF, but not MEK or ERK and authors suggest that the isoforms display distinct phenotypic differences due to their ability to interact with the downstream effector.

Indeed, there is plenty of evidence that isoform specific signalling arises from structural differences that result in differential localisation and effector engagement. As previously discussed, differential post-translational modifications of the HVR of each isoform has a significant influence on where each RAS isoform is localised in the cell membrane (Prior *et al.*, 2003; Hancock and Parton, 2005) (section 1.2.4). Each RAS isoform occupies distinct non-overlapping nanoclusters in the membranes that are thought to influence which RAS regulators and effectors each isoform is able to interact with, and mediate oncogenesis through (Prior *et al.*, 2003; Prior and Hancock, 2012; Abankwa *et al.*, 2010). Further evidence of isoform specific signalling arises from structural differences in the allosteric lobe (Mo, Coulson and Prior, 2018). Although there is almost 90% isoform sequence homology in the allosteric lobe, there is sequence divergence in residues that are thought to mediate nucleotide binding and conformational changes (Parker and Mattos, 2018). It has been reported that KRAS occupies the ‘closed’ GTP-bound state more readily than HRAS and NRAS (Johnson *et al.*, 2017). Considering the closed GTP-bound state promotes effector binding, the ability of each isoform to adopt the active conformation state could provide another reason for KRAS isoform mutation bias in human cancer.

1.3.2. RAS mutation specific signalling

Emerging evidence for the different functional outcomes of RAS codon mutations at amino acid positions G12, G13 and Q61, adds another layer of complexity to RAS biology (Hobbs, Der and Rossman, 2016). Although missense mutations at these three codon hotspots are activating, they are not all equally transforming (Hobbs and Der, 2019). In a study using site-directed mutagenesis to introduce 17 different amino acid substitutions in position Q61 of HRAS, authors reported that mutants varied over 100-fold in transforming potency (Der, Finkel and Cooper, 1986). Similar observations were also made in another in vitro mutagenesis study analysing the transforming potential of 20 different amino acid substitutions in HRAS at position 12 (Seeburg *et al.*, 1984).

Recent findings from biochemical studies may provide an explanation as to why RAS mutations aren't created equal. Studies revealed that mutation specific differences in intrinsic or GAP mediated GTP hydrolysis, GDP/GTP binding kinetics and effector interactions all contribute to distinct biologic behaviours (Smith, Neel and Ikura, 2013; Hunter *et al.*, 2015).

Hunter and colleagues created a model based on the biochemical and biophysical properties of individual KRAS mutants to predict biological readouts that ultimately may enable the rational selection of therapies targeting different RAS mutations (Hunter *et al.*, 2015). Most oncogenic mutants displayed marked GAP insensitivity indicating that inactivation is largely dependent on intrinsic GTP hydrolysis. Thus, authors concluded that mutation specific signalling may arise from differential intrinsic GTP hydrolysis rates that predominantly control the duration of RAS activation. Moreover, since RasGAPs are unable to compete with the nano affinity of RAS and RAF (Moodie *et al.*, 1995), authors used intrinsic hydrolysis rates alongside RBD-RAF affinities to predict the dependence of each mutant on the Raf-MAPK signalling cascade.

For example, authors predicted that the Q61L mutant mutants preferentially signal through the RAF kinase pathway, since the mutant Q61L has a high affinity to RAF and a low intrinsic GTP hydrolysis rate that promotes a longer duration of activation (Hunter *et al.*, 2015). The model also predicted that the G12V and G12R mutants are moderate activators of Raf due to the fact they have low affinity to RAF but a slow GTP hydrolysis rate that extends the duration of time RAS is in the active conformation and therefore bound to RAF. On the other end of the spectrum, the G12D mutant with its low affinity to RAF and high intrinsic hydrolysis rate is less likely to be dependent on RAF kinase pathway activation, however it is unknown whether this leads to the preferential binding of other signalling pathways such as PI3K and RalGDS.

Authors predicted that the G13D and G12C mutants would be moderate activators of RAF; whilst both mutants have a high affinity to RAF, both retain intrinsic levels of GTP hydrolysis that would attenuate prolonged effector interactions. Notably, unlike the other mutants, the KRAS G13D mutant displayed rapid nucleotide exchange kinetics (Hunter *et al.*, 2015). The rate of SOS independent exchange of GDP to GTP was one order of magnitude faster than KRAS wild type indicating that this mutant becomes spontaneously active rather than relying on GEF mediated regulation. Moreover, it has been reported that the fast-cycling K13D mutant may be more vulnerable to direct inhibition. Kevan Shokat and colleagues published a pioneering study showing that the KRAS G12C mutant can be directly targeted by covalent inhibition via the cysteine residue that locks it in its inactive GDP-bound state (Ostrem *et al.*, 2013). This was the first indication that RAS can be directly targeted (see section 1.4.1). It has been noted that rapid nucleotide cycling of mutant G13D may make the active site more assessable to a small molecule inhibitor (Hunter *et al.*, 2015).

There is independent evidence that supports the aforementioned classification scheme of KRAS mutations. Carla Mattos and colleagues also reported that the Q61L mutant more potently activates RAF compared to the G12V mutant due to differences in intrinsic GTP hydrolysis rates (Buhrman *et al.*, 2011). Cespedes et al. revealed that the G12D mutant preferentially associates with

PI3K, rather than RAF, thus supporting evidence that the G12D mutant is a poor activator of RAF (Céspedes *et al.*, 2006). Furthermore, authors also showed that the G12V mutant, which was classed as a moderate RAF activator, binds to both RAF and PI3K. However, it is important to note, the role of GEF stimulated nucleotide exchange remains unclear and the affinity of each mutant to other effector pathways needs to be elucidated in order to extend our understanding of how differences in the biochemical properties of RAS mutants result in distinct biological readouts.

Indeed, there is evidence supporting the notion that each activating RAS mutation elicits a distinct network response. Several studies have shown that KRAS codon 12 and 13 mutants harbour unique downstream responses that result in differential phenotypic outputs (Guerrero *et al.*, 2000; Vizan *et al.*, 2005; Hammond *et al.*, 2015). Furthermore, these differential responses can inform patient outcome and treatment responses in the clinic, further emphasizing that mutation specific signalling is biologically relevant (De Roock *et al.*, 2010). Patient data taken from the TCGA (The Cancer Genome Atlas) programme also suggests that mutation specific biology is relevant (Mo, Coulson and Prior, 2018). Each isoform is preferentially mutated at different codon hotspots, with KRAS predominantly mutated at codon 12, NRAS at codon 61 and HRAS at codon 12 and 61 (Figure 1.4) (Prior, Lewis and Mattos, 2012). Furthermore, the frequency of an amino acid missense substitution in a given RAS isoform is dependent on the cancer cell type. For example, in PDAC the most common mutation is KRAS G12D, whereas in NSCLC, KRAS G12C mutations are the most frequently seen (Hobbs, Der and Rossman, 2016).

Why RAS isoforms differentially and preferentially couple to specific cancers, codons and amino acid substitutions remains unclear. Whilst some studies suggest isoform specific mutagen exposure in different tissues may contribute to differences in cancer frequencies (Riely *et al.*, 2008), there is increasing amounts of evidence indicating that mutation specific oncogenicity is responsible (Mo, Coulson and Prior, 2018). For example, melanomas are predominantly associated with NRAS Q61 mutations and a study revealed that

NRAS Q61R efficiently promoted melanoma in mice, whilst NRAS K12D did not (Burd *et al.*, 2014). Moreover, Winters et al. used AAV/Cas-9 mediated gene editing to introduce 12 different KRAS mutations into mice (Winters *et al.*, 2017). Authors identified significant differences in the oncogenicity of each KRAS variant in each tissue type, in concordance with the frequencies observed in human cancers.

Finally, a recent study by Kevin Haigis and colleagues brings together several aspects of RAS isoform and mutation specific biology that help us to understand why RAS mutations aren't created equal (Poulin *et al.*, 2019; Hobbs and Der, 2019). The group used a multifaceted approach to profile the biological differences between two KRAS mutants, KRAS G12D and A146T. Whilst K12D mutations are commonly found in a variety of human cancers, A146T mutations are nearly exclusive to colorectal cancer. The aim of the study was to understand what is driving RAS mutational selection in specific tissues. Authors concluded that oncogenic potencies are the major contributing factor to the RAS mutational spectrums seen in different human cancers. Each mutant has distinct biochemical properties; KRAS G12D impairs GTP hydrolysis, whilst nucleotide exchange activities remain similar to wild type. Whereas the A126T mutant retained GTP hydrolysis activity but showed enhanced nucleotide exchange kinetics. Authors demonstrated the contrasting mechanisms of biochemical activation, that are likely to result in differences in the steady state level of KRAS-GTP, translate into distinct signalling properties. Furthermore, the authors showed that differential downstream signalling responses result in mutation specific phenotypic outputs. Moreover, the ability of each mutant to disrupt homeostasis in colorectal vs. pancreatic tumours was dependent on the intensity of downstream (MAPK) signalling. Thus, this study provides the first indication that variations in signalling downstream of different RAS mutations may drive the RAS mutational pattern seen in human cancers.

1.4. RAS targeting

1.4.1. Efforts to target RAS directly

Until recently, there has been limited success in targeting RAS. Early efforts to target RAS were confounded by the fact that RAS has picomolar affinity to GTP, together with a relatively flat surface that lacks a deep binding pocket for the binding of a small molecule inhibitor (Cox and Der, 2010). However, recent studies have emerged that have reinvigorated interest in RAS targeting and challenged the widely held perception that RAS is 'undruggable' (Stalnecker and Der, 2020).

Kevan Shokat and colleagues have led pioneering work in the development of direct RAS inhibitors (Ostrem *et al.*, 2013). Importantly, the inhibitors are expected to overcome toxicity concerns associated with the pan-inhibition of all RAS isoforms; KRAS is essential in mouse development, therefore there are concerns that targeting both wild-type and mutant proteins wouldn't be well tolerated (Koera *et al.*, 1997). The group developed a covalent inhibitor that specifically targets the glycine to cysteine mutation in KRAS at position 12 (KRAS G12C), a mutation often associated with smoking (Ostrem *et al.*, 2013) (Stalnecker and Der, 2020). The reactive cysteine residue in the active site of the protein can be covalently targeted by a small molecule inhibitor. As compounds rely on the reactive cysteine for binding, there is no effect on wild-type proteins (Moore *et al.*, 2020).

Crystallographic studies revealed a novel allosteric binding pocket beneath the switch II region of RAS-GDP (Ostrem *et al.*, 2013). The Shokat group used a tethering based approach to identify small molecule fragments that bound to the region, now termed the switch II pocket. The compounds irreversibly bind to the pocket and lock the K12C mutant in the GDP-bound state, thus leading to an accumulation of inactive protein. This in turn, attenuates effector engagement and downstream oncogenic signalling (Stalnecker and Der, 2020).

Most RAS mutations are GAP insensitive and have diminished intrinsic GTPase activity (Scheffzek *et al.*, 1997)(section 1.3.2). In contrast, it was reported that the G12C mutant has similar levels of intrinsic GTP hydrolysis to wild-type proteins (Hunter *et al.*, 2015). As a result, the mutant more frequently occupies the inactive GDP-bound state compared to other mutants, meaning the switch II pocket can be more readily accessed. This aspect, along with the cysteine reactive residue creates a unique therapeutic vulnerability to inhibition (Stalnecker and Der, 2020).

Several companies are currently developing KRAS G12C inhibitors, some of which have now entered phase 1/2 clinical trials (Stalnecker and Der, 2020). Initial observations have been promising, more so in NSCLC than CRC (Moore *et al.*, 2020). The first G12C molecule to enter clinical trials was AMG510; out of 13 NSCLC patients, 7 had partial response and 6 had stable disease. Results in CRC were less remarkable as only 1 out of 12 has a partial response (Moore *et al.*, 2020).

Although several more potent inhibitors are in the pipeline, it seems inevitable that acquired resistance to KRAS G12C inhibitors will arise. Considering that the compounds only bind to GDP-bound RAS, mechanisms of resistance are likely to include activation or mutation of proteins that either, promote the exchange of GDP to GTP, or diminish GTP hydrolysis (Moore *et al.*, 2020). Fortunately, it has been shown that AMG510 has synergistic growth inhibitory effects when combined with other inhibitors of the MAPK pathway, thus compensatory mechanisms may potentially be overcome by combinational therapies (Canon *et al.*, 2019).

KRAS G12C mutations only account for 12% of all KRAS mutations and are most commonly found in smoking associated NSCLC (Stalnecker and Der, 2020). Going forward, it will be important to find new strategies to target other more common RAS mutations (G12D and G12V) that lack the reactive cysteine substitution. Although, all RAS proteins possess the switch II binding pocket, it remains unclear whether targeting this region will be successful for other mutants that frequent the active GTP-bound state (Moore *et al.*, 2020).

A recent tethering screen has identified a ligand that can bind RAS in its GTP-bound state via a novel switch II groove adjacent to the switch II pocket (Gentile *et al.*, 2017). This discovery has prompted hope within the field that if RAS mutants can be targeted in either the active or inactive conformation, other individual RAS mutations may be 'druggable' (Moore *et al.*, 2020). Understanding the differences in the biochemical properties of each mutant will be critical for the evolution and development of more direct RAS inhibitors.

1.4.2. Targeting RAS localisation

Early efforts to target RAS focused on disrupting RAS processing to the membrane where it becomes activated (Cox and Der, 2010) (see section 1.2.4). As mentioned previously, the first step in RAS processing is catalysed by Farnesyl Transferase (Hancock *et al.*, 1991). Farnesyl Transferase Inhibitors (FTIs) were developed to prevent the prenylation of the cysteine residue of the CAAX motif, ultimately preventing membrane association and downstream RAS signalling (Moore *et al.*, 2020). These inhibitors were initially proved unsuccessful (Macdonald *et al.*, 2005). It was revealed that KRAS and NRAS proteins are resistant to FTIs as they can be alternatively prenylated by geranylgeranyl transferase (Whyte *et al.*, 1997; Fiordalisi *et al.*, 2003). However, recent work has indicated that this approach may be successful for treating HRAS mutant cancers (Moore *et al.*, 2020). HRAS proteins are exclusively prenylated by farnesyl transferase and therefore inhibition of this first critical modification may be successful in this subset of patient (Whyte *et al.*, 1997). Indeed, the FTI, Tipifarnib has showed promising results in a recent phase II clinical trial of HRAS mutant HNSCC and thyroid cancer (Moore *et al.*, 2020).

Other efforts to target RAS processing have focused on inhibiting downstream enzymes such as RCE1 and ICMT that control post-prenylation CAAX processing (Cox and Der, 2010). Efforts to target RCE1 have been confounded by toxicity issues, whilst ICMT inhibitors display limited potency *in vivo* (Cox, Der and Philips, 2015). Nevertheless, both RCE1 and ICMT were identified in a screen for essential genes in RAS driven Acute Myeloid leukaemia (AML)

(Wang *et al.*, 2017). Furthermore, a recent study has been published that identified a potent ICMT inhibitor that targets all four RAS isoforms in RAS driven AML and may lead the way to the development of more efficacious inhibitors (Marín-Ramos *et al.*, 2019).

1.4.3. Targeting the RAS pathway

Before the recent discovery of KRAS G12C inhibitors, anti-RAS drug discovery mainly focused on blocking RAS signalling by inhibiting the activity of upstream or downstream kinases (Cox and Der, 2010).

Targeting upstream of RAS has proven difficult. Cancers expressing mutant RAS are generally resistant to therapies targeting upstream RTKs (Moore *et al.*, 2020). Whilst, the use of monoclonal antibodies targeting EGFR have proved successful for the treatment of metastatic colorectal cancer (mCRC), they are limited to patients with wild type RAS alleles (Stalnecker and Der, 2020). Two examples are cetuximab and panitumumab that significantly improve overall and progression free survival in patients with RAS wild type cancer, but not patients with KRAS mutations. (Amado *et al.*, 2008; Karapetis *et al.*, 2008). As a result, the FDA recommend that patients with RAS mutations should not be candidates for treatment with anti-EGFR monoclonal antibodies (Stalnecker and Der, 2020). However, retrospective analysis of the mCRC clinical trials revealed that patients with KRAS G13D mutations may benefit from treatment with cetuximab (De Roock *et al.*, 2010). Again, this exemplifies the fact that RAS mutations should not be treated as one homologous group.

EGFR tyrosine kinase inhibitors (TKIs) have also proved ineffective in RAS mutant cancers. Erlotinib and gefitinib are used for the treatment of EGFR mutant NSCLC patients, yet patients with KRAS mutations are resistant to treatment (Mao *et al.*, 2010). It was revealed that mechanisms of resistance to EGFR inhibition converge on MEK activation, and therefore it has been suggested that targeting EGFR and MEK in combination may overcome any compensatory mechanisms (Troiani *et al.*, 2014). Indeed, there has been promising observations in lung and colorectal cancers; suppression of ERBB3

by afatinib sensitizes KRAS mutant NSCLC and CRC cells to MEK inhibition (Sun *et al.*, 2014). Furthermore, similar observations were made in NSCLC mouse models, where the combination of afatinib with trametinib improved survival of mice with KRAS G12D mutant tumours (Kruspig *et al.*, 2018).

Another promising combinational approach is the use of EGFR inhibitors with KRAS G12C inhibitors (Moore *et al.*, 2020). As previously discussed, KRAS G12C inhibitors only bind to RAS in the inactive GDP-bound state (Ostrem *et al.*, 2013). It has been reported that EGFR inhibition prevents GEF stimulated nucleotide exchange, which in turn, reduces the pool of GTP-bound RAS. Thus improving the efficacy of G12C inhibitors (Moore *et al.*, 2020).

There has been some success targeting downstream RAS signalling however, the development of inhibitors for downstream nodes has been met with similar problems concerning mechanisms of resistance (Stalnecker and Der, 2020). The majority of signalling nodes downstream of RAS are kinases (Wilson *et al.*, 2018). Although, kinases are readily druggable, the success of monotherapies for RAS mutant cancers is limited due to inhibitor driven induction of compensatory mechanisms (Moore *et al.*, 2020).

The development of resistance following therapy can occur through adaptive or acquired mechanisms of resistance (Wilson *et al.*, 2018). Adaptive resistance involves the rewiring of signalling pathways in response to inhibition, that ultimately results in the reactivation of the pathway. Whereas, acquired resistance develops over time and typically involves the mutation or gene amplification of a node within the pathway that confers a selective advantage over the effects of kinase inhibition.

For example, in RAS mutant cells, resistance to the BRAF inhibitor, vemurafenib, emerges via an adaptive mechanism of resistance involving the paradoxical activation of wild-type RAF (Hatzivassiliou *et al.*, 2010). Unexpectedly, the inhibitor promotes the formation and transactivation of RAF dimers, which in turn results in elevated downstream MEK and ERK signalling (Poulikakos *et al.*, 2010). Vemurafenib is approved for the treatment of BRAF

V600E mutant melanoma where RAF signals as a monomer; however, in some cases resistance can be acquired over time (Wilson *et al.*, 2018). Following vemurafenib treatment, an ERK dependent negative feedback loop is inactivated and results in the restoration of upstream RTK signalling (Lito *et al.*, 2012). Similar mechanisms of resistance to MEK inhibition have been described through which loss of activated ERK induces the reactivation of upstream RTKs or CRAF (Duncan *et al.*, 2012a) (Lito *et al.*, 2014).

Since monotherapies targeting RAF, MEK or ERK are considered clinically ineffective in RAS mutant cancers, the efficacy of combinational therapies is currently being evaluated in the clinic (Moore *et al.*, 2020). Indeed, clinical trials are currently in progress that aim to investigate the effect of combining RAF and MEK inhibitors, something which showed promising results in preclinical studies (Yen *et al.*, 2018).

In summary, whilst the recent discovery of KRAS G12C inhibitors have renewed optimism that RAS may be 'druggable', finding direct inhibitors that target the other common RAS mutants will remain challenging. What's more, even supposing the development of allele-specific inhibitors is achieved, mechanisms of resistance are likely to arise. Finding combinational strategies that negate emerging mechanisms of resistance, whilst improving the efficacy of new or existing treatments, will be critical to the success of targeting RAS. Firstly, it is imperative that we understand the requirements of specific RAS codon mutations and the context dependency of downstream kinase signalling. This may assist in the development of other allele specific RAS inhibitors, or more likely, inform effective drug combinations that will achieve maximal pathway suppression in a variety of RAS mutant cancers. Moreover, understanding what kinome rewiring occurs in response to RAS pathway inhibition will be crucial to achieving sustained suppression of RAS signalling.

1.5. The Human Kinome

1.5.1. Kinome overview

Protein kinases mediate protein function by catalysing the transfer of the ϒ-phosphate of ATP onto protein substrates, a process termed phosphorylation (Manning *et al.*, 2002). Phosphorylation occurs on the alcoholic amino acid side chains, Serine (S), Threonine (T) or Tyrosine (Y) of protein substrates and underpins much of biological signalling in eukaryotic cells (Wilson *et al.*, 2018). Recent evidence suggests that over 90% of proteins expressed in human cells are phosphorylated (Sharma *et al.*, 2014). Other regulators of phosphorylation include protein phosphatases that catalyse the removal of phosphate groups from proteins (Chen, Dixon and Manning, 2017). Together, protein kinases and phosphatases mediate most of cellular signalling in eukaryotic cells so it's not surprising that they have been described as the master regulators of signalling (Wilson *et al.*, 2018). Moreover, kinase dysregulation is commonly associated human disease and for this reason, they have been the subject of intensive pharmacological inhibition. (Fabbro, 2015)

The human kinome consists of 535 kinases (Wilson *et al.*, 2018). Most kinases belong to a superfamily that contain a eukaryotic protein kinase (ePK) catalytic domain. These 479 kinases can be subdivided into seven kinase families based on their primary structure. The ePK families include: AGC, CAMK, CK1, CMGC, STE, TK and TKL (Figure 1.5). A subgroup of ePK kinases that don't fall into these categories are described as the 'other' family. It is important to note that more recently, the AGC family has been reclassified and now belongs within the 'other' subgroup. The 56 remaining non ePK kinases are classed as 'atypical' kinases. This family possess an atypical kinase domain and display little sequence homology to the main superfamily (Wilson *et al.*, 2018).

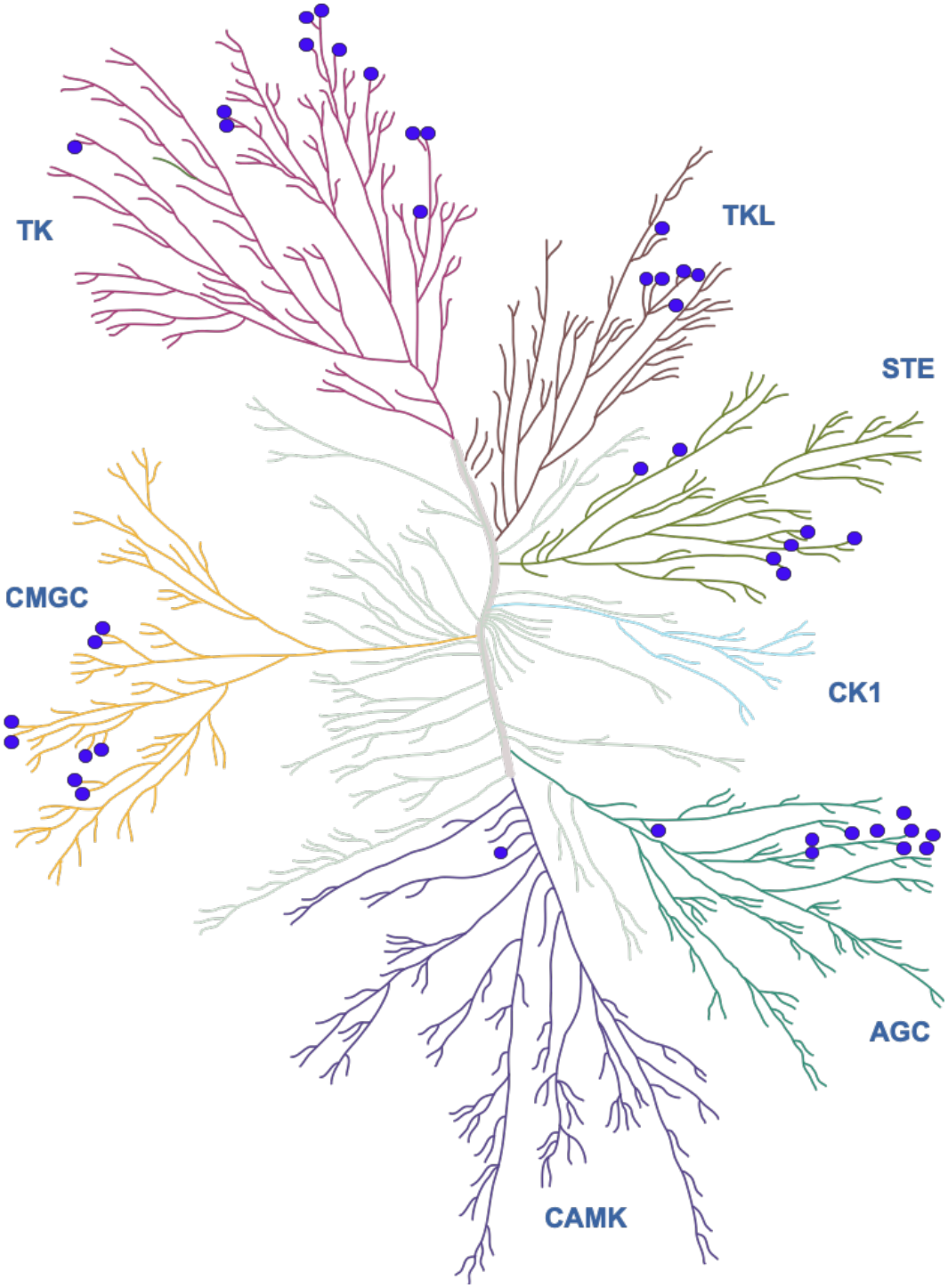

Figure 1.5. The human kinome

Kinases are visualized on the kinase dendrogram previously defined by Manning et al (Manning et al., 2002). The human kinome consists of 535 kinases. A total of 479 ePKs are displayed on the kinase dendrogram and can be further subclassified on the basis of primary sequence into seven major ePK families: TK, TKL, STE, CK1, AGC, CAMK, and CMGC. The remaining 56 atypical non-ePK kinases share little sequence homology with the major superfamily and are not included on the classical kinase dendrogram. Kinase nodes within the immediate RAS signalling network are highlighted in blue.

1.5.2. Kinase regulation

Protein kinases consist of two lobes: a small N terminal lobe comprised of a five-stranded β-sheet with an α-helix called the C-helix, and a large C-terminal lobe comprising six α-helices (Modi and Dunbrack, 2019). Generally, the N-lobe co-ordinates ATP binding, whilst the C-lobe binds protein substrates and catalyses phosphorylation (Wilson *et al.*, 2018). The two regions are connected by a flexible hinge region that forms a cleft for ATP binding (Kornev *et al.*, 2006). Kinases oscillate between an inactive conformation and an active catalytically competent conformation (Endicott, Noble and Johnson, 2012).

Although kinases are mainly regulated by phosphorylation, they can also be regulated by several other post-translational modifications, autoinhibition or binding to a regulatory partner (Johnson, Noble and Owen, 1996). Kinases adopt one or more of these mechanisms to promote or stabilize an active conformation (Wilson *et al.*, 2018). Several key interactions between conserved residues, ATP and the protein substrate are critical for kinase activation. In the N-lobe, one of the most important features is the conserved Lys-Glu pair (K72, E91). In the active conformation state, the C-helix is orientated in towards the active site and positions a glutamic acid residue in the helix so that it is able to form a salt bridge with a lysine residue in the β-sheet strand.

This interaction allows for hydrogen bonds to form between the lysine and the α and β phosphates of ATP, anchoring ATP in place (Kornev *et al.*, 2006). Another key feature in this region, is the glycine rich loop. More specifically, the three conserved glycine residues in the tip of the loop position the phosphates and poise ϒ-phosphate for transfer (Aimes, Hemmer and Taylor, 2000).

The C-lobe includes an activation loop. The activation segment consists of 20-35 residues beginning with the DFG motif (Asp–Phe–Gly). In the active conformation, the conserved aspartate residue in the DFG motif binds a magnesium ion that interacts with the β-phosphate of ATP (Modi and

Dunbrack, 2019). The phenylalanine residue of the DFG motif forms contacts with the HRD motif (usually His-Arg-Asp) of the catalytic loop facilitating the transfer of the ϒ-phosphate of ATP to the substrate (Fabbro, Cowan-Jacob and Moebitz, 2015). Importantly, the phenylalanine residue also makes contact with the C-helix and orientates the helix so that the Glu residue is in the correct position to form the salt bridge interaction that is essential for the ATP binding and therefore kinase activity (Endicott, Noble and Johnson, 2012).

It is important to note, that 52 non-enzymatic kinase members of the human kinome have been identified (Wilson *et al.*, 2018). These kinases belong to the pseudokinase group which represent approximately 10% of the human kinome and are distributed across all kinase families (Wilson *et al.*, 2018). Although pseudokinases lack the catalytic machinery required for phosphorylation, they are able to control the activity of proteins via alternative mechanisms (Eyers and Murphy, 2013). Pseudokinases can control enzymatic activity by acting as allosteric modulators, substrate competitors, scaffolding proteins or spatial anchors (Reiterer, Eyers and Farhan, 2014). Prominent examples include KSR1 and KSR2 that act as scaffolds to coordinate the assembly of RAF-MEK-ERK signalling pathway (Nguyen *et al.*, 2002). Thus, pseudokinases are still biologically relevant in human disease. In fact, mutation or overexpression of this group of kinases has been implicated in many human diseases including cancer, emphasizing that this non enzymatic group should not be overlooked (Bailey *et al.*, 2015).

1.5.3. The RAS regulated kinome

Deep proteomic analysis of 23 human cell lines revealed that cells typically express between 300-400 kinases (Wilson *et al.*, 2018). Yet, most kinase research has focused on a select number of kinases. The principle kinase nodes found upstream and downstream of RAS are highlighted on the kinase dendrogram in figure 1.5. These nodes alone, account for almost 35% of the approximately 120,000 kinome research publications (Wilson *et al.*, 2018). Therefore, unsurprisingly the nodes within the immediate RAS network are particularly well served by the 75 kinase chemical inhibitors currently approved

in the clinic (MRC) https://www.ppu.mrc.ac.uk/list-clinically-approved-kinase-inhibitors. In contrast, over 50% of kinome members account for less than 5% of kinome research publications and consequently, approximately 300 kinases still do not have an inhibitor that has ever reached clinical evaluation (Wilson *et al.*, 2018). Moreover, there is no structural information for over 200 of these kinases and therefore drug design would be challenging. This highlights an area of unmet need. The development of inhibitors will be vital to our understanding of kinase function, however counterintuitively, a lack of knowledge of kinase biology stifles any drug discovery efforts (Wilson *et al.*, 2018).

It is clear that global approaches to study the kinome are required to increase our understanding of the understudied members of the kinome. In a typical phosphoproteomic analysis, >10,000 phospho-sites can routinely be identified from low milligram quantities of starting material (Wilson *et al.*, 2018). The most commonly used enrichment strategies use metal oxides such as TiO2, which are highly specific for most phosphopeptides (Leitner, 2016). However, this method provides poor enrichment of the phospho-tyrosine (pTyr) pool and therefore, anti-pTyr antibody-based enrichment is typically employed to evaluate this less abundant modification (Leitner, 2016). Effective sampling of this subset is particularly important given the dominant role of tyrosine kinases in controlling early events in signalling that are frequently dysregulated in diseases such as cancer (Wilson *et al.*, 2018). However, fewer than 2% (5330 phospho-sites) have known regulatory consequences for their target proteins thus, illustrating the scale of the challenge for generating broad mechanistic insight from phospho-proteomic datasets (Wilson *et al.*, 2018).

The integration of global kinase profiling approaches with transcriptomic datasets will be essential for the systems-level understanding of kinome networks and their contributions in diseases such as cancer. However, whilst kinase profiling is used to determine drug specificity and sensitivity in vitro, profiling dynamic kinome adaptations in a cellular context remains challenging (Wilson *et al.*, 2018).

A method (MIB/MS) has recently been developed that claims to allow the simultaneous measurement of the relative expression and activities of hundreds of kinases within cells (Duncan *et al.*, 2012a). The method utilises broad specificity kinase inhibitors which are immobilised onto Sepharose beads to make up the Multiplexed Inhibitor Bead (MIB) slurry. Type I kinase inhibitors, which are thought to only bind to the ATP binding pocket of kinases in their active DFG-in conformation, are used to make the MIBs (Roskoski, 2016). The rationale is that binding of kinases to the column reflects kinase activity; increased binding of the kinase to the column indicates increased kinase activity. Quantitative mass spectrometry is used to identify and quantify the kinases in each sample. Incorporating a quantitative proteomic labelling technique, such as SILAC makes it possible to simultaneously measure and compare global kinome adaptions between multiple samples (Ong and Mann, 2005).

Considering that the RAS signalling network is enriched in kinases, I propose to use the method to profile RAS isoform and mutation specific signalling. Most of our understanding of RAS isoform biology has been based on studies with experimental systems using ectopic expression of activated RAS, rather than mutation of the endogenous RAS gene (Hood *et al.*, 2019). Whilst ectopic expression studies have reported that each isoform is preferentially coupled to a key RAS effector pathway (Yan *et al.*, 1998; Voice *et al.*, 1999), more recent endogenous expression studies revealed that there is significant heterogeneity for effector requirements of each RAS isoform (Tuveson *et al.*, 2004; Omerovic *et al.*, 2008; Hammond *et al.*, 2015; Hood *et al.*, 2019)(see section 1.3.1). Thus, there is now a general consensus that studying endogenous RAS signalling is more desirable. Moreover, there is an appreciation that RAS signalling is more context dependent than originally thought, and therefore profiling global kinome responses may reveal ‘dark’ kinases that are essential for RAS signalling.

For this reason, we have decided to use an isogenic cell system that has been engineered, using rAAV technology, to harbour different activating RAS mutations in the endogenous loci. We will use MIB/MS to profile kinome-wide

responses and thus characterise the context dependence of endogenous isoform-specific Ras-signalling responses. We propose that each RAS mutant activates distinct kinase driven tumourigenic pathways. If such patterns could be identified, it could provide a rationale for selecting novel kinase targets for drug discovery, inform treatment selection of existing therapies, or inform new combinational therapies to overcome mechanisms of resistance.

1.6. Aims and objectives

Aim

To understand the differential network responses downstream of common RAS codon mutations.

Objective

To use unbiased and global approaches to profile the kinome in RAS mutant cells.

Chapter 2 : Materials and methods

2.1. Cell biology

2.1.1. Cell culture

Unless otherwise stated, all cell culture reagents and Foetal bovine serum (FBS) were purchased from Gibco (Invitrogen, Paisley, UK). For all experiments, FBS was dialysed and heat-inactivated at 55^{o}C prior to use. All cell culture plasticware was purchased from Corning (NY, USA).

2.1.1.1. Cell lines

SW48

The SW48 cell line is an epithelial-like colorectal adenocarcinoma cell line established in 1973 from an 82-year-old female Caucasian patient (Leibovitz *et al.*, 1976). A panel of isogenic SW48 cells were obtained from Horizon Discovery (Cambridge, UK). The SW48 cells have been engineered, using rAAV technology, to harbour different activating RAS mutations in the endogenous loci (Mageean *et al.*, 2015). The panel have heterozygous knock-in of different activating RAS mutations (table 2.1); these are all derived from the same matched parental cell line that are homozygous wild-type RAS expressing cells. All Horizon's cell Lines are authenticated and validated by PCR amplification and Sanger Sequencing to confirm the mutation at the genomic level.

SW48 Parental and KRAS G12D cells containing doxycycline inducible shRNA targeting KRAS were used for knockdown studies (section 2.1.3.1).

Table 2.1: *Panel of isogenic SW48 cell lines*

Cell line	**Clone no.**	**Shorthand cell line ID**	**Horizon Catalogue no.**
Parental RAS^{wt}	MK2/238	PAR	HD PAR-006
KRAS G12D	C22	K12D	HD 103-011
KRAS G13D	C3D3	K13D	HD 103-002
KRAS G12V	c16	K12V	HD 103-007
HRAS G12V	878	H12V	HD 103-034
NRAS G12V	G9-1	N12V	*

*N. B: The NRAS mutant cell lines were made in-house by Simon Oliver.

MDA-MB-231

The MDA-MB-231 cell line is an epithelial, human breast adenocarcinoma cell line established in 1978 from a 51-year-old female Caucasian patient (Cailleau, Olivé and Cruciger, 1978). These cells are a metastatic triple negative breast cancer cell line derived from plural effusion and harbour a KRAS G13D mutation (Eckert *et al.*, 2004). The cells were purchased from the American Type Culture Collection (ATCC, Middlesex, UK) (cat no. ATCC® CRM-HTB-26™). All ATCC's cell lines are authenticated and validated by Short Tandem Repeat (STR) Profiling, Karyotyping and Cytochrome C Oxidase I (COI) Assay Testing.

2.1.1.2. Routine cell culture

Cells were cultured in 5% CO_2 at 37°C and typically passaged at 70-80% confluency, every 2-3 days. For maintenance, growth medium was aspirated, cells were washed with pre-warmed Phosphate-buffered saline (PBS) and then dissociated from flasks or dishes with 0.05% trypsin/EDTA (Gibco). Cells were resuspended in fresh medium and reseeded into new flasks or dishes at the ratios described in table 2.2. Cells were grown in culture for no longer than

30 passages and were routinely tested for mycoplasma using the EZ-PCR Mycoplasma Testing Kit (Geneflow, UK).

Table 2.2: *Cell culture medium and split ratio used for each cell line*

Cell line	Medium	Supplementation	Split ratio
SW48	McCoys 5A (modified) medium, with GlutaMAX™ supplement	10% (v/v) foetal bovine serum	1:3-1:4
MDA-MB-231	DMEM, high glucose, with GlutaMAX™ supplement, pyruvate	10% (v/v) foetal bovine serum	1:4-1:5

2.1.1.3. Cell line storage

Cells grown in a T175cm^2 flask were cultured as above, resuspended into fresh medium and pelleted by centrifugation (200g, 5mins). Pelleted cells were resuspended into 9mL of freezing medium (50% FBS, 45% serum-free medium, 5% DMSO). The cell suspension was aliquoted into cryovials (1mL/vial) and frozen to -80^{o}C in a 'Mr Frosty' freezing box. The cryovials were frozen slowly to -80^{o}C at a rate of 1^{o}C/min and subsequently transferred to liquid nitrogen for long term storage.

As required, cells were thawed rapidly at 37^{o}C and resuspended into a T25cm^2 flask containing pre-warmed medium. After 16-24h, the medium was replaced to remove any residual DMSO.

2.1.2. Cell treatments

2.1.2.1. Cell stimulation and inhibition

Growth factor stock solutions were prepared in filtered PBS and stored at -80^{O}C. Pervanadate was prepared from an equimolar solution containing

sodium orthovanadate ($NaVO_4$) and hydrogen peroxide (H_2O_2) (Sigma-Aldrich, Poole, UK).

Stock solutions of FBS, EGF, HGF or pervanadate were diluted in cell culture medium without FBS supplementation to the achieve the final concentrations listed in table 2.3. Cells were serum starved for 16h before each treatment was added. Treated cells were incubated in 5% CO_2 at 37°C for the length of time indicated in table 2.3 and subsequently harvested for immunoblotting or Mass spectrometry (see sections 2.2.1 and 2.4.2 for cell lysis).

Table 2.3: *Cell treatments*

Treatment	Type	Target	Conc.	Duration	Supplier
Foetal bovine serum (FBS)	Stimulation		20%(v/v)	5 minutes	Invitrogen, (Paisley, UK)
Epidermal growth factor (EGF)	Stimulation	EGFR	20 ng/mL	5 minutes	Protech, (London, UK)
Hepatocyte growth factor (HGF)	Stimulation	c-MET	50 ng/μl	0, 5. 10, 20 minutes	Protech, (London, UK)
Pervanadate ($H_6Na_3O_{10}V$)	Inhibitory	pTyr	100 μM	15 minutes	Sigma-Aldrich, (Poole, UK)

2.1.2.2. Drug treatments

Drug stocks were prepared in DMSO (Sigma-Aldrich, Pool, UK) and stored in 1 mL aliquots at -20°C. Prior to use, drug stocks were thawed and diluted in cell culture medium to yield the final drug concentration (5 μM). In every case, vehicle-only (DMSO) containing medium was used as a control. Cells were

serum starved for 16h and subsequently treated with Selumetinib for 4hr/ 24hrs in 5% CO_2 at 37°C.

Table 2.4: *Target and source of pharmacological inhibitor used*

Inhibitor	Target	Conc.	Duration	Supplier
Selumetinib	MEK1/2	5 μM	4hr or 24hr	Astra-Zeneca (Cambridge, UK)

2.1.3. Transfections

2.1.3.1. shRNA interference

Table 2.5: *shRNA sequences for KRAS knockdown*

Cell line	shRNA	Shorthand cell line ID.	shRNA sequence
KRAS G12D	#2	K12D sh2	Top strand: CCGGCGATACAGCTAATTCA GAATCCTCGAGGATTCTGAAT TAGCTGTATCGTTTTT, Bottom strand: AATTAAAAACGATACAGCTAA TTCAGAATCCTCGAGGATTCT GAATTAGCTGTATCG.
KRAS G12D	#3	K12D sh3	Top strand: CCGGCAGGCTCAGGACTTAG CAAGACCGAGTCTTGCTAAG TCCTGAGCCTGTTTTT, Bottom strand: AATTAAAAACAGGCTCAGGA CTTAGCAAGACTCGAGTCTT GCTAAGTCCTGAGCCTG.

SW48 Parental and KRAS G12D cell lines containing doxycycline inducible shRNA targeting KRAS were provided by Horizon Discovery (Cambridge, UK), details of which can be found in table 2.5.

Cells were maintained in medium containing 10% dialysed, tetracycline-free FBS. For knockdown of KRAS, cells were grown media containing 100 ng/ul doxycycline for 1 week. After one week, cells were harvested for immunoblotting, MIB/MS and NanoString studies (see sections 2.2, 2,3, 2,4).

2.1.3.2. DNA transfection

For transient DNA transfections, cells were seeded in 6cm dishes one day prior to transfection. The following day, two solutions were prepared for DNA transfection, the volumes for each are listed in table 2.6. Solution A contained 1μg transfected plasmid DNA encoding the different RAS G12V isoforms, n-terminally tagged with eGFP, diluted in optiMEM, to a total volume of 500μl. Solution B contained Lipofectamine 2000, diluted in optiMEM to a total volume of 500μl. Both mixtures were left at RT for 5 minutes before combining in a 1:1 ratio. The DNA-lipid complex was incubated for a further 20 minutes at room temperature (RT) before being added dropwise to the cells. Fresh medium was added to bring the total volume to 5mL.

Table 2.6: *Reaction mixes for transient DNA transfection*

Sol. A	**Sol. B**
1μg DNA	15ul Lipofectamine 2000
optiMEM	optiMEM
Mix (1:1)	

After 24hrs transfection efficiency was evaluated by visualising GFP expressing cells under a NIKON TiE microscope. A separate dish of cells was grown in parallel and harvested for analysis by immunoblotting.

2.2. Protein biochemistry

2.2.1. Preparation of whole cell lysates

For mass spectrometry, cells were lysed in MIB/MS buffer (section 2.4.2). Otherwise, cells were lysed in RIPA buffer supplemented with PhosSTOP phosphatase inhibitor tablets (Roche, Basel, Switzerland) and Mammalian Protease Inhibitors (MPI, Sigma Aldrich, Poole, UK).

Table 2.7: *Composition of RIPA Lysis buffer solution*

Solution	Contents
1x RIPA buffer	10mM Tris-Hcl pH7.5 150mM NaCl 1% (w/v) NP40 0.1% (w/v) SDS 1% sodium deoxycholate 1:250 mammalian protease buffers Phosphatase inhibitor cocktail tablets, 1 tablet/10mL

Cells grown in a 6cm or 10cm dish were placed on a bed of ice before cell lysis. Firstly, cells were washed twice with ice-cold PBS with the PBS being aspirated after each wash. Next, cells were placed on a rocker, on ice and incubated with 250μl of lysis buffer for ten minutes. The lysates were collected into a 1.5 mL microcentrifuge tube and then cleared of non-soluble material by centrifugation (14,000rpm, 10 minutes, 4^{o}C). The supernatant was collected into a 1.5mL Eppendorf tube for protein determination. Lysates were stored at -80 ^{o}C for long term storage.

2.2.2. Protein determination and sample preparation

Protein concentration was assessed using the Bio-Rad bicinchoninic acid (BCA) assay kit (Pierce, UK) using IgG to generate a standard curve. The standards and lysates were arranged in duplicate on a clear 96-well plate. For

protein determination, 10μl of diluted cell lysate was plated per well. 200μl of BCA reagent (50:1 reagent A:B) was added to all wells containing the standards and samples and plates were incubated for 30 minutes at 37^{o}C. A Glomax multi-detection system (Promega, WI, USA) was used to measure the colorimetric change observed after 30 minutes.

Following protein quantification, lysates were adjusted accordingly and combined with a 1x final concentration sample buffer (3% w/v SDS, 62.5mM Tris-HCl pH 6.8, 10 % glycerol, 3.2% β-mercaptoethanol stained with bromophenol blue). Samples were boiled for 5 minutes at 98 ^{o}C then left on ice to cool for 5 minutes before separation by SDS-PAGE. Samples were stored at -20 ^{o}C for long term storage.

2.2.3. SDS polyacrylamide electrophoresis (SDS-PAGE)

Samples were loaded on 4-12% pre-cast Bis-Tris gels (NuPage, Invitrogen, Paisley, UK) and separated by SDS-PAGE. Gels were run in tanks containing 1x MOPS or 1xMES running buffer (both NuPage, Invitrogen, Paisley, UK) depending on the molecular weight of the protein of interest. Separation typically took place at 100V for 15 minutes followed by 200V for 45 minutes. Samples were run alongside molecular weight markers: Rainbow Marker (GE healthcare, Amersham, UK) and Broad Range Marker (New England BioLabs, Herts, UK).

2.2.4. Western blotting

Following SDS-PAGE, separated proteins were transferred onto 0.45μM Protran nitrocellulose membrane (Geneflow, Lichfield, UK) using the GenieBlotter system (Idea Scientific, Minneapolis, USA). The transfer was performed at a constant current of 0.9A for one hour. After the transfer, the membrane was stained with Ponceau S (Sigma-Aldrich, Poole, UK) to visualise proteins and assess the quality of the protein transfer. Subsequently, membranes were destained using distilled water and cut into multiple sections when there was more than one protein of interest to probe per blot.

Membranes were incubated in a blocking buffer of either 5% milk/TBST (Marvel, Premier foods, UK) or 5% BSA/TBST (Bovine Serum Albumin, Sigma Aldrich, Poole, UK) for one hour at room temperature (see table 2.8). Primary antibodies were diluted in the same buffer used for the blocking step. See table 2.9 for concentrations and conditions. Membranes were incubated with primary antibody and placed on a gentle rocker at 4 ^{o}C overnight. The following day, the membranes were washed three times with TBST for 15 minutes in total. The secondary antibodies were made up in the same blocking buffer used for the primary antibody. See table 2.10 for concentrations and conditions. The membranes were incubated with secondary antibody in the dark, for one hour at RT. The membrane was washed again twice with TBST and once with TBS for a total of 15 minutes. Protein bands were visualised using the LI-COR Odyssey 2.1 infrared imaging system (LI-COR, Nebraska, USA). Images were analysed and quantified using the Odyssey ImageStudio Lite Software (LI-COR, Nebraska, USA).

Table 2.8: *Composition of western blotting solutions*

Solution	**Contents**
TBST	10mM Tris-HCl, pH 7.5 100mM NaCl 0.1% (v/v) Tween20
Transfer buffer	3.03g Tris base 14.4g Glycine 200ml Methanol 800ml dH20
Blocking buffer- 5% milk/TBST	10mM Tris-HCl, pH 7.5 100mM NaCl 0.1% (v/v) Tween20 5% (w/v) Marvel
Blocking buffer- 5% BSA/TBST	10mM Tris-HCl, pH 7.5 100mM NaCl 0.1% (v/v) Tween20 5% (w/v) BSA

Table 2.9: *Primary antibodies used for Western blotting*

Antibody	Species	Block/TBST	Dilution	Company	Cat. no.
AKT	Rabbit	Marvel	1:1000	Cell Signalling	9272
pAKT (S473)	Rabbit	Marvel	1:2000	Cell Signalling	4060
DCLK1 (short isoform)	Rabbit	Marvel	1:2000	Sigma	SAB4200186
EGFR	Goat	BSA	1:200	Santa Cruz	sc03-1005
pEGFR (pY1068)	Rabbit	BSA	1:1000	Cell Signalling	2234
ERK1/2	Rabbit	Marvel	1:1000	Cell Signalling	4695
pERK1/2 (pT202,Y204)	Rabbit	Marvel	1:2000	Cell Signalling	4370
KRAS	Mouse	Marvel	1:1000	Lifespan	3127
MEK	Rabbit	BSA	1:1000	Cell Signalling	9122
pMEK1/2 (S217,221)	Rabbit	BSA	1:1000	Cell Signalling	9154
MET	Mouse	BSA	1:1000	Cell Signalling	3127
pMET (T1234/1235)	Rabbit	BSA	1:1000	Cell Signalling	3129
MKK3	Rabbit	BSA	1:1000	Cell Signalling	8535
pMKK3 (S189/S207)	Rabbit	BSA	1:1000	Cell Signalling	12280
p21	Mouse	Marvel	1:200	Santa Cruz	sc-6246
p38	Rabbit	BSA	1:1000	Cell Signalling	8690
p-p38 (T180/Y182)	Rabbit	BSA	1:1000	Cell Signalling	4511
p53	Mouse	BSA	1:1000	Santa Cruz	sc-126
p-p53 (S15)	Mouse	BSA	1:1000	Cell Signalling	9286
p-p53 (S33)	Rabbit	BSA	1:1000	Cell Signalling	2526
p90 RSK2	Rabbit	BSA	1:1000	Cell Signalling	5528

p-p90 RSK2 (S227)	Rabbit	BSA	1:1000	Cell Signalling	3556
pan-RAS	Rabbit	Marvel	1:1000	Abcam	ab52939
RAC1	Mouse	Marvel	1:500	Upstate	05-389

Table 2.10: *Secondary antibodies used for Western blotting*

Antibody	**IRDye**	**Dilution (RT, 1h)**	**Company**	**Catalogue no.**
Donkey α Mouse	680LT	1:15000	Licor	926-68022
Donkey α Mouse	800CW			926-32212
Donkey α Rabbit	680LT			926-68023
Donkey α Rabbit	800CW			926-32213
Donkey α Goat	680LT			326-32224
Donkey α Goat	800CW			926-32214

2.3. NanoString

2.3.1. NanoString nCounter Human Kinase kit

N.B. All NanoString nCounter reagents and instruments were sourced from NanoString Technologies Inc., Seattle, USA.

The NanoString nCounter GX human kinase kit (NanoString) is a hybridisation-based profiling assay for detecting the expression of 522 kinase mRNAs in total RNA (Figure 2.1). The assay involves hybridising target sequences in the sample by complementary base pairing of two gene specific probes: the capture probe and the reporter probe. RNA is directly tagged with a capture probe and a reporter probe that are specific to the target of interest, creating a unique target-probe complex. Each reporter probe has a unique colour coded barcode made up from four possible colours placed in six possible configurations. After the hybridisation step, excess probes are removed on the nCounter prep station, leaving only purified target-probe complexes. These complexes are immobilised and aligned onto an imaging surface. The sample is scanned by the nCounter digital analyser (see section 2.3.5) where labelled barcodes are directly counted. After count normalisation with internal reference genes and controls, mRNA levels are quantified, and data is analysed using the nCounter advanced analysis software (see section 2.3.6).

2.3.2. Experimental set up

Figure 2.2 shows the experimental set up for each set of NanoString experiments (A and B). Three 6cm dishes of each cell line/ cell condition were grown in parallel; one dish was taken for mRNA extraction (section 2.3.3), one dish was lysed for western blotting analysis (section 2.2) and one was kept for the continuation of cell culture (section 2.1).

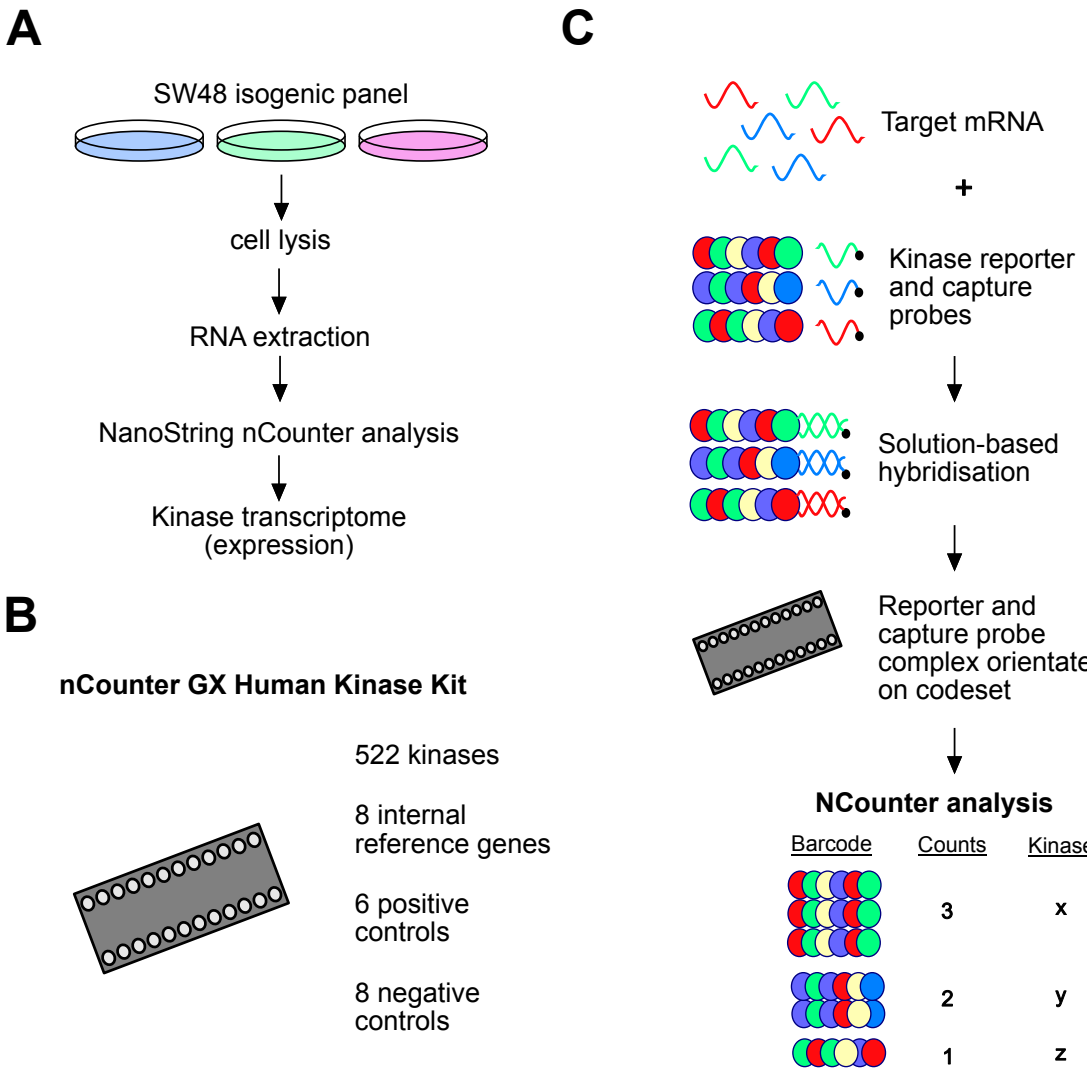

Figure 2.1. Overview of NanoString technology

A) An overview of workflow used to profile kinase transcript expression in SW48 cells. B) Each nCounter GX human kinase kit consists of 522 kinase genes, 8 internal reference genes, 6 positive controls and 8 negative controls. C) mRNA extracted from SW48 cells is mixed in solution with kinase reporter and capture probes. Each reporter probe has a unique colour coded barcode for each kinase of interest. mRNA is hybridised to 35-50 base target specific sequences and the complexes are orientated onto the codeset and analysed by the nCounter imaging software. The expression level of a kinase is measured by counting the number of times a unique barcode is detected.

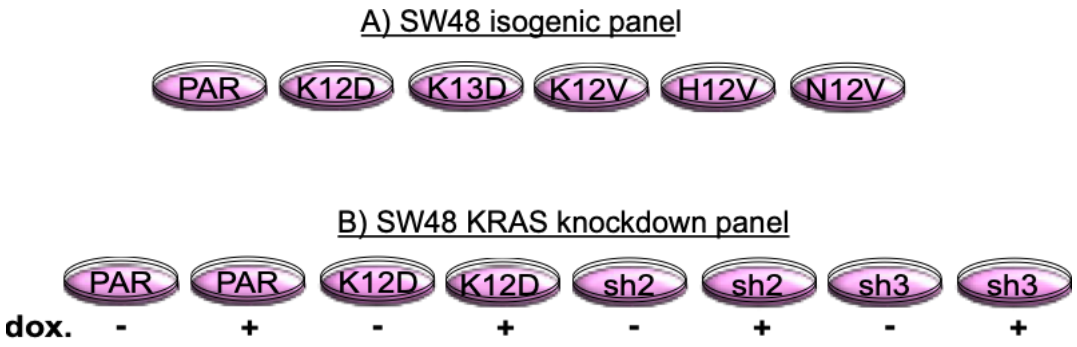

Figure 2.2. Experimental set up of cell lines used in NanoString experiments
A) The first set of NanoString experiments, outlined in chapter four, involved profiling the kinase transcriptome of SW48 isogenic mutant cells, in which one allele has been edited to harbour a specific RAS mutation. The panel included three KRAS mutant cell lines (K12D, K13D, K12V) and a HRAS (H12V) and NRAS (N12V) mutant cell line. The parental wild-type cell line was used as a reference to create log2 ratios for kinase expression for every cell line (see table 2.1 for more details). B) The second set of NanoString experiments, outlined in chapter 5, involved mapping kinase transcriptome adaptations to KRAS knockdown in the K12D mutant cell line. For KRAS knockdown experiments, two independent SW48 K12D cell lines with inducible expression of shRNAs targeting KRAS (sh2 and sh3) were used, along with the parental and K12D cell lines as controls (see section 2.1.3.1 for more details). Four biological replicates were conducted for each set of NanoString experiments.

2.3.3. mRNA extraction

To avoid RNase contamination, only RNase-free tips and tubes were used for RNA extraction. All work took place in a designated area washed down with an RNase cleaning spray, RNaseZAP (Thermo Fisher Scientific, MA, USA).

The RNeasy Mini kit (Qiagen, Germany) was used for the purification of total RNA from SW48 cells. Briefly, cells were washed with PBS, before a buffer containing guanidine thiocyanate (RLT buffer) was added to release RNA and inactivate RNases. For direct cell lysis, 350 μl of RLT buffer was added to the 6cm dish and the lysate was scrapped with a rubber policeman and collected into a 2mL microcentrifuge tube. The cell lysate was added to a QIA shredder spin column (Qiagen, Germany), placed into a collection tube and homogenised by centrifugation for 2 minutes at 15,000 rpm. One volume of 70% ethanol was added to the homogenised lysate to promote the selective binding of the RNA to the column. The sample was transferred into a RNeasy

spin column, placed over a 2mL collection tube and centrifuged for 15 seconds at 8000 x g. Total RNA adhered to the membrane and the contaminants were washed away during a series of wash steps. Columns were washed with 350 μl of RW1 buffer, followed by two 500μl washes with RPE buffer and the column was centrifuged for 15 seconds at 8,000g in between each wash step. The column was placed in a new collection tube, before 30 μl of RNase-free water was added. The column was centrifuged for 1 minute at 8,000g and the RNA eluted into the collection tube. Concentrations of RNA were quantified on a NanoDrop 1000 Spectrometer (Thermo Fisher Scientific, UK) (section 2.3.3).

2.3.4. Quality assessment of total RNA

The concentration and quality of total RNA samples were firstly assessed in-house, using a NanoDrop 1000 spectrometer (Thermo Fisher Scientific, UK). Nucleic acids were quantified using UV absorption at 260nM, and the A260/280 and A260/230 ratios were used to assess the quality of the sample. The A260/280 ratio was used to assess protein contamination, whilst the A260/230 ratio indicated the presence of organic contaminants. NanoString recommend a 260/280 ratio of >1.9 and a 260/230 ratio of >1.8 for optimal results. All samples met these criteria.

The concentration and quality of total RNA was also reviewed at the Centre of Genomic Research (CGR) at The University of Liverpool, where the NanoString instruments are based. The Qubit 2.0 fluorimeter (Thermo Fisher Scientific, UK) was used to quantify the total RNA, and an Agilent 2100 bioanalyser (Agilent Technologies Inc, CA, USA) was used to assess the quality of total RNA. Each sample was given an RNA integrity number (RIN) between 1-10, with 1 being the most degraded and 10 being of the highest quality. For pure RNA, a RIN of >7 was deemed acceptable. All samples scored 10/10 and therefore were taken forward for NanoString analysis.

Before NanoString analysis, all extracted RNA samples were adjusted to 100 ng/μl with RNase free water and the concentrations were confirmed on the Qubit 2.0 fluorimeter.

2.3.5. Solution phase hybridisation

Initially, a mastermix for the reporter probe was made by adding 70 μl of hybridisation buffer to the reporter codeset. Next, 8 μl of the reporter probe mastermix and 5 μl of sample (500 ng total RNA) was added to each of the individual strip tubes. Finally, 2 μl of the capture probeset was added to each tube, before the strip was capped and contents mixed briefly by centrifugation. The samples were added to a Veriti Thermal Cycler (Fisher Scientific, Loughborough, UK) at 65 ^{o}C for 16- 20 hours overnight.

2.3.6. Post hybridisation processing

The following day, the samples were removed from the thermal cycler and transferred to the NanoString nCounter prep station. The nCounter prep station is a fully automated liquid handling system that uses affinity purification to wash excess probes away. Briefly, magnetic beads are used to bind the capture probe whilst excess reporter probe is washed away. The sample is then eluted from the beads and the process repeated to wash away any excess capture probe. Finally, the hybridised samples are eluted and immobilised onto the surface of the nCounter cartridge.

The cartridge was transferred to the nCounter digital analyser for automated imaging and data collection. The samples were scanned by the automated fluorescence microscope and the images analysed at maximum FOV (555 fields of view). The barcodes were counted and tabulated into a reporter code count file (RCC file). The expression level of a gene was determined by counting the number of times its specific barcode was detected.

2.3.7. Data and statistical analysis

Data analysis was conducted using the nSolver 4.0 advanced analysis software which utilises the statistical software programme R 3.3.2 to perform each advanced analysis.

Firstly, a reporter library file (RLF file) that is specific to the nCounter GX human kinase codeset was downloaded, providing the software with information of which probe was assigned to which gene. Next, the reporter code count file (RCC file) containing barcode counts for each gene and control was downloaded into the software.

The nSolver software conducts a series of quality control (QC) and normalisation steps using the controls and internal reference genes. Firstly, the positive controls are used to assess the efficiency of the hybridisation reaction. The stepwise concentrations of the six positive controls are used to check the linearity performance of the assay; the R^2 value needed to be >0.95 to pass QC checks. Next, the negatives controls are used for background subtraction to account for any false discoveries produced by non-specific probe binding. For background correction, the geometric mean of the negative controls is subtracted from the raw counts of each kinase. Finally, in order to eliminate run to run and sample to sample variability, the internal reference genes are used for normalisation. The geNorm algorithm removes reference genes with the least stable expression relative to the other reference genes (Vandesompele *et al.*, 2002). The geometric mean of the most stable reference genes is then used to calculate a normalisation factor for each sample.

The normalised data was taken forward for advanced analysis. Gene expression data was analysed using the differential expression (DE) module.

Table 2.11 *Overview of Differential expression analyses*

Experiment	Description	Covariates for DE analysis
A	SW48 isogenic panel	K12D vs. PAR
		K13D vs. PAR
		K12V vs. PAR
		H12V vs. PAR
		N12V vs. PAR
B	SW48 knockdown panel	K12D vs. PAR
		KRAS knockdown vs. no knockdown (2x shRNA K12D cell lines +/- doxycycline)

The average counts from four biological replicates were used to generate log2 ratios for each kinase in respect to each covariate (table 2.11). Statistical t-testing was performed on log2 transformed data comparing the chosen covariates. The p-value was adjusted using the Benjamini-Hochberg method to eliminate the false discovery rate (FDR), as previously described ($p<0.001$)(Benjamini *et al.*, 2001). A volcano plot was generated for each DE analysis, displaying each kinase log2 fold change and -log10 (p-value) with respect to the chosen covariate.

2.4. Mass Spectrometry (MIB/MS)

Unless otherwise stated, all mass spectrometry grade (MS-grade) reagents were purchased from Sigma-Aldrich, Poole, UK. LoBind Eppendorf tubes (Fisher Scientific, Loughborough, UK) or glass vials were used throughout to maximise sample recovery,

2.4.1. SILAC labelling and experimental set up

SW48 cells were maintained in arginine and lysine free DMEM (Dundee cell products, cat no. LM010) and 10% dialyzed FBS (Life tech, cat no. 10270). To generate light, medium and heavy SILAC labelled cells the DMEM was supplemented with l-proline (Pro 0) and then either:

- **Light-** l-lysine (Lys0), l-arginine (Arg0)
- **Medium-** l-lysine-$^{2}H_4$(Lys4), l-arginine-U–$^{13}C_6$ (Arg6)
- **Heavy-** l-lysine- U–$^{13}C_6$-$^{15}N_2$ (Lys8), l-arginine-U–$^{13}C_6$–$^{15}N_4$ (Arg10)

The final concentrations were 28 mg/L for the arginine, 146 mg/L for the lysine and 200mg/mL for the proline amino acids (Sigma-Aldrich, Poole, UK). Cells were passaged 6-7 times in Medium containing amino acids, before MS analysis was conducted to test for label incorporation. Test labelling was conducted by carrying out an in-gel digest prior to MS analysis (sections 2.4.6 and 2.4.7 respectively). MaxQuant was used to assess the extent of label

incorporation (section 2.4.8) (>95% label incorporation was expected), as previously described (Geiger *et al.*, 2010).

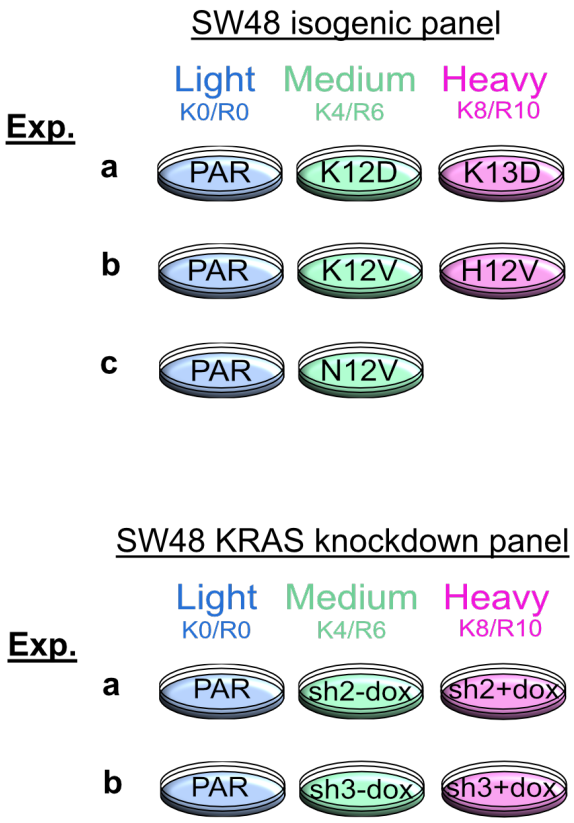

Figure 2.3. Experimental set up and SILAC configurations for SW48 MIB/MS experiments

The mutant cell lines were labelled with medium and heavy amino acids. The light labelled parental wild-type cell line was used as a reference in every case so comparisons could be made across all cell lines. The lysates were mixed in a 1:1:1 ratio and poured onto each MIB/MS column. Three biological replicates were conducted for each set of MIB/MS experiments. A) The first set of MIB/MS experiments, outlined in chapter four, involved profiling the kinome of SW48 isogenic mutant cells, in which one allele has been edited to harbour a specific RAS mutation. The mutant panel included three KRAS mutant cell lines (K12D, K13D, K12V) and a HRAS (H12V) and NRAS (N12V) mutant cell line. A total of 3 columns (a,b,c) were used per biological replicate. B) The second set of MIB/MS experiments, outlined in chapter 5, involved mapping kinase adaptations to KRAS knockdown in the K12D mutant cell line. For KRAS knockdown experiments, two independent SW48 K12D cell lines with inducible expression of shRNAs targeting KRAS (sh2 and sh3) were used (see section 2.1.3.1 for more details). A MIB column was run for each shRNA cell line.

2.4.2. Harvesting cells for MIB/MS

SW48 cells grown in 24.5cm (500cm^2) square dishes were placed on a bed of ice before cell lysis. Cells were washed twice with 75mLs of ice-cold PBS and the PBS discarded after each wash. Next, 10mL of ice-cold PBS was added to the dish and cells scraped using a window squeegee. The cells/PBS were placed into a 50mL centrifuge tube and pelleted by centrifugation (200g, 5mins). Pelleted cells were resuspended into 1mL of MIB/MS buffer (table 2.12) and placed on ice for ten minutes, inverting occasionally. Next, the lysates were sonicated (3 x 10 seconds), alternating to allow each sample to cool for at least 30 seconds on ice between pulses. The lysates were collected into a 2 mL microcentrifuge tube and then cleared of non-soluble material by centrifugation (14,000rpm, 10 minutes, 4^{o}C). A small aliquot was taken for protein determination by BCA assay (section 2.2.2). Clarified lysates were taken forward for MIB/MS analysis or stored at -80 ^{o}C for long term storage.

Table 2.12: Composition of MIB/MS lysis buffer

Solution	Contents
MIB Lysis Buffer	50 mM HEPES, pH 7.5 150 mM NaCl 0.5% Triton X-100 1 mM EDTA 1 mM EGTA 10 mM NaF 2.5 mM $NaVO_4$ Protease Inhibitor Cocktail, 2 tablets/50 mL Phosphatase Inhibitor Cocktail 2, 500µL/50mL Phosphatase Inhibitor Cocktail 3, 500µL/50mL

2.4.3. Production of Multiplexed Inhibitor Beads (MIBs)

For coupling inhibitors to beads, the inhibitors were weighed out into a 15mL falcon tube (table 2.13). The inhibitors were dissolved in 1mL of NN-

Dimethylformamide (DMF) (Sigma) and then diluted 1:1 with 50 mM sodium bicarbonate, pH 7.0.

Meanwhile, 2mL of Sepharose 4B beads (GE healthcare, 17-0571-01) were added into a crucible and drained by vacuuming. The beads were washed twice with 10mLs of 0.5M NaCl, gently swirling and draining in between each wash. Using the same method, the beads were washed with 10mLs of MilliQ water and finally 10mLs of coupling buffer (50% DMF: 50% 50mM sodium bicarbonate). The beads were vacuumed dried on the crucible for 30 seconds and transferred into the falcon containing the inhibitor solution. In a separate 50mL falcon, 0.3834g of EDC powder (Sigma) was weighed out to make a final concentration of 1M in 2mL solution. The EDC powder was added to the falcon containing the inhibitor and beads, inverting a few times to dissolve the powder. The tubes containing the reaction mixture were covered in foil and placed on a nutator overnight.

The following day, the beads were washed twice with 5mL of coupling buffer. To cap the unreactive groups on the kinobeads, the beads were incubated with 1M ethanolamine (Sigma) and 1M of EDC powder in 2mL of coupling buffer overnight.

On the final day, the beads were washed three times with 10mLs of coupling buffer, followed by three times with 10mLs of MilliQ water and once with 10mLs of 20% aqueous ethanol. The beads were stored in 20% aqueous ethanol at 4 ^{o}C until further use. See Figure 2.4 for more details.

Table 2.13. *Quantities of inhibitors used for MIB beads*

Inhibitor	Weight	Company	Catalogue no.
Bisindolylmaleimide (Bis-X)	20mg	SYNkinase	SYN-1021
CTx-0294885 (CTx)	14mg	SYNkinase	SYN-4001-100
CZC8004	20mg	SYNkinase	SYN-1037
Purvalanol B	20mg	SYNkinase	SYN-1070
PP58	20mg	MedChem Express	HY-18622
VI16832	0.8mg	MedChem Express	HY-18623

Bisindolylmaleimide X

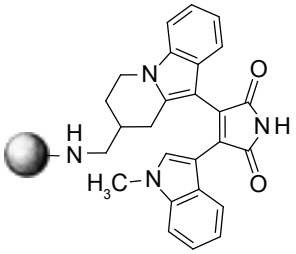

CTx-0294885

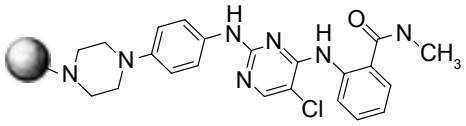

CZC8004

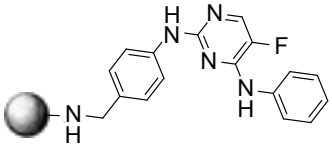

Purvalanol B

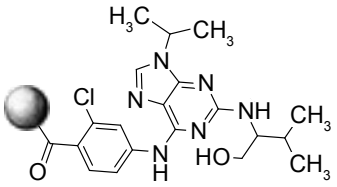

PP58

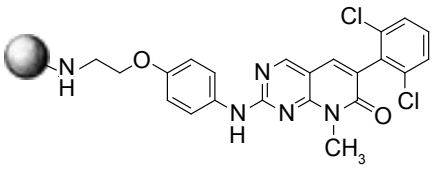

VI16832

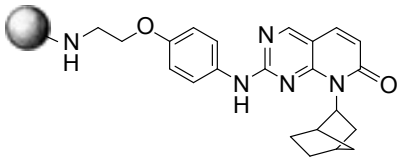

Figure 2.4. Structures of Multiplexed Inhibitor Beads (MIBs) used to profile the kinome
Broad-spectrum kinase inhibitors were immobilised on Sepharose beads through covalent linkage of their primary amino groups or carboxyl group (Purvalanol B). A mixture of six beads were used to enrich the kinase fraction from whole cell lysates.

2.4.4. MIB/MS experiments

Lysates (2mg of total protein) were thawed on ice before being equalised with MIB lysis buffer to 4mLs total volume. The samples were bought to 1M NaCl (850 μl per sample) using cold filtered 5M NaCl (Invitrogen, Paisley, UK).

The chromatography columns (BioRad, UK) (Cat no, 731-1550) were set up on a ring stand (BioRad, UK) (Cat no, 731-7005), two per sample: block

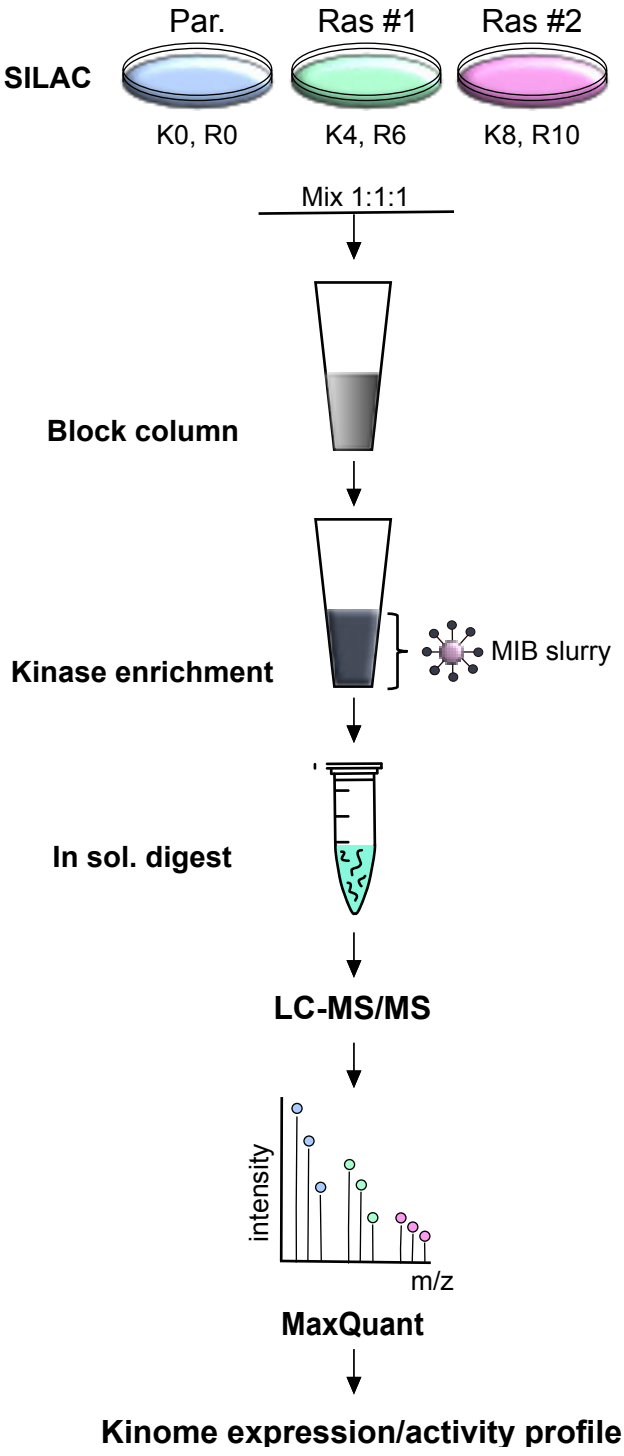

Figure 2.5. Overview of the workflow used to establish and compare the kinome profiles of isogenic SW48 cells

A panel of isogenic cell lines were labelled with SILAC allowing multiple samples to be compared in a single run. Total protein lysates were poured over a block column, containing un-conjugated Sepharose beads, to promote non-specific binding of any highly abundant non-kinase proteins. The flow through passes onto an affinity column containing a mixture of MIBs. Kinases eluted from the column were trypsin digested in-solution. Peptides are separated by Liquid Chromatography (LC) and identified and quantitated by Tandem Mass Spectrometry (MS-MS). Analysis of the MS dataset was conducted using MaxQuant software (n=3).

columns in the upper rack and the MIB columns on the lower rack. For the MIB column, 350μl of total MIB bead slurry was pipetted into each column (section 2.4.3). N.B. For most experiments, the MIB CTx was used alone, however a MIB slurry made up of all six MIBs in combination was tested (see section 3.2.1 for more details).

The MIB columns were washed with 2mL of high salt MIB wash buffer. For block columns, 200 μl of Sepharose 4B (block beads) were pipetted into each column and washed with 2mLs of high salt MIB wash buffer. After the washes had flowed through, the block columns were brought directly over the MIB columns. All sample flow through and washes were discarded into a Tupperware. For details of all buffers used in the MIB/MS experiments see table 2.14.

The lysates were gently poured into the block column and subsequently the block column was removed once the sample had flowed through. After the lysate had flowed through the MIB column below, several wash steps were conducted. The column was washed with 5mL of high salt MIB wash buffer, followed by 5mL of low salt MIB wash buffer and then 500 μl of SDS MIB wash buffer. The base of the MIB columns were firmly secured with caps, before 500 μl of elution buffer was added and the column tops capped. The MIB columns were boiled in a heat block at 95 ^{o}C for 15 minutes before collecting the eluate in a 1.5mL Eppendorf LoBind tube. A further 500 μl of elution buffer was added and the elution step was repeated bringing the total eluate volume to approximately 1mL.

The samples were then processed for MS analysis. Mainly, proteins were digested using an in-solution digest method (section 2.4.5) but an in-gel digestion method (section 2.4.6) was also tested. For more details see section 3.2.1.

Table 2.14: Composition of MIB/MS buffers

Solution	Contents
Low Salt MIB Wash Buffer	50 mM HEPES, pH 7.5 150 mM NaCl 0.5% Triton X-100 1 mM EDTA 1 mM EGTA
High Salt MIB Wash Buffer	50 mM HEPES, pH 7.5 1 M NaCl 0.5% Triton X-100 1 mM EDTA 1 mM EGTA
SDS MIB Wash Buffer	50 mM HEPES, pH 7.5 150 mM NaCl 0.5% Triton X-100 1 mM EDTA 1 mM EGTA 0.1% (w/v) SDS
MIB Elution Buffer	0.5% (w/v) SDS 1% (v/v) β-mercaptoethanol 0.1M Tris-HCl, pH 6.8 LC-MS grade water
C18 equilibration buffer	5% ACN 0.5% TFA LC-MS Grade water

2.4.5. In-solution digestion of proteins

2.4.5.1. Dithiothreitol and Iodoacetamide treatment

Dithiothreitol (DTT) (Sigma) is a reducing agent that is important for preventing intramolecular and intermolecular disulphide bonds from forming between cysteine residues of proteins by converting cystine disulphide bonds into cysteine free sulfhydryl groups (Gundry *et al.*, 2009). Firstly, samples were incubated with 10 μl of 500mM DTT in a heat block at 60 ºC for 25 minutes. The samples were left to come to room temperature on ice, before being incubated in the dark with 100 μl of 200mM iodoacetamide (IAA) (Sigma) for 30 minutes. IAA is an alkylating agent that caps the free sulfhydryl groups of cysteine residues, preventing disulphide bonds forming prior to tryptic digestion (Gundry *et al.*, 2009). Following incubation with IAA, 10 μl of 500mM DTT was added to each sample to stop the alkylation step. Finally, samples were concentrated using Amicon Millipore Ultra-4 (10K cut off) spin columns (cat no. UFC801008). The samples were poured into the columns and centrifuged for 30 minutes (4 ºC ,3000rpm). The concentrated samples (100 μl-150 μl) were transferred into 2mL LoBind microcentrifuge tubes ready for protein precipitation.

2.4.5.2. Methanol/ Chloroform precipitation of proteins

Protein precipitation was performed by adding MS-grade methanol, water and chloroform to each sample in a 4:3:1 ratio. Samples were centrifuged at top speed at 4 ºC for ten minutes to ensure an interphase layer of protein was formed. Using a pipette, the entire upper aqueous layer was removed, ensuring the white interphase layer of protein was still intact. Next, the samples were gently vortexed and centrifuged at 13,000rpm at 4 ºC for 5-10 minutes, ensuring that the opaque protein pellet was visible at the bottom of the tube. After the supernatant was removed, the protein pellet was washed twice with 500 μl of MS-grade methanol. Finally, the samples were dried in a speed vac at 37 ºC for approximately 5 minutes, ready for trypsin digestion.

2.4.5.3. Trypsin digestion

The protein pellet was resuspended in 100 μl of 50mM HEPES, pH8 buffer, using a pipette tip to dislodge the pellet from the side of the tube. The samples were incubated at 37 ^{o}C overnight with trypsin (4 ng/µL working concentration; Trypsin GOLD, sequencing grade, Promega, USA) to cleave C-terminal to arginine and lysine residues.

2.4.5.4. Ethyl acetate extraction for the removal of triton

Ethyl acetate was added to the samples for the removal of triton. Firstly, MS grade water was added to ethyl acetate in a 10:1 ratio in order to saturate ethyl acetate and prevent sample loss. 1mLs of saturated ethyl acetate was added to each sample. The samples were vortexed thoroughly before centrifugation at 13,000rpm for five minutes at RT. Next, the entire upper layer of ethyl acetate was removed in a fume hood. This extraction step was repeated twice more before residual ethyl acetate was evaporated by putting samples on a heat block for three minutes at 60 ^{o}C. Finally, samples were dried in a speed vac prior to desalting.

2.4.5.5. C-18 pepclean

The C-18 spin columns (Pierce, cat no, 89870) were placed in 2mL microcentrifuge tube to collect flow through from washes. The column resin was activated by adding 200 μl of 50% Acetonitrile (ACN) in MS grade water and centrifugation at 4400rpm for one minute. Next, the column was equilibrated by the centrifugation of 200 μl of C-18 buffer (5% ACN, 0.5% TFA, in MS water) at 4400rpm for one minute. The dried protein pellet was resuspended in 200 μl of C-18 buffer and loaded onto the C-18 column. The column was centrifuged at 4400rpm for one minute and the flow through discarded. The column was washed by centrifugation with 200 μl of C-18 buffer at 4400rpm for a further minute. Finally, samples were eluted from the column into a new 1.5mL LoBind Eppendorf tube by adding 2x 25 μl 50% ACN

to the column and centrifuging at 4000rpm for one minute. Samples were dried down in a speed vac prior to MS analysis.

2.4.6. In-gel digestion of proteins

2.4.6.1. SDS-PAGE

Samples were loaded on 4-12% pre-cast Bis-Tris gels (NuPage, Invitrogen, Paisley, UK) and separated by SDS-PAGE. Separation typically took place at 100V for 15 minutes followed by 200V for 45 minutes. The gels were placed in a 15cm dish and stained with Colloidal Blue staining (Invitrogen, Paisley, UK). Each sample lane was cut into 1x1mm pieces using a sterile scalpel (approx. 48 pieces). The gel pieces were transferred into 1.5mL LoBind Eppendorf tubes before being destained with 40 μl of 50mM Ambic/50% ACN at 37 ^{o}C. for ten minutes. Next, the gel slices were dehydrated by adding 100 μl of ACN and incubating for five minutes at RT. The supernatant was discarded, and samples dried for five minutes on a speed vac.

2.4.6.2. Dithiothreitol and Iodoacetamide treatment

The samples were reduced by adding 50 μl of 10mM DTT in 100mM of ambic and incubated for one hour at 56 ^{o}C. The supernatant was discarded, and samples were left to cool on ice for five minutes. Next, the samples were alkylated by adding 50 μl of 50mM IAA in 100mM ambic and incubated in the dark for 30 minutes at RT. The supernatant was discarded, before several wash steps were completed. Firstly, the gel pieces were washed with 300 μl of 100mM ambic for 15 minutes at RT. Again, the supernatant was discarded, before gel pieces were washed with 300 μl of 20mM ambic /50% ACN for 15 minutes at RT. Next, the gel slices were dehydrated by adding 100 μl of ACN for five minutes at RT. The supernatant was discarded, and the samples were dried by a Speed vac.

2.4.6.3. Trypsin digestion

The protein pellet was resuspended in 100 μl of reaction buffer (40mM ambic, 9%ACN) using the pipette tip to dislodge the pellet from the side of the tube. The samples were incubated at 37 ^{o}C overnight with trypsin (4 ng/µL working concentration; Trypsin GOLD, sequencing grade, Promega) to cleave C-terminal to arginine and lysine residues.

2.4.6.4. Peptide extraction

The following day, 100 μl of ACN was added to each digest and incubated for 30 minutes at 30 ^{o}C. The supernatant containing the peptides for analysis were transferred into a new 1.5mL LoBind Eppendorf. The remaining gel pieces were incubated with 1% formic acid for 20 minutes at RT before, the supernatant was transferred to the tube containing peptides for analysis. Finally, 150 μl of ACN was added to the gel pieces and incubated for ten minutes at RT before, the supernatant was again transferred to the tube containing peptides for analysis. The peptides were dried by a speed vac prior to MS analysis.

2.4.7. MS/MS

For label testing, samples were analysed in-house using our LTQ Orbitrap mass spectrometer. Dried protein pellets were resuspended in 1% formic acid and centrifuged at 13,000g for ten minutes before injection on the MS. A total of 5 µL of each sample was fractionated by nanoscale C18 high performance liquid chromatography (HPLC) on a Waters nanoACQUITY UPLC system coupled to an LTQ-OrbitrapXL (Thermo Fisher Scientific) fitted with a Proxeon nanoelectrospray source. Peptides were loaded onto a 5 cm × 180 µm trap column (BEH-C18 Symmetry; Waters Corporation) in 0.1% formic acid at a flow rate of 15 µL/min and then resolved using a 25 cm × 75 µm column using a 20 min linear gradient of 3 to 62.5% acetonitrile in 0.1% formic acid at a flow rate of 400 nL/min (column temperature of 65 °C). The mass spectrometer acquired full MS survey scans in the Orbitrap (R = 30 000; m/z range 300–

2000) and performed MSMS on the top five multiple charged ions in the linear quadrupole ion trap (LTQ) after fragmentation using collision-induced dissociation (30 ms at 35% energy) (Hammond *et al.*, 2015).

For MIB/MS experiments, samples were sent for analysis at the proteomics facility at the University of Warwick. Reversed phase chromatography was used to separate tryptic peptides prior to mass spectrometric analysis. Cell proteomes were analysed with two columns, an Acclaim PepMap μ-precolumn cartridge 300 μm i.d. x 5 mm, 5 μm, 100 Å and an Acclaim PepMap RSLC 75 μm i.d. x 25 cm, 2 μm, 100 Å (Thermo Fisher Scientific). The columns were installed on an Ultimate 3000 RSLCnano system (Thermo Fisher Scientific) at 40°C. Mobile phase buffer A was composed of 0.1% formic acid and mobile phase B was composed of acetonitrile containing 0.1% formic acid. Samples were loaded onto the μ-precolumn equilibrated in 2% aqueous acetonitrile containing 0.1% trifluoroacetic acid for 8 min at 10 μL min^{-1} after which peptides were eluted onto the analytical column at 300 nL min^{-1} by increasing the mobile phase B concentration from 8% B to 25% over 37 min, then to 35% B over 10 min, followed by a 3 min wash at 90% B and a 10 min re-equilibration at 4% B.

Eluting peptides were converted to gas-phase ions by means of electrospray ionization and analysed using an Orbitrap Fusion instrument (Thermo Fisher Scientific). Survey scans of peptide precursors from 375 to 1500 *m*/*z* were performed at 120K resolution (at 200 *m*/*z*) with a $2x10^5$ ion count target. The maximum injection time was set to 150 ms. Tandem MS was performed by isolation at 1.2 Th using the quadrupole, HCD fragmentation with normalized collision energy of 33, and rapid scan MS analysis in the ion trap. The MS^2 ion count target was set to $3x10^3$ and maximum injection time was 200 ms. Precursors with charge state 2–6 were selected and sampled for MS^2. The dynamic exclusion duration was set to 30 seconds with a 10-ppm tolerance around the selected precursor and its isotopes. Monoisotopic precursor selection was turned on and instrument was run in top speed mode.

2.4.8. MaxQuant data analysis

Raw MS data files were processed using MaxQuant software, as described previously (Hammond *et al.*, 2015). Data obtained from MaxQuant analyses were evaluated using Microsoft Excel and log2 ratios were generated for each kinase in respect to each covariate (table 2.11).

Chapter 3 : Using MIB/MS to profile kinome activity on a global scale

Traditional methods to measure kinase activity are relatively low throughput and limited to reagent availability, leaving much of the kinome understudied (Wilson *et al.*, 2018). The traditional 'gold' standard kinase assay, measures the transfer of radiolabelled ATP onto a kinase substrate and this is directly proportional to kinase activity (Hastie, McLauchlan and Cohen, 2006). Although highly sensitive, this method only provides biochemical analysis of individual enzymes. (Cann *et al.*, 2017). Western blotting is another traditional approach used to analyse the activity of select kinases via the presence of diagnostic phospho-sites (Stommel *et al.*, 2007). Again, this approach is relatively low throughput and limited to phospho-specific antibody availability. In addition, the multi-step nature of activation of some kinases that involves accessory proteins and structural changes, the phospho-site may not faithfully measure activation state (Johnson, Noble and Owen, 1996).

Advances in genomic technologies have allowed scientists to conduct high-throughput whole-genome and whole-transcriptome sequencing (Fleuren *et al.*, 2016). Scientists are therefore able measure the gene expression of kinases on a global scale and also map transcript changes in response to kinase inhibitors (Stuhlmiller, Earp and Johnson, 2014). This approach to studying the kinome however has some limitations. Firstly, the expression of a kinase at the transcript-level doesn't always correlate to the expression at the protein-level (Schwanhäusser *et al.*, 2011). Moreover, protein-level expression doesn't necessarily correlate to the enzymatic activity of the kinase (Graves *et al.*, 2013).

It has become apparent that to improve our understanding of the information flow between kinases and the wider signalling network, we need to be able to globally measure kinase expression at both the genetic and proteomic level, but more importantly to determine whether a kinase is active. Furthermore, establishing what proportion of the kinase is active and whether it's activation

status changes in response to activators or inhibitors will be critical to our understanding.

A method has recently been developed that purports to allow simultaneous measurement of the relative expression/activities of hundreds of kinases within cells (Duncan *et al.*, 2012a). The method utilises broad specificity kinase inhibitors which are immobilised onto Sepharose beads to make up the Multiplexed Inhibitor Bead (MIB) slurry. Type I kinase inhibitors, which are thought to only bind to the ATP binding pocket of kinases in their active DFG-in conformation, are used to make the MIBs (Roskoski, 2016). The rationale is that binding of kinases to the column reflects kinase activity; increased binding of the kinase to the column indicates increased kinase activity. Quantitative mass spectrometry is used to identify and quantify the kinases in each sample. Incorporating quantitative proteomic labelling techniques, such as SILAC or iTRAQ, make it possible to simultaneously measure and compare global kinome adaptions between multiple samples (Ong and Mann, 2005).

It is also important to note that the MIBs can also to bind pseudokinases; It was reported in a study by Murphy et al. that around 40% of pseudokinases still bind to ATP despite being catalytically inactive (Murphy *et al.*, 2014).

In the pioneering work by the Johnson lab, MIB/MS was used to profile kinome activity in response to MEK inhibition in TNBC cells (Duncan *et al.*, 2012b). The assay was used to map kinome adaptations caused by MEK inhibition, and as a result, the group were able to define a mechanism of drug resistance: Acute loss of MEK/ERK signalling causes degradation of c-myc and relieves transcriptional repression of several RTKs (Johnson *et al.*, 2013). An increase in RTK expression/activity thus causes an increase in downstream oncogenic MAPK signalling therefore providing the compensatory mechanism to MEK inhibition. The study provided the first example of how MIB/MS can be used to profile kinome activity, assess kinome rewiring in response to targeted inhibition, and therefore help rationally predict combinational therapy to overcome resistance in the clinic.

Many studies have since used MIB/MS to measure kinome reprogramming that occurs in response to targeted inhibition (Cox *et al.*, 2011; Duncan *et al.*, 2012a; Cooper *et al.*, 2013; Stuhlmiller *et al.*, 2015; Johnson *et al.*, 2014). MIB/MS has also been used to compare the differential signalling outputs of tumours or cells harbouring different mutations (Figure 2.5) (Gholami *et al.*, 2013). However, there seems to be some controversy as to what extent the MIB/MS assay reports activation-dependent binding and therefore what measuring kinome 'responsiveness' actually means. A recent paper was published opposing the notion that MIB/MS could be used to measure kinase activity; the authors state that binding to the MIBs is largely independent to kinase activation status (Ruprecht *et al.*, 2015). Instead, the group argue that enrichment mainly depends on kinase expression levels, the affinity of a kinase to the immobilised compound and kinase conformation state. Nevertheless, it is undisputed that the method is a good enrichment tool for kinases that are lowly abundant in cells and therefore a difficult group of enzymes to study simultaneously in the cellular context.

I propose to use MIB/MS to compare the differential signalling outputs of cells harbouring different Ras mutations. Since the Ras pathway is enriched in effectors that are kinases, MIB/MS would be useful for investigating the effect of Ras mutations on known downstream effectors but more importantly unknown Ras effectors that lie within the wider signalling networks. Before profiling differential kinome responses in Ras mutant cells, it will be imperative to elucidate to what extent the assay is able to report kinase activation status and therefore what type of 'response' we are measuring using the assay.

3.1. Objective

The objective of this chapter was to establish the MIB/MS kinome assay in the lab and determine to what extent the assay is able to report activation-dependent binding.

3.2. Results

The aims of the initial stages of the project was to establish and optimise the MIB/MS assay in the lab (Figure 3.1). Several stages of optimisation were conducted in order to:

i) Produce Multiplexed Inhibitor Beads (MIBs) in our lab.

ii) Validate the efficiency of six different MIBs in isolating kinases and potential binding partners.

iii) Optimise the sample processing pipeline.

3.2.1. CTx-0294885 is the most efficient MIB to isolate kinases

Multiplexed inhibitor beads (MIBs) comprise broad-spectrum kinase inhibitors immobilised on Sepharose beads through covalent linkage of their primary amino or carboxyl group. Previous studies had used columns containing up to six different MIBs to enrich kinases from cells or tissues (Cooper *et al.*, 2013; Cox *et al.*, 2011; Duncan *et al.*, 2012a; Stuhlmiller *et al.*, 2015). These included Bisindolylmaleimide-X, CTx-0294885, CZC8004, Purvalanol B, PP58 and VI16832 (Figure 2.4). Using published protocols, each kinase inhibitor was conjugated to Sepharose beads (Zhang *et al.*, 2013). I was able to observe a transfer of colour from the inhibitor solution to the beads which remained stable however, measuring conjugation efficiency by Mass Spectrometry should have been conducted to ensure that each inhibitor had linked with sepharose consistently, across all biological replicates.

The efficiency of each MIB to isolate kinases and potential binding partners was evaluated. Each MIB was individually tested over the indicated number of replicates and experimental conditions (Figure 3.2). Figure 3.2A, shows the proportion of kinases and non-kinases isolated by each bead type. The total number of proteins captured by each bead ranged from 349 to 757 proteins. Kinases represented between 5-16% of total proteins pulled down by each bead, a significant enrichment against the background rate of kinase

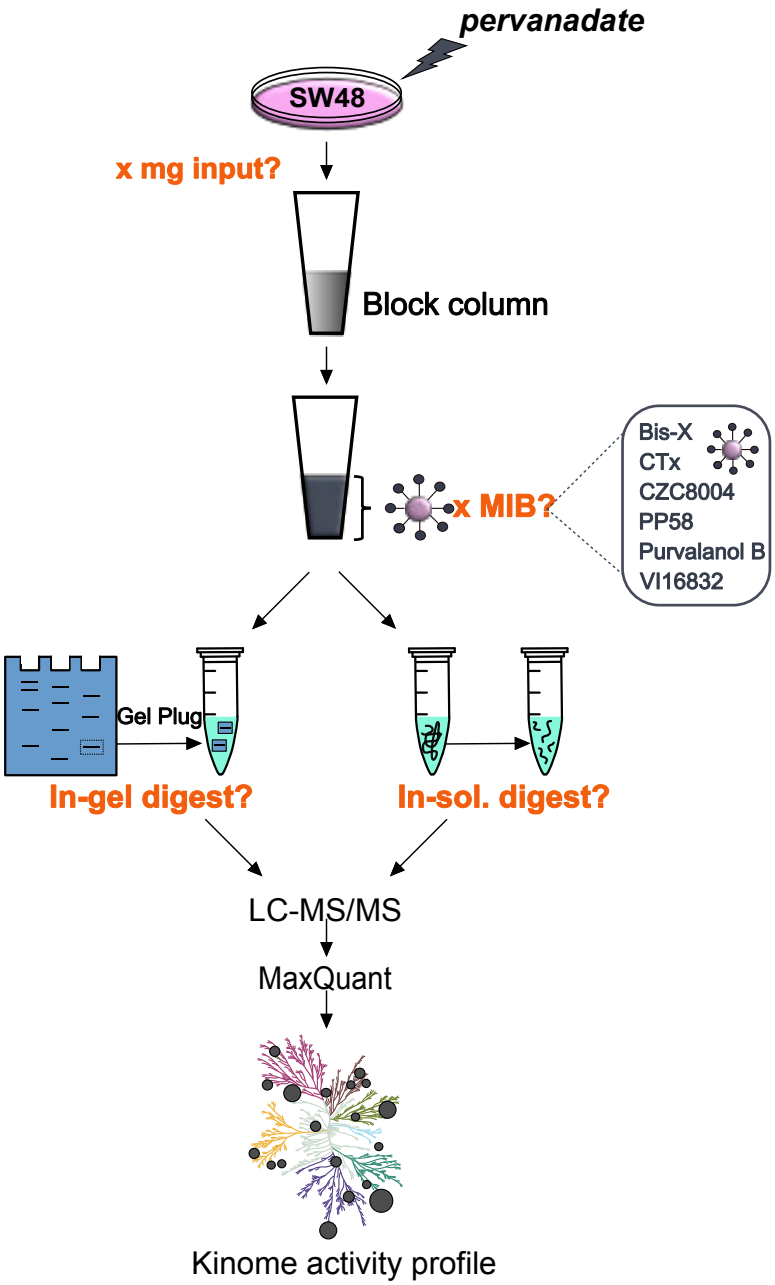

Figure 3.1. Overview of MIB/MS method optimisation.

When establishing the MIB/MS method in our lab, several aspects of the protocol were reviewed in order to achieve optimum kinome profiling in our cells (highlighted in orange). Prior to lysis, wild-type SW48 cells were treated with 100μM pervanadate for 15 mins at 37C. Different concentrations of cell lysate were loaded onto the column to determine if loading concentration correlated to the number of kinases detected by LC-MS/MS. Following passage through the block column, the lysate was passed through a column containing MIBs. Protein lysates were run over each bead type individually and also the six MIBs in combination to determine what combination provided the best coverage of the kinome (Bisindolylmaleimide, CTx-0294885, CZC8004, Purvalanol B, PP58, VI16832). To determine optimal tryptic digestion, an in-gel digest of proteins was compared to an in-solution digest approach.

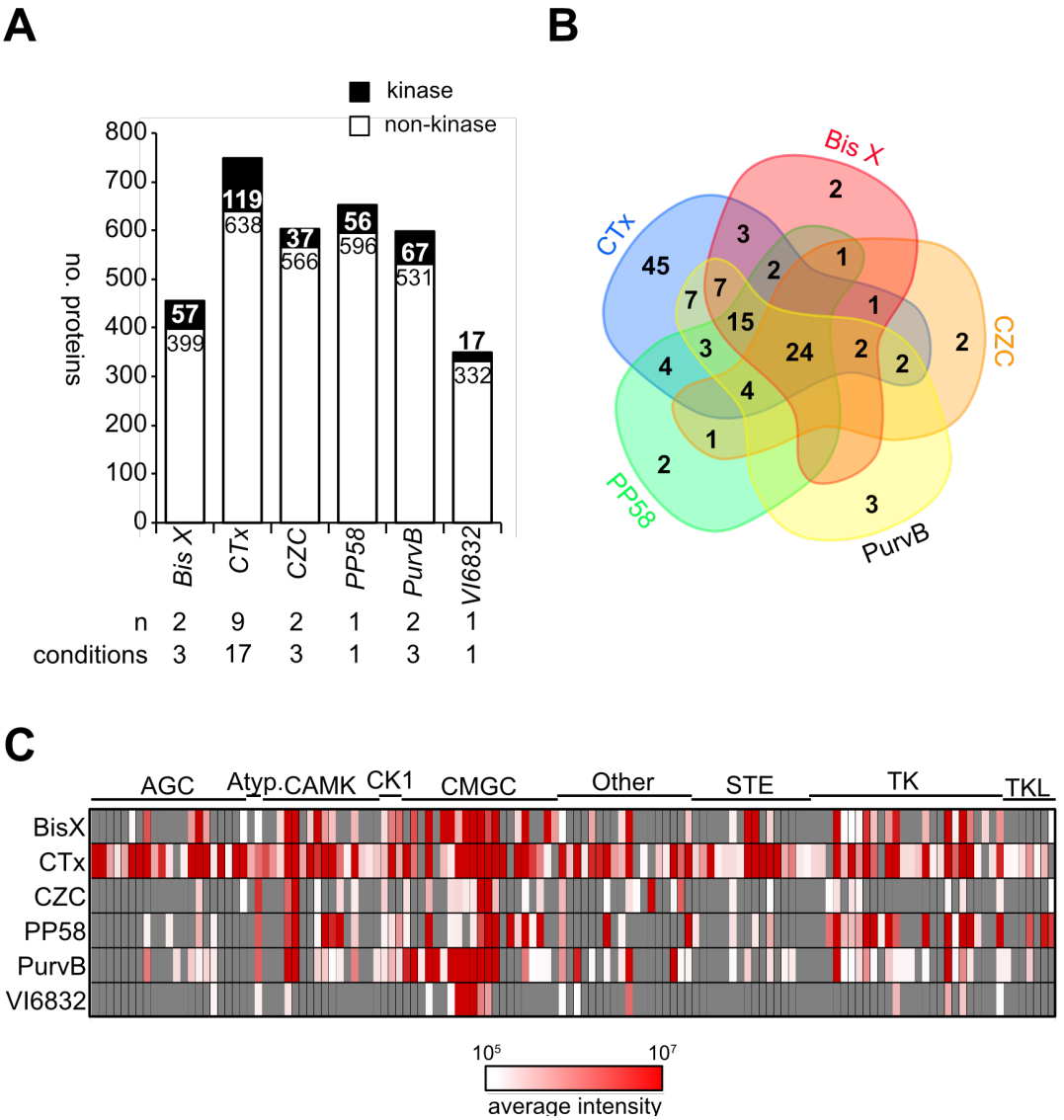

Figure 3.2. CTx-0294885 is the most efficient MIB in isolating kinases.

Protein lysates were run over each bead type (Bisindolylmaleimide, CTx-0294885, CZC8004, Purvalanol B, PP58, VI16832). Data derived from MaxQuant analysis illustrating: A) The total number of all kinase (black) and non-kinase (white) proteins pulled down by each MIB over several experiments under various experimental conditions. B) The overlap between protein kinases enriched by the six different MIBs. C) The average intensity of each kinase detected across the kinome. These data indicate that CTx provides the greatest coverage of the kinome.

expression in the human genome (2.6%). All 6 beads therefore successfully enriched for a subset of kinases but to various extents. The most efficient MIB is CTx-0294885 capturing approximately 20% of the kinome (119/535); CTx isolated 748 proteins, of which 119 were kinases. Given that previous studies had typically used five or more beads in combination, I wanted to determine what unique contribution each MIB provided. The Venn diagram in Figure 3.2B shows there is significant overlap between the kinases enriched by the six MIBs. However, the majority of kinases isolated from the cells at this stage were isolated by CTx, with 45 kinases unique to CTx alone. Furthermore, CTx clearly achieved the best coverage of the kinome, with kinases from all major kinase subfamilies captured by the MIB (Figure 3.2C). With this in mind, I decided to use the single bead CTx for further method optimisation.

3.2.2. Method optimisation

I wanted to ensure that the sample processing pipeline was as efficient as possible. Different concentrations of cell lysate were loaded onto a column containing MIBs and the number of kinases detected recorded. This series of experiments provided the opportunity to investigate whether loading concentration correlated to the number of kinases detected and also determine whether the method provides good kinase enrichment of SW48 cells. Figure 3.3A shows that we detected a greater number of kinases after loading more cellular material. However, less than 10% of the kinome was isolated in initial experiments using in-gel digestion. This was far lower than expected, considering the method is thought to be capable of enriching 50%-60% of the expressed kinome (Duncan *et al.*, 2012a). The only clear difference between the proteomic workflow that was adopted in our lab and that of the Johnson lab was that different types of proteolytic digest were utilised. Previous studies used an in-solution approach to digest proteins before peptides were separated by Liquid Chromatography (LC) and identified and quantified by Tandem Mass Spectrometry (MS-MS) (Duncan *et al.*, 2012a; Cooper *et al.*, 2013). I therefore wanted to see if kinase enrichment was improved after using an in-solution approach.

Optimum kinase enrichment was achieved using an in-solution digest. Nearly double the number of kinases were detected by LC/MS/MS after performing an in-solution digest vs. an in-gel digest (Figure 3.3A). For example, when 5mg of cell lysate was loaded, the in-solution digest yielded 88 kinases whilst the in-gel approach yielded 43. This trend was observed across all loading concentrations. Furthermore, it was found that to reach the maximal kinase enrichment, less loading material was needed using the in-solution digest vs. in-gel digest. For subsequent experiments, we decided to load 2mg of cell lysate as increasing the loading concentration in this context would not produce any greater benefit.

A comparison was made between the average intensities of all proteins detected over the experiments utilising an in-gel digest vs. an in-solution digest, and this provided an explanation as to why the in-solution digest is more favourable (Figure 3.3B). It is clear that the majority of proteins (kinase or non-kinase) are detected at a higher intensity after performing an in-solution digest. This suggests that the kinases are more abundant in a sample after this type of digestion and therefore are more likely to be detected.

We were interested in what makes a kinase more likely to be detected by the LC/MS/MS. One might expect that proteins with a higher molecular weight are more likely to be detected by LC/MS/MS, as there would a greater number of peptides in solution after digestion than lower molecular weight proteins. The data suggests, however, that there is no correlation between the number of occasions each kinase was observed and its molecular weight (Figure 3.3C) Instead, a relationship between the number of times a kinase was detected and its average intensity is evident; a kinase is more likely to be seen if it has a higher average intensity (Figure 3.3D). If we assume the intensity of a kinase is a measure of abundance, then we can deduce that kinase enrichment is based on protein abundance and is not influenced by molecular weight.

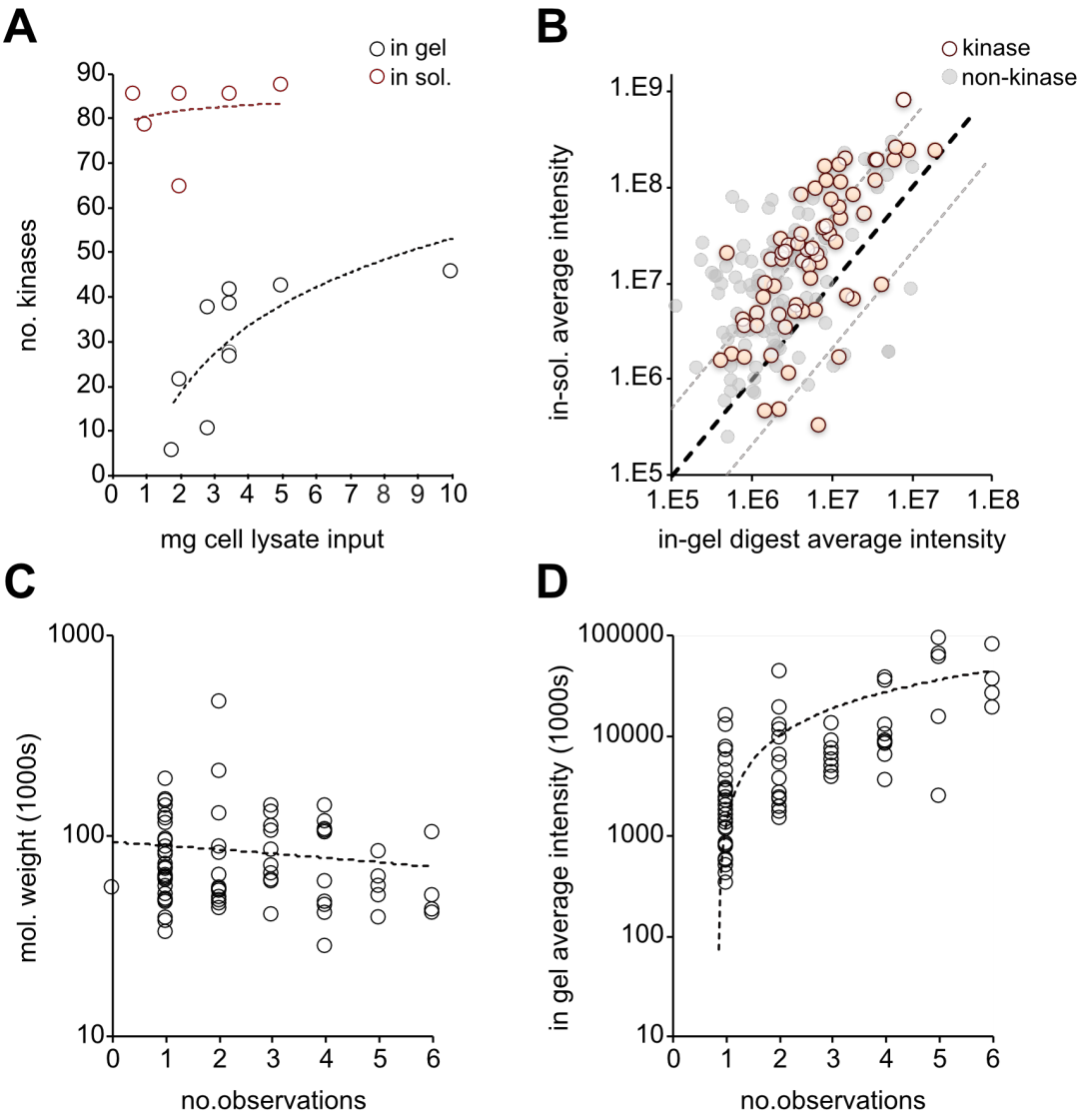

Figure 3.3. Improved enrichment of kinases observed using an in solution tryptic digest vs. in gel tryptic digest.

Data generated from multiple experiments using a single MIB, CTx only. MaxQuant analysis illustrating: A) The number of kinases detected using different concentrations of cell lysate over several in-gel digest (black) or in-solution digest (red) experiments. B) The intensities of all kinase (red) and non-kinase proteins (grey) detected in experiments utilising an in-gel digest vs. in-solution digest. C) Representation of the number of occasions protein kinases were detected based on their molecular weight. D) Correlation between the average intensity of each protein kinase and the number of occasions each kinase was detected over several in-gel digest experiments. Kinase enrichment is based on protein abundance and is not influenced by molecular weight.

3.2.3. The MIB assay does not profile kinase activation state in SW48 cells.

In the original MIB/MS study (Duncan ref), activation-dependent binding to MIBs was demonstrated by:

i) increased binding of MAPKs after cells were stimulated with EGF.

ii) increased binding of Tyrosine Kinases (TK) after cells were treated with the tyrosine phosphatase inhibitor, Pervanadate, which renders kinases in their active state.

I used the same approach to test activation-dependent binding in our SW48 parental cell line. SW48 cells were serum starved for 16h before treatment with 20% serum, 20ng/mL EGF or 100μM pervanadate. A simplified outline of the Ras signalling network is depicted in Figure 3.4A highlighting key nodes expected to be responsive after stimulation. The objective was to analyse the activation responses to each treatment and to see if this correlated to MIB binding.

Firstly, western blotting was performed to generate independent evidence of kinase responses to treatment with serum, EGF or pervanadate. A phospho-tyrosine (pY20) antibody was used to confirm pervanadate-induced TK activation. A global increase in the phosphorylation of TKs in SW48 cells treated with pervanadate was observed (Figure 3.4B). Additionally, using phospho-specific antibodies I observed increased activity of individual nodes in the MAPK and PI3K pathways induced by three treatments. The data generated was used to inform whether an increase in binding to MIBs is indicative of increased activation seen under each condition.

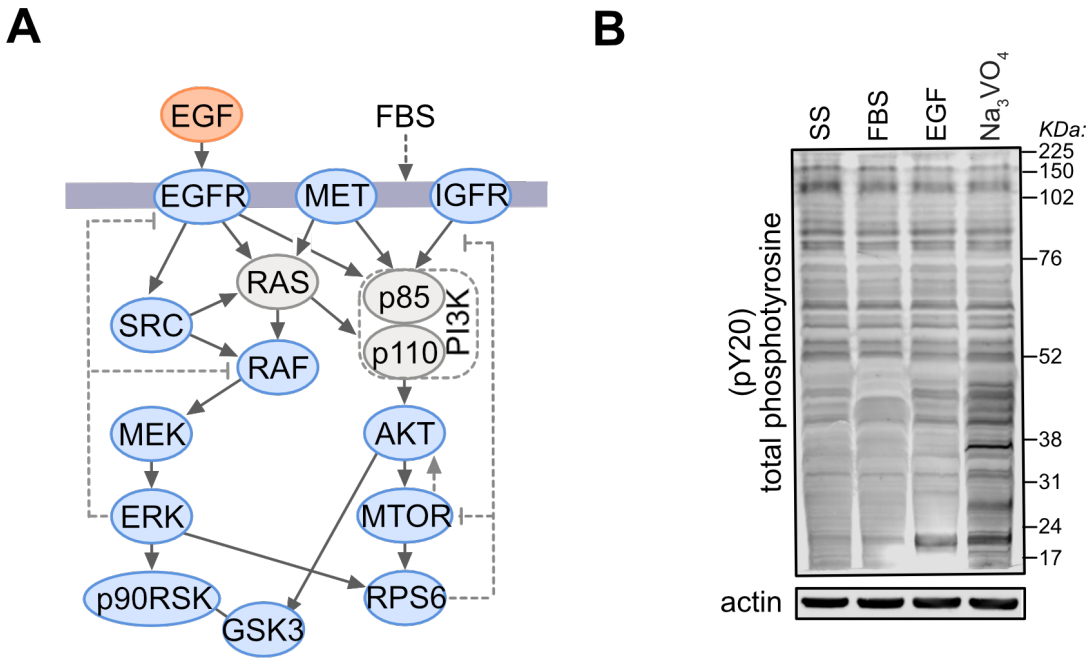

Figure 3.4. Signalling responses of SW48 wild-type cells after treatment with serum, EGF or pervanadate.

A) A simplified outline of the Ras signalling network. Ras proteins utilise various downstream effectors to illicit many signalling responses. Upon activation by RTKs, Ras can activate both the MAPK and PI3K pathways promoting cell differentiation and proliferation. B) SW48 wild-type cells were serum starved for 16hrs before treatment with 20% serum for 5 mins, 20ng/mL EGF for 5 mins or 100μM pervanadate for 15 minutes. Cells were subsequently lysed with RIPA buffer. Lysates were separated by SDS-page and western blots were probed with the indicated antibody.

Whilst evaluating whether the MIB/MS assay was capable of reporting changes in kinase activation in SW48 cells, several variations to the method were tested. These included comparing:

i) SILAC and label-free configurations (figure 3.5)

ii) CTx alone and a slurry of 6 MIBs in combination

3.2.3.1. SILAC with CTx

Firstly, the activity of serum starved SW48 cells were compared to cells that were treated with 20% serum. Lysates were combined and ran over a column containing CTx only. The heatmap in figure 3.6A clearly shows that there was no change in kinase enrichment after cells were stimulated with serum. Out of the 102 kinases that were captured, only one was 'responsive'. Responsive is

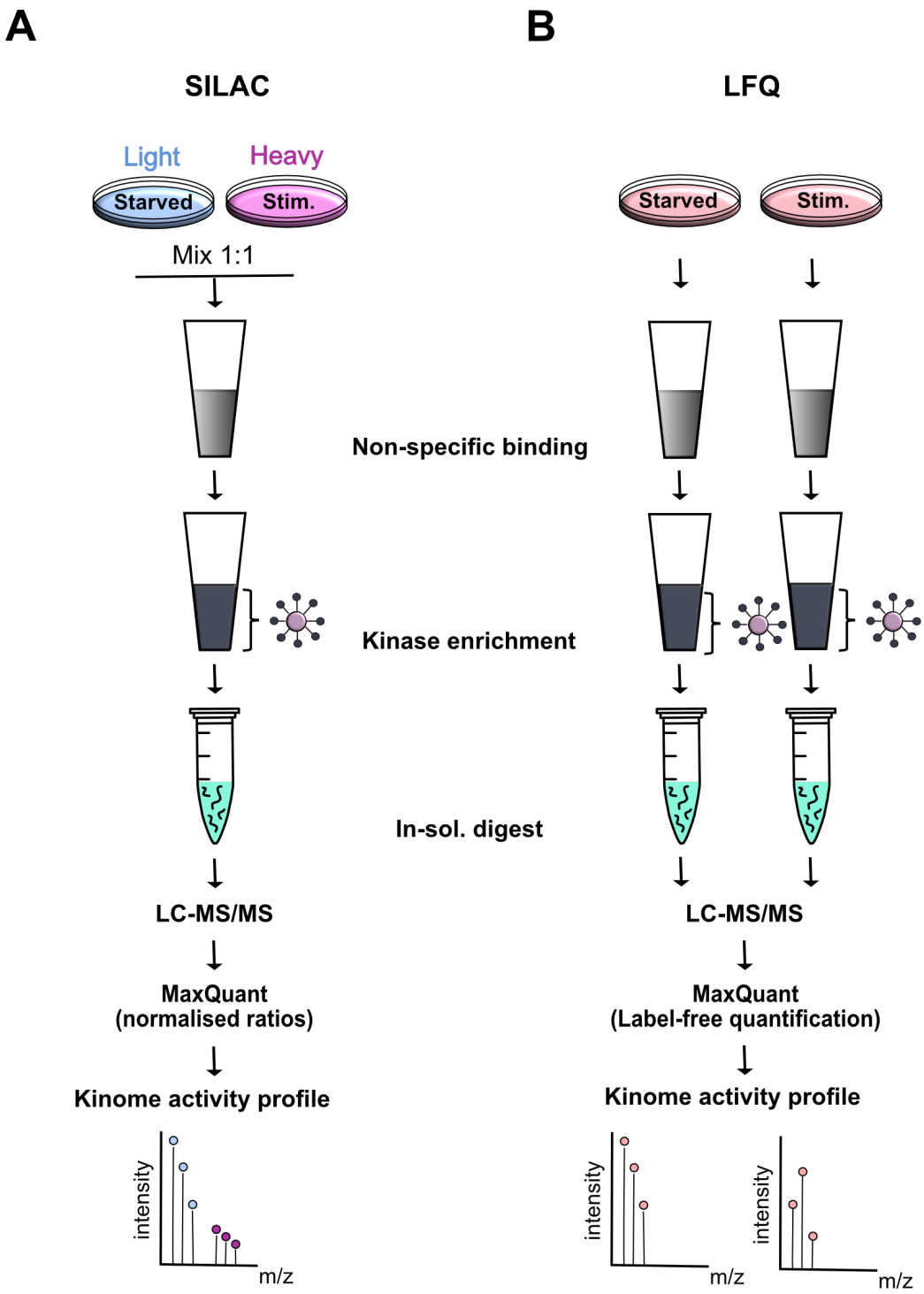

Figure 3.5. Experimental strategy for the characterisation of activity dependent binding to Multiplexed inhibitor beads (MIBs).

SW48 cells treated with serum, EGF or pervanadate were compared to serum starved cells to determine whether binding to the MIB column is dependent on kinase activation status. A) Cells were labelled with SILAC allowing two samples to be compared in a single run. Light labelled cells were serum starved and combined (1:1) with stimulated heavy labelled cells. B) Unlabelled cell lysates were ran over separate columns and label-free quantification was used to compare between the conditions.

defined by a 2-fold increase or decrease in activity after stimulation. Furthermore, there was no evidence of increased binding of key members of the MAPK pathway, whose activity we had previously shown to be induced by serum stimulation.

3.2.3.2. SILAC with COMBINED MIBs

Considering a slurry of six different MIBs (Bisindolylmaleimide-X, CTx-0294885, CZC8004, Purvalanol B, PP58 and VI16832) was used in the original study, I decided to test whether I could achieve activation-dependent binding using all six beads in combination. In this series of experiments, a comparison was made between the activity profiles of serum-starved cells vs. cells treated with serum, EGF or pervanadate. The heatmaps in Figure 3.6B, show that kinase enrichment is comparable between rested and treated cells. In all three cases, there were very few, if any kinases that were responsive. Furthermore, it is clear that again there is a lack of differential binding to MIBs of kinases known to be active after treatment with EGF or pervanadate (Figure 3.6C). There was no increase in binding of the kinases that had previously been seen to be activated by EGF stimulation. Similarly, there was no increase in the retention of tyrosine kinases shown to be indirectly activated by pervanadate.

At this stage, I started to consider why I couldn't emulate previous findings and whether it may be due to labelling technique I had used. The cells that I used had been labelled using SILAC. SILAC is advantageous because the label is introduced at the amino acid level. Multiple samples can be combined after lysis and therefore sample-sample variability is limited giving more reliable quantification (Geiger *et al.*, 2010). However, the original study employed iTRAQ to label samples (Duncan *et al.*, 2012a). iTRAQ differs from SILAC in that peptides are labelled post elution and digestion. I was concerned that I was unable to emulate the results from the previous study because the samples were mixed before loading onto the column. It was hypothesised that this could be due to cross-activation between samples when mixing lysates. I decided, therefore, to test a label-free approach using the MaxQuant software. This method would adjust for sample variation caused by running samples on

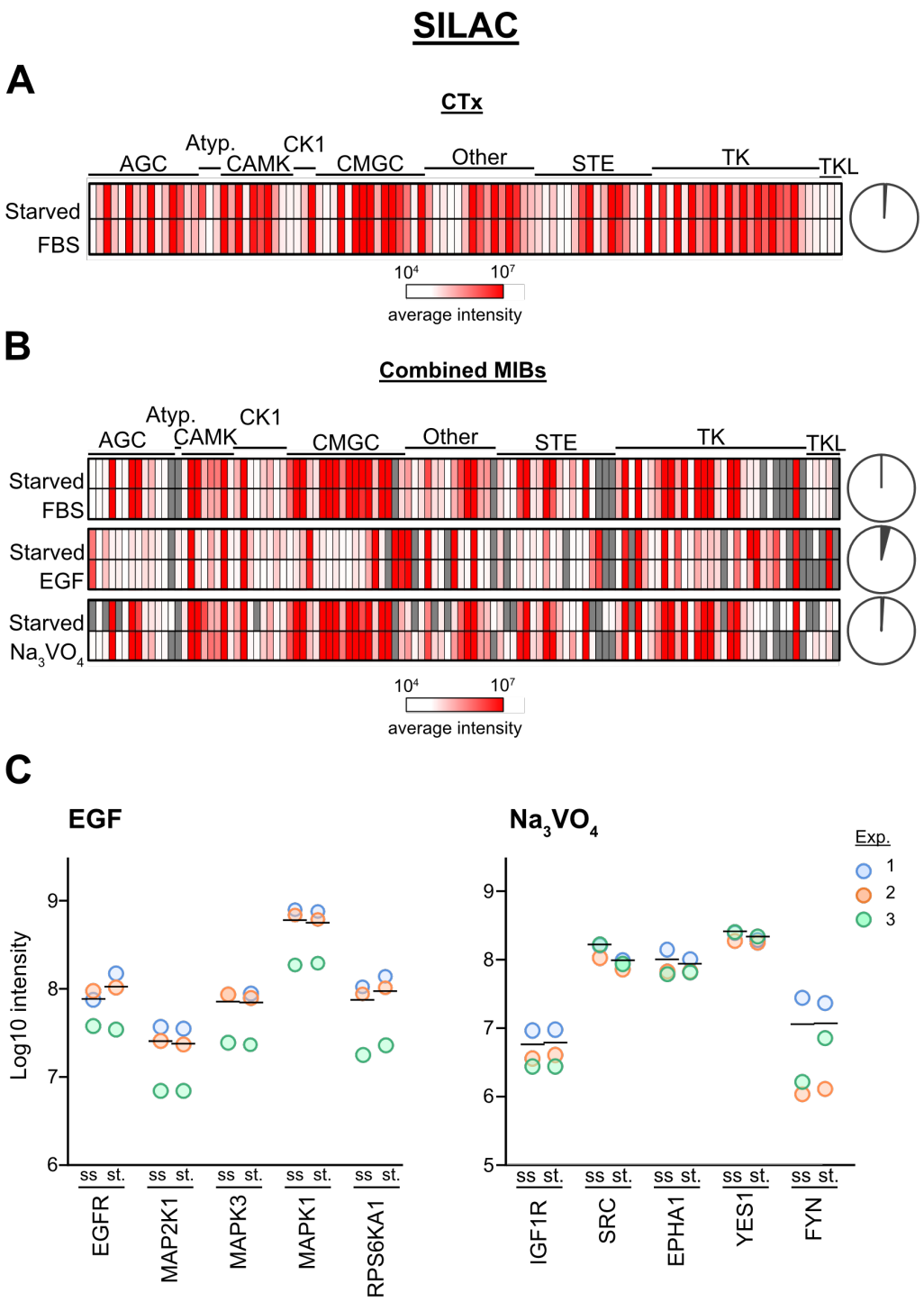

Figure 3.6. Binding proteins in SW48 cell extracts using SILAC

Data derived from MaxQuant illustrating there is no evidence of activation dependent binding following treatment of serum starved SW48 cells with serum, EGF or pervanadate. Heatmaps illustrating the kinase activation profile of SW48 cells employing A) CTx alone B) a combination of 6 MIBs (Bisindolylmaleimide, CTx-0294885, CZC8004, Purvalanol B, PP58, VI16832). The average intensities taken from 3 biological replicates were used to curate each heatmap. Pie charts show the ratio of kinases (grey) vs. non kinases (white) enriched under each experimental condition. C) Graphs showing the intensities of kinases in serum starved (ss) vs. stimulated (st.) cells. Kinases were selected based on expected activation changes in response to EGF stimulation and pervanadate treatment. Each data point represents the intensity from a single biological replicate.

separate columns but also solve the potential problem with cross-activation (Figure 3.7).

3.2.3.3. LABEL-FREE with CTx

Similar experiments were conducted using a label-free approach to see if there was evidence of differential binding in this context. Lysates that had been starved or stimulated with serum were ran over separate columns containing CTx only (Figure 3.7). Figure 3.7A, shows that there was differential kinase enrichment after cells were stimulated with serum. 82 out of the 90 kinases detected were deemed responsive however after closer inspection it was apparent that all intensities decreased after serum stimulation. This suggested that there was a decrease in the number of kinases bound to the column and therefore all responsive kinases were less active after stimulation. In this case it seems there may have been a problem with quantification. Label-Free Quantification (LFQ) relies on a population of peptides that minimally change between conditions for normalisation (Cox *et al.*, 2014). The software may be unable to carry out effective normalisation due to the relatively small number of proteins present within the enriched sample.

3.2.3.4. LABEL FREE with COMBINED MIBs

Subsequently, a label-free approach was tested using all six beads in combination. Similar to previous experiments, a comparison was made between the activity profiles of serum starved cells vs. cells treated with serum, EGF or pervanadate. In each case, there was a subset of responsive kinases that seemed to differentially bind to the column (Figure 3.7B). Unfortunately, increased binding of kinases known to be activated by EGF for pervanadate was not observed and therefore the I concluded that the differential binding we observed could not be entirely dependent on activation status (Figure 3.7C).

From this phase of experiments, I conclude that contrary to the previous studies, we are unable to use MIB/MS to profile the activation status of

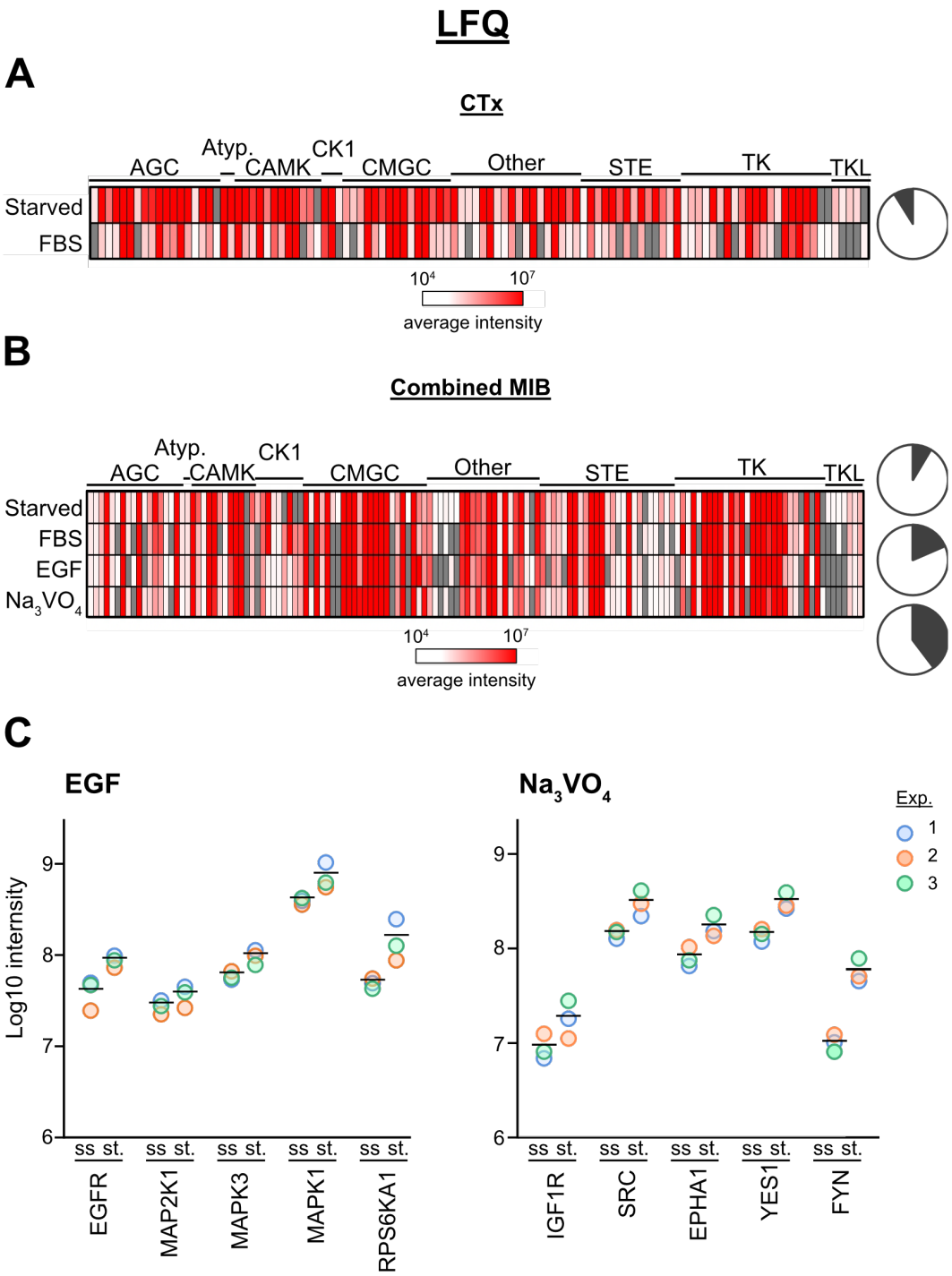

Figure 3.7. Binding proteins in SW48 cell extracts using LFQ

Data derived from MaxQuant illustrating there is no evidence of activation dependent following treatment of serum starved SW48 cells with serum, EGF or pervanadate. Heatmaps illustrating the kinase activation profile of SW48 cells employing A) CTx MIBs B) a combination of 6 MIBs (Bisindolylmaleimide, CTx-0294885, CZC8004, Purvalanol B, PP58, VI16832). The average intensities taken from 3 biological replicates were used to curate each heatmap. Pie charts show the ratio of kinases (grey) vs. non kinases (white) enriched under each experimental condition C) Graphs showing the intensities of kinases in serum starved (ss.) vs. stimulated (st.) cells. Kinases were selected based on expected activation changes in response to EGF stimulation and pervanadate treatment. Each data point represents the intensity from a single biological replicate.

individual kinases within the SW48 cell kinome regardless of bead type or labelling technique.

3.2.4. The MIB assay does not directly profile kinase activity in MDA-MB-231 cells.

In the original MIB/MS study, kinome activity and drug responsiveness was profiled in the TNBC cell lines, MDA-MB-231 and SUM159. (Duncan *et al.*, 2012a). SILAC labelled MDA-MB-231 cells were serum starved overnight and stimulated with 30ng/mL EGF for 15 minutes. Upon stimulation with EGF, there was a 10-fold increase in binding of EGFR to MIBs. Furthermore, there was increased binding of tyrosine kinases to MIBs following pervanadate treatment, however this was observed in Chronic Myeloid leukaemia cells.

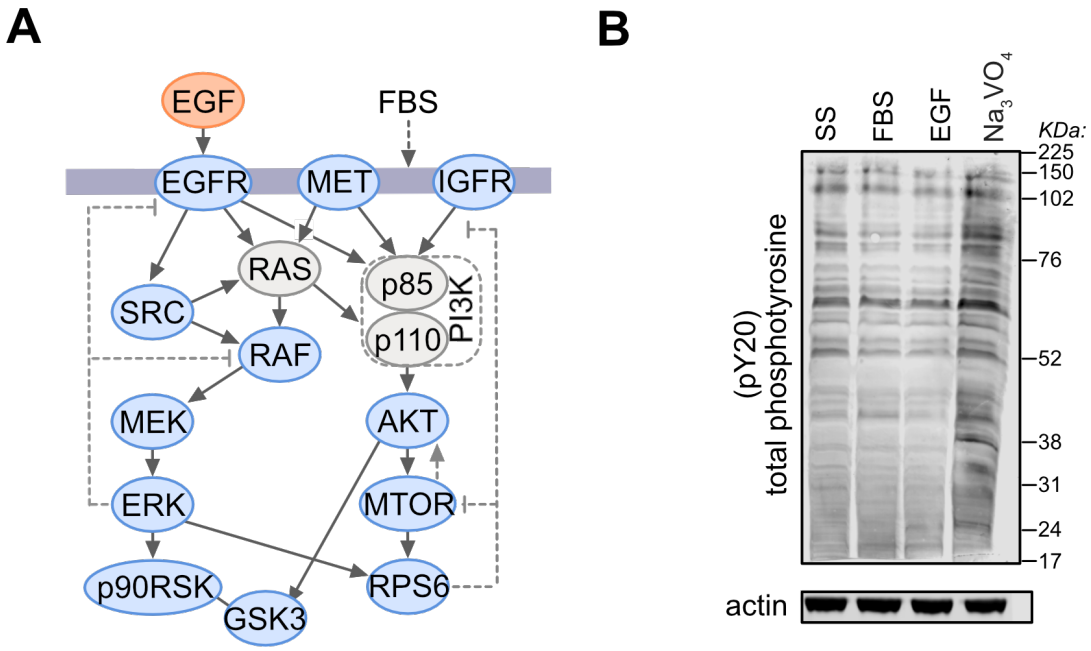

Figure 3.8. Signalling responses of MDA-MB-231 cells after treatment with serum, EGF or pervanadate.

A) A simplified outline of the Ras signalling network. Ras proteins utilise various downstream effectors to illicit many signalling responses. Upon activation by RTKs, Ras can activate both the MAPK and PI3K pathways promoting cell differentiation and proliferation. B) MDA-MB-231 cells were serum starved for 16hrs before treatment with 20% serum for 5 mins, 20ng/mL EGF for 5 mins or 100μM pervanadate for 15 minutes. Cells were subsequently lysed with RIPA buffer. Lysates were separated by SDS-page and western blots were probed with the indicated antibody.

Although I had not been able to profile activity in SW48 cells using MIB/MS, I decided to try to reproduce previous results in MDA-MB-231 cells. As before, the activation status of tyrosine kinases was confirmed by immunoblotting with a phospho-tyrosine (pY20) antibody (Figure 3.8B) and then, similar to previous experiments, I investigated to what extent kinase activity translated into MIB binding. Unfortunately, activation-dependent binding was not observed in MDA-MB-231 cells. There were no significant differences in kinase intensity after activation suggesting no differential binding in these cells (Figure 3.9). Furthermore, there was no significant increase of EGFR binding to MIBs after stimulation with EGF, nor retention of Tyrosine kinases to MIBs after treatment with pervanadate.

3.2.5. Pharmacological Kinase Inactivation does change affinity to MIBs

In the same study, the Johnson lab go on to demonstrate how the MIB/MS assay can be used as a tool to detect kinome reprogramming in response to targeted MEK inhibition (Duncan *et al.*, 2012a).

Firstly, using western blotting Johnson et al. showed a loss of ERK1/2 phosphorylation in TNBC cells treated with the MEK inhibitor, selumetinib for 4 hours. Reactivation of ERK1/2 was observed after treatment with the MEK inhibitor for 24 hours indicating that both TNBC cell lines circumvented MEK inhibition. MIB/MS was subsequently used to measure global kinome responses that occur after MEK inhibition. The assay reported an increase in binding of a group of receptor tyrosine kinases (RTKs) and it was hypothesised that this reprogramming could be responsible for resistance to MEK inhibition.

In SUM159 cells, the MIB/MS assay reported a clear increase in several RTKs such as: AXL, DDR1 and PDGFRb. However, there was a ‘less robust kinome response’ seen in the MDA-MB-231 cells, although a strong increase in PDGFRb binding was observed (Duncan *et al.*, 2012b). Unfortunately, we didn’t detect PDGFRb when we conducted the same MIB/MS experiment in our lab. This may have been due to sensitivity issues caused by using a different MS/MS instrument.

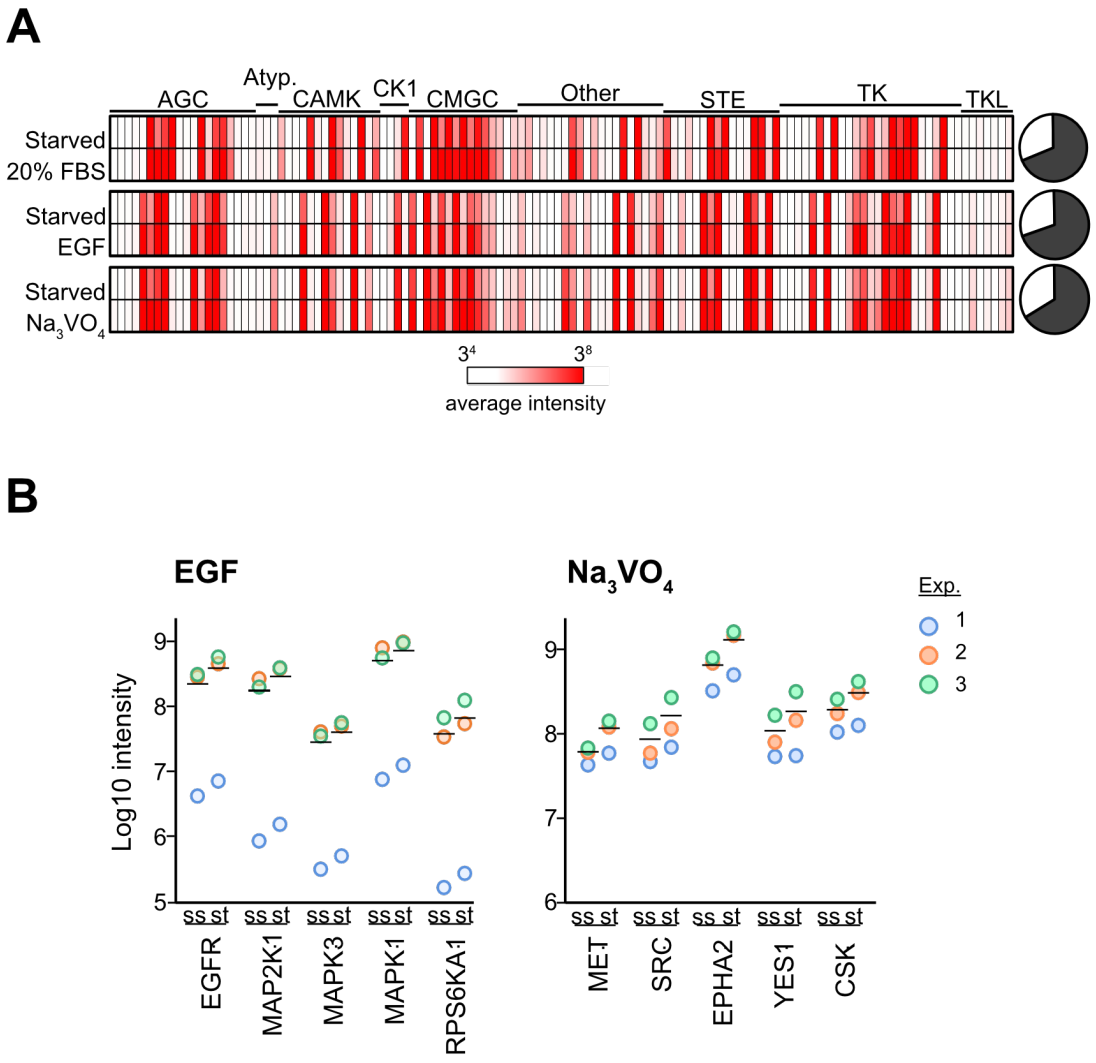

Figure 3.9. Binding proteins in MDA-MB-231 cell extracts

A) Data derived from MaxQuant illustrating there is no evidence of activation dependent following treatment of serum starved MDA-MB-231 cells with serum, EGF or pervanadate. Heatmaps illustrating the kinase activation profile of MDA-MB-231 cells using CTx alone. The average intensities taken from 3 biological replicates were used to curate each heatmap. Pie charts show the ratio of kinases (grey) vs. non kinases (white) enriched under each experimental condition. B) Graphs showing the intensities of kinases in serum starved (ss) vs. stimulated (st.) cells. Kinases were selected based on expected activation changes in response to EGF stimulation and pervanadate treatment. Each data point represents the intensity from a single biological replicate.

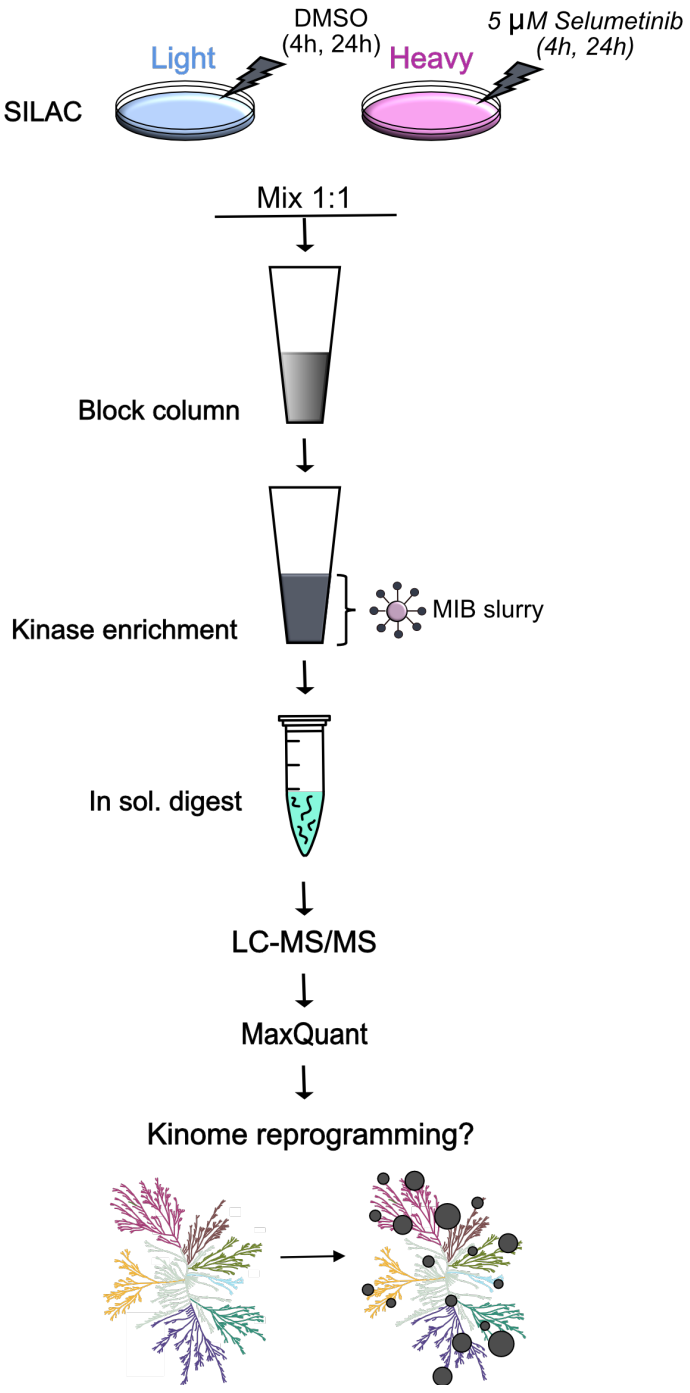

Figure 3.10. Overview of the workflow used to establish what kinome re-programming occurs in response to targeted inhibition of the Ras pathway.

The experimental strategy used to measure kinase activity of MDA-MB-231 cells following treatment with 5μM DMSO/Selumetinib (MEK inhibitor). SILAC labelling of MDA-MB-231 cells allows multiple samples to be ran in a single run. Total protein lysates were run over a block column, containing un-conjugated Sepharose beads, to promote non-specific binding of any highly abundant non-kinase proteins. The flow through passes onto an affinity column containing a mixture of MIBs. Kinases eluted from the column were trypsin digested in solution. Peptides are separated by Liquid-Chromatography (LC) and identified and quantitated by Tandem Mass Spectrometry (MS-MS). Analysis of the MS dataset is conducted using the MaxQuant software providing the possibility of predicting how cells circumvent inhibition of the Ras pathway.

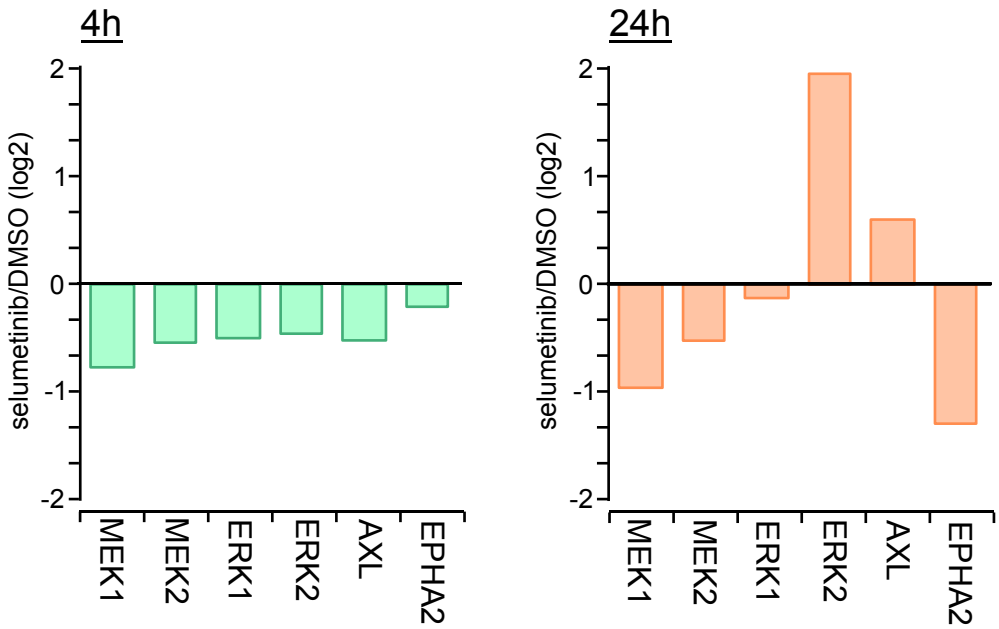

Figure 3.11. Evidence of activation dependent binding following targeted MEK inhibition in MDA-MB-231 cells.

MDA-MB-231 cells were serum starved for 16hrs before treatment with 5μM DMSO/Selumetinib for 4hrs or 24hrs. Graphs showing the quantitative changes in MIB binding as a log2 ratio of inhibitor treated cells/DMSO treated cells. Average intensities taken from three biological replicates were used to calculate a ratio for each kinase.

Figure 3.11 shows data derived from in-house MIB/MS experiments assessing kinome responses after MDA-MB-231 cells were treated with Selumetinib for 4h or 24h. Similar responses to the original study are observed for MEK1/2 at both time points. Furthermore, reactivation of ERK2 is seen after prolonged MEK inhibition. There is also a decrease of EPHA2 binding in our assay which was another significant response recorded in the original study.

It important to note that Duncan et al. reported a significant increase in expression of the RTK, AXL, in SUM159 cells, however they were unable to detect AXL in MDA-MB-231 cells using MIB/MS (Duncan *et al.*, 2012a). In our experiments, we were able to identify and detect an increase in AXL expression in MDA-MB-231 cells after 24h treatment. AXL was one of the 32 kinases unique to our dataset and it is probable that we were able to detect AXL as we used CTx alone and not a combination of beads.

In conclusion, we were able to reproduce some of Johnson et al. findings in the lab but due to a lack of responsiveness of the MDA-MB-231 cells, it would have been useful to conduct the experiments using SUM159 cells to provide a clearer insight into reprogramming in response to MEK inhibition.

3.3. Summary of results

- The MIB/MS assay has been successfully established and optimised in our lab to enrich kinases from cell lysates.
- Enrichment is a measure of protein abundance and/or activity
- It is unclear as to whether responses are indicative of changes in protein abundance or activity therefore further validation is required to discriminate between each possibility.

3.4. Discussion

The aim of this chapter was to establish the MIB/MS assay in the lab and to determine whether the assay reports changes in kinase activity. The method was successfully established in the lab and several stages of optimisation were carried out to achieve optimal kinase enrichment.

Whilst I was able to clearly enrich kinases from cell lysates (Figure 3.3), I struggled to obtain any evidence that MIB-binding was sensitive to the activation status of individual kinases. This included when I directly reproduced key elements of the experiments performed by the Johnson lab using the same cell line (Figure 3.9) and the same MIB bead composition (Figures 3.6 & 3.7). Although several early studies claimed that MIB beads capture kinases in their active conformation and therefore the assay has the ability to measure global kinome activation changes in response to stimuli or inhibitors (Johnson *et al.*, 2013; Stuhlmiller, Earp and Johnson, 2014; Cooper *et al.*, 2013), this notion was challenged by the Kuster lab, who suggested that MIB binding was largely independent of kinase activation state (Ruprecht *et al.*, 2015). Notably, the

Kuster lab found no evidence of increased binding of kinases known to be activated by pervanadate treatment and responsive kinases lay across all the kinase families (Ruprecht et al 2015. These findings are consistent with the data presented in this chapter.

A feature of all of these early studies is that they perform a large-scale MIB screen followed by very selective follow-up of individual kinases. They then generalise the observations made with these select few kinases to make their wider point in support or opposition to the notion that MIBs report kinase activation status across the entire kinome. Given the timing of these publications close to the beginning of my project, we approached the interpretation of MIB data with caution and were not necessarily surprised by the negative data that was generated.

Interestingly, in a more recent review discussing methods to study the kinome, Gary Johnson and co-authors address and support the contradictory findings presented in the Kuster publication and proceed to discuss the limitations of the assay (Cann *et al.*, 2017). It seems that the capability of the MIB/MS assay to profile kinome activity was previously overstated. It is now generally accepted that activation-dependent binding to MIBs depends on three main factors:

- the level of expression of a kinase in the cell
- kinase affinity to MIBs
- kinase conformation or activation status

Authors agree that the assay mainly reports changes in kinase abundance and in limited cases changes in kinase activity (Cann *et al.*, 2017; Ruprecht *et al.*, 2015). Evaluating the findings from this chapter also led me to the same conclusion; I found that a kinase was more likely to be detected by LC/MS/MS if it was more abundant in the cell lysate and that activation dependent binding was rare. It is also important to note that whether or not a true activation change can be detected depends on the proportion of active vs. inactive kinase in the cell lysate. In summary, the method is useful for looking at differential expression at the protein level; whilst evidence has been presented suggesting

that a fraction of the kinases captured on the column show activation dependent binding, this needs to be assessed on a case-by-case basis.

The data presented in the Kuster publication, helps us to appreciate that, whether or not kinase activation status is reported depends on the bead type and conformation status of the kinase. The efficiency of nine different inhibitor beads to bind kinases known to be activated by pervanadate treatment were evaluated; These included some of the MIBs used in the original study (Ruprecht *et al.*, 2015; Duncan *et al.*, 2012a). Consistent with my findings, there was a large degree of overlap in kinase specificity between different bead types. However, surprisingly each kinase was differentially bound to each bead after pervanadate treatment. For example, pervanadate treatment caused an increase in binding of EGFR to one bead and loss of binding to another (Ruprecht *et al.*, 2015). This indicates that MIBs can bind kinases in their active and inactive states and that there is bead conformation specificity. Gary Johnson presented data in a recent review supporting this premise (Cann *et al.*, 2017). The data showed that the capture of EGFR after EGF stimulation is dependent on bead type. As expected, an increase in EGFR capture to some MIBs such as PP58 and Purvalanol was observed; however, there was no increase in EGFR binding to the MIB CTx. This suggests that CTx preferentially binds EGFR in the inactive conformation; again, this is consistent with my findings. In the same study, it was shown that when CTx was added into a mixture of beads, it was enough to mask any increase in EGFR binding that would have been reported by the other beads alone (Cann *et al.*, 2017). Bead conformation specificity means that using a combination of beads in a single assay could obscure any potential activation dependent binding. The readout from a MIB correctly reporting a change in kinase activation state could be supressed by a MIB that preferentially binds kinases in their inactive state. I also found that there was no benefit in using several beads in combination and I decided to use the single MIB, CTx, going forward as it provided the best coverage of the kinome.

Whilst I was writing this chapter, it seems that the viewpoint on how the MIB/MS assay can be used to study the kinome has shifted. Many people,

including Gary Johnson have revoked claims that MIB/MS can report 'en masse' kinome activation changes (Cann *et al.*, 2017). A recent paper was published by the Duncan group, reporting kinome reprogramming in response to MEK inhibition in ovarian cancer (Kurimchak *et al.*, 2019). Although the study is very similar to the original TNBC study, there is no mention of activation-dependent binding throughout the paper (Kurimchak *et al.*, 2019; Duncan *et al.*, 2012a). Instead, the group integrated RNAseq and MIB/MS datasets to build a 'kinome signature' and any interesting hits were investigated further. Kuster also contributed to a recent paper that used a MIB pulldown to study the kinome in NSCLC cells (Mulder *et al.*, 2018). The paper combined proteome, kinome and phosphoproteome data to profile resistance to EGFR therapy.

Considering what we know now, I propose to use the MIB/MS assay in combination with other approaches to profile the kinome in RAS mutant cells. The MIB assay reports expression and/or activity of kinases; therefore, to discriminate between these possibilities we will pair it with a kinome gene expression screen. By integrating the two datasets I may be able to infer likely activation changes. However, it is important to note that a negative correlation between the two datasets could be due to other post translational modifications therefore it will be imperative to validate any responses by western blot where phospho-antibodies are available.

Chapter 4 : Profiling the kinome in Ras mutant cells

Most understanding of RAS isoform biology has derived from ectopic expression experiments. The studies describe preferential coupling of each isoform with key Ras effector pathways. KRAS was shown to be a more potent activator of the MAPK pathway whereas HRAS and NRAS were shown to more potently activate the PI3K pathway (Yan *et al.*, 1998; Voice *et al.*, 1999). This is in contrast to findings from studies using cell lines or mouse models with endogenously expressed mutant RAS; Very little evidence of preferential coupling to Ras effectors was presented suggesting that RAS signalling is more context dependent (Tuveson *et al.*, 2004; Omerovic *et al.*, 2008). It is now appreciated that ectopically expressed RAS proteins are often produced at supraphysiological levels and this can lead to mislocalisation or premature senescence (Serrano *et al.*, 1997). Thus, there is a general consensus that studying endogenous signalling in cells where endogenous levels of RAS are expressed is more desirable.

An isogenic panel of SW48 colorectal cancer cell lines have been developed to study endogenous RAS signalling. rAAV mediated homologous recombination was used to introduce different activating RAS mutations at the endogenous loci, in SW48 cells that otherwise have the same genetic background. Phosphoproteomic analysis of a panel of SW48 cell lines harbouring different activating mutations, at codons 12 or 13 of the KRAS gene, revealed that each mutant displays a unique signalling signature. Furthermore, codon 12 specific upregulation of kinases such as DCLK1 and MET was observed (Hammond *et al.*, 2015). Moreover, a recent study using a panel of SW48 G12V wild-type and mutant cells revealed that despite displaying significant Ras activation, the outputs directly downstream of oncogenic Ras mutants were minimal in the absence of growth factor inputs (Hood *et al.*, 2019).

Taking this into consideration and coupled with the fact that the RAS network is enriched in kinase effectors, I propose to conduct a kinome-wide analysis of RAS signalling using a panel of isogenic SW48 cell lines. We used a novel isogenic panel that includes SW48 cell lines harbouring different activating RAS mutations of the KRAS, HRAS and NRAS genes. By studying differential kinome responses of the individual mutants, we hope to gain a better understanding of the mechanisms underpinning both isoform and mutation specific RAS signalling.

535 kinases are encoded by the human genome (Wilson *et al.*, 2018). The NanoString nCounter platform allows gene expression analysis of 528 kinases therefore providing coverage of over 98% of the human kinome (Figure 2.1). Using the nCounter technology, I will be able to define the SW48 expressed kinome. Furthermore, analysis will reveal distinct kinome gene expression signatures of each mutant cell line. Subsequently, I will use MIB/MS to profile kinome responses at the protein level (Figure 2.5). The combination of methodologies allows large scale profiling of kinome expression and in some cases kinome activity; by integrating the two datasets, we may be able to infer likely protein expression versus activation changes within the kinomes of Ras mutant SW48 cells. The data generated from these global kinase assays will identify nodes sensitive to isoform and mutation specific Ras signalling.

4.1. Objective

The objective of this chapter is to understand the differential signalling occurring downstream of common RAS mutations. To achieve this, I aim to profile the kinome at both the transcript level and protein level in the isogenic SW48 panel. Finally, I will integrate the two datasets to reveal unique kinome signatures of each individual mutant cell line.

4.2. Results

4.2.1. NanoString analysis defines the expressed SW48 kinome and identifies differential kinome transcript signatures in SW48 isogenic cells

Using the NanoString nCounter platform, we were able to define the expressed SW48 cell kinome. The analysis indicates that SW48 cells typically express 362 kinases, representing 68% of the human kinome. Figure 4.1A displays the total expressed kinome and the proportion of kinases that are 'responsive' in SW48 mutant cells; Responsive can be defined as a 2-fold increase or decrease in gene expression in at least one mutant cell line compared to the Parental cell line. Of the 362 kinases expressed in the SW48 isogenic panel, 40 were responsive. This indicates that approximately 11% of the expressed kinome is differentially expressed upon the introduction of an activating RAS mutation into the parental SW48 cell line.

To examine the responsive subset in more detail, I considered the coverage of responsive kinases across the individual kinase families and the individual mutant cell lines (Figures 4.1B). The responsive subset is distributed across the majority of the kinome, although there is a notable enrichment of responsive kinases in the Tyrosine kinase (TK) family (Figure 4.1B). Figures 4.2C and D, illustrate the distribution of responsive kinases across the individual mutant cell lines. There are kinases unique to each cell line harbouring a G12V mutation, thus providing evidence of isoform specific kinome responses. However, the N12V cell line has notably less responsive kinases than the other isoforms, suggesting that kinase signalling in the NRAS mutant is relatively unchanged in comparison to the parental cell line. Furthermore, there is evidence of mutation specific signalling; Responses unique to each KRAS mutant cell line harbouring a different codon mutation were observed. It is important to note, that there is a marked increase in unique responses in the K12D cell line compared to the other KRAS mutant cell lines and it is, in fact, the most responsive cell line across the panel. In addition to isoform and mutation specific responses, responses shared amongst the mutant cell lines were observed. However, at this stage, it was impossible to

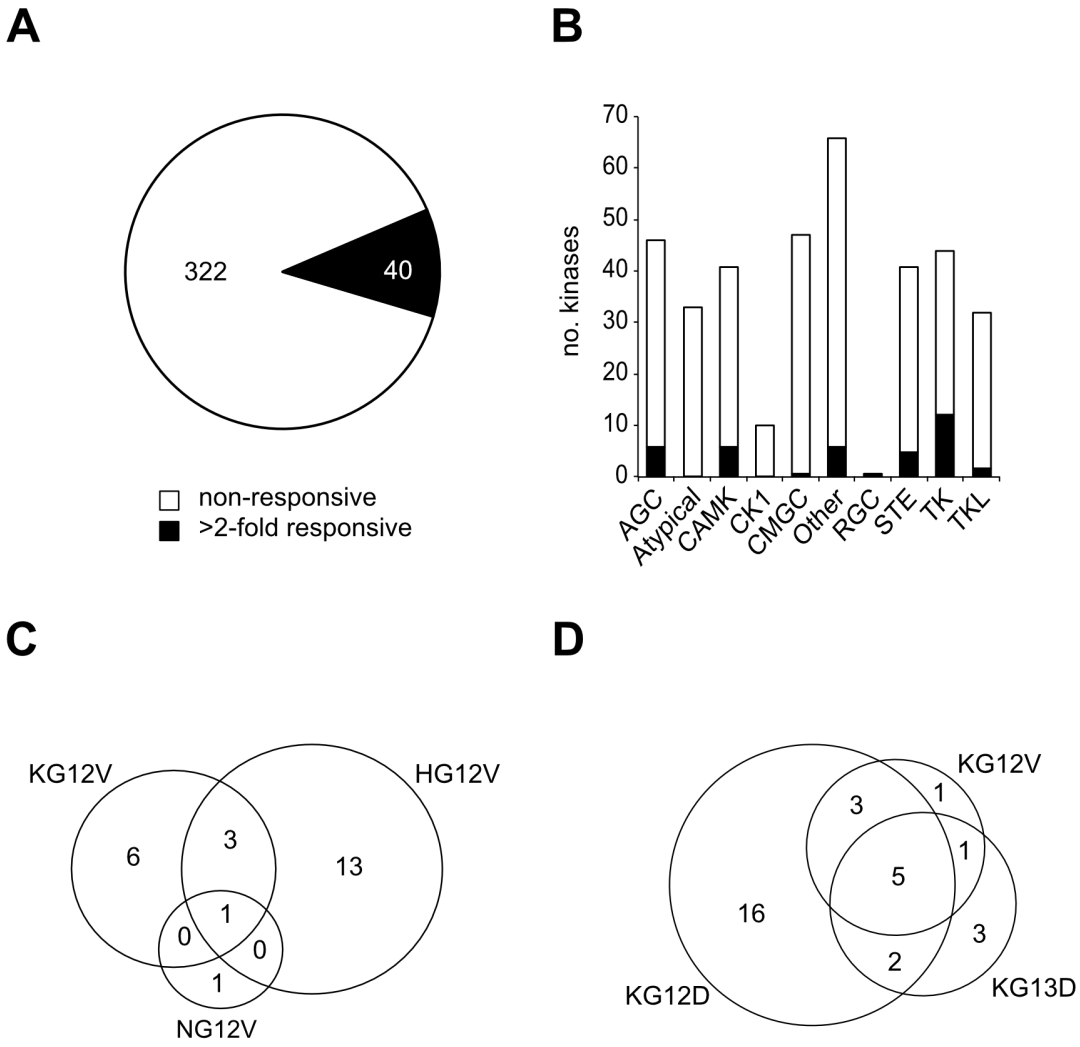

Figure 4.1. The kinase transcriptome of isogenic SW48 cells harbouring different RAS codon mutations

A) NanoString analysis reveals 362 kinases are expressed in SW48 cell lines. A subset of 40 kinases show differential expression in RAS mutant cells compared to Parental SW48 cells, based on a 2-fold change in expression. B) The bar chart displays the coverage of responsive and non-responsive kinases across the individual kinome families. C and D) Venn diagrams illustrate the overlap of responsive kinases between the different mutant RAS cell lines.

distinguish whether there was the same directional change in expression of these kinases across all mutant cell lines.

Hierarchical clustering of the responsive subset was performed to analyse the pattern of expression across each cell line (Figure 4.2A). Cell lines and genes were clustered based on the ratio (log2) of kinase expression in the mutant cell line vs. parental cell line. Interestingly, the KRAS mutant cell lines cluster together, away from the HRAS and NRAS cell lines. This indicates that the shared responses observed between the KRAS mutant cell lines follow a similar pattern of expression. Furthermore, within the KRAS mutant cell lines, the codon 12 mutants cluster together, away from the codon 13 mutant. The HRAS and NRAS mutant cell lines cluster together but don't appear to share the same degree of similarity that is observed in KRAS mutant cell lines.

On the whole, there are very few pan-RAS responses; Very few kinases have the same pattern of expression across all mutant cell lines. The most striking pan-responsive kinase is TRIB3, a pseudokinase which is significantly downregulated in all five mutant cell lines. In line with the background rate of expression in the human kinome (Wilson *et al.*, 2018), pseudokinases represent 10% of the expressed SW48 kinome. Five out of the 40 responsive kinases were pseudokinases. This suggests that despite lacking enzyme activity, this group of kinases may have a role in the regulation of oncogenic Ras signalling. Considering the lack of pan-RAS responses, I speculated whether or not the responsive kinases lay within the immediate RAS network. Taking into account the dogma derived from ectopic studies, I would have expected some common responses directly downstream of the oncogenic RAS mutants (Yan *et al.*, 1998; Voice *et al.*, 1999). For example, upregulation of nodes in the MAPK and PI3K pathways in the KRAS mutants and HRAS mutant respectively. However, only 1/10th of the responsive kinase subset lay within the direct RAS network (Figure 4.2B). Moreover, none of the responsive RAS related kinases show a pan-RAS response and are only defined as responsive in one or two mutant cell lines.

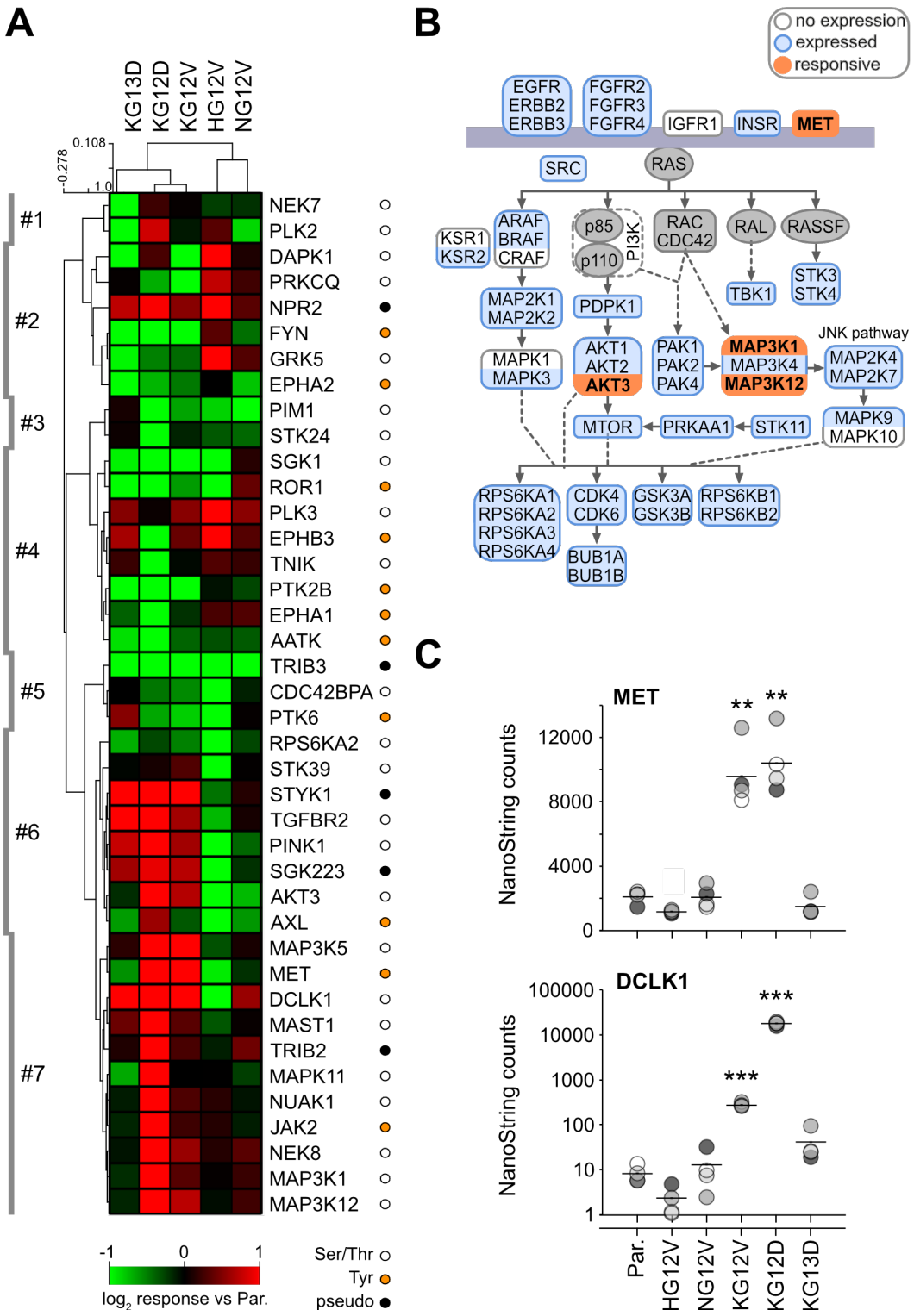

Figure 4.2. The responsive kinase transcriptome

A) Heatmap displaying responsive kinases; Responsive can be defined by a 2-fold change in gene expression in at least one mutant cell line vs. parental SW48 cell line. Responsive kinases are clustered by cell line and relative transcript changes. B) A simplified outline showing the responses within the immediate Ras network. Responsive kinases are highlighted in orange, unresponsive kinases are highlighted in blue and any kinases that are not expressed are left unshaded. C) The scatter plots show the raw counts of two kinases, DCLK1 and MET, used as positive controls. The graphs display counts for each kinase taken from four biological replicates.

As previously reported, a codon 12 specific upregulation of MET was observed in the KRAS mutant cell lines (Figure 4.2C) (Hammond *et al.*, 2015). Similarly, the kinase DCLK1 was significantly upregulated in the KRAS codon 12 mutant cell lines, again consistent with previous findings. MET and DCLK1 served as positive controls in our NanoString experiments and provided confidence in the other observed kinome responses.

Deeper differential expression analysis was conducted using the NanoString advanced analysis software, providing an insight into which responses were statistically significant. The software used statistical t testing to calculate a p-value for each kinase and the Benjamini-Hochberg method was applied to reduce the False Discovery Rate (FDR) (see section 2.3.7). The volcano plots in figure 4.3 the results of the differential expression analysis. The fold change (log2 ratio mutant/parental) and p value is displayed for each kinase. Highly statistically significant kinases fall above the p-value threshold ($p<0.05$) and differentially expressed kinases fall either side of the plot. The most statistically significant kinases are labelled for each mutant cell line. Any kinases that fell below the threshold, highlighted in grey, were removed from the responsive subset going forward. For example, initial analysis indicated that there were two differentially expressed kinases in the N12V line, however, this was reduced to 0 after statistical testing (Figure 4.3).

K12D/PAR

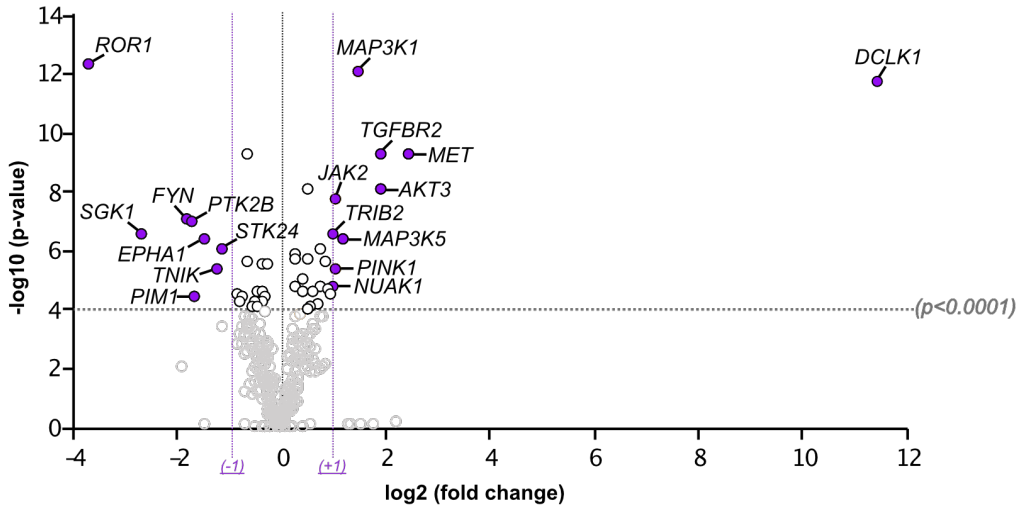

K13D/PAR

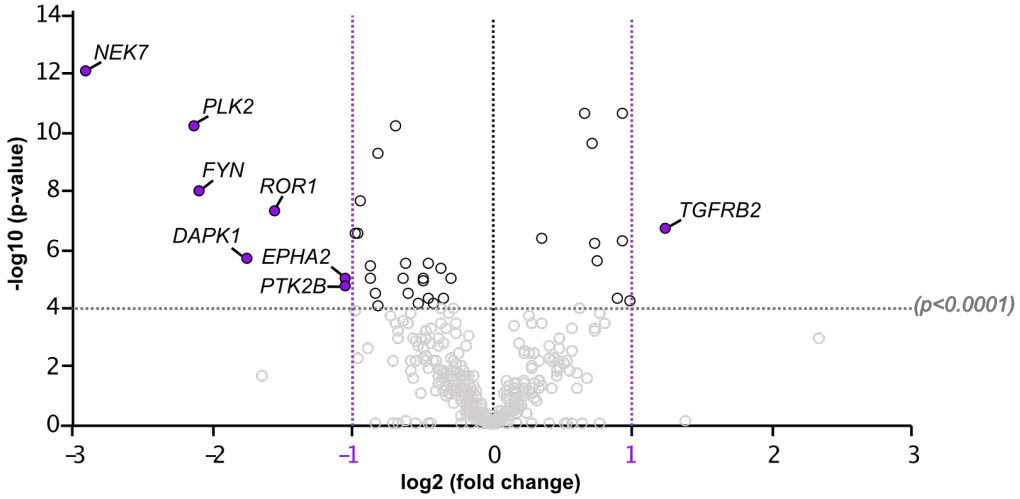

K12V/PAR

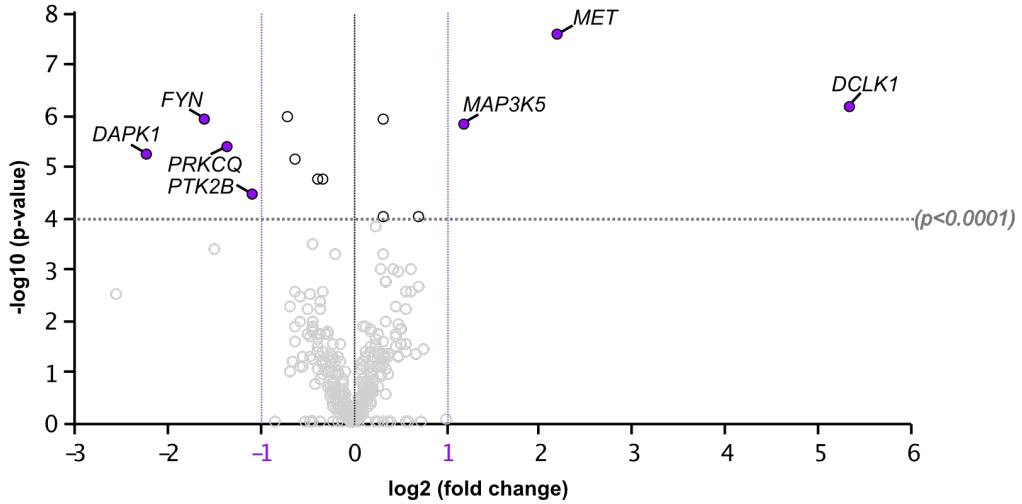

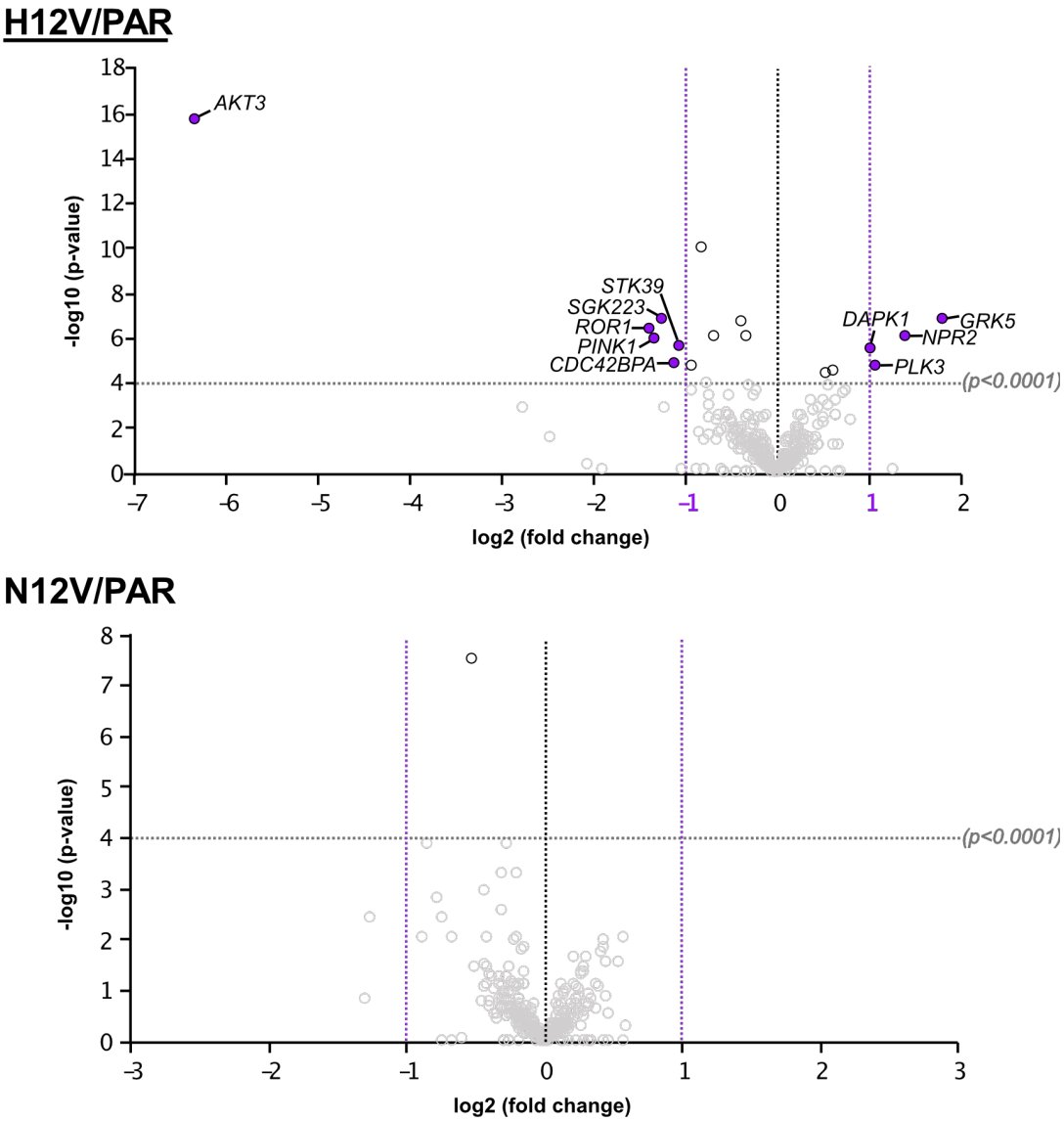

Figure 4.3. Differential gene expression analysis of isogenic SW48 cells harbouring different RAS codon mutations

The volcano plots display each kinase's log10 (p-value) and log2 fold change for mutant vs. parental SW48 cells. The most statistically significant kinase genes are labelled and highlighted in purple. (p<0.0001).

4.2.2. MIB/MS analysis reveals a subset of kinases that show differential protein expression in SW48 isogenic cells

Since transcript abundances only partially predict protein abundance (Schwanhäusser *et al.*, 2011), it was also essential to understand whether differential kinome protein expression also occurs (de Sousa Abreu *et al.*, 2009).

Using MIB/MS we were able to define and quantitate the expression of approximately 50% of the expressed SW48 kinome (Figure 4.4A). Of the 177 kinases pulled down by MIBs, 56 were defined as responsive; Responsive can be defined as a 2-fold increase or decrease in protein expression in at least one mutant cell line compared to the Parental cell line.

Similar observations can be made between the NanoString responsive dataset and the MIB responsive dataset: The MIB/MS responsive subset is distributed across every kinase family and again a notable enrichment of responsive kinases within the Tyrosine kinase family was observed (Figure 4.4B). Furthermore, there is evidence of isoform and mutation specific responses at the protein level. No shared responses were observed between the G12V mutant cell lines thus, providing evidence of isoform specific signalling (Figure 4.4C). Mutation specific responses were also observed amongst the KRAS mutant cell lines. Coinciding with the transcriptome data, the K12D mutant cell line was the most responsive mutant cell line; The K12D mutant had the greatest number of unique responses within the KRAS mutant cell lines together with the greatest number of overall responses seen across the panel of mutant cell lines. It is also important to note, that despite displaying no differential expression of kinases at the transcript level, the N12V mutant cell line harboured several responsive kinases at the protein level (Figure 4.4C).

Hierarchical clustering of the responsive subset was performed to analyse the pattern of expression across each cell line (Figure 4.5A). Cell lines and genes were clustered based on the ratio (log2) of kinase expression in the mutant cell line vs. parental cell line. Contrary to the NanoString responsive subset, the

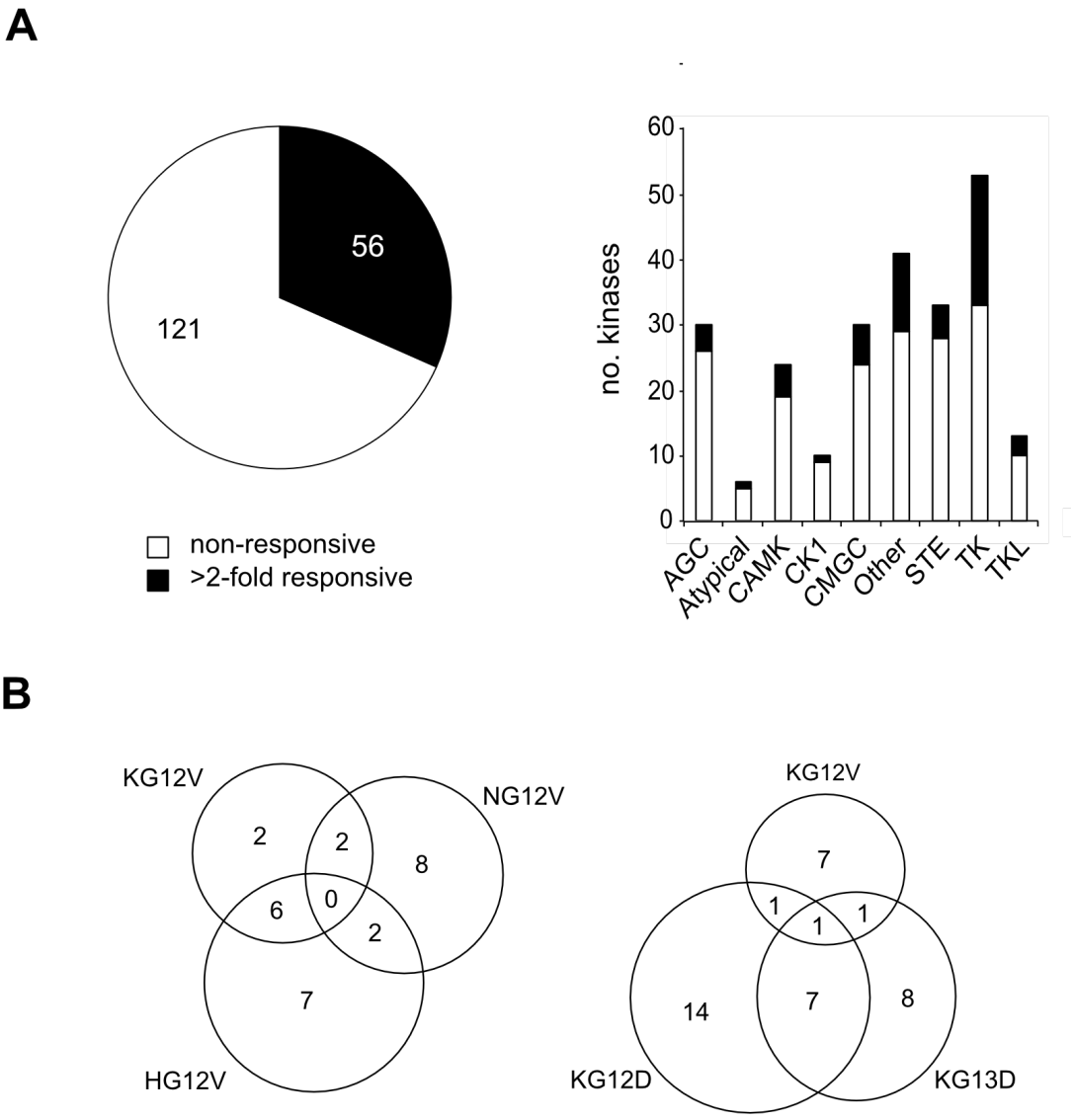

Figure 4.4. The protein kinome of isogenic SW48 cells harbouring different RAS codon mutations

A) MIB/MS enriched 177 kinases from SW48 cells. A subset of 56 kinases show differential expression in RAS mutant cells compared to Parental SW48 cells, based on a 2-fold change in expression. The bar chart displays the coverage of responsive and non-responsive kinases across the individual kinome families. B) Venn diagrams illustrate the overlap of responsive kinases between the different mutant RAS cell lines.

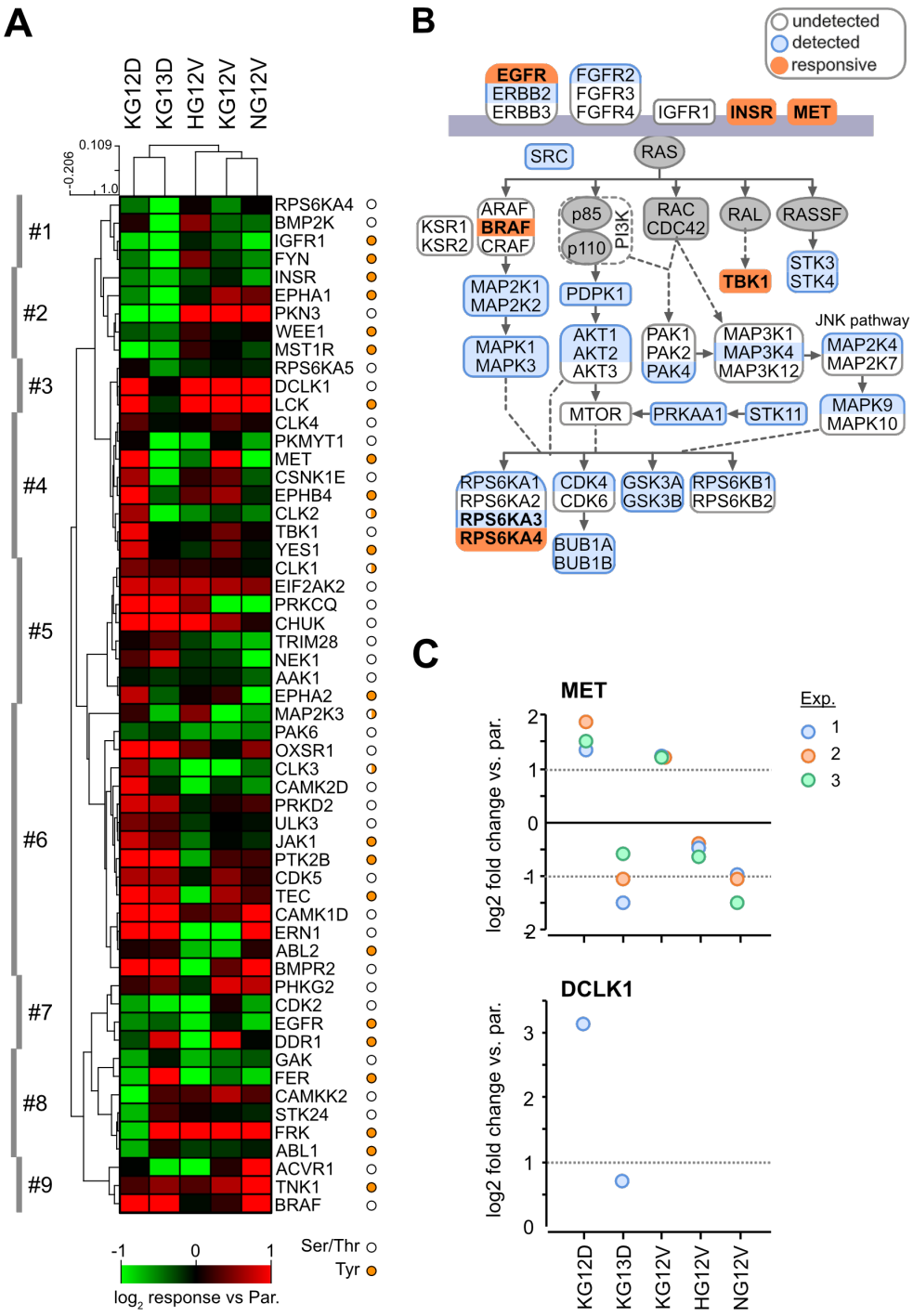

Figure 4.5. The responsive protein kinome

A) Heatmap displaying responsive kinases; Responsive can be defined by a 2-fold change in protein expression in at least one mutant cell line vs. parental SW48 cell line. Responsive kinases are clustered by cell line and relative changes in protein expression. B) A simplified outline showing the responses within the immediate Ras network. Responsive kinases are highlighted in orange, unresponsive kinases are highlighted in blue and any kinases that were not detected by MIB/MS are left unshaded. C) The scatter plots show the ratios log2 fold change (mutant/parental) of two kinases, DCLK1 and MET, used as positive controls. The graphs display ratios for each kinase taken from three biological replicates.

MIB/MS responsive subset cluster based on type of amino acid mutation rather than clustering in an isoform specific manner. All three isoforms harbouring a G12V mutation cluster together away from the two KRAS mutants harbouring an aspartic acid (D) mutation. Once more, there are very few pan-RAS responses across the mutant cell lines and very few responsive kinases that lie within the immediate RAS network (Figure 4.5B). As with the transcriptome responsive subset, only 1/10th of the responsive MIB/MS kinase subset lay within the immediate RAS network. Although there is a similar proportion of responsive kinases within the network in both datasets, only one kinase that was defined as responsive at the transcript level was detected by MIB/MS, so we are unable to correlate the pattern of responses across the two datasets.

MET was the only kinase within the RAS network that showed the same pattern of response at the transcript level and the protein level. The same codon 12 specific upregulation was observed in the KRAS mutant cell lines using MIB/MS (Figure 4.5C). In SW48 cells, MET expression is significantly upregulated in the K12D mutant vs. parental cells when they are serum starved, and downstream activity is induced by HGF stimulation (Figure 4.6). This suggests that MET upregulation is due to MET receptor overexpression rather than elevated levels of its ligand, HGF. Upregulation of DCLK1 was also observed in the K12D mutant cell line, although the kinase was only detected in one out of three biological replicates (Figure 4.5C).

4.2.3. Integrating transcript and protein kinase datasets reveals differential expression vs. activity profiles in Ras mutant cells

Using MIB/MS, we were able to profile 49% of the expressed SW48 kinome (Figure 4.7A). A larger proportion of the expressed kinome was defined as responsive at the protein level compared to the transcript level (Figure 4.7B). Moreover, there were very few common kinase responses across the two datasets (Figure 4.7B). The lack of commonalities between the two datasets is unsurprising considering it was previously shown that transcript abundance only partially predicts protein abundance; It is estimated that only ~40% of protein concentrations correlate with mRNA concentrations and that the

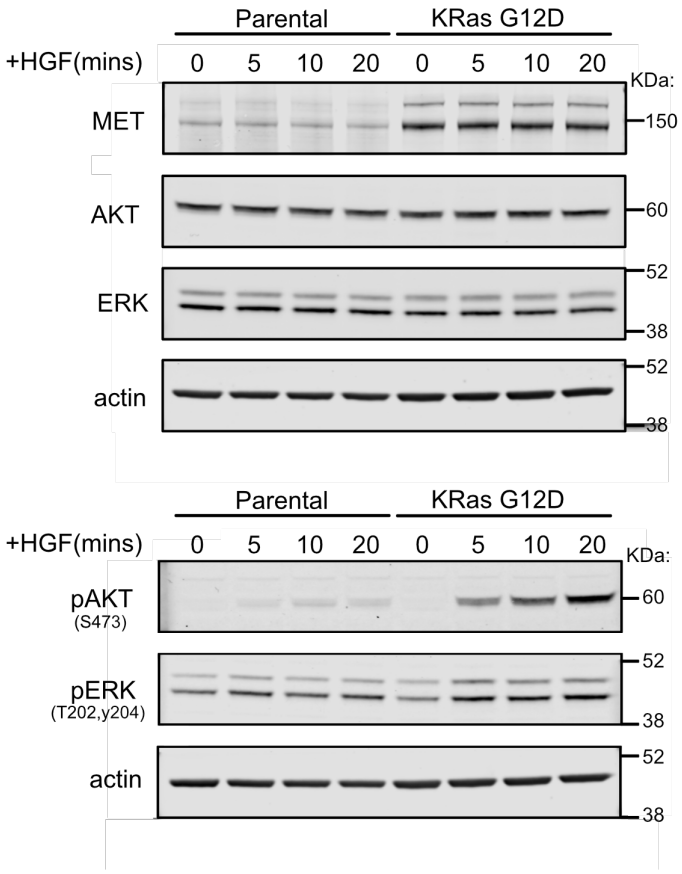

Figure 4.6. MET signalling in SW48 wild-type and KRAS G12D mutant

SW48 parental and K12D mutant cells were serum starved for 16hrs before treatment with HGF for 0, 5, 10, 20 mins. Cells were lysed with RIPA buffer. Lysates were separated by SDS-page and western blots probed with the indicated antibodies.

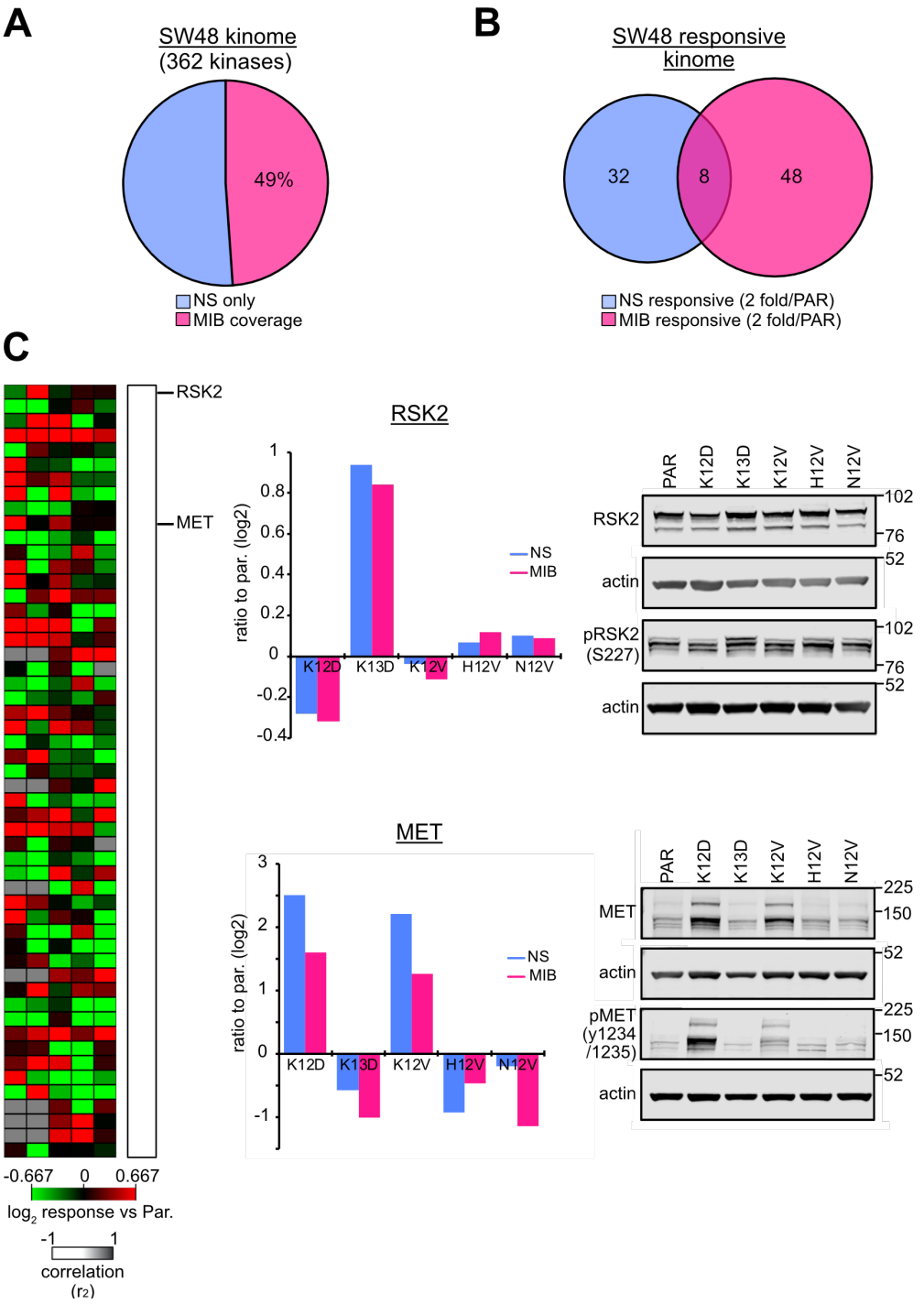

Figure 4.7. Correlation analysis between the NanoString and MIB/MS SW48 kinome datasets

A) The Venn diagram shows the number of expressed kinases defined by NanoString analysis vs. the number of kinases captured and identified by MIB/MS. B) The Venn diagram shows the overlap between kinases that were defined as responsive at the transcript level and at the protein level. C) A correlation analysis was carried between the responsive NanoString and MIB/MS datasets. Kinases were included if they were detected by MIB/MS and were defined as responsive. The heatmap displays all data included in the analysis. The heatmap is ranked based on correlation coefficient and the scale bar indicates the degree of correlation between the two datasets. Graphs show examples of kinases with high correlation coefficients; transcript (blue) and protein (pink) level responses are mapped across each cell line. Western blots were used for validation of the observed responses.

remaining 60% can be attributed to post transcriptional regulation (de Sousa Abreu *et al.*, 2009). It is now appreciated that protein abundance depends not only on mRNA concentration, but almost equally on regulatory mechanisms occurring after mRNA production. These include post translational modifications, translation efficiency and protein degradation of the existing protein (Vogel and Marcotte, 2012).

Going forward, I decided to consider what was significantly changing between the datasets, but more importantly, consider the pattern of mRNA expression vs. protein expression in order to build more a comprehensive kinase signature.

A correlation analysis was conducted between the NanoString and MIB/MS datasets to gain a clearer understanding of the differentially expressed kinome and how it may potentially be regulated (Figure 4.7C). Using the CORREL function in Microsoft excel, a correlation coefficient value was generated that indicates how closely related expression of a kinase was at the transcript vs. protein level. Kinases were included in the correlation analysis if they were detected by MIB/MS and were defined as responsive. There also needed to be a sufficient number of related pairs across the two datasets to generate a correlation coefficient. The heatmap in figure 4.7C displays the MIB/MS responsive data that met these criteria and was therefore included in the analysis. Kinases are ranked by correlation coefficient and the scale bar indicates the degree of correlation between the two datasets. A correlation coefficient of +1 indicates perfect correlation between the expression of a kinase at the transcript level and -1 indicates inverse expression.

Two examples of kinases with a high correlation coefficient were RSK2 and MET (R^2=0.99 and 0.93 respectively). The graphs in Figure 4.7C display the (log2) ratios of mutant vs. wild-type expression, at the transcript level (NS) and at the protein level (MIB). For both kinases, there is a high degree of correlation between the ratios generated from the NanoString and MIB/MS assays across all cell lines. Here, it is likely that transcript abundance is the main determinant

for protein abundance, and therefore provides an example of how the MIB column can report differential kinase expression across the mutant cell lines.

In each case, western blotting was used to confirm protein responses. It is important to note that changes in protein abundance can also correspond with changes in the amount of phosphorylated protein; If there is a larger pool of protein, a higher proportion may be available for phosphorylation. For example, elevated expression of RSK2 was observed in the K13D cell line at both the transcript level and at the protein level. Western blotting confirmed an increase in total RSK2 expression in the K13D cell line however the same elevation of p-RSK2 expression was also observed. The phospho-specific antibody detects RSK2 when it is phosphorylated at Serine 227, a site indicative of RSK2 activation. Thus, in this instance the MIB/MS assay is concomitantly reporting differential kinase expression and activity.

Western blotting also confirmed the codon 12 specific upregulation of MET in the KRAS mutant cell lines reported by NanoString and MIB/MS. Once more, western blotting revealed that changes in MET abundance also correlated with changes in the likely total active pool as inferred by the increased abundance of phosphor-MET.

Two examples of kinases with a low correlation coefficient were EPHA2 and MEK3 (MAP2K3) (both R^2<0.29). The graphs in Figure 4.8 display the ratios of mutant vs. wild-type expression at the transcript level (NS) and at the protein level (MIB). For EPHA2, there is little correlation between the transcript and protein concentrations recorded by NanoString or MIB/MS. A decrease in mRNA abundance was observed in the K12D mutant cell line versus the parental, whereas protein abundance increased. On the other hand, a decrease in mRNA abundance was also observed in the N12V mutant cell line versus the parental, but in this case protein abundance decreased almost 8-fold. This suggests that there is some post transcriptional regulation at play. Further work would be needed to elucidate such regulatory mechanisms. Protein responses were confirmed by western blot. Again, total EPHA2 and phospho-EPHA2 followed the same pattern of expression. Here, it is likely that

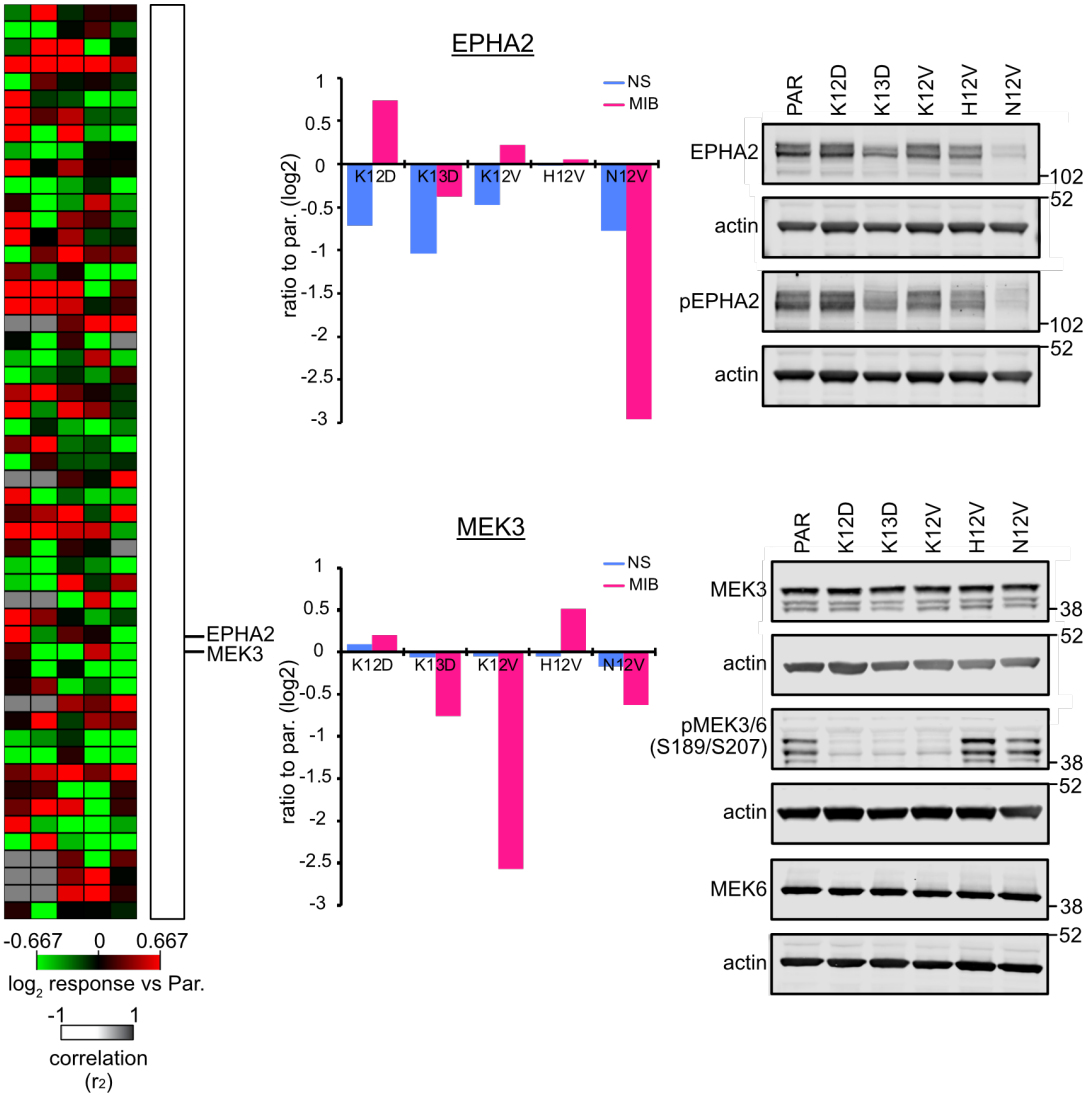

Figure 4.8. Correlation analysis between the NanoString and MIB/MS SW48 kinome datasets (2)

A correlation analysis was carried between the responsive NanoString and MIB/MS datasets. Kinases were included if they were detected by MIB/MS and were defined as responsive. The heatmap displays all data included in the analysis. The heatmap is ranked based on correlation coefficient and the scale bar indicates the degree of correlation between the two datasets. Graphs show examples of kinases with low correlation coefficients; transcript (blue) and protein (pink) level responses are mapped across each cell line. Western blots were used for validation of the observed responses.

the MIB/MS assay is reporting changes in expression, and as a result changes in kinase activity.

For MEK3, there was little, if any, differential MEK3 transcript expression in any of the mutant cell lines vs. parental. In contrast, the MIB/MS assay reported differential MEK3 protein responses in some of the mutant cell lines vs. parental; a significant decrease in MEK3 response was observed in the K12V cell line and to a lesser extent in the K13D cell line. A slight increase in MEK3 response was also recorded in the H12V mutant cell line.

Interestingly, there was also disparity between MEK3 responses reported by MIB/MS and levels of total MEK3 expression analysed by western blotting. Western blotting revealed that the levels of total MEK3 expression in all of the mutant cell lines remained similar to parental levels. The MEK3 protein expression data obtained by western blotting is comparable to the NanoString transcript data and therefore it is likely that MEK3 transcript abundance is the main determinant of MEK3 protein abundance. Considering the lack of correlation between the MIB/MS data and the transcript and protein expression data, it seems unlikely that the MIB column is reporting changes in kinase expression.

In fact, further western blotting analysis revealed that in this instance, MIB/MS is reporting changes in MEK3 phosphorylation. Blots were probed with a MEK3 phospho-antibody that detects phosphorylated MEK3/6 at serine residues 189 and 207, sites indicative of MEK3 activation. pMEK3/6 expression corresponds closely to the MEK3 responses reported by MIB/MS analysis indicating that in this case, MIB/MS is reporting changes in MEK3 activation status.

It is important to note that there was an inconsistency between the western blot and MIB/MS data for MEK3 activity in the K12D cell. One possible reason is that the MIB/MS assay only detected MEK3 in the K12D mutant in 1 out of the 3 biological replicates and therefore the ratio generated for the K12D mutant may not have been truly representative of MEK3 kinase activity. Taking this into consideration, it appears that there is a clear KRAS mutant specific

downregulation of MEK3 activity. Furthermore, evidence of upregulation of MEK3 activity in the HRAS mutant cell line is observed in MIB/MS and western blotting datasets.

4.3. Summary of results

- The expressed SW48 kinome has been defined using NanoString analysis.
- The NanoString and MIB/MS assays have been applied in order to identify RAS isoform and mutation specific kinome responses.
- I have demonstrated how integrating data from the NanoString and MIB/MS analyses can help infer differential kinome expression vs. activity in cells.
- The analyses reveal a subset of Ras responsive kinases for further analysis.

4.4. Discussion

Using a multi-omic approach, we have successfully performed large-scale kinome analysis of a panel of isogenic Ras mutant cells. Deep proteome analysis of 23 mammalian cell lines indicate that cell lines typically express 300-400 kinases (Wilson *et al.*, 2018). NanoString analysis revealed that SW48 cells express 362 kinases, thus falling within the expected range. Using MIB/MS, we achieved good coverage of the kinome. The method allowed the isolation and analysis of 50% of the SW48 expressed kinome, which is comparable to the coverage achieved in previous MIB/MS publications (Duncan *et al.*, 2012a). In the first pioneering MIB/MS study, Duncan et al., were able to profile 50%-60% of the kinome in two TNBC cell lines, over several MS runs.

Our studies demonstrate that the ability of MIB/MS to enrich for active vs. inactive kinases is context dependent and that kinase binding is a function of

kinase expression and in some cases kinase activity. By integrating transcriptomic and proteomic datasets, we were able to infer likely kinase expression and/or activity changes. High correlation between the transcriptomic and proteomic datasets indicated that transcript abundance likely determined protein abundance and that the MIB/MS column in this instance was reporting differential kinase expression across the mutant cell lines. Moreover, analysis revealed that low correlation between the two datasets could be due to post translational modification and that the MIB/MS column, in some cases, was able to report differential kinase activities. Western blotting analysis validated kinase responses reported by the MIB/MS column and also highlighted that changes in protein abundance can lead to a proportional increase in phosphorylation.

The combination of methodologies was applied to obtain an insight into cellular kinase adaptations to different oncogenic RAS mutations. Previous work in the laboratory, had focused on quantitative analysis of the proteome and phosphoproteome of a panel of isogenic SW48 cells harbouring different KRAS mutations (Hammond *et al.*, 2015). Our novel SW48 panel included a HRAS and NRAS mutant cell line to complement the existing KRAS mutant panel. Thus, the data generated from these studies provides the first kinome-wide analysis revealing nodes sensitive to endogenous RAS isoform and mutation specific signalling in an isogenic background.

On the whole there, there was very little evidence of pan-RAS responses. Seemingly, Tribbles 3 (TRIB3) was the only kinase to display the same pattern of response over the five mutant cell lines vs. the parental wild-type cell line; Significant downregulation of TRIB3 mRNA expression was observed in all five mutant cell lines. Previously, it has been shown that TRIB3 loss promotes tumorigenesis via dysregulation of AKT S473 phosphorylation (Salazar *et al.*, 2015). TRIB3 interacts with AKT and has a tumour inhibitory role by limiting the capacity of AKT to become activated. Loss of the TRIB3-AKT interaction enables hyper phosphorylation of AKT via the mTORC complex. This leads to the enhanced phosphorylation and inactivation of the transcription factor FOXO3, thought to be responsible for the more aggressive phenotype (Salazar

et al., 2015). TRIB3 is a pseudokinase and therefore it was not enriched by the ATP competitive inhibitor beads used in the MIB/MS assay. Western blot analysis would be needed to establish whether TRIB3 protein expression is also downregulated in the mutant cell lines vs. parental wild-type cells. Furthermore, RAS knockdown studies would corroborate whether the mutation in RAS is responsible for the genetic loss of TRIB3.

Phosphoproteomic analysis of the KRAS mutant SW48 panel revealed that very few proteins or phosphosites showed significant pan-KRAS mutation responses (Hammond *et al.*, 2015). Consistent with these findings, we observed very few KRAS isoform specific responses, with the exception of MEK3 whose activity was downregulated in all three KRAS mutant cell lines vs. the wild-type cell line. MEK3 (MAP2K3) belongs to the RAS related MAP kinase family. It has been previously shown that RAS regulates the activity of MEK3 and in turn, the downstream p38 pathway (Shin *et al.*, 2005). In the next chapter, I aim to elucidate the mechanism behind the potential isoform specific regulation of this kinase that may expose a therapeutic vulnerability in KRAS mutant cancers.

Although very few pan-KRAS responses were observed, Hammond et al. reported differential responses between the codon 12 and codon 13 KRAS mutant cell lines. Authors identified a cluster of proteins that were significantly upregulated in the codon 12 mutants only (Hammond *et al.*, 2015). Our transcriptome data also indicates that there is a divergence between codon 12 and codon 13 mutations. Clustering analysis revealed that at the transcript level, the KRAS codon 12 mutants share a similar pattern of responses across all expressed kinases that are distinct from the codon 13 mutant responses. On the contrary, at the protein level, KRAS mutant cell lines cluster based on the type of mutation rather than codon positioning. All three isoforms harbouring a G12V mutation cluster together away from the two KRAS mutants harbouring an aspartic acid (D) substitution. On the whole, it seems that both the type of amino acid substitution and the codon positioning of the mutation may influence the output of oncogenic RAS, however it is hard to distinguish which has the greatest effect.

Another layer of complexity is added by the fact that a number of responses were unique to each mutant cell line. Furthermore, the number of differential responses observed for each mutant cell line varied significantly. Across both datasets, there seems to be a significant bias for one particular variant; The KRAS G12D mutant cell line harboured the most differential kinase responses compared to the wild type cell line. Considering the fact that in colorectal cancer, the most prevalent mutation is KRAS G12D, I speculate whether the degree of responsiveness downstream of the RAS mutation mirrors the mutational frequencies observed in colorectal cancer?

A recent study concludes that oncogenic potency is the major determinant for tissue specific RAS mutational profiles (Poulin *et al.*, 2019). Authors show that context-dependent variations in signalling downstream of different RAS mutants may drive the RAS mutational pattern seen in cancer. Analysis reveals that different mutant forms of KRAS have different biochemical mechanisms of activation that can lead to profound differences in downstream signalling and that signalling is distinct to each tissue. One aspect of the study compared the proteomes of colons, pancreas, and spleens from mice expressing KRAS WT, KRAS G12D, or KRAS A146. Interestingly, they found that KRAS A146 which less potently drives tumorigenesis in the colon, has a more similar proteomic signature to WT than KRAS G12D (Poulin *et al.*, 2019). This may explain why we see more differential kinome responses in our K12D cell line vs. wild type cells and less in the N12V cell line for example and emphasises that RAS mutations should not be treated equally (Hobbs and Der, 2019).

Although many mutation specific responses were observed, I would have expected some common responses directly downstream of RAS. As previously stated, we had confidence that the NanoString assay was able to map the transcript kinome adaptations of the entire expressed SW48 kinome. Whilst the MIB/MS assay only enriched 50% of the expressed kinome, there was good coverage of the majority of kinase families, including many of the Tyrosine Kinases that lie upstream and downstream of RAS. Taking into

account the dogma derived from ectopic studies, it seems surprising that there were very few responses within the immediate RAS network. Furthermore, we did not observe preferential coupling of each RAS isoform to a particular pathway, as previously described (Yan *et al.*, 1998; Voice *et al.*, 1999). In concordance with our data, many studies investigating endogenous RAS signalling did not observe high levels of MAPK and PI3K pathway activity, suggesting that oncogenic RAS may cause a subtler, network response (Tuveson *et al.*, 2004; Omerovic *et al.*, 2008) (Hood *et al.*, 2019). For many years, research has focused on the kinase nodes within the MAPK and PI3K pathways. The 12 principle MAPK/PI3K nodes account for 20% of all kinome publications, whilst over 300 kinases account for only 5% of research publications (Wilson *et al.*, 2018). As a result, much of the kinome is understudied and therefore untargeted. Our global, unbiased approaches to study the kinome have enabled us to study RAS isoform specific signalling in the wider context. Our results suggest there needs to be greater attention and appreciation of the effects of RAS isoform and mutation specific signalling in the wider signalling network and highlights the unmet need within the kinome.

The panel of isogenic SW48 cell lines have been well characterised previously within the lab (Hood *et al.*, 2019). The abundance of mutant RAS has been quantified in each cell line and it has been shown that the lack of downstream effector activation is not due to a lack of active RAS (Mageean *et al.*, 2015; Hood *et al.*, 2019). Another potential explanation for low effector stimulation is that SW48 cells harbour an $EGFR^{G719S}$ mutation. This promotes ligand independent activation of MAPK signalling which could result in pre-existing negative feedback mechanisms. However, it was shown that the engagement of negative feedback mechanisms only occurs when the cells are stimulated with EGF. Moreover, the observation of low effector activation was also extended to a broader panel of colorectal cancer cell lines harbouring mutated RAS suggesting that this observation is not specific to SW48 cells(Hood *et al.*, 2019).

Another possible criticism of the SW48 cell line is that they are not dependent on RAS to be viable and therefore are not a true representation of RAS driven

oncogenesis. I aim to address this in the next chapter by conducting RAS knockdown studies. I will evaluate the RAS dependency of the differentially expressed kinases highlighted in this chapter. This will provide a further layer of validation whilst allowing me to shortlist any potentially interesting hits.

Chapter 5 : Evaluating the RAS dependency of RAS responsive kinases

In Chapter four, we performed the first kinome-wide analysis of endogenous isoform and mutation specific RAS signalling. Using an isogenic panel of SW48 cell lines, we were able to study the effects of different oncogenic mutations in RAS without the confounding effects of variations in the genetic background. Using NanoString and MIB/MS, we conducted a comparative analysis of five RAS mutant cell lines versus the RAS wild-type cell line. The combination of transcriptomic and proteomic approaches generated a list of differentially expressed genes and proteins for each mutant cell line. Although the SW48 cell panel is isogenic, it is important to confirm there is a direct connectivity between differentially expressed kinases and oncogenic RAS, and that regulation of kinase expression and/or activity does not result from an irreversible adaption or selection pressure.

In this chapter, I will conduct knockdown experiments to evaluate the RAS dependency of the responsive kinase list. The KRAS G12D mutant (K12D) differentially regulated more kinases at both, the transcript and protein level, compared to the other mutant cell lines and therefore was classed as our most 'responsive' RAS mutant cell line. For this reason, I have decided to initially focus on evaluating the RAS dependency of kinases that were differentially regulated by the K12D SW48 cell line. To achieve KRAS knockdown, I will use isogenic SW48 cell lines with stably expressing shRNAs targeting KRAS. One advantage of using shRNA versus siRNA is that we are able to control shRNA expression using inducible promoters. Furthermore, shRNA is delivered directly into the nucleus and uses the endogenous processing machinery allowing a more sustained knockdown with fewer off target effects (Rao *et al.*, 2009).

I will use the NanoString and MIB/MS assays to study kinome adaptations to KRAS knockdown at the transcript level and protein level, respectively. To confirm RAS dependency, upon knockdown we must observe a reversal of the

regulation of gene/protein expression of a responsive kinase back towards wild-type levels. In other words, after RAS knockdown the kinase should no longer be differentially expressed in the mutant cell line versus the parental cell line and therefore no longer defined as responsive.

DCLK1 was the most significantly upregulated kinase in the K12D mutant cells. DCLK1 is frequently upregulated in colorectal cancer and is associated with poor prognosis (Gagliardi *et al.*, 2012) (Gao *et al.*, 2016). It has been shown that DCLK1 expression promotes tumour proliferation and also increases chemoresistance in colorectal cancer cells (Li, Jones and Mei, 2019). Moreover, depletion of the related kinase DCLK2 has been shown to reduce the viability of RAS mutant DLD-1 cells (Luo *et al.*, 2009). Furthermore, a direct link between the overexpression of DCLK1 and RAS activation has been revealed in PDAC (Qu *et al.*, 2019). It was previously shown in the lab, that KRAS codon 12 specific upregulation of DCLK1 was reversed upon KRAS knockdown, thus providing further evidence of the biological relevance of this kinase in oncogenic RAS signalling (Hammond *et al.*, 2015). As I am using the same cell system, I will use DCLK1 as a positive control for KRAS knockdown.

A similar pattern of KRAS codon 12 specific upregulation was observed for the receptor tyrosine kinase, MET. Although MET sits upstream of RAS, potential negative feedback from downstream kinases may regulate the expression of the receptor. Unlike DCLK1, the RAS dependency of MET upregulation was not previously evaluated in SW48 cell lines (Hammond *et al.*, 2015). In this chapter, I will investigate whether the upregulation of MET in K12D cells is directly KRAS-dependent.

Additionally, I will explore the potential interplay between RAS and MEK3 (MAP2K3) activation. Significant downregulation of MEK3 phosphorylation was observed in all three KRAS mutant cell lines. In contrast, an increase in MEK3 activation was observed in the HRAS mutant cell line. Therefore, it will be interesting to validate these findings and see if MEK3 has opposing isoform-specific effects. MEK3 activation is observed in human cancers although it remains unclear if it is an oncogene or a tumour suppressor gene. In lung

cancer, MEK3 is tumour promoting (Galan-Moya *et al.*, 2011), whereas in breast cancer it is tumour suppressive (Jia *et al.*, 2010; MacNeil *et al.*, 2014).

It was previously reported that HRAS, but not NRAS, induces MEK3/p38 pathway activation, leading to an invasive and migrative phenotype in human breast cancer cells (Shin *et al.*, 2005). Since Rac1 had been shown to induce p38 activation previously, a Rac1 activity assay was conducted to see whether HRAS and NRAS differentially regulated levels of Rac1-GTP (Zhang *et al.*, 1995). Activation of Rac1 was induced by HRAS and not NRAS, in line with HRAS stimulating MCF10A cell motility. Moreover, MEK3/6 and p38 activation was shown to be dependent on Rac1 activity (Shin *et al.*, 2005). In this chapter, I aim to establish whether HRAS specific upregulation of MEK3 activity occurs via Rac1 and whether subsequent p38 activation leads to an invasive and migrative phenotype in SW48 HRAS G12V cells.

Paradoxically, it has been reported that oncogenic RAS can induce cellular senescence via MEK3 and p38 activation (Wang *et al.*, 2002). The study showed that the activation of MEK3/6, and subsequent activation of p38 induces premature senescence in primary human fibroblasts. Furthermore, inhibition of p38 activity rescued cells from cell cycle arrest indicating that p38 is essential for RAS induced senescence. Moreover, MEK3 and p38 is stimulated by RAS following MEK and ERK activation; Premature senescence induced by MEK3/p38 pathway activation is dependent on MEK1 activity revealing an interaction between the two linear pathways (Wang *et al.*, 2002; Deng *et al.*, 2004). Signalling between the two pathways is thought to be indirect since MEK3 activation occurs several days after MAPK activation however the intermediate steps linking ERK and MEK3 are unclear (Iwasa, Han and Ishikawa, 2003).

It is well documented that RAS induced senescence acts a homeostatic mechanism in response to prolonged RAS signalling and that tumour cells may evade this anti-proliferative mechanism for transformation (Serrano *et al.*, 1997; Ferbeyre *et al.*, 2002). SW48 KRAS mutant cells may evade cellular senescence by downregulating MEK3 pathway activation. In this chapter, I aim

to establish the mechanism by which KRAS may be potentially regulating MEK3 activity. Furthermore, I will look to dissect the mechanism linking the MAPK and MEK3/p38 pathways by looking at potential upstream regulators of MEK3.

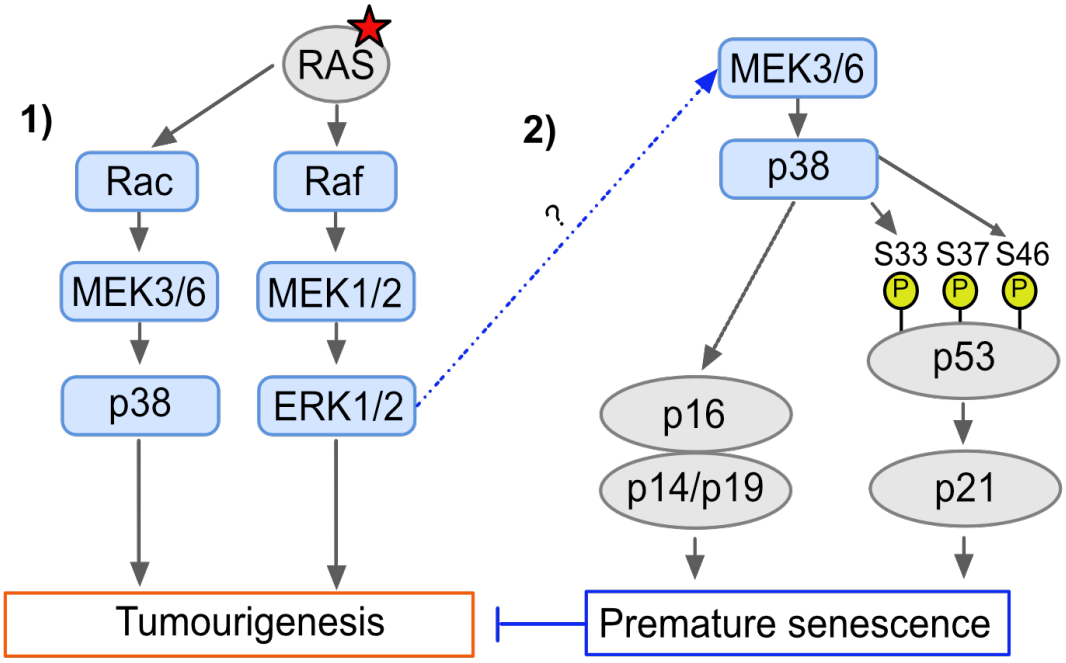

Figure 5.1. Potential mechanisms for RAS induced MEK3/6 activation

MEK3 activation can result in a 1) tumourgenic or 2) tumour suppressive phenotype in RAS mutant cells. 1) HRAS specific up regulation of MEK3/6 occurs via Rac1 activation leading to tumourigenesis in human breast cancer cells. 2) RAS induced senescence via MEK3/p38 pathway. MAPK activation indirectly increases in MEK3/p38 pathway activation, causing premature senescence. Mutant RAS cells may evade this homeostatic protective mechanism by down regulating the MEK3/p38 pathway activation.

5.1. Objective

The objective of this chapter is to evaluate the RAS dependency of kinases that are differentially regulated in RAS mutant versus wild-type cells. I aim to achieve this by knocking down KRAS in the K12D mutant cell line and analysing KRAS-dependent regulation of kinase expression and/or activity. Moving on from this, I will follow up any potential RAS isoform and mutation specific responsive kinases identified in Chapter Four.

5.2. Results

5.2.1. Stable knockdown of KRAS by shRNA in SW48 KRAS G12D mutant cells

To examine the effects of the knockdown of oncogenic KRAS, we used a panel of four isogenic cell lines: The Parental and K12D cell lines as controls, and two independent K12D cell lines stably expressing doxycycline-inducible KRAS-specific shRNAs. As expected, the induced expression of both shRNAs resulted in significant decreases in KRAS expression (Figure 5.2). Approximately, a 73% and 63% loss of KRAS protein expression can be observed in response to the induced expression of shRNA2 and shRNA3 respectively. Moreover, consistent with previous observations, KRAS loss was accompanied by a significant loss of DCLK1 protein expression, thus giving further affirmation of KRAS knockdown (Hammond *et al.*, 2015). It is important to note, we were able to achieve similar levels of KRAS knockdown over several biological replicates with the shRNA2 construct consistently producing a higher level of protein knockdown.

5.2.2. NanoString analysis after KRAS knockdown reveals KRAS dependent transcript responses

NanoString analysis was conducted to measure transcript level changes in the kinome after KRAS knockdown. Both shRNAs were used in the analysis, thus providing two technical replicates for each biological replicate (n=4, t=8). KRAS knockdown was confirmed by western blotting before the lysates were processed by the NanoString nCounter platform (Figure 5.3).

Differential expression (DE) analysis was conducted using the NanoString advanced analysis software, providing an insight into which kinases were significantly changing: A) in the K12D mutant vs. Parental cell line and B) after knockdown of oncogenic KRAS in the mutant K12D cell lines. The software used statistical t testing to calculate a p-value for each kinase and the Benjamini-Hochberg method was applied to reduce the False Discovery Rate

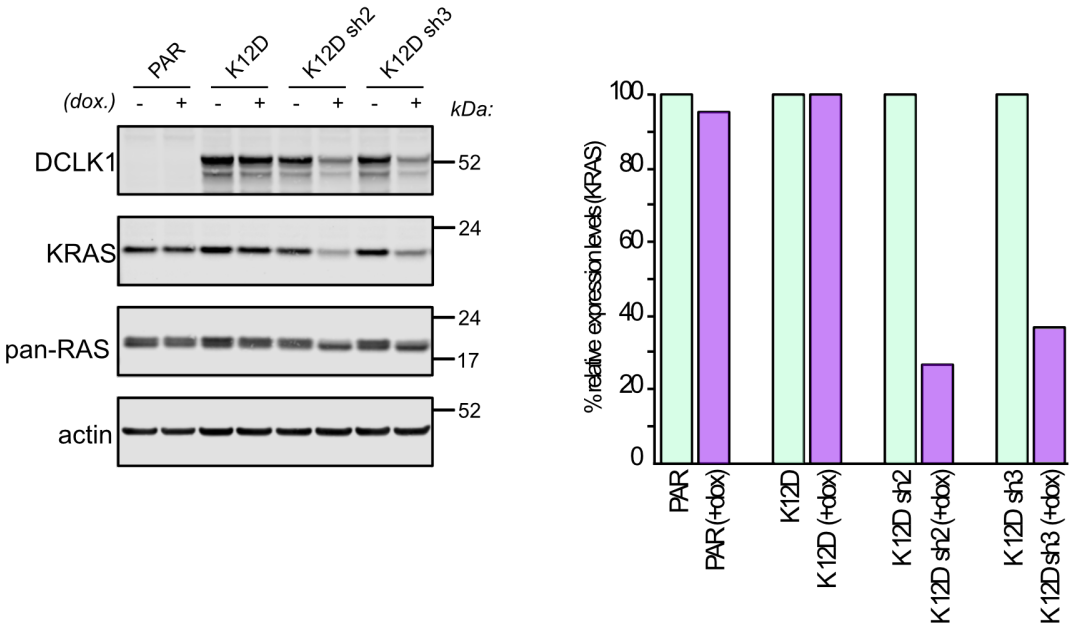

Figure 5.2. Stable knockdown of KRAS by shRNA in SW48 KRAS G12D mutant cells reduces DCLK1 expression

SW48 K12D cells with inducible expression of 2 different shRNAs targeting KRAS (sh2 and sh3) were treated with 100ng/mL doxycycline for 1 week to induce shRNA expression where indicated. Cells were lysed using RIPA buffer and separated using SDS-PAGE. Western blots were probed with the indicated antibodies. The pan-RAS antibody recognizes all 3 isoforms and detects a doublet band; the top band represents KRAS expression and the bottom band both HRAS and NRAS expression. Approximately, a 73% and 63% loss of KRAS protein expression can be observed in response to the induced expression of shRNA2 and shRNA3 respectively.

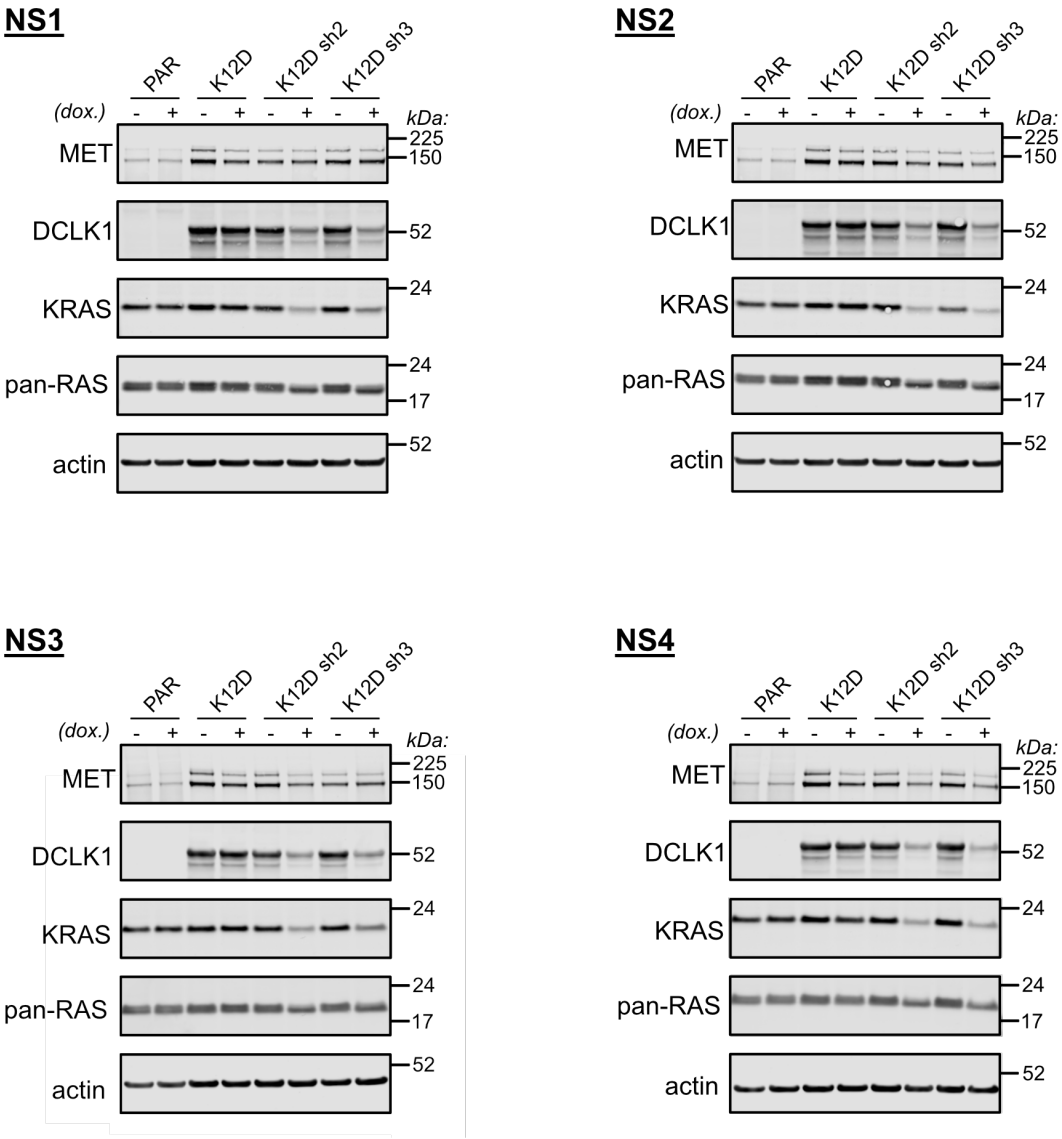

Figure 5.3. KRAS knockdown in SW48 KRAS G12D mutant cells reduces expression of DCLK1.

Western blot analysis displays KRAS knockdown over four biological replicates (NS1-NS4). SW48 K12D cells with inducible expression of 2 different shRNAs targeting KRAS (sh2 and sh3) were treated with 100ng/mL doxycycline for 1 week to induce shRNA expression where indicated. Cells were lysed in RIPA buffer and saved for NanoString analysis. A small proportion of the lysates were taken for western blotting analysis. Lysates were separated by SDS-PAGE and western blots were probed with the indicated antibodies.

(FDR) (see section 2.3.7). The volcano plots in figure 5.4 display the results of the differential expression analysis. The fold change (log2 ratio) and p-value is displayed for each kinase. Highly statistically significant kinases fall above the p-value threshold ($p<0.0001$) and differentially expressed kinases fall either side of the plot. Some of the most statistically significant kinases are labelled for each condition. Any kinases that fell below the threshold, highlighted in grey, were removed from further analyses.

The aim was to identify kinase adaptations that show dependency to mutant KRAS. To confirm KRAS dependency, upon KRAS knockdown we needed to observe a reversal of mRNA expression levels in the mutant K12D cell line back towards parental levels. For example, as expected DCLK1 mRNA expression was significantly upregulated in the K12D mutant cell line vs. parental cell line (Figure 5.4). Upon KRAS knockdown, DCLK1 mRNA expression levels decreased by over 2-fold, back towards parental wild-type levels (Figure 5.4).

Figure 5.5 displays a shortlist of kinases extracted from the differential expression analysis, that like DCLK1, show some dependence on oncogenic KRAS. To be shortlisted, the differential expression of each kinase had to be significant in both DE analyses (MUT/WT and KD/MUT $p>0.0001$). The kinases are grouped based on the degree of RAS dependence characterised by fold-changes before and after knockdown.

Group One represents kinases that show the highest degree of KRAS dependency; Kinases included in this group were differentially regulated >1.5-fold in the mutant K12D cell line vs. parental wild-type cell line, and upon KRAS knockdown mRNA expression shifted >1.5-fold back towards parental levels. Alongside DCLK1, examples of kinases in Group One included EPHA1 and MET. EPHA1 mRNA expression was downregulated by over 2-fold in the K12D mutant vs. parental cell line. After KRAS knockdown, EPHA1 mRNA levels were restored back to near parental levels. MET mRNA expression was upregulated almost 7-fold in the K12D mutant vs. wild-type cell line. Upon

A

Mutant vs. WT

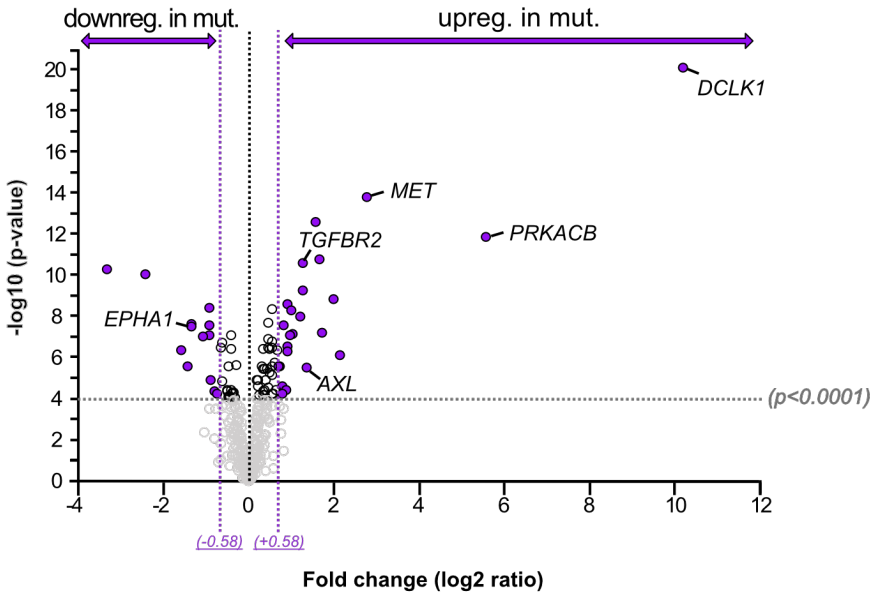

B

Knockdown vs. mutant

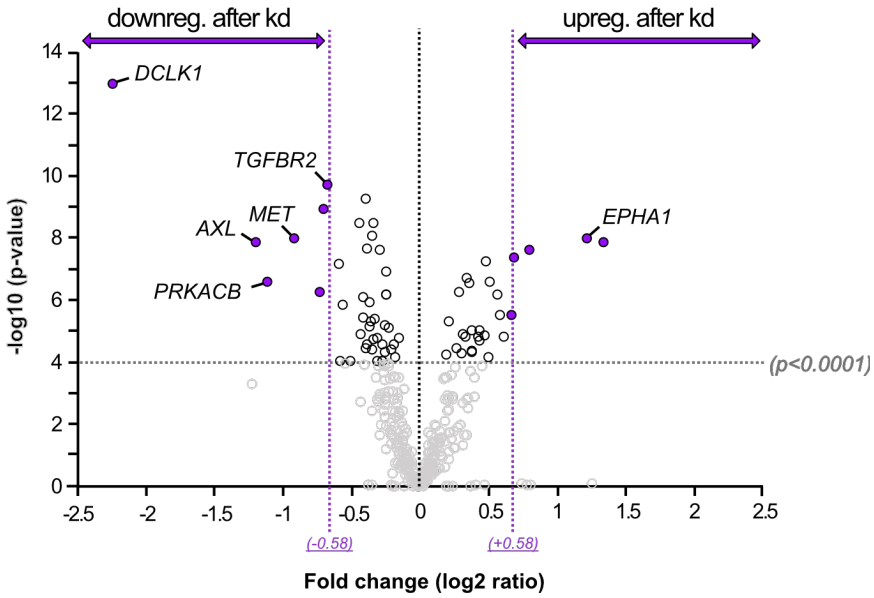

Figure 5.4. NanoString analysis after KRAS knockdown reveals KRAS dependent transcript responses

SW48 K12D cells with inducible expression of 2 different shRNAs targeting KRAS (sh2 and sh3) were treated with 100ng/mL doxycycline for 1 week to induce shRNA expression and lysates analysed using the NanoString platform. Volcano plots displaying the differential expression of kinases in A) SW48 K12D mutant cells vs. SW48 parental (WT) cells and B) SW48 K12D mutant cells after KRAS knockdown. Only kinases that show a 1.5-fold-change in transcript expression and p-values in the significant range are coloured or annotated (n=4).

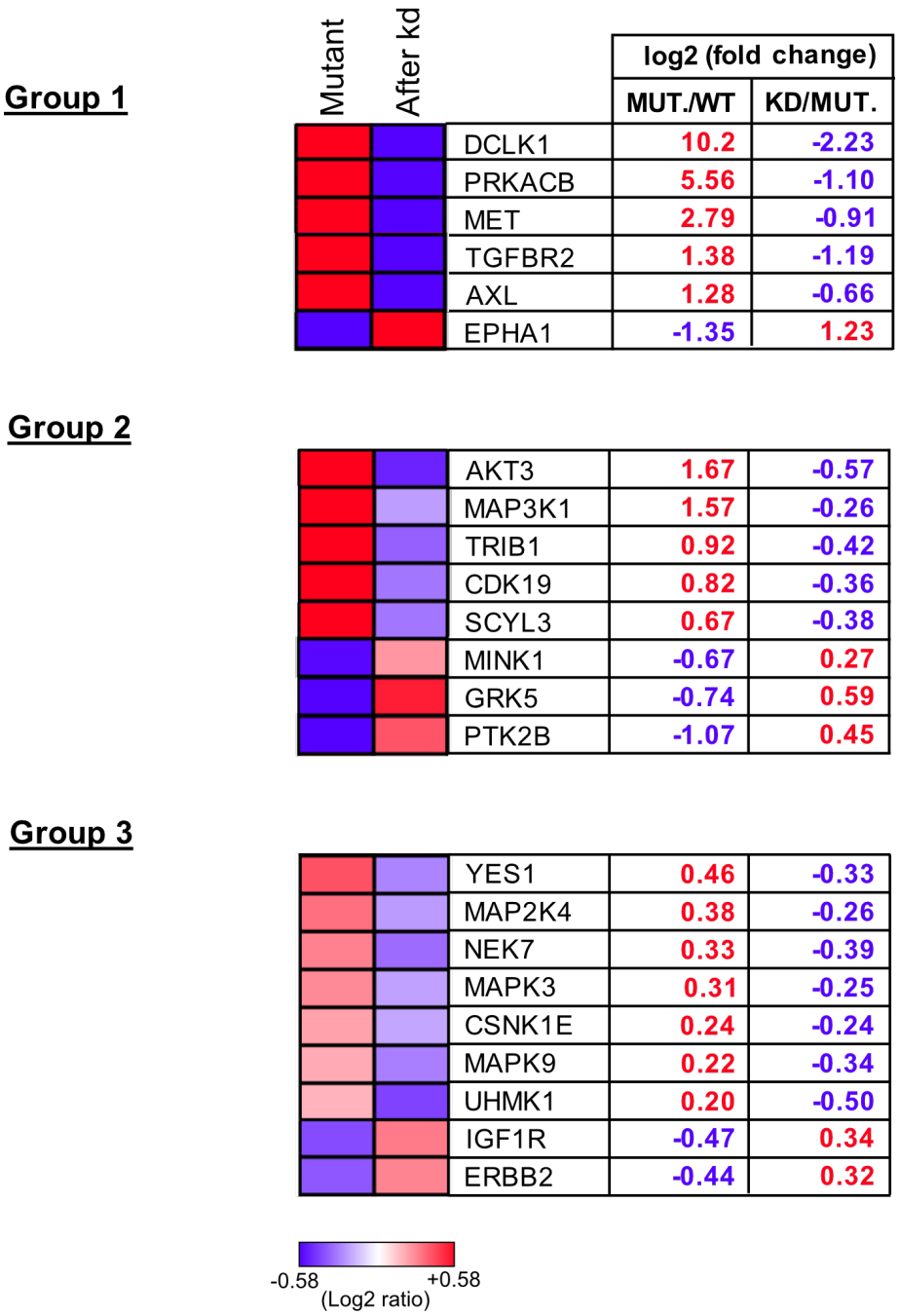

Figure 5.5. Shortlisting KRAS dependent transcript responses reveals MET up regulation is KRAS dependent

Only kinases with significant p-values in both differential expression analyses were shortlisted (MUT/WT and KD/MUT p>0.0001). Kinases were grouped based on fold-change. Group 1 represents kinases that showed >1.5-fold change in MUT vs. WT, and upon knockdown mRNA expression shifted >1.5-fold back towards parental levels. Group 2 represents kinases that were differentially regulated >1.5 fold in MUT vs. WT however, upon knockdown expression shifted <1.5-fold back towards parental levels. Group 3 represents kinases that significantly changed in opposing directions however not to a significant level.

KRAS knockdown, mRNA expression decreased by almost 2-fold, suggesting MET upregulation is in fact dependent on mutant KRAS.

Group Two represents kinases that were differentially regulated >1.5-fold in the mutant K12D cell line vs. parental cell line; however, upon KRAS knockdown, expression shifted <1.5-fold back towards parental levels. Considering, we don't achieve full KRAS knockdown in SW48 cells, we may only see a partial reversal in mRNA expression back towards parental levels after knockdown. In some cases, KRAS gene knockout would be required in order to observe a complete reversal of mRNA expression back to parental levels. Thus, (Group Two) kinase mRNA regulation may still prove to be dependent on KRAS.

Group Three kinases are not significantly regulated by oncogenic KRAS; however, upon KRAS knockdown, any subtle changes in mRNA expression that were observed, are reversed back toward parental levels. These data may prove useful when looking at the information flow of a particular pathway. Although they are not significantly changing kinases, they could still represent nodes within a KRAS dependent pathway, where the regulation of a combination of kinases may produce an effect.

5.2.3. MIB/MS analysis after KRAS knockdown reveals KRAS dependent protein responses

MIB/MS analysis was conducted to measure protein level adaptations in the kinome after KRAS knockdown. Figure 5.6A. describes the experimental set up for the MIB/MS knockdown experiments. Individual MIB columns were run for each shRNA cell line, making a total of two technical replicates for each biological replicate (n=3, t=6). Stable Isotopic Labelling (SILAC) provides the opportunity to compare three cell conditions in a single run, these were: the parental wild-type cell line vs. the K12D mutant cell line, with and without, doxycycline induced KRAS shRNA expression. The light labelled parental cell lysates were mixed in a 1:1:1 ratio with medium labelled K12D mutant cells (no knockdown) and heavy labelled K12D mutant cells (with knockdown).

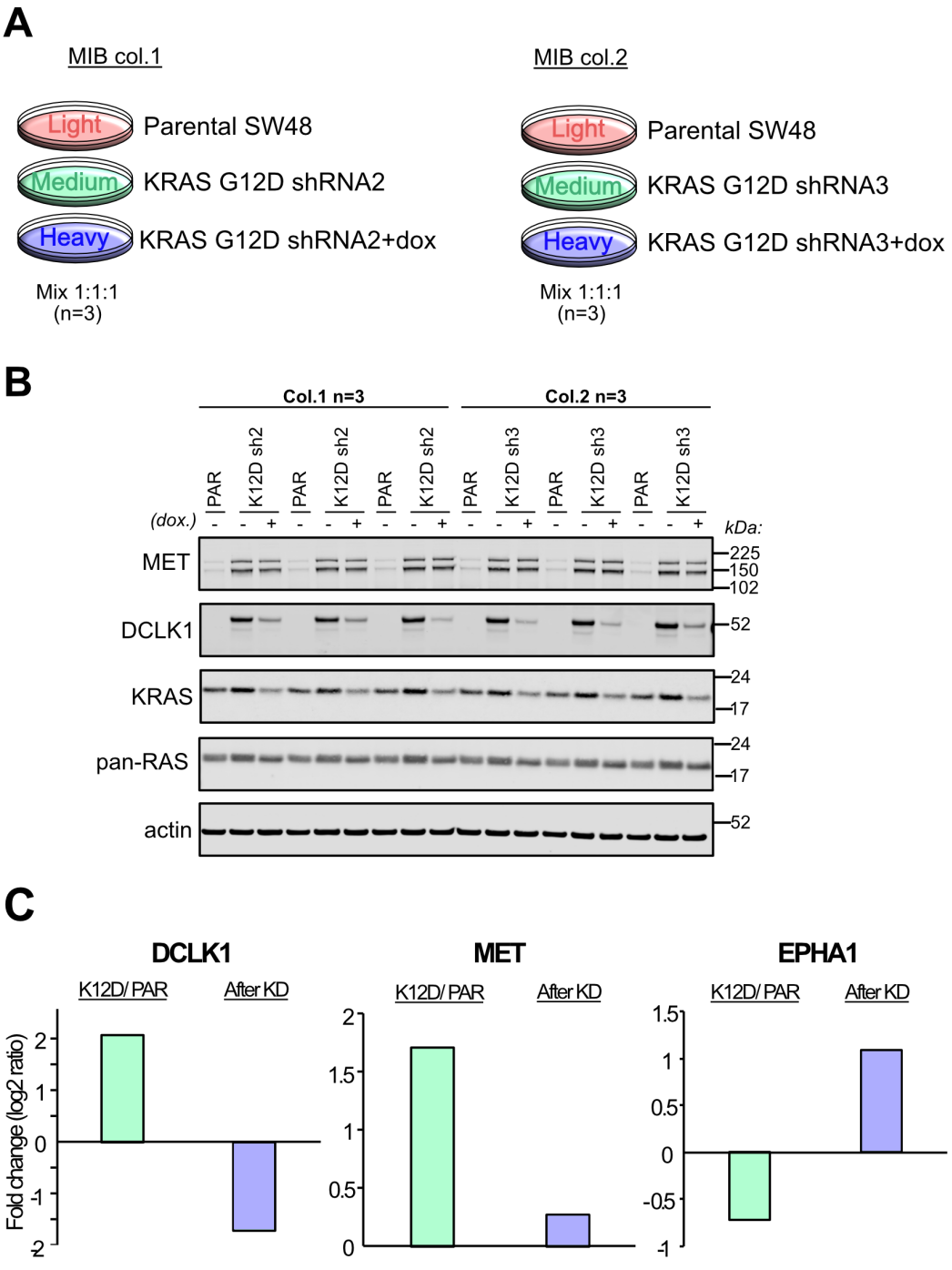

Figure 5.6. MIB/MS analysis after KRAS knockdown reveals KRAS dependent protein responses

SW48 K12D cells with inducible expression of 2 different shRNAs targeting KRAS (sh2 and sh3) were treated with 100ng/mL doxycycline for 1 week to induce shRNA expression. A) Experimental set up of MIB/MS knockdown experiments. SILAC labelled lysates: SW48 parental (light), K12D no knockdown (medium) and K12D with knockdown (heavy) were mixed in a 1:1:1 ratio and loaded onto a column containing MIB beads. B) Western blotting analysis validates that KRAS knockdown was successfully achieved in all cell lysates loaded onto the MIB columns, over 3 biological and 6 technical replicates. Cells were lysed using RIPA buffer and separated with SDS-PAGE. Western blots probed with the indicated antibodies (n=3). C) MIB/MS analysis. The average intensities taken across three biological replicates were used to determine the fold change in expression (log2 ratio) 1) SW48 K12D mutant cells vs. parental cells and 2) SW48 K12D mutant cells +/- knockdown (n=3).

It is important to note, that KRAS knockdown was confirmed by western blotting before the lysates were mixed and loaded onto the MIB columns (Figure 5.6B). Consistent with previous analyses, DCLK1 upregulation in the K12D mutant seems to be dependent on KRAS expression. Unlike DCLK1, the KRAS dependency of MET upregulation was not previously evaluated in SW48 cell lines (Hammond *et al.*, 2015). Figure 5.6B, displays MET protein expression before and after KRAS knockdown. Two bands are visualised using the MET antibody. One represents the precursor Pro-MET (170kDa) that matures through proteolytic cleavage by Furin. The cleavage leads to the formation of a disulphide linked heterodimer, comprised of an alpha subunit (45kDa) and a beta subunit (145kDa) (Fernandes, Duplaquet and Tulasne, 2019). The second band visualised in the blot in figure 5.6B represents the beta subunit of the mature MET protein.

MET follows a similar pattern of expression to DCLK1 in the parental and K12D mutant cells, however only marginal decreases in protein expression is observed after KRAS knockdown. NanoString analysis revealed that MET mRNA regulation was directly dependent on KRAS expression however, we do not observe the same compelling evidence for MET protein expression dependency. It is important to note, that there does seem to be more convincing evidence of RAS dependency in the K12D shRNA2 cell line vs. shRNA3 cell line, consistent with a higher level of KRAS knockdown achieved using the shRNA 2 oligo.

The graphs in Figure 5.6C display data collated from the MIB/MS experiments using the same lysates. As anticipated, a 4-fold increase in DCLK1 protein expression was observed in the K12D mutant cell line vs. parental cell line. Moreover, DCLK1 expression reduced by over 3-fold, back towards parental levels after knockdown, giving confidence the MIB/MS column could report KRAS dependency. The MIB/MS assay reported a 3-fold upregulation in MET protein expression in the K12D mutant vs. parental cell line however, in concordance with the western blot analyses, no reduction of MET protein expression was observed post knockdown. The final graph shows data for the Ephrin receptor, EPHA1; EPHA1 protein expression is downregulated by over

1.5-fold in the mutant vs. parental cell line and is restored back to parental levels after KRAS knockdown. This is similar to what we observed at the transcript level and therefore EPHA1 seems like an interesting KRAS dependent hit to take forward.

5.2.4. Regulation of Ephrin Receptor Tyrosine Kinases by oncogenic KRAS

EphA1 belongs to the largest family of receptor tyrosine kinases (RTKs) comprising of 16 Ephrin receptors (Ephs) and 9 ephrin ligands (Lisabeth, Falivelli and Pasquale, 2013). There are two subgroups of Eph receptors: EphA receptors (A1-A10) and EphB receptors (B1-B6). Ephs are present in the majority of cancer cells however both upregulation and downregulation of Eph expression has been reported (Kou and Kandpal, 2018). Furthermore, it has been well documented that different Eph family members can either promote or inhibit tumour progression in different cancer types (Herath and Boyd, 2010).

Considering many members of the Eph receptor family are paradoxically regulated in a variety of different cancers, I decided to investigate the family as a whole. Figure 5.7 displays data taken from A) NanoString analyses and B) MIB/MS analyses following KRAS knockdown. As previously stated, EphA1 showed a high degree of KRAS dependency at both the transcript and protein level. In both cases, EphA1 was downregulated in the mutant vs. parental cell line. Upon knockdown, EphA1 mRNA and protein expression increased by over two-fold and was restored back to near parental levels. NanoString analysis also revealed that SW48 cells express a further 6 EPH receptors making a total of: 3 EphA and 4 EphB receptors (Figure 5.7A) Moreover, EphA2, A4, B2, and B3 showed some degree of RAS dependence at the transcript level. There was less coverage of the Eph family using MIB/MS however, once more, some degree of RAS dependency was observed for EphB2 at the protein level (Figure 5.7B). Notably, despite the fact that EphA2 seems to be differentially regulated at the transcript level and protein level, both mRNA and protein expression appear to be RAS dependent.

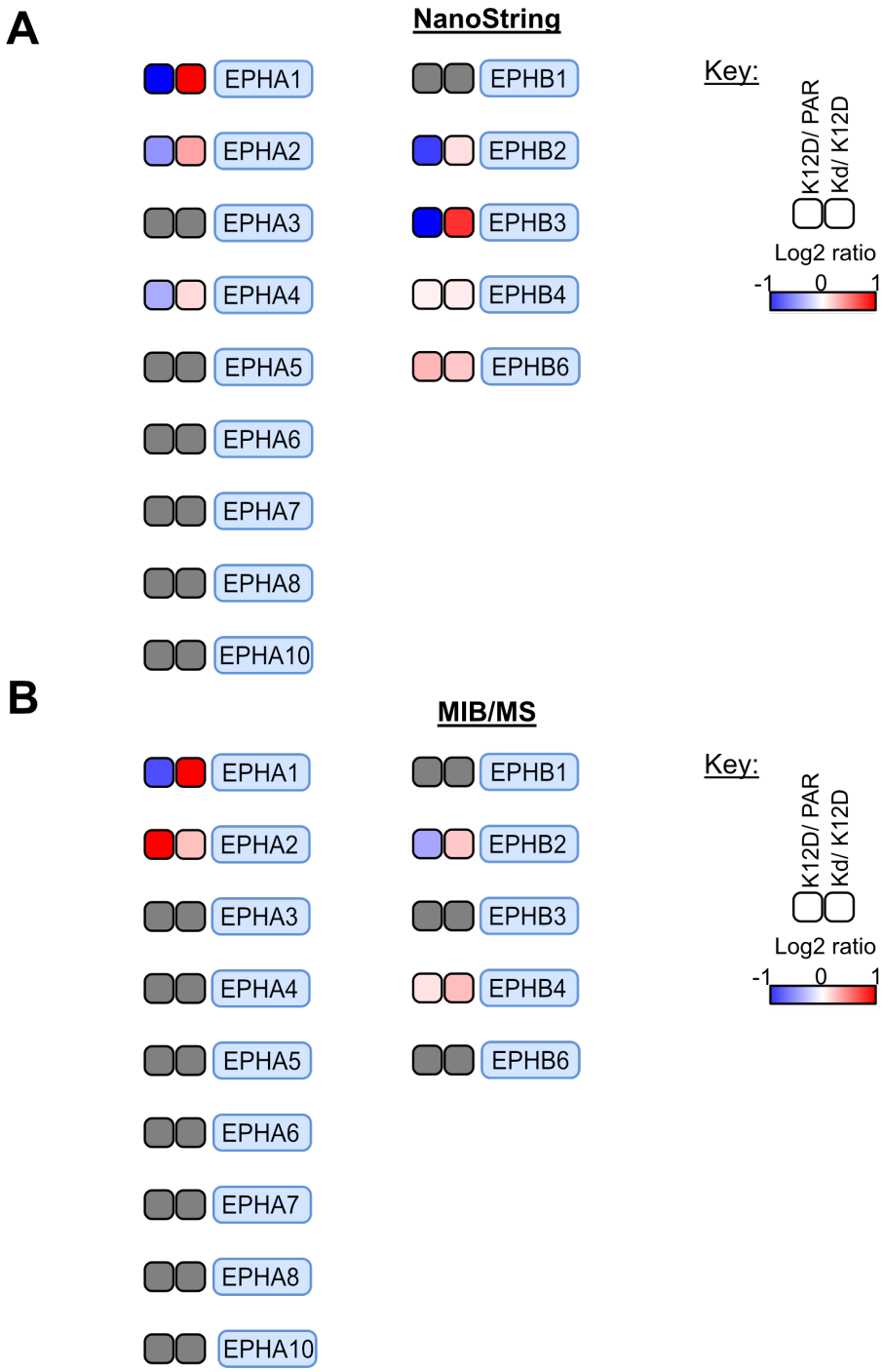

Figure 5.7.NanoString and MIB/MS analyses reveal KRAS dependent group of Ephrin Receptor Tyrosine Kinases in SW48 K12D cells

SW48 KRAS G12D cells with inducible expression of shRNA targeting KRAS were treated with 100 ng/mL doxycycline for 1 week to induce knockdown of KRAS and analysed using A) NanoString analysis (n=4) and B) MIB/MS analysis (n=3). The average counts taken across all biological replicates were used to determine the fold change (log2 ratio) in expression of the 1) K12D mutant cell line vs. the parental SW48 cell line and 2) the K12D cell +/- KRAS knockdown. Ephrin RTKs that are not expressed/detected in SW48 cells are coloured in grey.

Since the majority of expressed Ephs show some degree of RAS dependence, I decided to review Eph expression across all mutant SW48 cell lines to determine whether RAS mutations generally regulate this group of kinases. Figure 5.8 displays the expression data for Eph receptors across all five mutant cell lines, in relation to parental expression levels (data is derived from the (A) NanoString and (B) MIB/MS experiments conducted in Chapter four). With the exception of the K12V cell line at the protein level, EphA1 expression is downregulated in all KRAS mutant cell lines at both the transcript level and protein level. This suggests that EphA1 downregulation may be KRAS specific, however western blotting would be needed to confirm protein responses. Once again, we observe differential regulation of the EphA2 kinase at the protein level vs. transcript level. Furthermore, whilst we don't see any significant changes to EphA4 mRNA expression, the MIB column reports significant upregulation of EphA4 expression/activity in the KRAS and HRAS mutant cell lines. A diverse range of responses were observed for the EphB group of receptors at the transcript level, and protein expression was only measured for 2/4 EphB receptors.

Western blotting was conducted to confirm EphA protein responses and gain a greater insight into EphB protein regulation (Figure 5.9). Unfortunately, we observed a lack of antibody sensitivity and specificity for EphA1. EphA1 was one of the most highly abundant proteins measured by MIB/MS in SW48 cells, so we would expect to see protein expression by western blotting. Despite several stages of antibody optimisation, I was unable to detect a band for total EphA1 and phosphorylated EphA1. Although the NanoString and MIB/MS assay provide us with a level of confidence that EphA1 expression is RAS regulated, a suitable antibody would need to be sourced for further validation.

Western blotting analysis confirmed EphA2 protein responses reported by MIB/MS across all cell lines (Figure 5.9). Changes in EphA2 protein abundance correlated with the amount of active protein; The phospho-antibody detects EphA2 when its phosphorylated at Tyrosine 772 (Y772), a site indicative of activation. Across all cell lines, there appears to be a similar pattern of expression/activation to another RTK, MET (Figure 4.7).

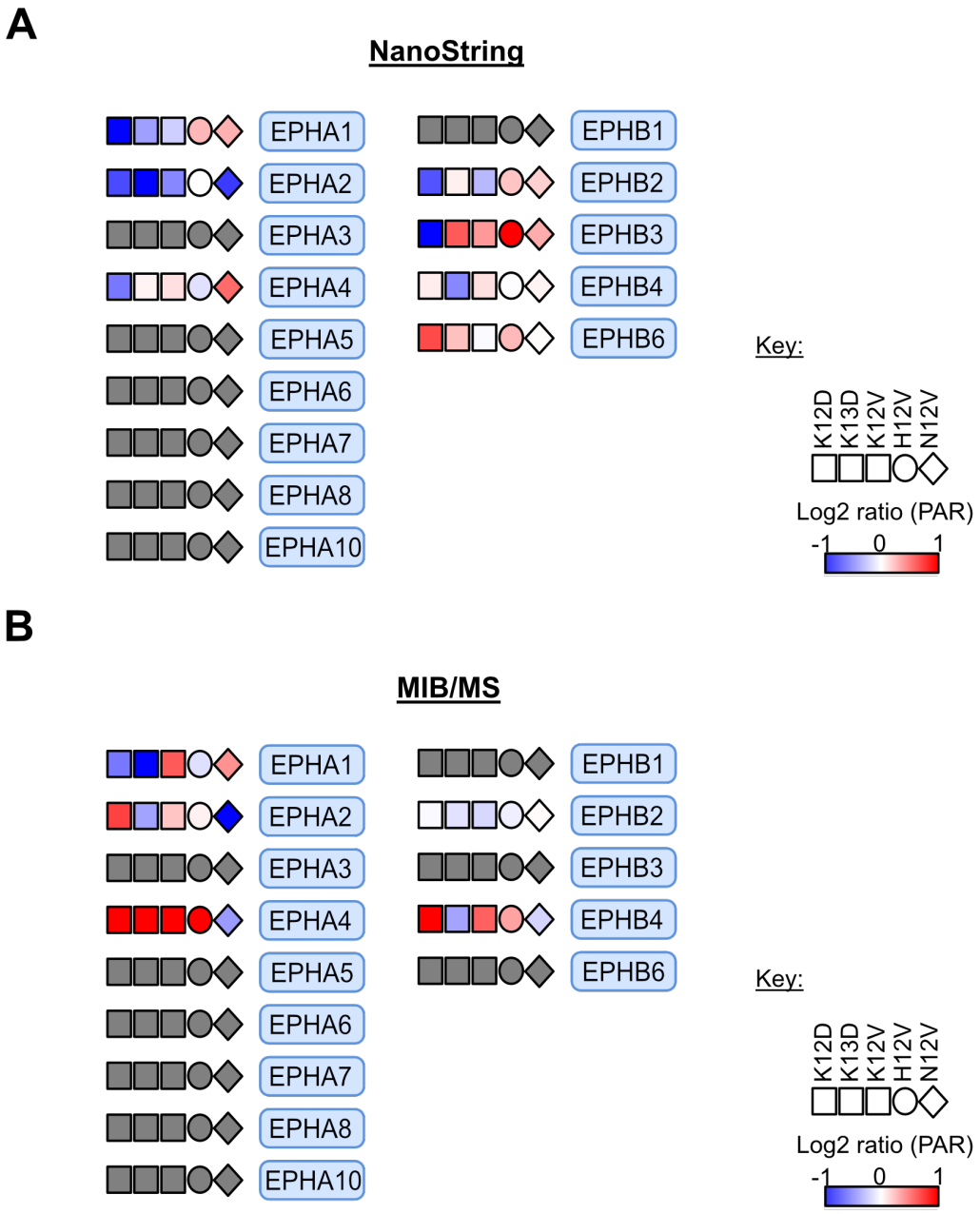

Figure 5.8. NanoString and MIB/MS analyses reveal transcript-level and protein level expression of Ephrin Receptor Tyrosine Kinases in isogenic SW48 cells harbouring different RAS codon mutations

A) NanoString analysis (n=4) and B) MIB/MS analysis (n=3) of isogenic SW48 cells reveals differential expression of Ephrin receptors at the transcript-level and protein-level. The square data points represent the panel of KRAS mutant SW48 cells, the HRAS mutant cell line is represented by the circular data point and the NRAS mutant by the diamond data point. For each mutant, the average counts/intensities taken from all biological replicates were used to determine the fold change (log2 ratio MUT/PAR) in expression in comparison to parental SW48 cells. Each point is coloured based on the magnitude of change in expression compared to the parental SW48 cell line. Ephrin RTKs that are not expressed/detected in SW48 cells are coloured in grey.

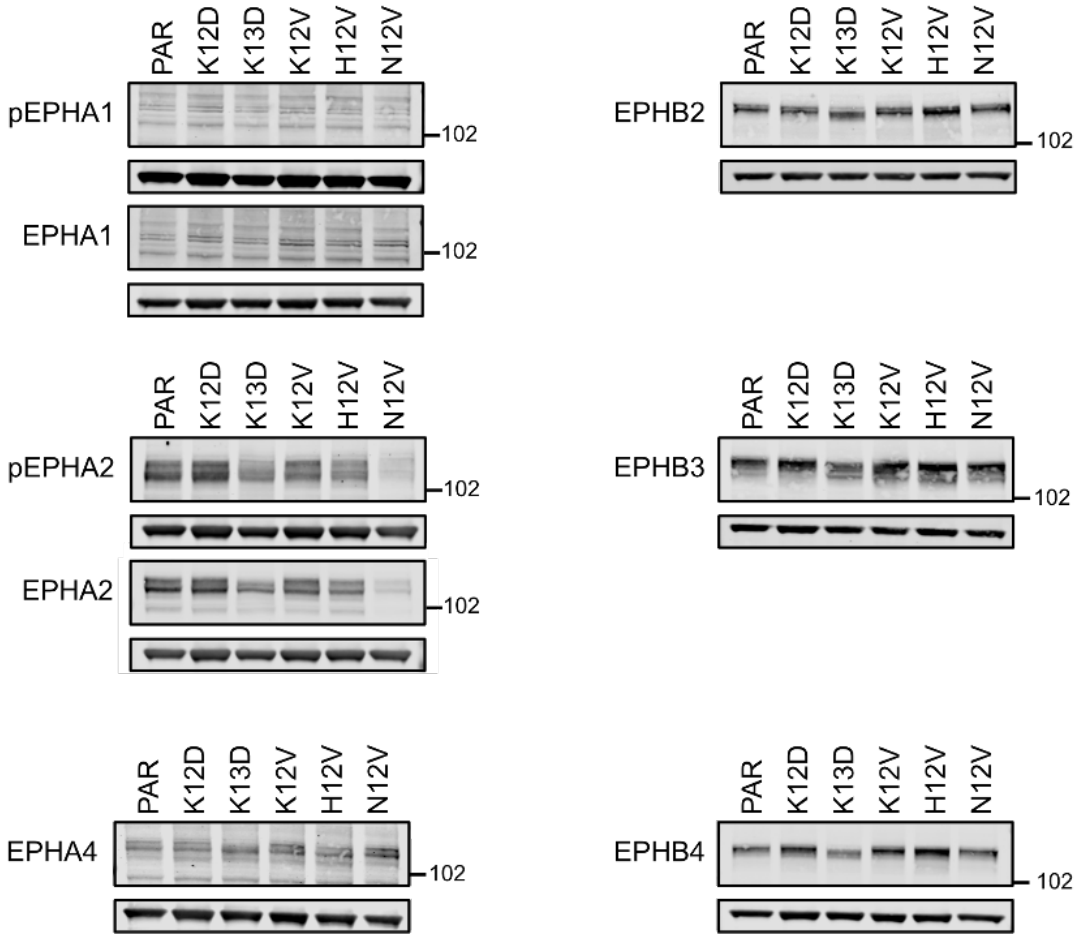

Figure 5.9. Western blotting analysis confirms protein responses of Ephrin Receptor Tyrosine Kinases in isogenic SW48 cells harbouring different RAS codon mutations

SW48 cells were grown in 10%FBS and subsequently lysed in RIPA buffer. Lysates were separated by SDS-PAGE and western blots were probed with the indicated antibodies (n=3).

Experiments to establish any potential relationship between EphA2 and MET may provide an insight into why EphA2 is differentially regulated at the transcript level and protein level. Moreover, western blotting would be required to confirm the RAS dependency of EphA2.

For EphA4, protein responses measured by western blotting and MIB/MS do not correlate; a significant upregulation in EphA4 was reported by MIB/MS however it is important to note, that the assay may have been reporting changes in activation state rather than protein abundance, and therefore it would be important to blot for active protein.

Western blotting analysis for EphB4 closely mapped the protein responses reported by MIB/MS (Figure 5.9). Although there was weak coverage of the other EphB receptors using MIB/MS, we were able to measure protein responses by western blot. Interestingly, the three EphB receptors follow a similar pattern of expression across all SW48 cell lines suggesting that there may be reciprocal activity between this subgroup of Eph receptors.

5.2.5. Regulation of MEK3 activation by oncogenic RAS

Figure 5.10A displays the potential mechanisms regulating MEK3/6 activity in SW48 RAS mutant cells. There seems to be a dichotomy between whether MEK3/6 pathway activation leads to tumour promoting or tumour inhibitory properties. Whilst levels of MEK3 mRNA remained constant, MIB/MS reported differential MEK3 activity across the mutant cell lines (Figure 5.10B). An ~0.5-fold upregulation of MEK3 activity was observed in the HRAS mutant cell line vs. parental cell line, mapping to increased retention of p38 to the MIB column. On the other hand, MIB/MS reported downregulation of MEK3 in 2/3 KRAS mutant cell lines; however, subsequent western blotting revealed MEK3 activity was in fact significantly downregulated in all three KRAS mutant cell lines.

The HRAS- and KRAS-dependent MEK3 responses suggested different mechanisms of regulation and effect that I investigated further.

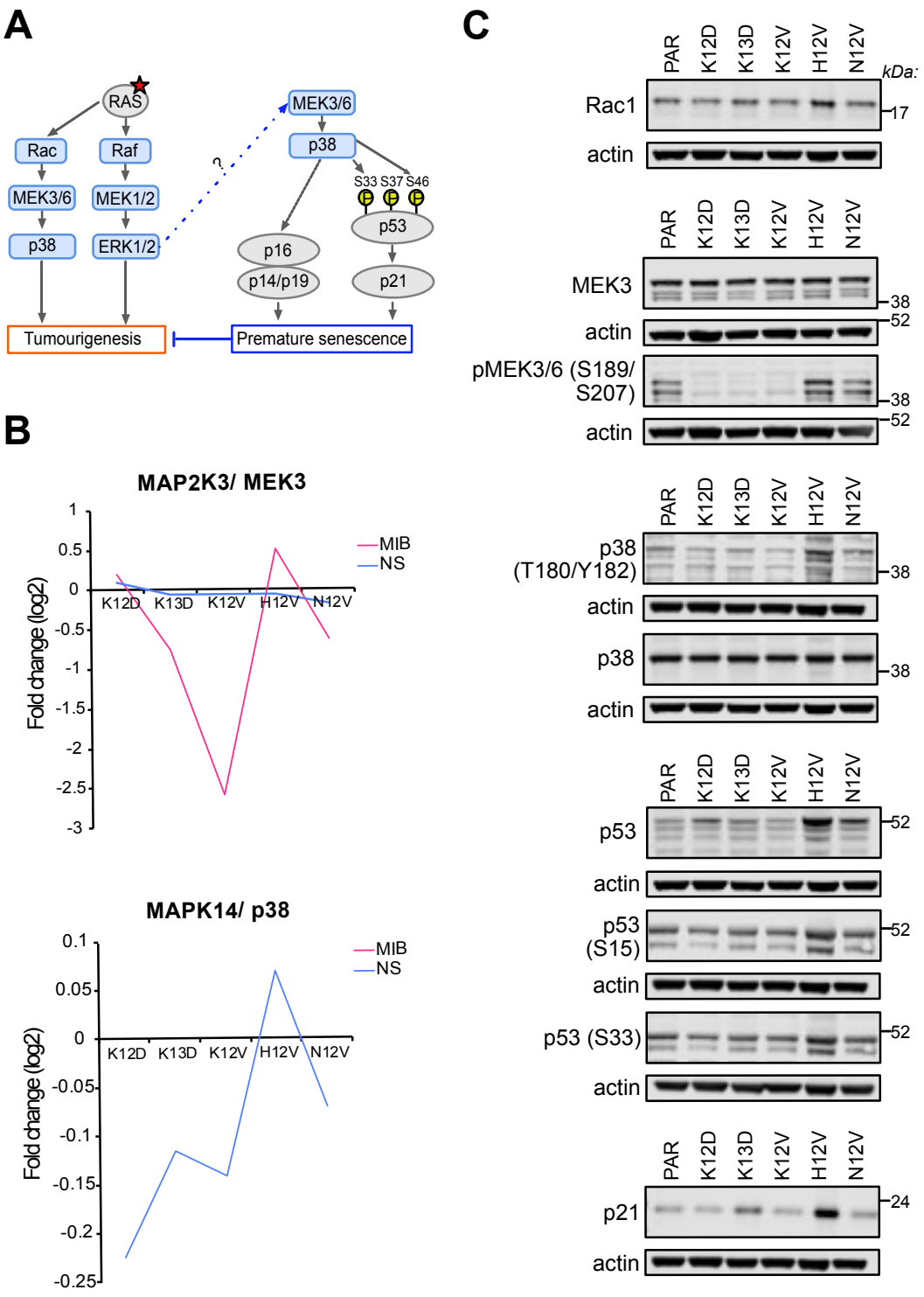

Figure 5.10. MEK3/p38 pathway regulation by oncogenic RAS

A) A simplified outline of potential mechanisms for RAS induced MEK3/6 pathway activation. B) NanoString (blue) and MIB/MS (pink) analyses reveal differential expression of MEK3 and p38 across the mutant SW48 panel vs. parental SW48 cell line. Data is derived from the NanoString (n=4) and MIB/MS experiments (n=3) conducted in Chapter Four. The average counts/intensities taken across all biological replicates were used to determine the fold change in expression of the mutant panel vs. parental cell line (log2 ratio MUT/PAR). C) Western blotting analysis of nodes within the MEK3/p38 pathway. SW48 cells were grown in 10%FBS and subsequently lysed in RIPA buffer. Lysates were separated by SDS-PAGE and western blots were probed with the indicated antibodies (n=3).

5.2.5.1. HRAS

The HRAS-specific upregulation of MEK3 required further investigation to identify the signalling route from Ras to MEK3. Two pathways depicted in Figure 5.10A link via the MAPK pathway or via Rac1. Focussing on the Rac1 link, I measured Rac1 protein abundance. The first western blot in Figure 5.10C shows an increase in Rac1 expression in the HRAS mutant cell line, corresponding with an increase in downstream MEK3 activity inferred by phosphorylation of S189/S207 of MEK3. Furthermore, Rac1 expression remains fairly constant across all other cell lines indicating that MEK3 regulation via Rac1 may be HRAS specific, as previously described (Shin *et al.*, 2005). An increase in phosphorylated p38 is observed in the HRAS mutant, providing further evidence of HRAS-specific activation of the MEK3 pathway. Shin et al. had previously linked HRAS-specific upregulation of MEK3/6 with an invasive and migrative phenotype. However, further downstream an upregulation of total and phosphorylated levels of p53 is observed; SW48 cells have wild type p53 status, so one would expect an increase in p53 would have a tumour suppressive effect on the H12V mutant cell line. Furthermore, levels of p21 are also upregulated in the HRAS mutant vs. parental cell line. Further analyses would be needed to reveal the effect of MEK3 activity on SW48 HRAS mutant cell phenotype.

5.2.5.2. KRAS

MIB/MS also reported KRAS-specific downregulation of p38, a kinase downstream of MEK3. Western blotting analysis was performed in order to confirm p38 protein responses, and also probe the effects on downstream readouts depicted in Figure 5.10A. Firstly, I wanted to investigate whether SW48 KRAS mutant cells were downregulating MEK3 pathway activation in order to evade cellular senescence. Western blotting revealed that MEK3 activation status has no effect on total p38 levels (Figure 5.10C). Instead, loss of MEK3 phosphorylation correlates with a loss of p38 activation in the KRAS mutant cell lines; The phospho-antibody detects p38 when its phosphorylated at threonine 180 and tyrosine 182 (T180/Y182), sites indicative of activation

by MEK3 and MEK6 respectively (ref needed). Further downstream, whilst total levels of p53 remain fairly consistent across the KRAS mutant panel, phosphorylated levels of p53 appear also to be marginally downregulated. Expression of p21 is variable across the KRAS mutant panel and we were unable to probe p16 expression due to reagent availability. On the whole, western blotting analyses has provided some evidence that the KRAS mutant cell panel may be downregulating nodes of the MEK3 pathway in order to evade cellular senescence via p53, however further studies measuring senescence markers would be required to confirm this hypothesis.

It was previously shown that MEK3 pathway activation is dependent on MAPK activity (Wang *et al.*, 2002). Considering the intermediate steps linking MAPK and MEK3 pathway activation are still unclear, I wanted to examine the potential upstream regulators of MEK3; The expression/activity of a potential regulator of MEK3 may be downregulated in the KRAS mutant cell lines at either the transcript or protein level, which could in turn downregulate MEK3 activity. Figure 5.11 displays the A) transcript and B) protein level expression of 16 MAP3Ks that could potentially regulate MEK3 (MAP2K3) activity. At the transcript level, two kinases: TPL2 and MINK1 are downregulated in 2/3 KRAS mutant cell lines. At the protein level, MINK1 is significantly downregulated in 2/3 KRAS mutant cell lines whilst, TPL2 wasn't retained on the MIB column.
To prove a direct link between MAPK and MEK3 pathway activation, a potential regulator of MEK3 should show RAS dependency upon KRAS knockdown. Figure 5.12 displays the expression of the same 16 potential regulators, before and after KRAS knockdown in the K12D cell line. NanoString analysis revealed that both TPL2 and MINK1 display dependency on KRAS; Both kinases are downregulated in the K12D mutant, and upon knockdown, mRNA expression is restored back towards parental levels. Western blotting would be required to prove TPL2 and MINK1 upregulation is dependent on KRAS at the protein level. Moreover, measuring the effect of MEK3 activity after knockdown of either kinase could prove direct dependency.

Thus far, we had obtained evidence of reduced MEK3 activity in three independent KRAS mutant cell lines vs. the wild type cell line. Furthermore,

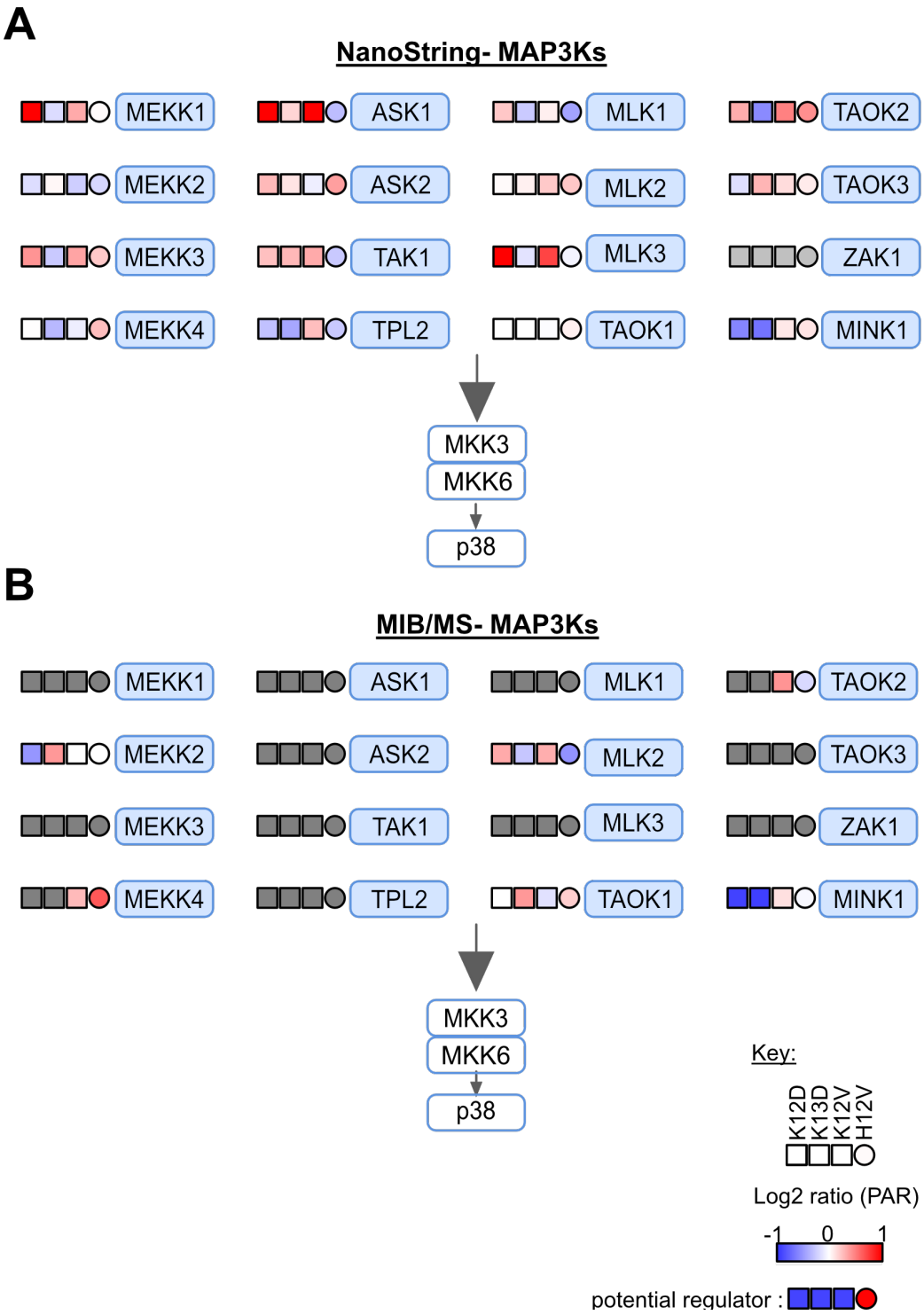

Figure 5.11. NanoString and MIB/MS analyses reveals potential upstream regulators of MKK3/6 in isogenic SW48 cells

NanoString (n=4) and MIB/MS (n=3) analyses were used to measure transcript and protein responses of potential MEK3 upstream regulators. The square data points represent the panel of KRAS mutant SW48 cells and the HRAS mutant cell line is represented by the circular data point. For each mutant, the average counts taken across all biological replicates were used to determine the fold change in expression in comparison to the parental SW48 cells (log2 ratio MUT/PAR). Each point is coloured based on the magnitude of change in expression compared to the parental SW48 cell line. Kinases that were not expressed/detected in SW48 cells are coloured in grey.

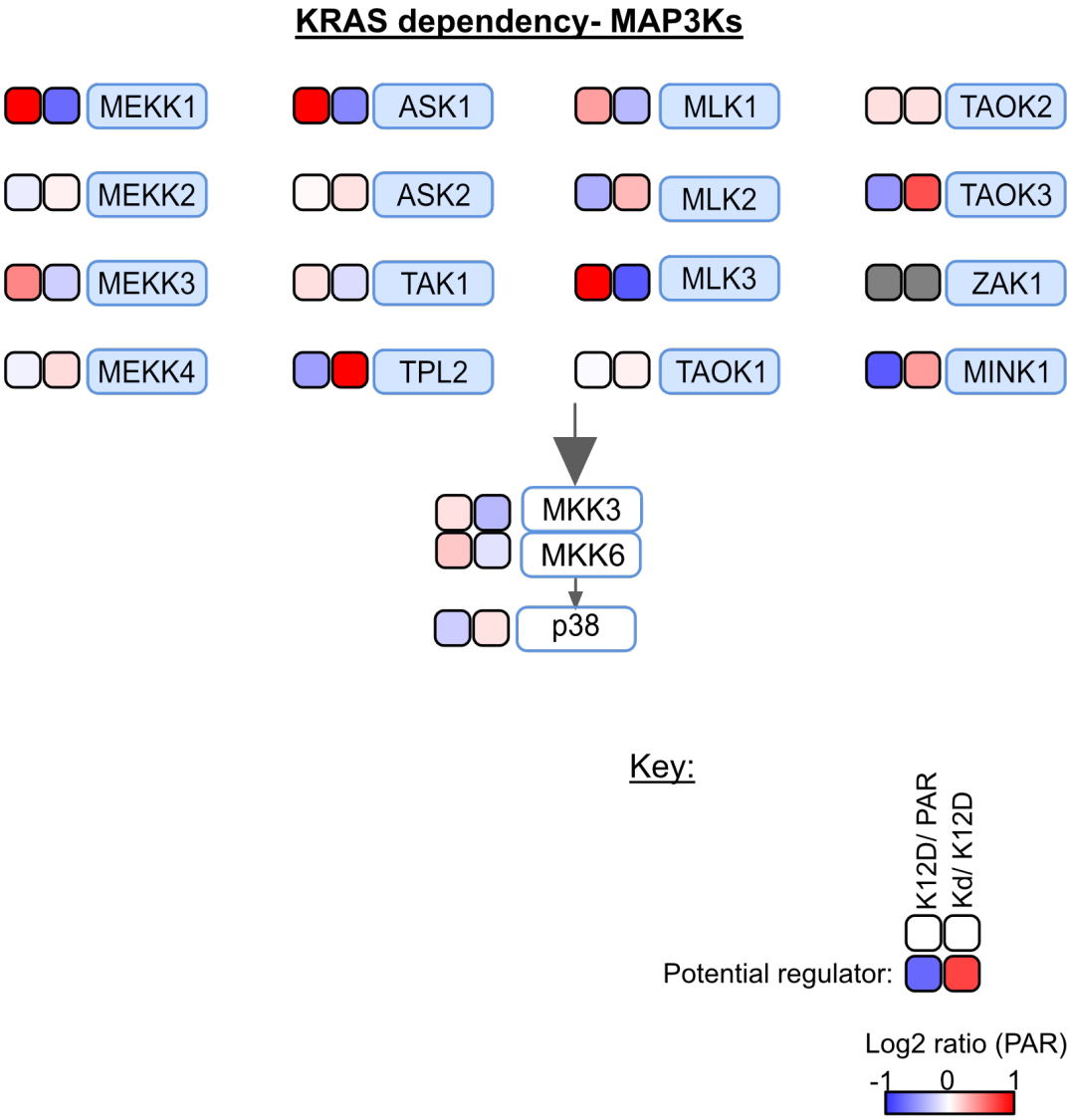

Figure 5.12. NanoString analysis after KRAS knockdown reveals the KRAS dependent upstream regulators of MEK3/6 in SW48 K12D cells

SW48 KRAS G12D cells with inducible expression of shRNA targeting KRAS were treated with 100 ng/mL doxycycline for 1 week to induce knockdown of KRAS and then analysed using NanoString analysis (n=4). The average counts taken from four biological replicates were used to determine the fold change (log2 ratio) in expression of the 1) K12D mutant cell line vs. the parental SW48 cells and 2) K12D mutant +/- knockdown. The expression of a potential Ras dependent regulator of pMKK3/6 would be downregulated in the K12D mutant cell line compared to the parental levels and then restored back towards parental levels upon KRAS knockdown.

we observed some reduction in the phosphorylation and activation of downstream nodes. We also identified potential upstream regulators of MEK3 and evaluated their dependency on KRAS.

For MEK3 itself, we were unable to confirm KRAS dependency by NanoString and MIB/MS analysis. Differential MEK3 regulation was observed at the protein level, making NanoString analysis after KRAS knockdown redundant. Plus, we were unable to detect MEK3 by MIB/MS in any of the knockdown experiments (figure 5.6). Using western blotting analysis, we were unable to confirm KRAS dependency for MEK3 (Figure 5.13). As expected, levels of phosphorylated MEK3 were significantly downregulated in the K12D mutant vs. parental cell line, however no change was observed upon KRAS knockdown; after KRAS knockdown, one would expect pMEK3 levels to increase back toward parental levels.

Figure 5.14 displays data from preliminary DNA transfection experiments. Plasmid DNA encoding the different RAS G12V isoforms, N-terminally tagged with EGFP, were transfected into parental SW48 cells. There was no reduction in pMEK3 levels when the KRAS plasmid was transfected into parental SW48 cells. However, an increase in pMEK3 was observed upon HRAS plasmid transfection, when total MEK3 levels remained constant across all cell lines. It is important to note that this is preliminary data and experimental conditions need to be optimised.

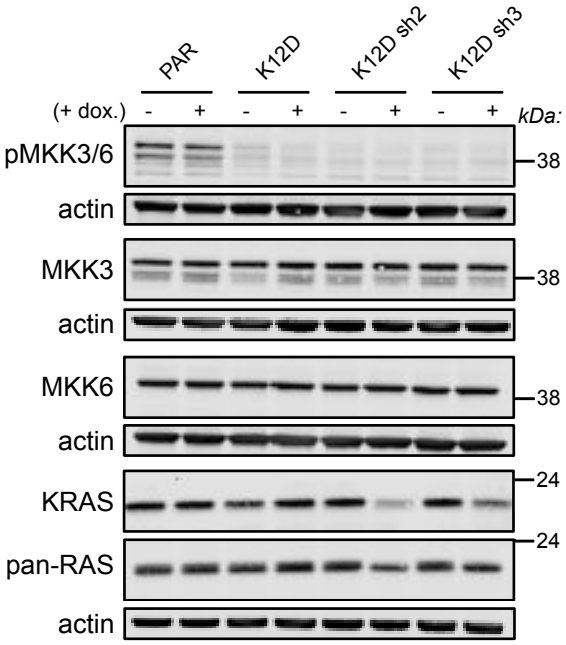

Figure 5.13. KRAS knockdown in SW48 KRAS G12D mutant cells has no effect on pMKK3/6 expression

SW48 K12D cells with inducible expression of 2 different shRNAs targeting KRAS (sh1 and sh2) were treated with 100ng/mL doxycycline for 1 week to induce shRNA expression. Cells were lysed using RIPA buffer and separated with SDS-PAGE. Western blots probed with the indicated antibodies (n=3).

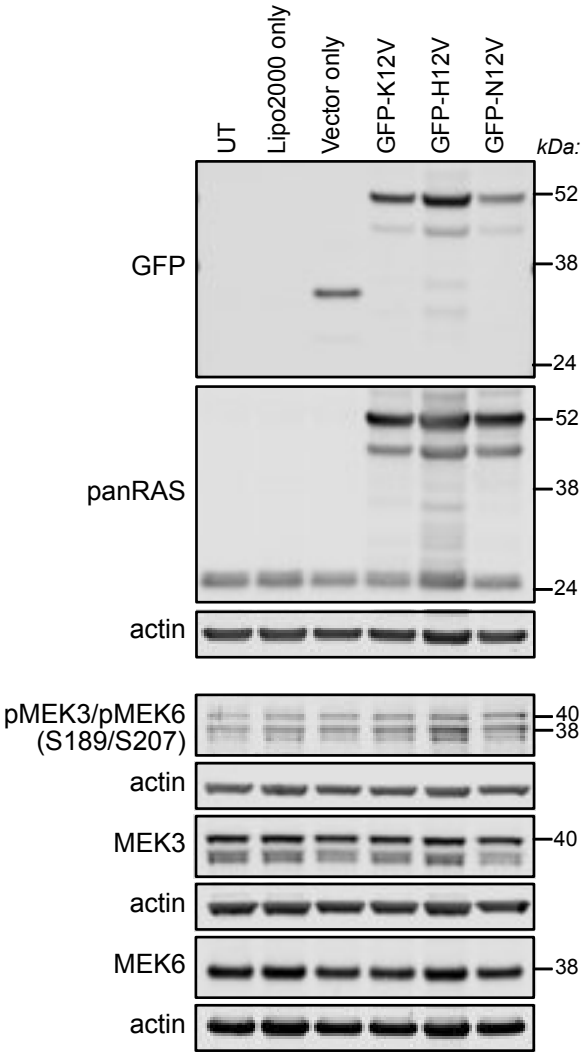

Figure 5.14. Transient expression of mutant RAS isoforms in Parental SW48 cells

Plasmid DNA encoding the different RAS G12V isoforms, n-terminally tagged with EGFP, were transfected into parental SW48 cells using the Lipofectamine 2000 transfection system. The DNA-lipid complex was incubated for 20 minutes at room temperature before being added dropwise to the cells. After 24hrs transfection efficiency was evaluated by visualising GFP expressing cells under a NIKON TiE microscope. A separate dish of cells were grown in parallel and harvested for western blotting analysis (see above). Cells were lysed using RIPA buffer and separated using SDS-PAGE. Western blots were probed with the indicated antibodies (n=1).

5.3. Summary of results

- The induced expression of two independent shRNAs specific for KRAS resulted in significant loss of KRAS expression in SW48 K12D cells.
- NanoString, MIB/MS and Western blotting analyses were used to study kinome adaptations after KRAS knockdown. The methods were applied to determine whether there is a direct link between oncogenic KRAS G12D and differentially regulated kinases.
- A significant loss of DCLK1 expression was observed in response to either of the two independent shRNAs for KRAS.
- NanoString analysis revealed a direct link between oncogenic KRAS and MET mRNA upregulation.
- Oncogenic KRAS differentially regulates the group of Ephrin receptor tyrosine kinases (Eph RTKs).
- Whilst the link between oncogenic RAS and MEK3 activity is not clear, nodes within the pathway were probed by western blotting and their RAS dependence evaluated using NanoString and MIB/MS assays.

5.4. Discussion

In this chapter, I successfully evaluated the RAS dependency of kinases that are differentially regulated in the K12D vs. Parental SW48 cell line. The induced expression of two independent shRNAs specific for KRAS resulted in significant loss of KRAS expression. Using this cell system and a combination of NanoString, MIB/MS and western blotting analyses, we were able to identify KRAS dependent regulation of kinase expression and/or activity. Furthermore, I have been able to investigate some of the KRAS isoform and allele specific responses identified in chapter four.

Our studies provide corroborating evidence of a link between DCLK1 upregulation and oncogenic KRAS. DCLK1 was the most significantly upregulated kinase in the KRAS codon 12 mutant cell lines. NanoString,

MIB/MS and western blotting analysis all confirmed that DCLK1 upregulation is dependent on oncogenic KRAS. Indeed, a direct connectivity between DCLK1 overexpression and RAS activation has been described in these cells previously, but also in another recent study in PDAC (Hammond *et al.*, 2015; Qu *et al.*, 2019). In fact, DCLK1 is upregulated in several cancers, including colorectal cancer, and therefore is a promising drug target (Li, Jones and Mei, 2019). However, it is a relatively understudied kinase and its biology remains poorly understood. Drug Discovery efforts tend to focus on kinases with well-established roles in cancer cell signalling, therefore it is not surprising that up until April 2020, no selective inhibitor for DCLK1 had been described (Ferguson *et al.*, 2020). The recent study describes the first potent chemical inhibitor of DCLK1, DCLK1-IN1. Using multi-omic approaches, authors reveal that DCLK1 inhibition in PDAC organoids regulates proteins and pathways involved in cell motility, although studies thus far are limited to in vitro (Ferguson *et al.*, 2020). DCLK1 is one of 300 members of the kinome that still don't have any inhibitors that have entered a clinical trial (Wilson *et al.*, 2018). This highlights an area of unmet need within the kinome; understudied kinases lack selective inhibitors however, counterintuitively a lack of inhibitor availability stifles our understanding of kinase biology.

The receptor tyrosine kinase, MET was also upregulated in the KRAS codon 12 mutant cells. MET overexpression has previously been reported in several different epithelial cancers including thyroid (Di Renzo *et al.*, 1992), ovarian (Di Renzo *et al.*, 1994), pancreatic (Di Renzo *et al.*, 1995b), colorectal and gastric cancers (Di Renzo *et al.*, 1991) (Liu, Park and Tsao, 1992). A study of colorectal carcinomas concluded that MET is overexpressed without gene amplification in the large majority of cases (Di Renzo *et al.*, 1995a). Moreover, activated oncogenes such as RAS can induce MET overexpression in cancer by enhancing cMET transcription (Gambarotta *et al.*, 1996) (Ivan *et al.*, 1997).

In SW48 cells, MET expression is significantly upregulated in the K12D mutant vs. parental cells when they are serum starved, and downstream activity is induced by HGF stimulation (Figure 4.6). This suggests that MET upregulation is due to MET receptor overexpression rather than elevated levels of its ligand,

HGF. Our studies reveal that MET overexpression is dependent on oncogenic KRAS. Knockdown of KRAS in SW48 K12D mutant cells resulted in a significant reduction of MET mRNA suggesting that, like previously described, MET overexpression occurs from oncogene induced enhanced transcription (Gambarotta *et al.*, 1996) (Ivan *et al.*, 1997).

It is important to note that although NanoString analysis revealed that MET mRNA deregulation was directly dependent on KRAS, we did not see a reduction in MET protein expression after KRAS knockdown. The half-life of MET protein has been shown to be approximately 5h, therefore a reduction in protein expression should have been observed after a week of doxycycline treatment (Giordano *et al.*, 1989). Marginal decreases in MET protein expression were seen in the K12D cell line with induced sh2 oligo expression. Considering that a higher level of KRAS knockdown was achieved using this shRNA, one could speculate that higher levels of KRAS knockdown or complete knockout would be needed to see an effect on MET protein expression by western blotting. One other possible reason may be due to antibody specificity; the MET antibody recognises the beta subunit (145kDa) of MET whereas, KRAS may regulate the expression of the alpha subunit (45kDa). Impaired degradation may also cause an accumulation of MET protein even when there is less mRNA available for translation. It has been revealed that activated MET variants display resistance to degradation suggesting impaired degradation may contribute to tumorigenesis (Mak *et al.*, 2007; Joffre *et al.*, 2011). Along with enhanced cMET transcription, defective degradation of the receptor may also contribute to MET overexpression in SW48 K12D cells; after KRAS knockdown, MET mRNA levels reduce however if the cells have become resistant to degradation, we may not necessarily see a reduction in receptor expression.

Forced degradation through targeting one of the many mechanisms of MET degradation, has now become a promising therapeutic strategy. Proteolysis targeting chimera (PROTACs), a technology for post-translational protein degradation, has been developed against MET and other RTKs (Burslem *et al.*, 2018). The group employed a selective inhibitor of MET, foretinib as a

recruiting element, tethered to an E3 ligase, to target Met for proteasomal degradation. When compared to conventional TKIs, PROTACs provided a more potent and sustained effect on MET signalling inhibition that was also less susceptible to kinome rewiring (Burslem *et al.*, 2018). There has also been some success with monoclonal antibodies that primarily target the interaction between HGF and MET, but unexpectedly induce its internalisation and degradation. One example, DN30, inhibits MET signalling by inducing the cleavage of MET on the cell surface by metalloproteases such as ADAM10. The fragments can then be internalised and degraded by the lysosome (Petrelli *et al.*, 2006).

Other efforts to target MET directly using monoclonal antibodies or TKIs, have been confounded by drug resistance. There is increasing evidence that RAS mutations confer resistance to MET inhibition, and that targeting MET in combination with nodes of the MAPK pathway, may circumvent kinome rewiring (Leiser *et al.*, 2015; Suzawa *et al.*, 2019; Rotow *et al.*, 2020). Taking this into consideration, I would like to extend our findings to a panel of KRAS mutant cell lines. If KRAS codon 12 specific upregulation of MET occurs generally in colorectal cancer, targeting the MAPK pathway and MET in combination could be beneficial in this setting and may inform treatment choices in the clinic.

Another kinase that displayed strong evidence of KRAS dependency was EPHA1. Downregulation of EPHA1 expression has been associated with an invasive and migrative phenotype in breast cancer (Fox and Kandpal, 2004) and colorectal cancer cells (Dong *et al.*, 2009). Epigenetic silencing of EPHA1 in colorectal cancer is correlated with poorer survival (Herath *et al.*, 2009). Furthermore, knockdown of EPHA1 promotes adhesion and motility in HRT18 colorectal cancer cells (Wu *et al.*, 2016). NanoString and MIB/MS analysis revealed EPHA1 expression is downregulated in the panel of SW48 cells harbouring KRAS mutations. Moreover, we found evidence at the transcript and protein level that EPHA1 downregulation was directly dependent on oncogenic KRAS. One unique property of this receptor compared with other RTKs is its ability to inhibit RAS and MAPK signalling (Miao *et al.*, 2001); SW48

KRAS mutant cells may downregulate EPHA1 expression in order to bypass the effects of EPHA1 on MAPK inhibition. Unfortunately, due to poor antibody specificity we were unable to confirm protein responses by western blotting, a common obstacle often encountered in kinase studies.

Whilst EPHA1 is generally thought of as a tumour suppressor, its most closely related family member EPHA2 has been described as tumour promoting in a variety of different cancers (Kou and Kandpal, 2018). EPHA2 is overexpressed in several cancer types, including breast (Zelinski *et al.*, 2001), melanoma (Udayakumar *et al.*, 2011) and prostate cancer (Walker-Daniels *et al.*, 1999). Moreover, it has been shown that EPHA2 promotes invasion and migration in colorectal cancer and is associated with poor survival (Dunne *et al.*, 2016). In SW48 K12D cells, we observed KRAS dependent upregulation of EPHA2 protein expression. Notably, at the transcript level, EPHA2 was differentially regulated whilst also being KRAS dependent; EPHA2 mRNA was downregulated and upon knockdown its expression increased.

A RAS-EPHA2 feedback loop has been described which may provide an explanation of why EPHA2 mRNA and protein levels are differentially regulated in SW48 cells (Macrae *et al.*, 2005). It has been shown that whilst RAS/MAPK signalling induces EPHA2 expression, ligand stimulated EPHA2 downregulates MAPK signalling. In cancer cells, the EPHA2 ligand, ephrin-A1 is downregulated in order to bypass negative regulation of MAPK signalling; the expression of EPHA2 and ephrin-A1 was inversely proportional in a panel of breast cancer cell lines and this was shown to contribute to hyperactive RAS signalling (Macrae *et al.*, 2005). Indeed, MIB/MS analysis revealed that oncogenic KRAS upregulates EPHA2 expression in SW48 K12D cells however, I would be interested to probe ephrin-A1 expression to see if EPHA2 and ephrin-A1 expression is inversely proportional. One could expect that SW48 KRAS mutant cells downregulate ephrin-A1 expression in order to circumvent the ligand dependent negative feedback loop. If this mechanism is typically adopted in KRAS mutant colorectal cancer cells, targeting EPHA2 with a molecule that mimics ephrin-A1 thus downregulating MAPK signalling, may be a promising therapeutic strategy in RAS mutant cells.

Interestingly, EPHA2 and MET expression and activation status correlated across the SW48 cell panel. An RNA sequencing study of 675 human cancer cells revealed that EPHA2 expression is strongly correlated with other RTKs, such as MET and EGFR (Klijn *et al.*, 2015). Moreover, it was shown that the expression of these co-expressed genes is regulated by MAPK or PI3K signalling. A recent study has identified EPHA2 as a biomarker of resistance to anti-EGFR therapy (Martini *et al.*, 2019). Enhanced EPHA2 levels is a mechanism of resistance to cetuximab therapy and inhibition of EPHA2 could overcome resistance in RAS mutant colorectal cancer cells. Considering RAS mutations also confer resistance to MET inhibition, targeting MET in combination with EPHA2, may circumvent kinome rewiring. Therefore, I would be interested in targeting MET and EPHA2 in the SW48 KRAS codon 12 mutant panel to see whether this may be a promising combinational therapy.

In this chapter, we also investigated the potential interplay between oncogenic RAS and MEK3 regulation. MIB/MS and western blotting analyses revealed RAS isoform specific activation of MEK3; MEK3 activation was upregulated in the HRAS mutant cell line, whilst MEK3 activity was downregulated in the KRAS mutant panel.

HRAS specific upregulation of MEK3 has previously been described in breast cancer cells (Shin *et al.*, 2005). Authors showed that HRAS, but not NRAS, upregulates MEK3 activity via Rac1, leading to an invasive and migrative phenotype. Western blotting analysis revealed that Rac1 expression is upregulated in the SW48 HRAS mutant vs. parental cell line, corresponding with elevated levels of pMEK3 and p38. However, we would need to knockdown Rac1 to confirm direct connectivity between Rac1 and MEK3/p38 activity. Surprisingly, further downstream, there was evidence of p53 and p21 upregulation in the HRAS mutant vs. parental cell line. Considering p53 and p21 are markers of cellular senescence, further analyses would be needed to reveal the effect of MEK3 activation in this context. HRAS specific upregulation of the MEK3/p38 pathway may result in cellular senescence and may potentially act as a protective mechanism to prolonged RAS signalling (Serrano *et al.*, 1997). Notably, SW48 HRAS mutant cell morphology is larger

and flatter than the other SW48 cell lines. Going forward, I would like to measure B-galactosidase levels across the cell lines to determine whether the cells are in fact senescent.

Indeed, oncogenic RAS can induce cellular senescence via MEK3 and p38 activation (Wang *et al.*, 2002). SW48 KRAS mutant cells may evade cellular senescence by downregulating MEK3 pathway activation. Western blotting analyses reported downregulation of the downstream nodes, p38 and p53 in SW48 KRAS mutant cells; whilst total expression of p38 and p53 remained constant across the SW48 panel, marginal decreases in p38 and p53 activation were observed in the KRAS mutant panel. However, I would suggest caution as to whether the level of downregulation downstream of MEK3 is significant enough to produce a phenotypic effect.

Although there is evidence of reduced MEK3 activity in three independent KRAS mutant cell lines, it was notable that MEK3 levels did not change in either the KRAS knockdown (Figure 5.12) or KRAS over-expression experiments (Figure 5.13). This may indicate stable rewiring of the signalling network regulating MEK3 expression so that it is now independent of KRAS. There are a variety of links between Ras and MEK3 that may be responsible, one is via MINK1. A study in ovarian epithelial cells, revealed that the kinase, MINK1, may be involved in RAS induced cellular senescence (Nicke *et al.*, 2005). Authors showed that RAS activates MINK1, which in turn activates MEK3 and p38, resulting in cellular senescence through elevated levels of p21. Furthermore, it was shown that oxidative stress is necessary for the activation of MINK1 downstream of RAS. RAS activates MINK1 with delayed kinetics involving reactive oxygen species (ROS), and this may provide the missing link between RAS and MEK3 pathway induction. They identified MINK1 as a potential tumour suppressor that could limit the oncogenic potential of cancer cells (Nicke *et al.*, 2005).

In SW48 cells we found evidence of reduced MINK1 expression. NanoString and MIB/MS analyses revealed that like MEK3, MINK1 was downregulated in the KRAS mutant panel. Moreover, we were also able to confirm that MINK1

mRNA downregulation is directly dependent on KRAS. Further work would be needed to elucidate whether KRAS mutant cells are potentially downregulating MINK1 and MEK3 activation in order to evade cellular senescence. Going forward, I would like to confirm direct dependency between MINK1 and MEK3 and also measure levels of ROS in the mutant vs. parental cell lines.

In this chapter, I have successfully identified kinases that are regulated by oncogenic RAS isoforms and I have suggested follow-up work that would be necessary to identify potential mechanisms. We were hampered by a lack of specific inhibitors and antibodies; however, our data highlight the utility of the discovery-based MIB/NanoString approach for identifying new areas of Ras-relevant biology.

Chapter 6 : Final discussion

In the initial stages of my PhD, I successfully established and optimised the MIB/MS assay in our lab. During this time, the viewpoint on how the MIB/MS assay can be used to study the kinome shifted. Whilst it was originally claimed to be sensitive to kinase activation state, data emerged suggesting that the ability to differentially enrich for active vs. inactive kinases is likely to be highly context dependent (Ruprecht *et al.*, 2015). Evaluating the findings from Chapter three led me to similar conclusions. I established that the assay mainly reports changes in kinase abundance, and in limited cases, changes in kinase activity. Concurrent with the data presented by the Kuster lab, the data generated in this thesis contributed to understanding within the field as to how the method can be used to profile the kinome. It is now widely accepted that the capability of the MIB/MS assay to report dynamic changes in kinase activation depends on three main factors:

- The level of expression of a kinase in a cell
- Kinase affinity to MIBs
- Kinase conformation or activation status

Nevertheless, due to low cellular abundance, kinases are often underrepresented in proteomic and phosphoproteomic datasets and therefore the assay is still a good tool for enrichment (Daub *et al.*, 2008). The method allowed the isolation and analysis of 50% of the SW48 expressed kinome, which is comparable to the coverage achieved in previous MIB/MS publications (Duncan *et al.*, 2012a). In Chapter four, I demonstrated how integrating data from MIB/MS analyses with transcriptomic analyses can help infer differential kinome expression vs. activity in cells. However, it is important to note that further validation is required to discriminate between each possibility.

The combination of methodologies was applied to obtain an insight into cellular kinase adaptations to different oncogenic RAS mutations. Most of our

understanding of RAS isoform specific signalling has been inferred from studies of mouse development (Koera *et al.*, 1997; Esteban *et al.*, 2001). Furthermore, cancer mutational studies have helped us to understand that there is distinct tissue specific RAS mutational profiles for each RAS isoform (Prior, Lewis and Mattos, 2012; Prior, Hood and Hartley, 2020). However, why RAS isoforms differentially and preferentially couple to specific cancers, codons and amino acid substitutions remains unclear. Classical studies of ectopically expressed activated RAS describe preferential coupling of the RAS isoforms to key kinase effectors, RAF and PI3K (Yan *et al.*, 1998; Voice *et al.*, 1999). However, studies of endogenous RAS expression have helped us to appreciate that this perception was likely to be over-simplistic and RAS signalling is in fact more context dependent (Tuveson *et al.*, 2004; Omerovic *et al.*, 2008; Hood *et al.*, 2019). Moreover, ectopically expressed RAS proteins are often produced at supraphysiological levels and can alter cell signalling and even induce cellular senescence (Serrano *et al.*, 1997).

For these reasons, we used an isogenic panel of SW48 colorectal cancer cell lines to study endogenous RAS signalling. Isogenic cell models provide the opportunity to study the cellular consequences of RAS mutations, without the additional effects of differences in the genetic background. Furthermore, a matched parental cell line can be used as a reference and therefore comparisons can be made across the whole panel of mutations. To date, most studies have focused on comparative analysis of KRAS mutant vs. wild type cells (Hammond *et al.*, 2015; Winters *et al.*, 2017). However, our cell line panel included a G12V mutant in all three isoforms, alongside a KRAS panel harbouring different codon mutations. This novel cell line panel has enabled us to carry out the first kinome wide analysis of endogenous isoform and mutation specific Ras signalling.

One of the possible criticisms of the SW48 cell line is that they are not dependent on RAS to be viable and therefore are not a true representation of RAS driven oncogenesis. To address this, we conducted RAS knockdown studies to determine whether there was a direct link between oncogenic RAS and differentially regulated kinases.

NanoString and MIB/MS analyses revealed a subset of Ras responsive kinases for further analysis. A notable observation was the lack of responses within the immediate RAS network; in concordance with many studies investigating endogenous RAS isoform signalling, effector activation was minimal downstream of mutant RAS (Tuveson *et al.*, 2004; Omerovic *et al.*, 2008; Hood *et al.*, 2019). It seems likely that RAS induces oncogenesis through a complex network of signalling nodes rather than just the classical linear pathways we have come to know. Our global, unbiased approaches to study the kinome have enabled us to study RAS isoform specific signalling in the wider context. Our data suggests there needs to be greater attention and appreciation of the effects of RAS isoform and mutation specific signalling in the wider signalling network and highlights the unmet need within the kinome.

Another key observation was that there were very few common responses across the RAS mutant panel. Furthermore, there was evidence of divergence between codon 12 and codon 13 mutations in the KRAS mutant panel; in concordance with previous data generated in the lab, we identified a cluster of proteins that were significantly upregulated in the KRAS codon 12 mutants only (Hammond *et al.*, 2015). A final layer of complexity was added by the fact that each RAS mutant cell line activated distinct kinase networks. Altogether, this emphasises the point that RAS mutations should not be treated equally. In the clinic, patients with RAS mutant tumours are often treated as one homologous group. Our data suggests that differential signalling occurs downstream of different RAS mutations and therefore RAS mutations need to be assessed on a case-by-case basis. Moreover, RAS isoform specific signalling needs to be investigated in the context of different tissues.

Going forward, I would have liked to extend my findings to a wider panel of colorectal cancer cell lines in order to identify common isoform/mutation specific kinase responses to oncogenic RAS. Moreover, these global kinase profiling approaches could be applied to other cancer types to help characterise the context dependence of endogenous isoform-specific Ras-signalling responses in different tissues. Interestingly, there was a significant bias towards the KRAS G12D variant; the mutant cell line harboured the most

differential kinase responses compared to the wild type cell line. A recent study provided the first indication that variations in signalling downstream of different RAS mutations may drive the RAS mutational pattern seen in human cancers (Poulin *et al.*, 2019). Considering KRAS G12D is the most prevalent mutation in colorectal cancer, it may be likely that we see more responses downstream of this variant due to its oncogenic potency in this tissue type. It would be interesting to investigate whether, there would be similar observations for NRAS in melanoma, for example.

Using the discovery based NanoString/MIB approach, I was able to successfully identify kinases that are regulated by oncogenic RAS variants. Unfortunately, we were hampered by a lack of specific antibodies and inhibitors, an often-common challenge in kinome studies, and therefore follow up work would need to be done to validate any potential mechanisms. Nevertheless, our data highlight the utility of these global kinase approaches in identifying new areas of RAS relevant biology. These approaches could be used to identify novel targets downstream of RAS or inform the rationale selection of existing treatments for different RAS mutant tumours. Moreover, the combination of methodologies could be used to understand what kinome rewiring occurs in response to RAS pathway inhibition. Several studies have used the MIB/MS approach to inform the rationale selection of new combinational therapies that may overcome resistance in patients (Duncan *et al.*, 2012a; Johnson *et al.*, 2014; Stuhlmiller *et al.*, 2015; Kurimchak *et al.*, 2019). Furthermore, considering that resistance is likely to arise in response to direct RAS inhibition, understanding the specific requirements of each RAS mutation will be essential going forward.

Bibliography

Abankwa, D., Gorfe, A. A., Inder, K. and Hancock, J. F. (2010) 'Ras membrane orientation and nanodomain localization generate isoform diversity', *Proc Natl Acad Sci U S A,* 107(3), pp. 1130-5.

Aimes, R. T., Hemmer, W. and Taylor, S. S. (2000) 'Serine-53 at the tip of the glycine-rich loop of cAMP-dependent protein kinase: role in catalysis, P-site specificity, and interaction with inhibitors', *Biochemistry,* 39(28), pp. 8325-32.

Amado, R. G., Wolf, M., Peeters, M., Van Cutsem, E., Siena, S., Freeman, D. J., Juan, T., Sikorski, R., Suggs, S., Radinsky, R., Patterson, S. D. and Chang, D. D. (2008) 'Wild-type KRAS is required for panitumumab efficacy in patients with metastatic colorectal cancer', *J Clin Oncol,* 26(10), pp. 1626-34.

Apolloni, A., Prior, I. A., Lindsay, M., Parton, R. G. and Hancock, J. F. (2000) 'H-ras but not K-ras traffics to the plasma membrane through the exocytic pathway', *Mol Cell Biol,* 20(7), pp. 2475-87.

Aronheim, A., Engelberg, D., Li, N., al-Alawi, N., Schlessinger, J. and Karin, M. (1994) 'Membrane targeting of the nucleotide exchange factor Sos is sufficient for activating the Ras signaling pathway', *Cell,* 78(6), pp. 949-61.

Bailey, F. P., Byrne, D. P., McSkimming, D., Kannan, N. and Eyers, P. A. (2015) 'Going for broke: targeting the human cancer pseudokinome', *Biochem J,* 465(2), pp. 195-211.

Ballester, R., Marchuk, D., Boguski, M., Saulino, A., Letcher, R., Wigler, M. and Collins, F. (1990) 'The NF1 locus encodes a protein functionally related to mammalian GAP and yeast IRA proteins', *Cell,* 63(4), pp. 851-9.

Benjamini, Y., Drai, D., Elmer, G., Kafkafi, N. and Golani, I. (2001) 'Controlling the false discovery rate in behavior genetics research', *Behav Brain Res,* 125(1-2), pp. 279-84.

Bonfini, L., Karlovich, C. A., Dasgupta, C. and Banerjee, U. (1992) 'The Son of sevenless gene product: a putative activator of Ras', *Science,* 255(5044), pp. 603-6.

Bos, J. L., Rehmann, H. and Wittinghofer, A. (2007) 'GEFs and GAPs: critical elements in the control of small G proteins', *Cell,* 129(5), pp. 865-77.

Bowtell, D., Fu, P., Simon, M. and Senior, P. (1992) 'Identification of murine homologues of the Drosophila son of sevenless gene: potential activators of ras', *Proc Natl Acad Sci U S A,* 89(14), pp. 6511-5.

Broek, D., Toda, T., Michaeli, T., Levin, L., Birchmeier, C., Zoller, M., Powers, S. and Wigler, M. (1987) 'The S. cerevisiae CDC25 gene product regulates the RAS/adenylate cyclase pathway', *Cell,* 48(5), pp. 789-99.

Brunner, D., Dücker, K., Oellers, N., Hafen, E., Scholz, H. and Klämbt, C. (1994) 'The ETS domain protein pointed-P2 is a target of MAP kinase in the sevenless signal transduction pathway', *Nature,* 370(6488), pp. 386-9.

Buday, L. and Downward, J. (1993) 'Epidermal growth factor regulates p21ras through the formation of a complex of receptor, Grb2 adapter protein, and Sos nucleotide exchange factor', *Cell,* 73(3), pp. 611-20.

Buday, L., Warne, P. H. and Downward, J. (1995) 'Downregulation of the Ras activation pathway by MAP kinase phosphorylation of Sos', *Oncogene,* 11(7), pp. 1327-31.

Buhrman, G., Kumar, V. S., Cirit, M., Haugh, J. M. and Mattos, C. (2011) 'Allosteric modulation of Ras-GTP is linked to signal transduction through RAF kinase', *J Biol Chem,* 286(5), pp. 3323-31.

Burd, C. E., Liu, W., Huynh, M. V., Waqas, M. A., Gillahan, J. E., Clark, K. S., Fu, K., Martin, B. L., Jeck, W. R., Souroullas, G. P., Darr, D. B., Zedek, D. C., Miley, M. J., Baguley, B. C., Campbell, S. L. and Sharpless, N. E. (2014) 'Mutation-specific RAS oncogenicity explains NRAS codon 61 selection in melanoma', *Cancer Discov,* 4(12), pp. 1418-29.

Burslem, G. M., Smith, B. E., Lai, A. C., Jaime-Figueroa, S., McQuaid, D. C., Bondeson, D. P., Toure, M., Dong, H., Qian, Y., Wang, J., Crew, A. P., Hines, J. and Crews, C. M. (2018) 'The Advantages of Targeted Protein Degradation Over Inhibition: An RTK Case Study', *Cell Chem Biol,* 25(1), pp. 67-77.e3.

Buss, J. E. and Sefton, B. M. (1986) 'Direct identification of palmitic acid as the lipid attached to p21ras', *Mol Cell Biol,* 6(1), pp. 116-22.

Cailleau, R., Olivé, M. and Cruciger, Q. V. (1978) 'Long-term human breast carcinoma cell lines of metastatic origin: preliminary characterization', *In Vitro,* 14(11), pp. 911-5.

Cann, M. L., McDonald, I. M., East, M. P., Johnson, G. L. and Graves, L. M. (2017) 'Measuring Kinase ActivityA Global Challenge', *Journal of Cellular Biochemistry,* 118(11), pp. 3595-3606.

Canon, J., Rex, K., Saiki, A. Y., Mohr, C., Cooke, K., Bagal, D., Gaida, K., Holt, T., Knutson, C. G., Koppada, N., Lanman, B. A., Werner, J., Rapaport, A. S., San Miguel, T., Ortiz, R., Osgood, T., Sun, J. R., Zhu, X., McCarter, J. D., Volak, L. P., Houk, B. E., Fakih, M. G., O'Neil, B. H., Price, T. J., Falchook, G. S., Desai, J., Kuo, J., Govindan, R., Hong, D. S., Ouyang, W., Henary, H., Arvedson, T., Cee, V. J. and Lipford, J. R. (2019) 'The clinical KRAS(G12C) inhibitor AMG 510 drives anti-tumour immunity', *Nature,* 575(7781), pp. 217-223.

Capon, D. J., Seeburg, P. H., McGrath, J. P., Hayflick, J. S., Edman, U., Levinson, A. D. and Goeddel, D. V. (1983) 'Activation of Ki-ras2 gene in human

colon and lung carcinomas by two different point mutations', *Nature,* 304(5926), pp. 507-13.

Casar, B., Arozarena, I., Sanz-Moreno, V., Pinto, A., Agudo-Ibáñez, L., Marais, R., Lewis, R. E., Berciano, M. T. and Crespo, P. (2009) 'Ras subcellular localization defines extracellular signal-regulated kinase 1 and 2 substrate specificity through distinct utilization of scaffold proteins', *Mol Cell Biol,* 29(5), pp. 1338-53.

Casey, P. J., Solski, P. A., Der, C. J. and Buss, J. E. (1989) 'p21ras is modified by a farnesyl isoprenoid', *Proc Natl Acad Sci U S A,* 86(21), pp. 8323-7.

Castellano, E. and Downward, J. (2011) 'RAS Interaction with PI3K: More Than Just Another Effector Pathway', *Genes Cancer,* 2(3), pp. 261-74.

Chardin, P., Camonis, J. H., Gale, N. W., van Aelst, L., Schlessinger, J., Wigler, M. H. and Bar-Sagi, D. (1993) 'Human Sos1: a guanine nucleotide exchange factor for Ras that binds to GRB2', *Science,* 260(5112), pp. 1338-43.

Chen, M. J., Dixon, J. E. and Manning, G. (2017) 'Genomics and evolution of protein phosphatases', *Sci Signal,* 10(474).

Chien, Y., Kim, S., Bumeister, R., Loo, Y. M., Kwon, S. W., Johnson, C. L., Balakireva, M. G., Romeo, Y., Kopelovich, L., Gale, M., Yeaman, C., Camonis, J. H., Zhao, Y. and White, M. A. (2006) 'RalB GTPase-mediated activation of the IkappaB family kinase TBK1 couples innate immune signaling to tumor cell survival', *Cell,* 127(1), pp. 157-70.

Chien, Y. and White, M. A. (2003) 'RAL GTPases are linchpin modulators of human tumour-cell proliferation and survival', *EMBO Rep,* 4(8), pp. 800-6.

Choy, E., Chiu, V. K., Silletti, J., Feoktistov, M., Morimoto, T., Michaelson, D., Ivanov, I. E. and Philips, M. R. (1999) 'Endomembrane trafficking of ras: the CAAX motif targets proteins to the ER and Golgi', *Cell,* 98(1), pp. 69-80.

Clark, R., Wong, G., Arnheim, N., Nitecki, D. and McCormick, F. (1985) 'Antibodies specific for amino acid 12 of the ras oncogene product inhibit GTP binding', *Proc Natl Acad Sci U S A,* 82(16), pp. 5280-4.

Clark, S. G., Stern, M. J. and Horvitz, H. R. (1992) 'C. elegans cell-signalling gene sem-5 encodes a protein with SH2 and SH3 domains', *Nature,* 356(6367), pp. 340-4.

Cooper, M. J., Cox, N. J., Zimmerman, E. I., Dewar, B. J., Duncan, J. S., Whittle, M. C., Nguyen, T. A., Jones, L. S., Roy, S. G., Smalley, D. M., Kuan, P. F., Richards, K. L., Christopherson, R. I., Jin, J., Frye, S. V., Johnson, G. L., Baldwin, A. S. and Graves, L. M. (2013) 'Application of Multiplexed Kinase Inhibitor Beads to Study Kinome Adaptations in Drug-Resistant Leukemia', *Plos One,* 8(6).

Cox, A. D. and Der, C. J. (2010) 'Ras history: The saga continues', *Small GTPases,* 1(1), pp. 2-27.

Cox, A. D., Der, C. J. and Philips, M. R. (2015) 'Targeting RAS Membrane Association: Back to the Future for Anti-RAS Drug Discovery?', *Clin Cancer Res,* 21(8), pp. 1819-27.

Cox, J., Hein, M. Y., Luber, C. A., Paron, I., Nagaraj, N. and Mann, M. (2014) 'Accurate proteome-wide label-free quantification by delayed normalization and maximal peptide ratio extraction, termed MaxLFQ', *Mol Cell Proteomics,* 13(9), pp. 2513-26.

Cox, N. J., Zimmerman, E. I., Dewar, B. J., Duncan, J., Whittle, M., Jin, J., Frye, S. V., Johnson, G. L. and Graves, L. M. (2011) 'Profiling the Kinome of Drug Resistant Chronic Myelogenous Leukemia', *Faseb Journal,* 25.

Céspedes, M. V., Sancho, F. J., Guerrero, S., Parreño, M., Casanova, I., Pavón, M. A., Marcuello, E., Trias, M., Cascante, M., Capellà, G. and Mangues, R. (2006) 'K-ras Asp12 mutant neither interacts with Raf, nor signals through Erk and is less tumorigenic than K-ras Val12', *Carcinogenesis,* 27(11), pp. 2190-200.

Daub, H., Olsen, J. V., Bairlein, M., Gnad, F., Oppermann, F. S., Körner, R., Greff, Z., Kéri, G., Stemmann, O. and Mann, M. (2008) 'Kinase-selective enrichment enables quantitative phosphoproteomics of the kinome across the cell cycle', *Mol Cell,* 31(3), pp. 438-48.

De Roock, W., Jonker, D. J., Di Nicolantonio, F., Sartore-Bianchi, A., Tu, D., Siena, S., Lamba, S., Arena, S., Frattini, M., Piessevaux, H., Van Cutsem, E., O'Callaghan, C. J., Khambata-Ford, S., Zalcberg, J. R., Simes, J., Karapetis, C. S., Bardelli, A. and Tejpar, S. (2010) 'Association of KRAS p.G13D mutation with outcome in patients with chemotherapy-refractory metastatic colorectal cancer treated with cetuximab', *JAMA,* 304(16), pp. 1812-20.

de Sousa Abreu, R., Penalva, L. O., Marcotte, E. M. and Vogel, C. (2009) 'Global signatures of protein and mRNA expression levels', *Mol Biosyst,* 5(12), pp. 1512-26.

de Vos, A. M., Tong, L., Milburn, M. V., Matias, P. M., Jancarik, J., Noguchi, S., Nishimura, S., Miura, K., Ohtsuka, E. and Kim, S. H. (1988) 'Three-dimensional structure of an oncogene protein: catalytic domain of human c-H-ras p21', *Science,* 239(4842), pp. 888-93.

Deng, Q., Liao, R., Wu, B. L. and Sun, P. (2004) 'High intensity ras signaling induces premature senescence by activating p38 pathway in primary human fibroblasts', *J Biol Chem,* 279(2), pp. 1050-9.

Deng, T. and Karin, M. (1994) 'c-Fos transcriptional activity stimulated by H-Ras-activated protein kinase distinct from JNK and ERK', *Nature,* 371(6493), pp. 171-5.

Dent, P., Haser, W., Haystead, T. A., Vincent, L. A., Roberts, T. M. and Sturgill, T. W. (1992) 'Activation of mitogen-activated protein kinase kinase by v-Raf in NIH 3T3 cells and in vitro', *Science,* 257(5075), pp. 1404-7.

Der, C. J., Finkel, T. and Cooper, G. M. (1986) 'Biological and biochemical properties of human rasH genes mutated at codon 61', *Cell,* 44(1), pp. 167-76.

Der, C. J., Krontiris, T. G. and Cooper, G. M. (1982) 'Transforming genes of human bladder and lung carcinoma cell lines are homologous to the ras genes of Harvey and Kirsten sarcoma viruses', *Proc Natl Acad Sci U S A,* 79(11), pp. 3637-40.

Di Renzo, M. F., Narsimhan, R. P., Olivero, M., Bretti, S., Giordano, S., Medico, E., Gaglia, P., Zara, P. and Comoglio, P. M. (1991) 'Expression of the Met/HGF receptor in normal and neoplastic human tissues', *Oncogene,* 6(11), pp. 1997-2003.

Di Renzo, M. F., Olivero, M., Ferro, S., Prat, M., Bongarzone, I., Pilotti, S., Belfiore, A., Costantino, A., Vigneri, R. and Pierotti, M. A. (1992) 'Overexpression of the c-MET/HGF receptor gene in human thyroid carcinomas', *Oncogene,* 7(12), pp. 2549-53.

Di Renzo, M. F., Olivero, M., Giacomini, A., Porte, H., Chastre, E., Mirossay, L., Nordlinger, B., Bretti, S., Bottardi, S. and Giordano, S. (1995a) 'Overexpression and amplification of the met/HGF receptor gene during the progression of colorectal cancer', *Clin Cancer Res,* 1(2), pp. 147-54.

Di Renzo, M. F., Olivero, M., Katsaros, D., Crepaldi, T., Gaglia, P., Zola, P., Sismondi, P. and Comoglio, P. M. (1994) 'Overexpression of the Met/HGF receptor in ovarian cancer', *Int J Cancer,* 58(5), pp. 658-62.

Di Renzo, M. F., Poulsom, R., Olivero, M., Comoglio, P. M. and Lemoine, N. R. (1995b) 'Expression of the Met/hepatocyte growth factor receptor in human pancreatic cancer', *Cancer Res,* 55(5), pp. 1129-38.

Dickson, B., Sprenger, F., Morrison, D. and Hafen, E. (1992) 'Raf functions downstream of Ras1 in the Sevenless signal transduction pathway', *Nature,* 360(6404), pp. 600-3.

Dong, Y., Wang, J., Sheng, Z., Li, G., Ma, H., Wang, X., Zhang, R., Lu, G., Hu, Q., Sugimura, H. and Zhou, X. (2009) 'Downregulation of EphA1 in colorectal carcinomas correlates with invasion and metastasis', *Mod Pathol,* 22(1), pp. 151-60.

Downward, J., Riehl, R., Wu, L. and Weinberg, R. A. (1990) 'Identification of a nucleotide exchange-promoting activity for p21ras', *Proc Natl Acad Sci U S A,* 87(15), pp. 5998-6002.

Duncan, J. S., Whittle, M. C., Nakamura, K., Abell, A. N., Midland, A. A., Zawistowski, J. S., Johnson, N. L., Granger, D. A., Jordan, N. V., Darr, D. B., Usary, J., Kuan, P. F., Smalley, D. M., Major, B., He, X. P., Hoadley, K. A.,

Zhou, B., Sharpless, N. E., Perou, C. M., Kim, W. Y., Gomez, S. M., Chen, X., Jin, J., Frye, S. V., Earp, H. S., Graves, L. M. and Johnson, G. L. (2012a) 'Dynamic Reprogramming of the Kinome in Response to Targeted MEK Inhibition in Triple-Negative Breast Cancer', *Cell,* 149(2), pp. 307-321.

Duncan, J. S., Whittle, M. W., Graves, L. M. and Johnson, G. L. (2012b) 'Reprogramming of the cancer kinome in response to targeted kinase inhibition', *Clinical Cancer Research,* 18(10).

Dunne, P. D., Dasgupta, S., Blayney, J. K., McArt, D. G., Redmond, K. L., Weir, J. A., Bradley, C. A., Sasazuki, T., Shirasawa, S., Wang, T., Srivastava, S., Ong, C. W., Arthur, K., Salto-Tellez, M., Wilson, R. H., Johnston, P. G. and Van Schaeybroeck, S. (2016) 'EphA2 Expression Is a Key Driver of Migration and Invasion and a Poor Prognostic Marker in Colorectal Cancer', *Clin Cancer Res,* 22(1), pp. 230-242.

Eckert, L. B., Repasky, G. A., Ulkü, A. S., McFall, A., Zhou, H., Sartor, C. I. and Der, C. J. (2004) 'Involvement of Ras activation in human breast cancer cell signaling, invasion, and anoikis', *Cancer Res,* 64(13), pp. 4585-92.

Egan, S. E., Giddings, B. W., Brooks, M. W., Buday, L., Sizeland, A. M. and Weinberg, R. A. (1993) 'Association of Sos Ras exchange protein with Grb2 is implicated in tyrosine kinase signal transduction and transformation', *Nature,* 363(6424), pp. 45-51.

Endicott, J. A., Noble, M. E. and Johnson, L. N. (2012) 'The structural basis for control of eukaryotic protein kinases', *Annu Rev Biochem,* 81, pp. 587-613.

Esteban, L. M., Vicario-Abejón, C., Fernández-Salguero, P., Fernández-Medarde, A., Swaminathan, N., Yienger, K., Lopez, E., Malumbres, M., McKay, R., Ward, J. M., Pellicer, A. and Santos, E. (2001) 'Targeted genomic disruption of H-ras and N-ras, individually or in combination, reveals the dispensability of both loci for mouse growth and development', *Mol Cell Biol,* 21(5), pp. 1444-52.

Eyers, P. A. and Murphy, J. M. (2013) 'Dawn of the dead: protein pseudokinases signal new adventures in cell biology', *Biochem Soc Trans,* 41(4), pp. 969-74.

Fabbro, D. (2015) '25 years of small molecular weight kinase inhibitors: potentials and limitations', *Mol Pharmacol,* 87(5), pp. 766-75.

Fabbro, D., Cowan-Jacob, S. W. and Moebitz, H. (2015) 'Ten things you should know about protein kinases: IUPHAR Review 14', *Br J Pharmacol,* 172(11), pp. 2675-700.

Feig, L. A., Bast, R. C., Knapp, R. C. and Cooper, G. M. (1984) 'Somatic activation of rasK gene in a human ovarian carcinoma', *Science,* 223(4637), pp. 698-701.

Ferbeyre, G., de Stanchina, E., Lin, A. W., Querido, E., McCurrach, M. E., Hannon, G. J. and Lowe, S. W. (2002) 'Oncogenic ras and p53 cooperate to induce cellular senescence', *Mol Cell Biol,* 22(10), pp. 3497-508.

Ferguson, F. M., Nabet, B., Raghavan, S., Liu, Y., Leggett, A. L., Kuljanin, M., Kalekar, R. L., Yang, A., He, S., Wang, J., Ng, R. W. S., Sulahian, R., Li, L., Poulin, E. J., Huang, L., Koren, J., Dieguez-Martinez, N., Espinosa, S., Zeng, Z., Corona, C. R., Vasta, J. D., Ohi, R., Sim, T., Kim, N. D., Harshbarger, W., Lizcano, J. M., Robers, M. B., Muthaswamy, S., Lin, C. Y., Look, A. T., Haigis, K. M., Mancias, J. D., Wolpin, B. M., Aguirre, A. J., Hahn, W. C., Westover, K. D. and Gray, N. S. (2020) 'Discovery of a selective inhibitor of doublecortin like kinase 1', *Nat Chem Biol,* 16(6), pp. 635-643.

Fernandes, M., Duplaquet, L. and Tulasne, D. (2019) 'Proteolytic cleavages of MET: the divide-and-conquer strategy of a receptor tyrosine kinase', *BMB Rep,* 52(4), pp. 239-249.

Fiordalisi, J. J., Johnson, R. L., Weinbaum, C. A., Sakabe, K., Chen, Z., Casey, P. J. and Cox, A. D. (2003) 'High affinity for farnesyltransferase and alternative prenylation contribute individually to K-Ras4B resistance to farnesyltransferase inhibitors', *J Biol Chem,* 278(43), pp. 41718-27.

Fleuren, E. D. G., Zhang, L. X., Wu, J. M. and Daly, R. J. (2016) 'The kinome 'at large' in cancer', *Nature Reviews Cancer,* 16(2), pp. 83-98.

Fox, B. P. and Kandpal, R. P. (2004) 'Invasiveness of breast carcinoma cells and transcript profile: Eph receptors and ephrin ligands as molecular markers of potential diagnostic and prognostic application', *Biochem Biophys Res Commun,* 318(4), pp. 882-92.

Gagliardi, G., Goswami, M., Passera, R. and Bellows, C. F. (2012) 'DCLK1 immunoreactivity in colorectal neoplasia', *Clin Exp Gastroenterol,* 5, pp. 35-42.

Galan-Moya, E. M., de la Cruz-Morcillo, M. A., Llanos Valero, M., Callejas-Valera, J. L., Melgar-Rojas, P., Hernadez Losa, J., Salcedo, M., Fernández-Aramburo, A., Ramon y Cajal, S. and Sánchez-Prieto, R. (2011) 'Balance between MKK6 and MKK3 mediates p38 MAPK associated resistance to cisplatin in NSCLC', *PLoS One,* 6(12), pp. e28406.

Gale, N. W., Kaplan, S., Lowenstein, E. J., Schlessinger, J. and Bar-Sagi, D. (1993) 'Grb2 mediates the EGF-dependent activation of guanine nucleotide exchange on Ras', *Nature,* 363(6424), pp. 88-92.

Gallego, C., Gupta, S. K., Heasley, L. E., Qian, N. X. and Johnson, G. L. (1992) 'Mitogen-activated protein kinase activation resulting from selective oncogene expression in NIH 3T3 and rat 1a cells', *Proc Natl Acad Sci U S A,* 89(16), pp. 7355-9.

Gambarotta, G., Boccaccio, C., Giordano, S., Andŏ, M., Stella, M. C. and Comoglio, P. M. (1996) 'Ets up-regulates MET transcription', *Oncogene,* 13(9), pp. 1911-7.

Gao, T., Wang, M., Xu, L., Wen, T., Liu, J. and An, G. (2016) 'DCLK1 is up-regulated and associated with metastasis and prognosis in colorectal cancer', *J Cancer Res Clin Oncol,* 142(10), pp. 2131-40.

Geiger, T., Cox, J., Ostasiewicz, P., Wisniewski, J. R. and Mann, M. (2010) 'Super-SILAC mix for quantitative proteomics of human tumor tissue', *Nat Methods,* 7(5), pp. 383-5.

Gentile, D. R., Rathinaswamy, M. K., Jenkins, M. L., Moss, S. M., Siempelkamp, B. D., Renslo, A. R., Burke, J. E. and Shokat, K. M. (2017) 'Ras Binder Induces a Modified Switch-II Pocket in GTP and GDP States', *Cell Chem Biol,* 24(12), pp. 1455-1466.e14.

Gholami, A. M., Hahne, H., Wu, Z., Auer, F. J., Meng, C., Wilhelm, M. and Kuster, B. (2013) 'Global proteome analysis of the NCI-60 cell line panel', *Cell Rep,* 4(3), pp. 609-20.

Gibbs, J. B., Sigal, I. S., Poe, M. and Scolnick, E. M. (1984) 'Intrinsic GTPase activity distinguishes normal and oncogenic ras p21 molecules', *Proc Natl Acad Sci U S A,* 81(18), pp. 5704-8.

Gimple, R. C. and Wang, X. (2019) 'RAS: Striking at the Core of the Oncogenic Circuitry', *Front Oncol,* 9, pp. 965.

Giordano, S., Di Renzo, M. F., Narsimhan, R. P., Cooper, C. S., Rosa, C. and Comoglio, P. M. (1989) 'Biosynthesis of the protein encoded by the c-met proto-oncogene', *Oncogene,* 4(11), pp. 1383-8.

González-García, A., Pritchard, C. A., Paterson, H. F., Mavria, G., Stamp, G. and Marshall, C. J. (2005) 'RalGDS is required for tumor formation in a model of skin carcinogenesis', *Cancer Cell,* 7(3), pp. 219-26.

Graves, L. M., Duncan, J. S., Whittle, M. C. and Johnson, G. L. (2013) 'The dynamic nature of the kinome', *Biochemical Journal,* 450, pp. 1-8.

Guerrero, S., Casanova, I., Farré, L., Mazo, A., Capellà, G. and Mangues, R. (2000) 'K-ras codon 12 mutation induces higher level of resistance to apoptosis and predisposition to anchorage-independent growth than codon 13 mutation or proto-oncogene overexpression', *Cancer Res,* 60(23), pp. 6750-6.

Gundry, R. L., White, M. Y., Murray, C. I., Kane, L. A., Fu, Q., Stanley, B. A. and Van Eyk, J. E. (2009) 'Preparation of proteins and peptides for mass spectrometry analysis in a bottom-up proteomics workflow', *Curr Protoc Mol Biol,* Chapter 10, pp. Unit10.25.

Haigis, K. M., Kendall, K. R., Wang, Y., Cheung, A., Haigis, M. C., Glickman, J. N., Niwa-Kawakita, M., Sweet-Cordero, A., Sebolt-Leopold, J., Shannon, K.

M., Settleman, J., Giovannini, M. and Jacks, T. (2008) 'Differential effects of oncogenic K-Ras and N-Ras on proliferation, differentiation and tumor progression in the colon', *Nat Genet,* 40(5), pp. 600-8.

Hall, A., Marshall, C. J., Spurr, N. K. and Weiss, R. A. (1983) 'Identification of transforming gene in two human sarcoma cell lines as a new member of the ras gene family located on chromosome 1', *Nature,* 303(5916), pp. 396-400.

Hamad, N. M., Elconin, J. H., Karnoub, A. E., Bai, W., Rich, J. N., Abraham, R. T., Der, C. J. and Counter, C. M. (2002) 'Distinct requirements for Ras oncogenesis in human versus mouse cells', *Genes Dev,* 16(16), pp. 2045-57.

Hammond, D. E., Mageean, C. J., Rusilowicz, E. V., Wickenden, J. A., Clague, M. J. and Prior, I. A. (2015) 'Differential reprogramming of isogenic colorectal cancer cells by distinct activating KRAS mutations', *J Proteome Res,* 14(3), pp. 1535-46.

Han, M., Golden, A., Han, Y. and Sternberg, P. W. (1993) 'C. elegans lin-45 raf gene participates in let-60 ras-stimulated vulval differentiation', *Nature,* 363(6425), pp. 133-40.

Hanahan, D. and Weinberg, R. A. (2011) 'Hallmarks of cancer: the next generation', *Cell,* 144(5), pp. 646-74.

Hancock, J. F., Cadwallader, K., Paterson, H. and Marshall, C. J. (1991) 'A CAAX or a CAAL motif and a second signal are sufficient for plasma membrane targeting of ras proteins', *EMBO J,* 10(13), pp. 4033-9.

Hancock, J. F., Magee, A. I., Childs, J. E. and Marshall, C. J. (1989) 'All ras proteins are polyisoprenylated but only some are palmitoylated', *Cell,* 57(7), pp. 1167-77.

Hancock, J. F. and Parton, R. G. (2005) 'Ras plasma membrane signalling platforms', *Biochem J,* 389(Pt 1), pp. 1-11.

Hancock, J. F., Paterson, H. and Marshall, C. J. (1990) 'A polybasic domain or palmitoylation is required in addition to the CAAX motif to localize p21ras to the plasma membrane', *Cell,* 63(1), pp. 133-9.

HARVEY, J. J. (1964) 'AN UNIDENTIFIED VIRUS WHICH CAUSES THE RAPID PRODUCTION OF TUMOURS IN MICE', *Nature,* 204, pp. 1104-5.

Hastie, C. J., McLauchlan, H. J. and Cohen, P. (2006) 'Assay of protein kinases using radiolabeled ATP: a protocol', *Nature Protocols,* 1(2), pp. 968-971.

Hatzivassiliou, G., Song, K., Yen, I., Brandhuber, B. J., Anderson, D. J., Alvarado, R., Ludlam, M. J., Stokoe, D., Gloor, S. L., Vigers, G., Morales, T., Aliagas, I., Liu, B., Sideris, S., Hoeflich, K. P., Jaiswal, B. S., Seshagiri, S., Koeppen, H., Belvin, M., Friedman, L. S. and Malek, S. (2010) 'RAF inhibitors prime wild-type RAF to activate the MAPK pathway and enhance growth', *Nature,* 464(7287), pp. 431-5.

Herath, N. I. and Boyd, A. W. (2010) 'The role of Eph receptors and ephrin ligands in colorectal cancer', *Int J Cancer,* 126(9), pp. 2003-11.

Herath, N. I., Doecke, J., Spanevello, M. D., Leggett, B. A. and Boyd, A. W. (2009) 'Epigenetic silencing of EphA1 expression in colorectal cancer is correlated with poor survival', *Br J Cancer,* 100(7), pp. 1095-102.

Hill, M. and Hillova, J. (1971) 'Recombinational events between exogenous mouse DNA and newly synthesized DNA strands of chicken cells in culture', *Nat New Biol,* 231(26), pp. 261-5.

Hobbs, G. A. and Der, C. J. (2019) 'RAS Mutations Are Not Created Equal', *Cancer Discov,* 9(6), pp. 696-698.

Hobbs, G. A., Der, C. J. and Rossman, K. L. (2016) 'RAS isoforms and mutations in cancer at a glance', *J Cell Sci,* 129(7), pp. 1287-92.

Hofer, F., Fields, S., Schneider, C. and Martin, G. S. (1994) 'Activated Ras interacts with the Ral guanine nucleotide dissociation stimulator', *Proc Natl Acad Sci U S A,* 91(23), pp. 11089-93.

Hood, F. E., Klinger, B., Newlaczyl, A. U., Sieber, A., Dorel, M., Oliver, S. P., Coulson, J. M., Blüthgen, N. and Prior, I. A. (2019) 'Isoform-specific Ras signaling is growth factor dependent', *Mol Biol Cell,* 30(9), pp. 1108-1117.

Hornberg, J. J., Binder, B., Bruggeman, F. J., Schoeberl, B., Heinrich, R. and Westerhoff, H. V. (2005) 'Control of MAPK signalling: from complexity to what really matters', *Oncogene,* 24(36), pp. 5533-42.

Howe, L. R., Leevers, S. J., Gómez, N., Nakielny, S., Cohen, P. and Marshall, C. J. (1992) 'Activation of the MAP kinase pathway by the protein kinase raf', *Cell,* 71(2), pp. 335-42.

Hruban, R. H., Goggins, M., Parsons, J. and Kern, S. E. (2000) 'Progression model for pancreatic cancer', *Clin Cancer Res,* 6(8), pp. 2969-72.

Hunter, J. C., Manandhar, A., Carrasco, M. A., Gurbani, D., Gondi, S. and Westover, K. D. (2015) 'Biochemical and Structural Analysis of Common Cancer-Associated KRAS Mutations', *Mol Cancer Res,* 13(9), pp. 1325-35.

Hurley, J. B., Simon, M. I., Teplow, D. B., Robishaw, J. D. and Gilman, A. G. (1984) 'Homologies between signal transducing G proteins and ras gene products', *Science,* 226(4676), pp. 860-2.

Ivan, M., Bond, J. A., Prat, M., Comoglio, P. M. and Wynford-Thomas, D. (1997) 'Activated ras and ret oncogenes induce over-expression of c-met (hepatocyte growth factor receptor) in human thyroid epithelial cells', *Oncogene,* 14(20), pp. 2417-23.

Iwasa, H., Han, J. and Ishikawa, F. (2003) 'Mitogen-activated protein kinase p38 defines the common senescence-signalling pathway', *Genes Cells,* 8(2), pp. 131-44.

Jainchill, J. L., Aaronson, S. A. and Todaro, G. J. (1969) 'Murine sarcoma and leukemia viruses: assay using clonal lines of contact-inhibited mouse cells', *J Virol,* 4(5), pp. 549-53.

Jia, M., Souchelnytskyi, N., Hellman, U., O'Hare, M., Jat, P. S. and Souchelnytskyi, S. (2010) 'Proteome profiling of immortalization-to-senescence transition of human breast epithelial cells identified MAP2K3 as a senescence-promoting protein which is downregulated in human breast cancer', *Proteomics Clin Appl,* 4(10-11), pp. 816-28.

Joffre, C., Barrow, R., Ménard, L., Calleja, V., Hart, I. R. and Kermorgant, S. (2011) 'A direct role for Met endocytosis in tumorigenesis', *Nat Cell Biol,* 13(7), pp. 827-37.

Johnson, C. W., Reid, D., Parker, J. A., Salter, S., Knihtila, R., Kuzmic, P. and Mattos, C. (2017) 'The small GTPases K-Ras, N-Ras, and H-Ras have distinct biochemical properties determined by allosteric effects', *J Biol Chem,* 292(31), pp. 12981-12993.

Johnson, G. L., Amos, K. D., Duncan, J. S., Whittle, M., Zawistowki, J., Goulet, D., He, X. P., Noe, J., Perou, C. M., Earp, S. and Carey, L. A. (2013) 'Kinome reprogramming response to MEK inhibition: A window-of-opportunity trial in triple-negative breast cancer (TNBC)', *Journal of Clinical Oncology,* 31(15).

Johnson, G. L., Stuhlmiller, T. J., Angus, S. P., Zawistowski, J. S. and Graves, L. M. (2014) 'Molecular Pathways: Adaptive Kinome Reprogramming in Response to Targeted Inhibition of the BRAF-MEK-ERK Pathway in Cancer', *Clinical Cancer Research,* 20(10), pp. 2516-2522.

Johnson, L., Greenbaum, D., Cichowski, K., Mercer, K., Murphy, E., Schmitt, E., Bronson, R. T., Umanoff, H., Edelmann, W., Kucherlapati, R. and Jacks, T. (1997) 'K-ras is an essential gene in the mouse with partial functional overlap with N-ras', *Genes Dev,* 11(19), pp. 2468-81.

Johnson, L. N., Noble, M. E. and Owen, D. J. (1996) 'Active and inactive protein kinases: structural basis for regulation', *Cell,* 85(2), pp. 149-58.

Kamata, T. and Feramisco, J. R. (1984) 'Epidermal growth factor stimulates guanine nucleotide binding activity and phosphorylation of ras oncogene proteins', *Nature,* 310(5973), pp. 147-50.

Karapetis, C. S., Khambata-Ford, S., Jonker, D. J., O'Callaghan, C. J., Tu, D., Tebbutt, N. C., Simes, R. J., Chalchal, H., Shapiro, J. D., Robitaille, S., Price, T. J., Shepherd, L., Au, H. J., Langer, C., Moore, M. J. and Zalcberg, J. R. (2008) 'K-ras mutations and benefit from cetuximab in advanced colorectal cancer', *N Engl J Med,* 359(17), pp. 1757-65.

Karnoub, A. E. and Weinberg, R. A. (2008) 'Ras oncogenes: split personalities', *Nat Rev Mol Cell Biol,* 9(7), pp. 517-31.

Khokhlatchev, A., Rabizadeh, S., Xavier, R., Nedwidek, M., Chen, T., Zhang, X. F., Seed, B. and Avruch, J. (2002) 'Identification of a novel Ras-regulated proapoptotic pathway', *Curr Biol,* 12(4), pp. 253-65.

Kirsten, W. H. and Mayer, L. A. (1967) 'Morphologic responses to a murine erythroblastosis virus', *J Natl Cancer Inst,* 39(2), pp. 311-35.

Klijn, C., Durinck, S., Stawiski, E. W., Haverty, P. M., Jiang, Z., Liu, H., Degenhardt, J., Mayba, O., Gnad, F., Liu, J., Pau, G., Reeder, J., Cao, Y., Mukhyala, K., Selvaraj, S. K., Yu, M., Zynda, G. J., Brauer, M. J., Wu, T. D., Gentleman, R. C., Manning, G., Yauch, R. L., Bourgon, R., Stokoe, D., Modrusan, Z., Neve, R. M., de Sauvage, F. J., Settleman, J., Seshagiri, S. and Zhang, Z. (2015) 'A comprehensive transcriptional portrait of human cancer cell lines', *Nat Biotechnol,* 33(3), pp. 306-12.

Koera, K., Nakamura, K., Nakao, K., Miyoshi, J., Toyoshima, K., Hatta, T., Otani, H., Aiba, A. and Katsuki, M. (1997) 'K-ras is essential for the development of the mouse embryo', *Oncogene,* 15(10), pp. 1151-9.

Kornev, A. P., Haste, N. M., Taylor, S. S. and Eyck, L. F. (2006) 'Surface comparison of active and inactive protein kinases identifies a conserved activation mechanism', *Proc Natl Acad Sci U S A,* 103(47), pp. 17783-8.

Kou, C. J. and Kandpal, R. P. (2018) 'Differential Expression Patterns of Eph Receptors and Ephrin Ligands in Human Cancers', *Biomed Res Int,* 2018, pp. 7390104.

Krontiris, T. G. and Cooper, G. M. (1981) 'Transforming activity of human tumor DNAs', *Proc Natl Acad Sci U S A,* 78(2), pp. 1181-4.

Kruspig, B., Monteverde, T., Neidler, S., Hock, A., Kerr, E., Nixon, C., Clark, W., Hedley, A., Laing, S., Coffelt, S. B., Le Quesne, J., Dick, C., Vousden, K. H., Martins, C. P. and Murphy, D. J. (2018) 'The ERBB network facilitates KRAS-driven lung tumorigenesis', *Sci Transl Med,* 10(446).

Kurimchak, A. M., Shelton, C., Herrera-Montávez, C., Duncan, K. E., Chernoff, J. and Duncan, J. S. (2019) 'Intrinsic Resistance to MEK Inhibition through BET Protein-Mediated Kinome Reprogramming in NF1-Deficient Ovarian Cancer', *Mol Cancer Res,* 17(8), pp. 1721-1734.

Kyriakis, J. M., App, H., Zhang, X. F., Banerjee, P., Brautigan, D. L., Rapp, U. R. and Avruch, J. (1992) 'Raf-1 activates MAP kinase-kinase', *Nature,* 358(6385), pp. 417-21.

Lambert, J. M., Lambert, Q. T., Reuther, G. W., Malliri, A., Siderovski, D. P., Sondek, J., Collard, J. G. and Der, C. J. (2002) 'Tiam1 mediates Ras activation of Rac by a PI(3)K-independent mechanism', *Nat Cell Biol,* 4(8), pp. 621-5.

Land, H., Parada, L. F. and Weinberg, R. A. (1983) 'Tumorigenic conversion of primary embryo fibroblasts requires at least two cooperating oncogenes', *Nature,* 304(5927), pp. 596-602.

Leibovitz, A., Stinson, J. C., McCombs, W. B., McCoy, C. E., Mazur, K. C. and Mabry, N. D. (1976) 'Classification of human colorectal adenocarcinoma cell lines', *Cancer Res,* 36(12), pp. 4562-9.

Leiser, D., Medová, M., Mikami, K., Nisa, L., Stroka, D., Blaukat, A., Bladt, F., Aebersold, D. M. and Zimmer, Y. (2015) 'KRAS and HRAS mutations confer resistance to MET targeting in preclinical models of MET-expressing tumor cells', *Mol Oncol,* 9(7), pp. 1434-46.

Leitner, A. (2016) 'Enrichment Strategies in Phosphoproteomics', *Methods Mol Biol,* 1355, pp. 105-21.

Li, L., Jones, K. and Mei, H. (2019) 'Doublecotin-Like Kinase 1 Increases Chemoresistance of Colorectal Cancer Cells through the Anti-Apoptosis Pathway', *J Stem Cell Res Ther,* 9(3).

Li, N., Batzer, A., Daly, R., Yajnik, V., Skolnik, E., Chardin, P., Bar-Sagi, D., Margolis, B. and Schlessinger, J. (1993) 'Guanine-nucleotide-releasing factor hSos1 binds to Grb2 and links receptor tyrosine kinases to Ras signalling', *Nature,* 363(6424), pp. 85-8.

Lisabeth, E. M., Falivelli, G. and Pasquale, E. B. (2013) 'Eph receptor signaling and ephrins', *Cold Spring Harb Perspect Biol,* 5(9).

Lito, P., Pratilas, C. A., Joseph, E. W., Tadi, M., Halilovic, E., Zubrowski, M., Huang, A., Wong, W. L., Callahan, M. K., Merghoub, T., Wolchok, J. D., de Stanchina, E., Chandarlapaty, S., Poulikakos, P. I., Fagin, J. A. and Rosen, N. (2012) 'Relief of profound feedback inhibition of mitogenic signaling by RAF inhibitors attenuates their activity in BRAFV600E melanomas', *Cancer Cell,* 22(5), pp. 668-82.

Lito, P., Saborowski, A., Yue, J., Solomon, M., Joseph, E., Gadal, S., Saborowski, M., Kastenhuber, E., Fellmann, C., Ohara, K., Morikami, K., Miura, T., Lukacs, C., Ishii, N., Lowe, S. and Rosen, N. (2014) 'Disruption of CRAF-mediated MEK activation is required for effective MEK inhibition in KRAS mutant tumors', *Cancer Cell,* 25(5), pp. 697-710.

Liu, C., Park, M. and Tsao, M. S. (1992) 'Overexpression of c-met proto-oncogene but not epidermal growth factor receptor or c-erbB-2 in primary human colorectal carcinomas', *Oncogene,* 7(1), pp. 181-5.

Lowenstein, E. J., Daly, R. J., Batzer, A. G., Li, W., Margolis, B., Lammers, R., Ullrich, A., Skolnik, E. Y., Bar-Sagi, D. and Schlessinger, J. (1992) 'The SH2 and SH3 domain-containing protein GRB2 links receptor tyrosine kinases to ras signaling', *Cell,* 70(3), pp. 431-42.

Luo, J., Emanuele, M. J., Li, D., Creighton, C. J., Schlabach, M. R., Westbrook, T. F., Wong, K. K. and Elledge, S. J. (2009) 'A genome-wide RNAi screen identifies multiple synthetic lethal interactions with the Ras oncogene', *Cell,* 137(5), pp. 835-48.

Macdonald, J. S., McCoy, S., Whitehead, R. P., Iqbal, S., Wade, J. L., Giguere, J. K. and Abbruzzese, J. L. (2005) 'A phase II study of farnesyl transferase inhibitor R115777 in pancreatic cancer: a Southwest oncology group (SWOG 9924) study', *Invest New Drugs,* 23(5), pp. 485-7.

MacNeil, A. J., Jiao, S. C., McEachern, L. A., Yang, Y. J., Dennis, A., Yu, H., Xu, Z., Marshall, J. S. and Lin, T. J. (2014) 'MAPK kinase 3 is a tumor suppressor with reduced copy number in breast cancer', *Cancer Res,* 74(1), pp. 162-72.

Macrae, M., Neve, R. M., Rodriguez-Viciana, P., Haqq, C., Yeh, J., Chen, C., Gray, J. W. and McCormick, F. (2005) 'A conditional feedback loop regulates Ras activity through EphA2', *Cancer Cell,* 8(2), pp. 111-8.

Mageean, C. J., Griffiths, J. R., Smith, D. L., Clague, M. J. and Prior, I. A. (2015) 'Absolute Quantification of Endogenous Ras Isoform Abundance', *PLoS One,* 10(11), pp. e0142674.

Mak, H. H., Peschard, P., Lin, T., Naujokas, M. A., Zuo, D. and Park, M. (2007) 'Oncogenic activation of the Met receptor tyrosine kinase fusion protein, Tpr-Met, involves exclusion from the endocytic degradative pathway', *Oncogene,* 26(51), pp. 7213-21.

Malliri, A., van der Kammen, R. A., Clark, K., van der Valk, M., Michiels, F. and Collard, J. G. (2002) 'Mice deficient in the Rac activator Tiam1 are resistant to Ras-induced skin tumours', *Nature,* 417(6891), pp. 867-71.

Malumbres, M. and Barbacid, M. (2003) 'RAS oncogenes: the first 30 years', *Nat Rev Cancer,* 3(6), pp. 459-65.

Manning, B. D. and Toker, A. (2017) 'AKT/PKB Signaling: Navigating the Network', *Cell,* 169(3), pp. 381-405.

Manning, G., Whyte, D. B., Martinez, R., Hunter, T. and Sudarsanam, S. (2002) 'The protein kinase complement of the human genome', *Science,* 298(5600), pp. 1912-34.

Manser, E., Leung, T., Salihuddin, H., Zhao, Z. S. and Lim, L. (1994) 'A brain serine/threonine protein kinase activated by Cdc42 and Rac1', *Nature,* 367(6458), pp. 40-6.

Mao, C., Qiu, L. X., Liao, R. Y., Du, F. B., Ding, H., Yang, W. C., Li, J. and Chen, Q. (2010) 'KRAS mutations and resistance to EGFR-TKIs treatment in patients with non-small cell lung cancer: a meta-analysis of 22 studies', *Lung Cancer,* 69(3), pp. 272-8.

Margolis, B. and Skolnik, E. Y. (1994) 'Activation of Ras by receptor tyrosine kinases', *J Am Soc Nephrol,* 5(6), pp. 1288-99.

Martin, G. A., Viskochil, D., Bollag, G., McCabe, P. C., Crosier, W. J., Haubruck, H., Conroy, L., Clark, R., O'Connell, P. and Cawthon, R. M. (1990)

'The GAP-related domain of the neurofibromatosis type 1 gene product interacts with ras p21', *Cell,* 63(4), pp. 843-9.

Martini, G., Cardone, C., Vitiello, P. P., Belli, V., Napolitano, S., Troiani, T., Ciardiello, D., Della Corte, C. M., Morgillo, F., Matrone, N., Sforza, V., Papaccio, G., Desiderio, V., Paul, M. C., Moreno-Viedma, V., Normanno, N., Rachiglio, A. M., Tirino, V., Maiello, E., Latiano, T. P., Rizzi, D., Signoriello, G., Sibilia, M., Ciardiello, F. and Martinelli, E. (2019) 'EPHA2 Is a Predictive Biomarker of Resistance and a Potential Therapeutic Target for Improving Antiepidermal Growth Factor Receptor Therapy in Colorectal Cancer', *Mol Cancer Ther,* 18(4), pp. 845-855.

Marín-Ramos, N. I., Balabasquer, M., Ortega-Nogales, F. J., Torrecillas, I. R., Gil-Ordóñez, A., Marcos-Ramiro, B., Aguilar-Garrido, P., Cushman, I., Romero, A., Medrano, F. J., Gajate, C., Mollinedo, F., Philips, M. R., Campillo, M., Gallardo, M., Martín-Fontecha, M., López-Rodríguez, M. L. and Ortega-Gutiérrez, S. (2019) 'A Potent Isoprenylcysteine Carboxylmethyltransferase (ICMT) Inhibitor Improves Survival in Ras-Driven Acute Myeloid Leukemia', *J Med Chem,* 62(13), pp. 6035-6046.

McGrath, J. P., Capon, D. J., Goeddel, D. V. and Levinson, A. D. (1984) 'Comparative biochemical properties of normal and activated human ras p21 protein', *Nature,* 310(5979), pp. 644-9.

Miao, H., Wei, B. R., Peehl, D. M., Li, Q., Alexandrou, T., Schelling, J. R., Rhim, J. S., Sedor, J. R., Burnett, E. and Wang, B. (2001) 'Activation of EphA receptor tyrosine kinase inhibits the Ras/MAPK pathway', *Nat Cell Biol,* 3(5), pp. 527-30.

Milburn, M. V., Tong, L., deVos, A. M., Brünger, A., Yamaizumi, Z., Nishimura, S. and Kim, S. H. (1990) 'Molecular switch for signal transduction: structural differences between active and inactive forms of protooncogenic ras proteins', *Science,* 247(4945), pp. 939-45.

Mitin, N., Rossman, K. L. and Der, C. J. (2005) 'Signaling interplay in Ras superfamily function', *Curr Biol,* 15(14), pp. R563-74.

Mo, S. P., Coulson, J. M. and Prior, I. A. (2018) 'RAS variant signalling', *Biochem Soc Trans,* 46(5), pp. 1325-1332.

Modi, V. and Dunbrack, R. L. (2019) 'Defining a new nomenclature for the structures of active and inactive kinases', *Proc Natl Acad Sci U S A,* 116(14), pp. 6818-6827.

Molloy, C. J., Bottaro, D. P., Fleming, T. P., Marshall, M. S., Gibbs, J. B. and Aaronson, S. A. (1989) 'PDGF induction of tyrosine phosphorylation of GTPase activating protein', *Nature,* 342(6250), pp. 711-4.

Moodie, S. A., Paris, M., Villafranca, E., Kirshmeier, P., Willumsen, B. M. and Wolfman, A. (1995) 'Different structural requirements within the switch II region

of the Ras protein for interactions with specific downstream targets', *Oncogene,* 11(3), pp. 447-54.

Moodie, S. A., Willumsen, B. M., Weber, M. J. and Wolfman, A. (1993) 'Complexes of Ras.GTP with Raf-1 and mitogen-activated protein kinase kinase', *Science,* 260(5114), pp. 1658-61.

Moore, A. R., Rosenberg, S. C., McCormick, F. and Malek, S. (2020) 'RAS-targeted therapies: is the undruggable drugged?', *Nat Rev Drug Discov,* 19(8), pp. 533-552.

MRC *List of clinically approved kinase inhibitors*. Available at: https://www.ppu.mrc.ac.uk/list-clinically-approved-kinase-inhibitors.

Mulcahy, L. S., Smith, M. R. and Stacey, D. W. (1985) 'Requirement for ras proto-oncogene function during serum-stimulated growth of NIH 3T3 cells', *Nature,* 313(5999), pp. 241-3.

Mulder, C., Prust, N., van Doorn, S., Reinecke, M., Kuster, B., van Bergen En Henegouwen, P. and Lemeer, S. (2018) 'Adaptive Resistance to EGFR-Targeted Therapy by Calcium Signaling in NSCLC Cells', *Mol Cancer Res,* 16(11), pp. 1773-1784.

Murphy, J. M., Zhang, Q., Young, S. N., Reese, M. L., Bailey, F. P., Eyers, P. A., Ungureanu, D., Hammaren, H., Silvennoinen, O., Varghese, L. N., Chen, K., Tripaydonis, A., Jura, N., Fukuda, K., Qin, J., Nimchuk, Z., Mudgett, M. B., Elowe, S., Gee, C. L., Liu, L., Daly, R. J., Manning, G., Babon, J. J. and Lucet, I. S. (2014) 'A robust methodology to subclassify pseudokinases based on their nucleotide-binding properties', *Biochem J,* 457(2), pp. 323-34.

Murray, M. J., Shilo, B. Z., Shih, C., Cowing, D., Hsu, H. W. and Weinberg, R. A. (1981) 'Three different human tumor cell lines contain different oncogenes', *Cell,* 25(2), pp. 355-61.

Nguyen, A., Burack, W. R., Stock, J. L., Kortum, R., Chaika, O. V., Afkarian, M., Muller, W. J., Murphy, K. M., Morrison, D. K., Lewis, R. E., McNeish, J. and Shaw, A. S. (2002) 'Kinase suppressor of Ras (KSR) is a scaffold which facilitates mitogen-activated protein kinase activation in vivo', *Mol Cell Biol,* 22(9), pp. 3035-45.

Nicke, B., Bastien, J., Khanna, S. J., Warne, P. H., Cowling, V., Cook, S. J., Peters, G., Delpuech, O., Schulze, A., Berns, K., Mullenders, J., Beijersbergen, R. L., Bernards, R., Ganesan, T. S., Downward, J. and Hancock, D. C. (2005) 'Involvement of MINK, a Ste20 family kinase, in Ras oncogene-induced growth arrest in human ovarian surface epithelial cells', *Mol Cell,* 20(5), pp. 673-85.

Olivier, J. P., Raabe, T., Henkemeyer, M., Dickson, B., Mbamalu, G., Margolis, B., Schlessinger, J., Hafen, E. and Pawson, T. (1993) 'A Drosophila SH2-SH3

adaptor protein implicated in coupling the sevenless tyrosine kinase to an activator of Ras guanine nucleotide exchange, Sos', *Cell,* 73(1), pp. 179-91.

Omerovic, J., Hammond, D. E., Clague, M. J. and Prior, I. A. (2008) 'Ras isoform abundance and signalling in human cancer cell lines', *Oncogene,* 27(19), pp. 2754-62.

Omerovic, J., Laude, A. J. and Prior, I. A. (2007) 'Ras proteins: paradigms for compartmentalised and isoform-specific signalling', *Cell Mol Life Sci,* 64(19-20), pp. 2575-89.

Ong, S. E. and Mann, M. (2005) 'Mass spectrometry-based proteomics turns quantitative', *Nat Chem Biol,* 1(5), pp. 252-62.

Ostrem, J. M., Peters, U., Sos, M. L., Wells, J. A. and Shokat, K. M. (2013) 'K-Ras(G12C) inhibitors allosterically control GTP affinity and effector interactions', *Nature,* 503(7477), pp. 548-51.

Parada, L. F., Tabin, C. J., Shih, C. and Weinberg, R. A. (1982) 'Human EJ bladder carcinoma oncogene is homologue of Harvey sarcoma virus ras gene', *Nature,* 297(5866), pp. 474-8.

Parker, J. A. and Mattos, C. (2018) 'The K-Ras, N-Ras, and H-Ras Isoforms: Unique Conformational Preferences and Implications for Targeting Oncogenic Mutants', *Cold Spring Harb Perspect Med,* 8(8).

Perucho, M., Goldfarb, M., Shimizu, K., Lama, C., Fogh, J. and Wigler, M. (1981) 'Human-tumor-derived cell lines contain common and different transforming genes', *Cell,* 27(3 Pt 2), pp. 467-76.

Petrelli, A., Circosta, P., Granziero, L., Mazzone, M., Pisacane, A., Fenoglio, S., Comoglio, P. M. and Giordano, S. (2006) 'Ab-induced ectodomain shedding mediates hepatocyte growth factor receptor down-regulation and hampers biological activity', *Proc Natl Acad Sci U S A,* 103(13), pp. 5090-5.

Potenza, N., Vecchione, C., Notte, A., De Rienzo, A., Rosica, A., Bauer, L., Affuso, A., De Felice, M., Russo, T., Poulet, R., Cifelli, G., De Vita, G., Lembo, G. and Di Lauro, R. (2005) 'Replacement of K-Ras with H-Ras supports normal embryonic development despite inducing cardiovascular pathology in adult mice', *EMBO Rep,* 6(5), pp. 432-7.

Poulikakos, P. I., Zhang, C., Bollag, G., Shokat, K. M. and Rosen, N. (2010) 'RAF inhibitors transactivate RAF dimers and ERK signalling in cells with wild-type BRAF', *Nature,* 464(7287), pp. 427-30.

Poulin, E. J., Bera, A. K., Lu, J., Lin, Y. J., Strasser, S. D., Paulo, J. A., Huang, T. Q., Morales, C., Yan, W., Cook, J., Nowak, J. A., Brubaker, D. K., Joughin, B. A., Johnson, C. W., DeStefanis, R. A., Ghazi, P. C., Gondi, S., Wales, T. E., Iacob, R. E., Bogdanova, L., Gierut, J. J., Li, Y., Engen, J. R., Perez-Mancera, P. A., Braun, B. S., Gygi, S. P., Lauffenburger, D. A., Westover, K. D. and

Haigis, K. M. (2019) 'Tissue-Specific Oncogenic Activity of KRAS', *Cancer Discov,* 9(6), pp. 738-755.

Prior, I. A. and Hancock, J. F. (2012) 'Ras trafficking, localization and compartmentalized signalling', *Semin Cell Dev Biol,* 23(2), pp. 145-53.

Prior, I. A., Hood, F. E. and Hartley, J. L. (2020) 'The Frequency of Ras Mutations in Cancer', *Cancer Res,* 80(14), pp. 2969-2974.

Prior, I. A., Lewis, P. D. and Mattos, C. (2012) 'A comprehensive survey of Ras mutations in cancer', *Cancer Res,* 72(10), pp. 2457-67.

Prior, I. A., Muncke, C., Parton, R. G. and Hancock, J. F. (2003) 'Direct visualization of Ras proteins in spatially distinct cell surface microdomains', *J Cell Biol,* 160(2), pp. 165-70.

Pulciani, S., Santos, E., Lauver, A. V., Long, L. K., Aaronson, S. A. and Barbacid, M. (1982) 'Oncogenes in solid human tumours', *Nature,* 300(5892), pp. 539-42.

Qu, D., Weygant, N., Yao, J., Chandrakesan, P., Berry, W. L., May, R., Pitts, K., Husain, S., Lightfoot, S., Li, M., Wang, T. C., An, G., Clendenin, C., Stanger, B. Z. and Houchen, C. W. (2019) 'Overexpression of DCLK1-AL Increases Tumor Cell Invasion, Drug Resistance, and KRAS Activation and Can Be Targeted to Inhibit Tumorigenesis in Pancreatic Cancer', *J Oncol,* 2019, pp. 6402925.

Quilliam, L. A., Huff, S. Y., Rabun, K. M., Wei, W., Park, W., Broek, D. and Der, C. J. (1994) 'Membrane-targeting potentiates guanine nucleotide exchange factor CDC25 and SOS1 activation of Ras transforming activity', *Proc Natl Acad Sci U S A,* 91(18), pp. 8512-6.

Rajalingam, K., Schreck, R., Rapp, U. R. and Albert, S. (2007) 'Ras oncogenes and their downstream targets', *Biochim Biophys Acta,* 1773(8), pp. 1177-95.

Rao, D. D., Vorhies, J. S., Senzer, N. and Nemunaitis, J. (2009) 'siRNA vs. shRNA: similarities and differences', *Adv Drug Deliv Rev,* 61(9), pp. 746-59.

Rapp, U. R., Goldsborough, M. D., Mark, G. E., Bonner, T. I., Groffen, J., Reynolds, F. H. and Stephenson, J. R. (1983) 'Structure and biological activity of v-raf, a unique oncogene transduced by a retrovirus', *Proc Natl Acad Sci U S A,* 80(14), pp. 4218-22.

Reddy, E. P., Reynolds, R. K., Santos, E. and Barbacid, M. (1982) 'A point mutation is responsible for the acquisition of transforming properties by the T24 human bladder carcinoma oncogene', *Nature,* 300(5888), pp. 149-52.

Reiterer, V., Eyers, P. A. and Farhan, H. (2014) 'Day of the dead: pseudokinases and pseudophosphatases in physiology and disease', *Trends Cell Biol,* 24(9), pp. 489-505.

Riely, G. J., Kris, M. G., Rosenbaum, D., Marks, J., Li, A., Chitale, D. A., Nafa, K., Riedel, E. R., Hsu, M., Pao, W., Miller, V. A. and Ladanyi, M. (2008) 'Frequency and distinctive spectrum of KRAS mutations in never smokers with lung adenocarcinoma', *Clin Cancer Res,* 14(18), pp. 5731-4.

Robinson, L. C., Gibbs, J. B., Marshall, M. S., Sigal, I. S. and Tatchell, K. (1987) 'CDC25: a component of the RAS-adenylate cyclase pathway in Saccharomyces cerevisiae', *Science,* 235(4793), pp. 1218-21.

Rodriguez-Viciana, P., Warne, P. H., Dhand, R., Vanhaesebroeck, B., Gout, I., Fry, M. J., Waterfield, M. D. and Downward, J. (1994) 'Phosphatidylinositol-3-OH kinase as a direct target of Ras', *Nature,* 370(6490), pp. 527-32.

Rogge, R. D., Karlovich, C. A. and Banerjee, U. (1991) 'Genetic dissection of a neurodevelopmental pathway: Son of sevenless functions downstream of the sevenless and EGF receptor tyrosine kinases', *Cell,* 64(1), pp. 39-48.

Roskoski, R. (2016) 'Classification of small molecule protein kinase inhibitors based upon the structures of their drug-enzyme complexes', *Pharmacol Res,* 103, pp. 26-48.

Rotow, J. K., Gui, P., Wu, W., Raymond, V. M., Lanman, R. B., Kaye, F. J., Peled, N., Fece de la Cruz, F., Nadres, B., Corcoran, R. B., Yeh, I., Bastian, B. C., Starostik, P., Newsom, K., Olivas, V. R., Wolff, A. M., Fraser, J. S., Collisson, E. A., McCoach, C. E., Camidge, D. R., Pacheco, J., Bazhenova, L., Li, T., Bivona, T. G. and Blakely, C. M. (2020) 'Co-occurring Alterations in the RAS-MAPK Pathway Limit Response to MET Inhibitor Treatment in MET Exon 14 Skipping Mutation-Positive Lung Cancer', *Clin Cancer Res,* 26(2), pp. 439-449.

Rozakis-Adcock, M., Fernley, R., Wade, J., Pawson, T. and Bowtell, D. (1993) 'The SH2 and SH3 domains of mammalian Grb2 couple the EGF receptor to the Ras activator mSos1', *Nature,* 363(6424), pp. 83-5.

Ruprecht, B., Zecha, J., Heinzlmeir, S., Medard, G., Lemeer, S. and Kuster, B. (2015) 'Evaluation of Kinase Activity Profiling Using Chemical Proteomics', *Acs Chemical Biology,* 10(12), pp. 2743-2752.

Salazar, M., Lorente, M., García-Taboada, E., Pérez Gómez, E., Dávila, D., Zúñiga-García, P., María Flores, J., Rodríguez, A., Hegedus, Z., Mosén-Ansorena, D., Aransay, A. M., Hernández-Tiedra, S., López-Valero, I., Quintanilla, M., Sánchez, C., Iovanna, J. L., Dusetti, N., Guzmán, M., Francis, S. E., Carracedo, A., Kiss-Toth, E. and Velasco, G. (2015) 'Loss of Tribbles pseudokinase-3 promotes Akt-driven tumorigenesis via FOXO inactivation', *Cell Death Differ,* 22(1), pp. 131-44.

Santos, E., Martin-Zanca, D., Reddy, E. P., Pierotti, M. A., Della Porta, G. and Barbacid, M. (1984) 'Malignant activation of a K-ras oncogene in lung

carcinoma but not in normal tissue of the same patient', *Science,* 223(4637), pp. 661-4.

Santos, E., Tronick, S. R., Aaronson, S. A., Pulciani, S. and Barbacid, M. (1982) 'T24 human bladder carcinoma oncogene is an activated form of the normal human homologue of BALB- and Harvey-MSV transforming genes', *Nature,* 298(5872), pp. 343-7.

Scheffzek, K., Ahmadian, M. R., Kabsch, W., Wiesmüller, L., Lautwein, A., Schmitz, F. and Wittinghofer, A. (1997) 'The Ras-RasGAP complex: structural basis for GTPase activation and its loss in oncogenic Ras mutants', *Science,* 277(5324), pp. 333-8.

Schlichting, I., Almo, S. C., Rapp, G., Wilson, K., Petratos, K., Lentfer, A., Wittinghofer, A., Kabsch, W., Pai, E. F. and Petsko, G. A. (1990) 'Time-resolved X-ray crystallographic study of the conformational change in Ha-Ras p21 protein on GTP hydrolysis', *Nature,* 345(6273), pp. 309-15.

Schwanhäusser, B., Busse, D., Li, N., Dittmar, G., Schuchhardt, J., Wolf, J., Chen, W. and Selbach, M. (2011) 'Global quantification of mammalian gene expression control', *Nature,* 473(7347), pp. 337-42.

Scolnick, E. M., Papageorge, A. G. and Shih, T. Y. (1979) 'Guanine nucleotide-binding activity as an assay for src protein of rat-derived murine sarcoma viruses', *Proc Natl Acad Sci U S A,* 76(10), pp. 5355-9.

Scolnick, E. M. and Parks, W. P. (1974) 'Harvey sarcoma virus: a second murine type C sarcoma virus with rat genetic information', *J Virol,* 13(6), pp. 1211-9.

Scolnick, E. M., Rands, E., Williams, D. and Parks, W. P. (1973) 'Studies on the nucleic acid sequences of Kirsten sarcoma virus: a model for formation of a mammalian RNA-containing sarcoma virus', *J Virol,* 12(3), pp. 458-63.

Seeburg, P. H., Colby, W. W., Capon, D. J., Goeddel, D. V. and Levinson, A. D. (1984) 'Biological properties of human c-Ha-ras1 genes mutated at codon 12', *Nature,* 312(5989), pp. 71-5.

Sefton, B. M., Trowbridge, I. S., Cooper, J. A. and Scolnick, E. M. (1982) 'The transforming proteins of Rous sarcoma virus, Harvey sarcoma virus and Abelson virus contain tightly bound lipid', *Cell,* 31(2 Pt 1), pp. 465-74.

Serrano, M., Lin, A. W., McCurrach, M. E., Beach, D. and Lowe, S. W. (1997) 'Oncogenic ras provokes premature cell senescence associated with accumulation of p53 and p16INK4a', *Cell,* 88(5), pp. 593-602.

Sharma, K., D'Souza, R. C., Tyanova, S., Schaab, C., Wiśniewski, J. R., Cox, J. and Mann, M. (2014) 'Ultradeep human phosphoproteome reveals a distinct regulatory nature of Tyr and Ser/Thr-based signaling', *Cell Rep,* 8(5), pp. 1583-94.

Shih, C., Padhy, L. C., Murray, M. and Weinberg, R. A. (1981) 'Transforming genes of carcinomas and neuroblastomas introduced into mouse fibroblasts', *Nature,* 290(5803), pp. 261-4.

Shih, C., Shilo, B. Z., Goldfarb, M. P., Dannenberg, A. and Weinberg, R. A. (1979a) 'Passage of phenotypes of chemically transformed cells via transfection of DNA and chromatin', *Proc Natl Acad Sci U S A,* 76(11), pp. 5714-8.

Shih, T. Y., Weeks, M. O., Young, H. A. and Scholnick, E. M. (1979b) 'Identification of a sarcoma virus-coded phosphoprotein in nonproducer cells transformed by Kirsten or Harvey murine sarcoma virus', *Virology,* 96(1), pp. 64-79.

Shimizu, K., Goldfarb, M., Suard, Y., Perucho, M., Li, Y., Kamata, T., Feramisco, J., Stavnezer, E., Fogh, J. and Wigler, M. H. (1983) 'Three human transforming genes are related to the viral ras oncogenes', *Proc Natl Acad Sci U S A,* 80(8), pp. 2112-6.

Shin, I., Kim, S., Song, H., Kim, H. R. and Moon, A. (2005) 'H-Ras-specific activation of Rac-MKK3/6-p38 pathway: its critical role in invasion and migration of breast epithelial cells', *J Biol Chem,* 280(15), pp. 14675-83.

Simon, M. A., Dodson, G. S. and Rubin, G. M. (1993) 'An SH3-SH2-SH3 protein is required for p21Ras1 activation and binds to sevenless and Sos proteins in vitro', *Cell,* 73(1), pp. 169-77.

Sjölander, A., Yamamoto, K., Huber, B. E. and Lapetina, E. G. (1991) 'Association of p21ras with phosphatidylinositol 3-kinase', *Proc Natl Acad Sci U S A,* 88(18), pp. 7908-12.

Smith, M. J., Neel, B. G. and Ikura, M. (2013) 'NMR-based functional profiling of RASopathies and oncogenic RAS mutations', *Proc Natl Acad Sci U S A,* 110(12), pp. 4574-9.

Spaargaren, M. and Bischoff, J. R. (1994) 'Identification of the guanine nucleotide dissociation stimulator for Ral as a putative effector molecule of R-ras, H-ras, K-ras, and Rap', *Proc Natl Acad Sci U S A,* 91(26), pp. 12609-13.

Stalnecker, C. A. and Der, C. J. (2020) 'RAS, wanted dead or alive: Advances in targeting RAS mutant cancers', *Sci Signal,* 13(624).

Stommel, J. M., Kimmelman, A. C., Ying, H. Q., Nabioullin, R., Ponugoti, A. H., Wiedemeyer, R., Stegh, A. H., Bradner, J. E., Ligon, K. L., Brennan, C., Chin, L. and DePinho, R. A. (2007) 'Coactivation of receptor tyrosine kinases affects the response of tumor cells to targeted therapies', *Science,* 318(5848), pp. 287-290.

Stuhlmiller, T. J., Earp, H. S. and Johnson, G. L. (2014) 'Adaptive Reprogramming of the Breast Cancer Kinome', *Clinical Pharmacology & Therapeutics,* 95(4), pp. 413-415.

Stuhlmiller, T. J., Miller, S. M., Zawistowski, J. S., Nakamura, K., Beltran, A. S., Duncan, J. S., Angus, S. P., Collins, K. A. L., Granger, D. A., Reuther, R. A., Graves, L. M., Gomez, S. M., Kuan, P. F., Parker, J. S., Chen, X., Sciaky, N., Carey, L. A., Earp, H. S., Jin, J. and Johnson, G. L. (2015) 'Inhibition of Lapatinib-Induced Kinome Reprogramming in ERBB2-Positive Breast Cancer by Targeting BET Family Bromodomains', *Cell Reports,* 11(3), pp. 390-404.

Sun, C., Hobor, S., Bertotti, A., Zecchin, D., Huang, S., Galimi, F., Cottino, F., Prahallad, A., Grernrum, W., Tzani, A., Schlicker, A., Wessels, L. F., Smit, E. F., Thunnissen, E., Halonen, P., Lieftink, C., Beijersbergen, R. L., Di Nicolantonio, F., Bardelli, A., Trusolino, L. and Bernards, R. (2014) 'Intrinsic resistance to MEK inhibition in KRAS mutant lung and colon cancer through transcriptional induction of ERBB3', *Cell Rep,* 7(1), pp. 86-93.

Suzawa, K., Offin, M., Lu, D., Kurzatkowski, C., Vojnic, M., Smith, R. S., Sabari, J. K., Tai, H., Mattar, M., Khodos, I., de Stanchina, E., Rudin, C. M., Kris, M. G., Arcila, M. E., Lockwood, W. W., Drilon, A., Ladanyi, M. and Somwar, R. (2019) 'Activation of KRAS Mediates Resistance to Targeted Therapy in MET Exon 14-mutant Non-small Cell Lung Cancer', *Clin Cancer Res,* 25(4), pp. 1248-1260.

Sweet, R. W., Yokoyama, S., Kamata, T., Feramisco, J. R., Rosenberg, M. and Gross, M. (1984) 'The product of ras is a GTPase and the T24 oncogenic mutant is deficient in this activity', *Nature,* 311(5983), pp. 273-5.

Tabin, C. J., Bradley, S. M., Bargmann, C. I., Weinberg, R. A., Papageorge, A. G., Scolnick, E. M., Dhar, R., Lowy, D. R. and Chang, E. H. (1982) 'Mechanism of activation of a human oncogene', *Nature,* 300(5888), pp. 143-9.

Takács, T., Kudlik, G., Kurilla, A., Szeder, B., Buday, L. and Vas, V. (2020) 'The effects of mutant Ras proteins on the cell signalome', *Cancer Metastasis Rev*.

Taparowsky, E., Suard, Y., Fasano, O., Shimizu, K., Goldfarb, M. and Wigler, M. (1982) 'Activation of the T24 bladder carcinoma transforming gene is linked to a single amino acid change', *Nature,* 300(5894), pp. 762-5.

Trahey, M. and McCormick, F. (1987) 'A cytoplasmic protein stimulates normal N-ras p21 GTPase, but does not affect oncogenic mutants', *Science,* 238(4826), pp. 542-5.

Trahey, M., Wong, G., Halenbeck, R., Rubinfeld, B., Martin, G. A., Ladner, M., Long, C. M., Crosier, W. J., Watt, K. and Koths, K. (1988) 'Molecular cloning of two types of GAP complementary DNA from human placenta', *Science,* 242(4886), pp. 1697-700.

Troiani, T., Napolitano, S., Vitagliano, D., Morgillo, F., Capasso, A., Sforza, V., Nappi, A., Ciardiello, D., Ciardiello, F. and Martinelli, E. (2014) 'Primary and acquired resistance of colorectal cancer cells to anti-EGFR antibodies

converge on MEK/ERK pathway activation and can be overcome by combined MEK/EGFR inhibition', *Clin Cancer Res,* 20(14), pp. 3775-86.

Tuveson, D. A., Shaw, A. T., Willis, N. A., Silver, D. P., Jackson, E. L., Chang, S., Mercer, K. L., Grochow, R., Hock, H., Crowley, D., Hingorani, S. R., Zaks, T., King, C., Jacobetz, M. A., Wang, L., Bronson, R. T., Orkin, S. H., DePinho, R. A. and Jacks, T. (2004) 'Endogenous oncogenic K-ras(G12D) stimulates proliferation and widespread neoplastic and developmental defects', *Cancer Cell,* 5(4), pp. 375-87.

Udayakumar, D., Zhang, G., Ji, Z., Njauw, C. N., Mroz, P. and Tsao, H. (2011) 'EphA2 is a critical oncogene in melanoma', *Oncogene,* 30(50), pp. 4921-9.

Urano, T., Emkey, R. and Feig, L. A. (1996) 'Ral-GTPases mediate a distinct downstream signaling pathway from Ras that facilitates cellular transformation', *EMBO J,* 15(4), pp. 810-6.

Vandesompele, J., De Preter, K., Pattyn, F., Poppe, B., Van Roy, N., De Paepe, A. and Speleman, F. (2002) 'Accurate normalization of real-time quantitative RT-PCR data by geometric averaging of multiple internal control genes', *Genome Biol,* 3(7), pp. RESEARCH0034.

Vetter, I. R. and Wittinghofer, A. (2001) 'The guanine nucleotide-binding switch in three dimensions', *Science,* 294(5545), pp. 1299-304.

Vizan, P., Boros, L. G., Figueras, A., Capella, G., Mangues, R., Bassilian, S., Lim, S., Lee, W. N. and Cascante, M. (2005) 'K-ras codon-specific mutations produce distinctive metabolic phenotypes in NIH3T3 mice [corrected] fibroblasts', *Cancer Res,* 65(13), pp. 5512-5.

Vogel, C. and Marcotte, E. M. (2012) 'Insights into the regulation of protein abundance from proteomic and transcriptomic analyses', *Nat Rev Genet,* 13(4), pp. 227-32.

Vogelstein, B., Fearon, E. R., Hamilton, S. R., Kern, S. E., Preisinger, A. C., Leppert, M., Nakamura, Y., White, R., Smits, A. M. and Bos, J. L. (1988) 'Genetic alterations during colorectal-tumor development', *N Engl J Med,* 319(9), pp. 525-32.

Voice, J. K., Klemke, R. L., Le, A. and Jackson, J. H. (1999) 'Four human ras homologs differ in their abilities to activate Raf-1, induce transformation, and stimulate cell motility', *J Biol Chem,* 274(24), pp. 17164-70.

Vos, M. D. and Clark, G. J. (2006) 'RASSF family proteins and Ras transformation', *Methods Enzymol,* 407, pp. 311-22.

Walker-Daniels, J., Coffman, K., Azimi, M., Rhim, J. S., Bostwick, D. G., Snyder, P., Kerns, B. J., Waters, D. J. and Kinch, M. S. (1999) 'Overexpression of the EphA2 tyrosine kinase in prostate cancer', *Prostate,* 41(4), pp. 275-80.

Wallace, M. R., Marchuk, D. A., Andersen, L. B., Letcher, R., Odeh, H. M., Saulino, A. M., Fountain, J. W., Brereton, A., Nicholson, J. and Mitchell, A. L. (1990) 'Type 1 neurofibromatosis gene: identification of a large transcript disrupted in three NF1 patients', *Science,* 249(4965), pp. 181-6.

Wang, T., Yu, H., Hughes, N. W., Liu, B., Kendirli, A., Klein, K., Chen, W. W., Lander, E. S. and Sabatini, D. M. (2017) 'Gene Essentiality Profiling Reveals Gene Networks and Synthetic Lethal Interactions with Oncogenic Ras', *Cell,* 168(5), pp. 890-903.e15.

Wang, W., Chen, J. X., Liao, R., Deng, Q., Zhou, J. J., Huang, S. and Sun, P. (2002) 'Sequential activation of the MEK-extracellular signal-regulated kinase and MKK3/6-p38 mitogen-activated protein kinase pathways mediates oncogenic ras-induced premature senescence', *Mol Cell Biol,* 22(10), pp. 3389-403.

Warne, P. H., Viciana, P. R. and Downward, J. (1993) 'Direct interaction of Ras and the amino-terminal region of Raf-1 in vitro', *Nature,* 364(6435), pp. 352-5.

Wei, W., Mosteller, R. D., Sanyal, P., Gonzales, E., McKinney, D., Dasgupta, C., Li, P., Liu, B. X. and Broek, D. (1992) 'Identification of a mammalian gene structurally and functionally related to the CDC25 gene of Saccharomyces cerevisiae', *Proc Natl Acad Sci U S A,* 89(15), pp. 7100-4.

Wennerberg, K., Rossman, K. L. and Der, C. J. (2005) 'The Ras superfamily at a glance', *J Cell Sci,* 118(Pt 5), pp. 843-6.

Westwick, J. K., Cox, A. D., Der, C. J., Cobb, M. H., Hibi, M., Karin, M. and Brenner, D. A. (1994) 'Oncogenic Ras activates c-Jun via a separate pathway from the activation of extracellular signal-regulated kinases', *Proc Natl Acad Sci U S A,* 91(13), pp. 6030-4.

White, M. A., Vale, T., Camonis, J. H., Schaefer, E. and Wigler, M. H. (1996) 'A role for the Ral guanine nucleotide dissociation stimulator in mediating Ras-induced transformation', *J Biol Chem,* 271(28), pp. 16439-42.

Whyte, D. B., Kirschmeier, P., Hockenberry, T. N., Nunez-Oliva, I., James, L., Catino, J. J., Bishop, W. R. and Pai, J. K. (1997) 'K- and N-Ras are geranylgeranylated in cells treated with farnesyl protein transferase inhibitors', *J Biol Chem,* 272(22), pp. 14459-64.

Wigler, M., Pellicer, A., Silverstein, S. and Axel, R. (1978) 'Biochemical transfer of single-copy eucaryotic genes using total cellular DNA as donor', *Cell,* 14(3), pp. 725-31.

Willingham, M. C., Pastan, I., Shih, T. Y. and Scolnick, E. M. (1980) 'Localization of the src gene product of the Harvey strain of MSV to plasma membrane of transformed cells by electron microscopic immunocytochemistry', *Cell,* 19(4), pp. 1005-14.

Willumsen, B. M., Christensen, A., Hubbert, N. L., Papageorge, A. G. and Lowy, D. R. (1984a) 'The p21 ras C-terminus is required for transformation and membrane association', *Nature,* 310(5978), pp. 583-6.

Willumsen, B. M., Norris, K., Papageorge, A. G., Hubbert, N. L. and Lowy, D. R. (1984b) 'Harvey murine sarcoma virus p21 ras protein: biological and biochemical significance of the cysteine nearest the carboxy terminus', *EMBO J,* 3(11), pp. 2581-5.

Wilson, L. J., Linley, A., Hammond, D. E., Hood, F. E., Coulson, J. M., MacEwan, D. J., Ross, S. J., Slupsky, J. R., Smith, P. D., Eyers, P. A. and Prior, I. A. (2018) 'New Perspectives, Opportunities, and Challenges in Exploring the Human Protein Kinome', *Cancer Res,* 78(1), pp. 15-29.

Winters, I. P., Chiou, S. H., Paulk, N. K., McFarland, C. D., Lalgudi, P. V., Ma, R. K., Lisowski, L., Connolly, A. J., Petrov, D. A., Kay, M. A. and Winslow, M. M. (2017) 'Multiplexed in vivo homology-directed repair and tumor barcoding enables parallel quantification of Kras variant oncogenicity', *Nat Commun,* 8(1), pp. 2053.

Wolfman, A. and Macara, I. G. (1990) 'A cytosolic protein catalyzes the release of GDP from p21ras', *Science,* 248(4951), pp. 67-9.

Wood, K. W., Sarnecki, C., Roberts, T. M. and Blenis, J. (1992) 'ras mediates nerve growth factor receptor modulation of three signal-transducing protein kinases: MAP kinase, Raf-1, and RSK', *Cell,* 68(6), pp. 1041-50.

Wu, B. O., Jiang, W. G., Zhou, D. and Cui, Y. X. (2016) 'Knockdown of EPHA1 by CRISPR/CAS9 Promotes Adhesion and Motility of HRT18 Colorectal Carcinoma Cells', *Anticancer Res,* 36(3), pp. 1211-9.

Xu, G. F., O'Connell, P., Viskochil, D., Cawthon, R., Robertson, M., Culver, M., Dunn, D., Stevens, J., Gesteland, R. and White, R. (1990) 'The neurofibromatosis type 1 gene encodes a protein related to GAP', *Cell,* 62(3), pp. 599-608.

Yan, J., Roy, S., Apolloni, A., Lane, A. and Hancock, J. F. (1998) 'Ras isoforms vary in their ability to activate Raf-1 and phosphoinositide 3-kinase', *J Biol Chem,* 273(37), pp. 24052-6.

Yen, I., Shanahan, F., Merchant, M., Orr, C., Hunsaker, T., Durk, M., La, H., Zhang, X., Martin, S. E., Lin, E., Chan, J., Yu, Y., Amin, D., Neve, R. M., Gustafson, A., Venkatanarayan, A., Foster, S. A., Rudolph, J., Klijn, C. and Malek, S. (2018) 'Pharmacological Induction of RAS-GTP Confers RAF Inhibitor Sensitivity in KRAS Mutant Tumors', *Cancer Cell,* 34(4), pp. 611-625.e7.

Zelinski, D. P., Zantek, N. D., Stewart, J. C., Irizarry, A. R. and Kinch, M. S. (2001) 'EphA2 overexpression causes tumorigenesis of mammary epithelial cells', *Cancer Res,* 61(5), pp. 2301-6.

Zhang, L., Holmes, I. P., Hochgräfe, F., Walker, S. R., Ali, N. A., Humphrey, E. S., Wu, J., de Silva, M., Kersten, W. J., Connor, T., Falk, H., Allan, L., Street, I. P., Bentley, J. D., Pilling, P. A., Monahan, B. J., Peat, T. S. and Daly, R. J. (2013) 'Characterization of the novel broad-spectrum kinase inhibitor CTx-0294885 as an affinity reagent for mass spectrometry-based kinome profiling', *J Proteome Res,* 12(7), pp. 3104-16.

Zhang, S., Han, J., Sells, M. A., Chernoff, J., Knaus, U. G., Ulevitch, R. J. and Bokoch, G. M. (1995) 'Rho family GTPases regulate p38 mitogen-activated protein kinase through the downstream mediator Pak1', *J Biol Chem,* 270(41), pp. 23934-6.

Zhang, X. F., Settleman, J., Kyriakis, J. M., Takeuchi-Suzuki, E., Elledge, S. J., Marshall, M. S., Bruder, J. T., Rapp, U. R. and Avruch, J. (1993) 'Normal and oncogenic p21ras proteins bind to the amino-terminal regulatory domain of c-Raf-1', *Nature,* 364(6435), pp. 308-13.

Ünal, E. B., Uhlitz, F. and Blüthgen, N. (2017) 'A compendium of ERK targets', *FEBS Lett,* 591(17), pp. 2607-2615.